On (pseudo-) polymorphic phase transformations

Dissertation
zur Erlangung des akademischen Grades

Doktor-Ingenieurin (Dr.-Ing.)

Genehmigt durch die

Mathematisch-Naturwissenschaftlich-Technische Fakultät
(Ingenieurwissenschaftlicher Bereich)
der Martin-Luther-Universität Halle-Wittenberg

von Frau Dipl.-Ing. Christine Strege
geb. am 24.07.1973 in Nienburg / Weser

Dekan der Fakultät: Prof. Dr.-Ing. habil. H. Altenbach
Gutachter:
1. Prof. Dr.-Ing. habil. J. Ulrich
2. Prof. Dr. rer. nat. habil. D. A. Lempe
3. Prof. Dr. A. S. Myerson

Halle (Saale), 09. August 2004

Danksagung

Die vorliegende Arbeit entstand zwischen Oktober 1999 und September 2003 während meiner Tätigkeit als wissenschaftliche Mitarbeiterin an einer „Außenstelle" der Martin-Luther-Universität Halle-Wittenberg, am Institut für Verfahrenstechnik / TVT des Fachbereichs Ingenieurwissenschaften in Merseburg.

Mein herzlicher Dank gilt an erster Stelle meinem Doktorvater Herrn Prof. Dr.-Ing. J. Ulrich, der mir die Möglichkeit zur Promotion gab, und mich stets, wie auch schon zu Studienzeiten, unterstützt und gefördert hat. Ich möchte Herrn Prof. Dr.-Ing. J. Ulrich ferner für die Gewährung der großen Freiräume bei der Bearbeitung des Promotionsthemas danken, und natürlich auch für die Möglichkeit zur Teilnahme an zahlreichen Dienstreisen zu Konferenzen oder Workshops.

Bei Herrn Prof. Dr. rer. nat. D. A. Lempe möchte ich mich für die kritische Begutachtung meiner Arbeit bedanken.

I want to warmly thank Prof. Dr. A. S. Myerson for giving me his opinion on my thesis. I already got to know Prof. Dr. A. S. Myerson many years ago as a student during an internship in New York, and ever since I appreciated him as a competent and pleasant conversationalist.

Dank geht an dieser Stelle ebenfalls an das K+S-Forschungsinstitut der Kali und Salz GmbH für die finanzielle Unterstützung eines Teils des Projekts.

Einen großen Beitrag zum Gelingen dieser Arbeit haben auch die beteiligten Schüler, (Austausch-) Studenten und insbesondere die Studienarbeiter Raik Stolle, Eric Römbach und Max Wellerdiek geleistet.

Mir wird besonders die angenehme Arbeitsatmosphäre an der MLU in Erinnerung bleiben – und die aus dieser Zeit entstandenen Freundschaften. Einen großen Dank an alle, die zu diesem freundschaftlichen Arbeitsklima beigetragen haben, wie z.B. Andrea, Bernd, Conny, Kai, Mandy, Tero, Torsten und Uta. Besonders erwähnen möchte ich an dieser Stelle noch Mirko, mit dem mich seit der Hallenser Zeit eine enge Freundschaft verbindet.

Mein besonderer Dank gilt meiner Mutter, die mich immer und in allem unterstützt hat. Danke!

München, im November 2004

1. Introduction

The phenomenon of the same substance having different crystalline modifications is known as polymorphism. Polymorphs are chemically identical solids, but exhibit differences in their physical properties. Often two polymorphs of the same substance exhibit for instance distinct differences in their solubility, dissolution rate, crystal habit, density, crystal hardness or melting point /MYE02/. Substances incorporating solvent in their crystal lattice represent a special type of polymorphism. These substances are called solvates or hydrates, if water molecules are part of the crystal structure. Solvates and hydrates are summarized with the term "pseudopolymorphs". Due to the incorporation of solvent, pseudopolymorphs are chemically not identical and therefore not only the physical but also the chemical properties may be quite different /BYR82/.

The crystallization of pseudopolymorphs might raise some problems. Firstly, the operating conditions have to be fixed under which the process has to be conducted to produce the desired product in a stable and reproducible way. In this context the temperature, pressure, supersaturation and the residence time of the crystals in the crystallizer have to be mentioned. Besides the operating conditions, thermodynamics and kinetics have to be considered. Attention has to be paid to the fact that different solvents or impurity concentrations might for instance influence the solubility, growth rate or the induction time for the transformation of a metastable pseudopolymorph into a more stable modification. However, often the impurity concentration cannot be directly influenced since e.g. the raw material has varying purities.

Besides the unintentional influence on crystallization processes caused by solution by-products, often substances are deliberately added to achieve specific effects. Examples for an intentional addition of an additive would be for instance the change of habit from needle-like to a more compact form in order to have a more efficient filterability or the delay of phase transformations to stabilize a metastable product. In many cases, crystallization leads to the formation of a metastable (pseudo-) polymorph, which will eventually transform into a more stable one. Sometimes transformation is not certain even though a system enters a condition that will thermodynamically allow it. Transformation rates of (pseudo-) polymorphs strongly depend on kinetics. Therefore, the transformation of a metastable phase into a more stable phase is not certain even though the system enters a condition in which, considering solely thermodynamics, a transformation would have to take place. Phase transformations can only be assured if a more stable solid phase is already present, is introduced by seeding, or makes its appearance by nucleation /MOHN01, MUL00/.

The motivation for this work is to carry out further basic research in the field of phase transformations, concerning the predictability of phase transformations and the possibility to influence phase transformations, either promoting or retarding the transformations. Furthermore, the course of phase transformations with organic and inorganic substances will be explored to find out about general conformities and differences.

2. State of the art

A multitude of crystalline substances exhibits polymorphism and / or pseudopolymorphism /HEN97/. The knowledge of potential factors influencing the outcome of the crystallization process and the control of the process itself is the prerequisite for obtaining crystalline products with given quality. Crystallization processes executed at random may either produce an unexpected modification right from the beginning or phase transformations during processing or storage may be induced inadvertently.

2.1 Nucleation

The state of supersaturation is an essential requirement for crystallization operations, however, supersaturated solutions are not at equilibrium. Since every system strives to reach equilibrium, supersaturated solutions finally crystallize. Crystallization from solution can be subdivided into two kinetic steps: The first kinetic step is a phase separation, called nucleation, and the second step is the subsequent growth of nuclei to crystals. The relation of the degree of nucleation to crystal growth determines important product properties, such as product crystal size and size distribution. Nucleation is also strongly interrelated to the width of the metastable zone or the metastability of a system, respectively /KLE85, MUL00, MYE02, VAU92/.

2.1.1 Metastable zone

The nucleation rate, i.e. the number of nuclei formed per unit time and unit volume, is neglectable for small supersaturations. Only when a critical supersaturation is reached, it increases distinctly. This may be taken as an explanation for the so-called metastable zone, which constitutes the allowable supersaturation level for all crystallization operations. Although the existence of a metastable zone is not doubted, no standardized definition is given in literature. Therefore, the following diagram, *Figure 2.1-1*, represents a summary of published definitions /BEC03a, MER95, MUL00, MYE02, NYV85, ULR02a/.

From *Figure 2.1-1* it can be seen that various stages of stability exist in solution crystallization for primary nucleation. Below the solubility curve all solutions are unsaturated. Since no crystallization is possible in unsaturated solutions, this region is said to be stable. The solubility curve represents an equilibrium state where growth and dissolution processes take place at the same magnitude, thus the induction time for nucleation is infinite. Assuming a cooling crystallization, solutions will be supersaturated when reaching a temperature below the saturation temperature. However, supersaturated solutions do not necessarily crystallize, but the tendency to crystallize increases with increasing supersaturation. At a certain temperature a point is reached, where the induction time equals zero, meaning that when a solution is cooled to that temperature, instantaneous crystallization starts. This point, defined by temperature and concentration, is called the metastable limit. The zone between the saturation curve and this supersaturation limit is called metastable zone. The metastability describes a state in

which instantaneous nucleation does not take place, however, after a certain induction period nucleation cannot be excluded. Furthermore, crystals present in the solution or added to it, will grow and therewith deplete supersaturation. In laboratory experiments it has been shown that this metastable limit can be exceeded and a transitional state will be obtained. In this case, a level of supersaturation is reached at which the liquid becomes to viscous to nucleate. At even higher supersaturations a system is said to be unstable. In practice, this region can hardly be reached in solution crystallization, because of the presence of dust and dirt, the employed cooling rate, use of agitation etc., as described later in this section. However, e.g. for some systems in melt crystallization, the unstable region has been proven to exist.
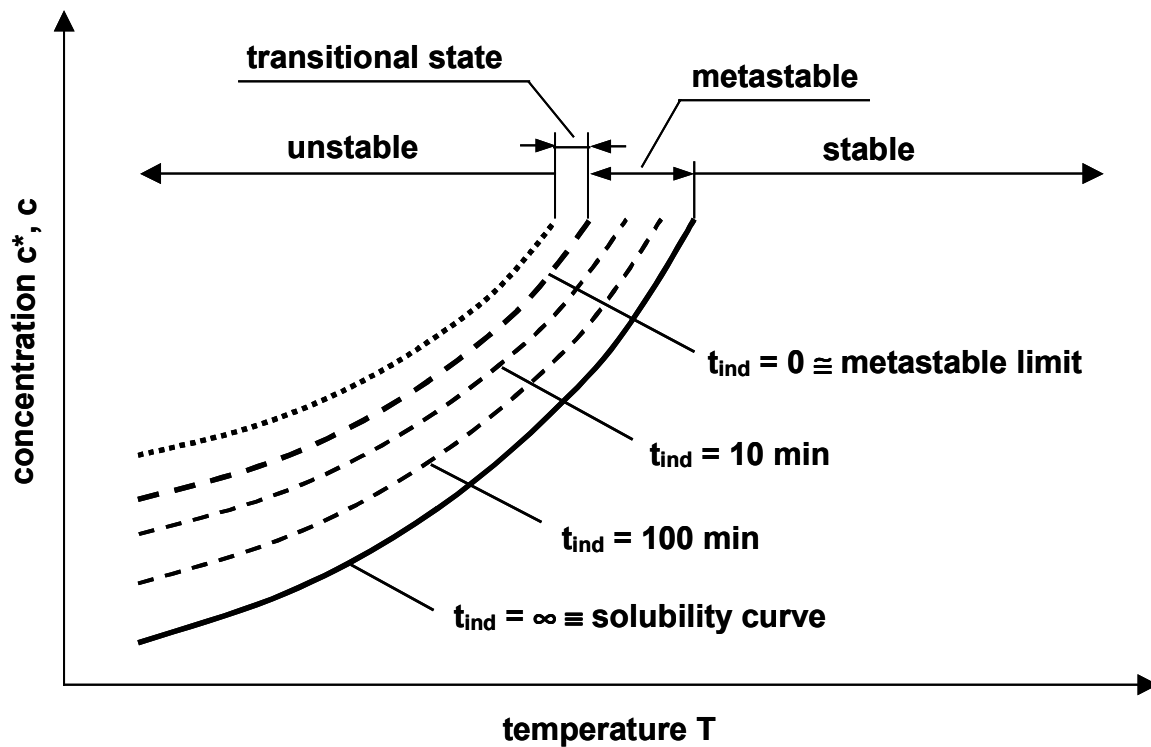
Fig. 2.1-1   Stages of stability in solution crystallization

The metastable limit is, in contrast to the solubility curve, thermodynamically not founded and kinetically not well defined. The width of the metastable zone depends on a number of parameters such as temperature level, rate of generating the supersaturation, solution history, impurities, fluid dynamics, viscosity, mechanical forces, friction, extreme pressures etc. /MER80, MUL00, MYE02, ULR02/.

The width of the metastable zone can also be influenced by the use of seed crystals. In general, the width of the metastable zone for seeded solutions is smaller in comparison to solutions without crystals being present. For solutions of KCl and $NaClO_3$ it has been shown that an increasing size of seed crystals leads to a decrease of the metastable zone width /HER01/. Furthermore, it is reported that the addition of single crystals results in a clearly lower scattering of the supercooling temperatures than the addition of two or more

crystals. Even one crystal at rest in an unstirred solution is sufficient to reduce the metastable zone width significantly /KLE85, LAC99, MER96/.

In *Figure 2.1-2* a diagrammatic representation of the metastable zone for different nucleation mechanisms is shown. Besides the lower continuous solubility curve, three broken supersolubility curves indicate different mechanisms for nucleation.
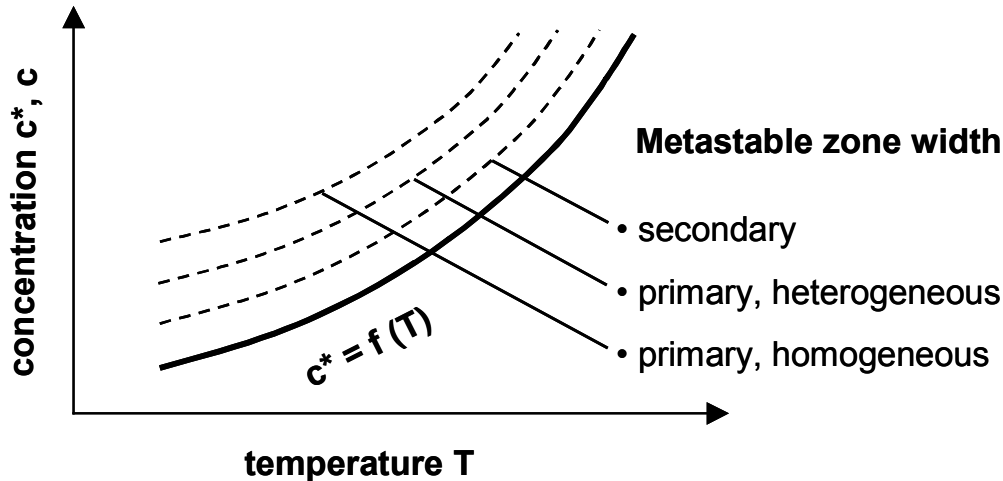
Fig. 2.1-2   Metastable zone width for different nucleation mechanisms /MER95/

Common is a differentiation between primary and secondary nucleation. Primary nucleation is the formation of nuclei that are able to grow without presence of any crystalline matter, whereas secondary nucleation requires the presence of crystals.

Primary nucleation can be subdivided into *homogeneous nucleation* – spontaneous in the solution bulk - and *heterogeneous nucleation* - induced e.g. by surface roughness, and especially by foreign micro and nano particles that cannot be excluded from being present in the solution. Homogeneous nucleation is not very common, in most cases dissolved impurities and physical features such as crystallizer walls, stirrers, and baffles function as heteronuclei to induce crystal formation. The reason for this is the energetic barrier to build a species with a large surface area to volume ratio where the full stabilization of the bulk is not given for many of the molecules. A heteronucleus reduces the energetic barrier by providing stabilization of a growing face of the crystal. Therefore, nucleation in a heterogeneous system generally occurs at a lower supersaturation than in a homogeneous system.

Secondary nuclei can originate from attrition fragments, i.e. from seed crystals interacting with the above-mentioned physical features. Furthermore, secondary nuclei are formed either as preordered species, as clusters in the boundary layer of the crystal surface, or on the crystal surface by dendritic growth and dendrite coarsening. These parent crystals have a catalyzing effect on the nucleation phenomena, and thus, nucleation occurs at a lower supersaturation than needed for primary nucleation. Mechanisms of secondary

nucleation are e.g. initial breeding, polycrystalline breeding, macroabrasion, dendritic, fluid shear, and contact nucleation. Secondary nucleation is the most relevant mechanism for industrial crystallization operations /KLE85, LAC99, MAT03, MER96, MUL00, MYE02, VAU92/.

A control of the actual supersaturation in the crystallizer is mandatory to be able to exert a targeted influence on nucleation and growth processes and therewith on the product quality. Very high supersaturations usually cause primary nucleation, and thus a large number of nuclei. For this reason many fine crystals are obtained, and a product with a specified mean crystal size distribution is not recoverable anymore. Furthermore, at very high supersaturations crystal growth is well enhanced, and often the outcome is dendritic growth and a diminished purity due to liquid inclusions. On the other hand, operating a crystallizer close to the saturation curve results in slow growth rates and high purities. However, this is not desirable for economic reasons, because slow growth rates require too long retention times of the product in the solution. On this account, in industrial crystallization a compromise has to be made between product quality and process safety or economical efficiency. According to a rule of thumb the crystallizer should be operated approximately in the middle of the metastable zone /HOF91/.

2.1.2 Fundamentals of nucleation

Nucleation theories are presented elsewhere in detail /KAS00, ZET69/, and only a few aspects will be mentioned here.

When the solubility of a solution is exceeded and it is supersaturated, the molecules start to associate and form clusters, or concentration fluctuations. Under the assumption that these clusters or nuclei are spherical, the equation for the free enthalpy (Gibbs free energy) change required to form a nuclei with the radius r, the volume $4\pi r^3/3$, and the surface $4\pi r^2$ is:

$$\Delta G = \Delta G_v + \Delta G_s = \frac{4}{3}\pi r^3 \Delta G_v + 4\pi r^2 \sigma \qquad \text{(2.1-1)}$$

The first term is the volume term, being the number of molecules inside the nucleus. The second term is the surface term, representing the excess energy expended in creating the nucleus surface /BOI88, KLE85, MUL00, MYE02/.

Under given conditions of temperature and pressure, a process in a system runs spontaneously, if during this process the free enthalpy G of the system decreases. A supersaturated phase has a higher free enthalpy than the stable phase, and should therefore spontaneously transform into it. The formation of a nucleus of the new, stable phase within the supersaturated phase, will cause a (negative) change of the free

enthalpy ΔG_v, that is proportional to the volume of the nucleus. However, with the formation of this nucleus also a new phase boundary emerges and its interfacial energy causes a (positive) change of the free enthalpy ΔG_s, which is proportional to the surface of the nucleus. For very small particles this positive change of the free enthalpy is comparable to ΔG_v, and therefore the thermodynamic probability of nucleation is drastically diminished. Since the surface term ΔG_s predominates with small r, the free energy of the system is increased when a small nucleus is formed, i.e. energy has to be expended /KLE85/.

Due to the competition between volume and surface terms, the Gibbs free energy change passes through a maximum, representing the critical size of a nucleus. The critical size r_{crit} represents the minimum size of a stable nucleus. If one molecule is withdrawn from it, it dissolves spontaneously. On the other hand, if one molecule is added to it, it grows spontaneously. Both processes are taking place with a reduction of the free energy. As soon as stable nuclei, i.e. particles larger than the critical size, have been formed, they begin to grow into crystals of visible size. The maximum of the free energy ΔG_{crit} corresponds to the critical nucleus r_{crit}:

$$\Delta G_{crit} = \frac{4}{3}\pi r_{crit}^2 \sigma \qquad\qquad (2.1\text{-}2)$$

A plot of the Gibbs free energy change as a function of the size of a nucleus (see *Figure 2.1-3*) illustrates that as the nucleus' size increases a point is reached where the Gibbs free energy change is negative, and the nucleus will grow spontaneously. At this point, nucleation will occur. The reason that supersaturated solutions are metastable is, therefore, because a nucleus of critical size needs to form. As the supersaturation increases, the critical size decreases and due to this reason, solutions become less and less stable as the supersaturation increases /BOI88, MUL00, MYE02/.

Summing up, it may be said that classical nucleation theory comprises two distinct steps. First, the aggregation of dissolved molecules in the supersaturated solution into organized nuclei and second, the growth of the nuclei once a critical size is overcome. However, new theoretical approaches indicate that classical nucleation theory fails in various situations /WEIS03/.

Experimental studies of structures of supersaturated solutions at the onset of crystallization have provided proof for the existence of clusters. In classical theory is assumed that clusters of approximately spherical molecules should also be almost spherical. In contrast to this, modern nucleation theories propound the hypothesis of clusters adopting a variety of arrangements and shapes, some of which resemble the crystals into which they will eventually grow. In new approaches, the shape and internal structure of critical nuclei is considered variable, because the shape of a critical nucleus

could have a large effect on its energy and therefore on the rate of formation of crystals /WEIS03/.
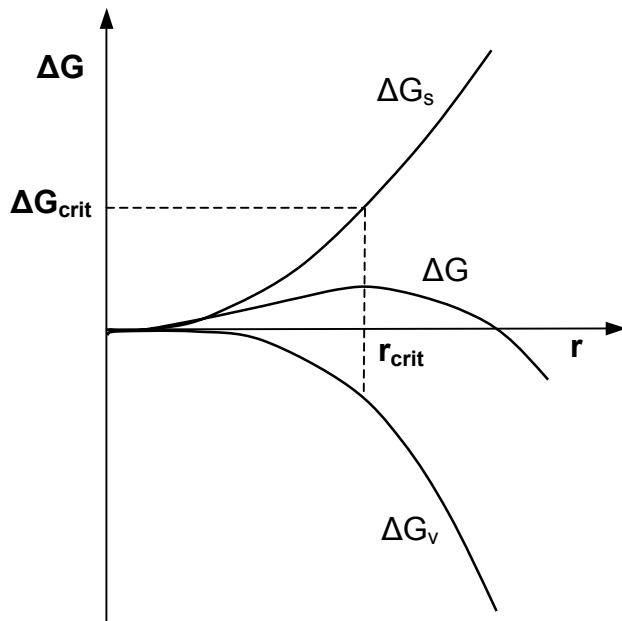
Fig. 2.1-3   Gibbs free energy change ΔG as a function of the size of a nucleus r /KLE85/

Nuclei are formed spontaneously at the end of an induction time, which depends e.g. on the system, supersaturation, viscosity of the solution, and impurities. The diameter of metastable GIBBS-nuclei lies within the range of 1...1000 nm. The number of molecules constituting a stable nucleus depends on the system and can vary from about ten to several thousand /MUL00, VAU92/.

2.1.2.1   Induction time

The period of time, which usually elapses between the achievement of supersaturation and the point at which crystals are first detected, is generally referred to as the induction period. The induction period can be divided into several parts: At the beginning, a certain relaxation time t_r is required for this system to achieve a quasi-steady-state distribution of molecular clusters. Further time is required for the formation of a stable nucleus, t_n, and then for the nucleus to grow to a detectable size, t_g. However, in practice it is difficult to isolate these separate quantities. The relaxation time depends to a great extent on the viscosity of the solution and, hence, on the diffusivity. The nucleation time depends on the supersaturation which affects the size of the critical nucleus, and the growth time depends on the size at which nuclei can be detected, thus on the measuring technique.

In some systems, particularly at low supersaturation, another time lag may be observed, which is referred to as the latent period. To distinguish it from the induction period, the latent period is defined as the period of time between the achievement of supersaturation and the onset of a significant change in the system, e.g. the occurrence of massive

nucleation or some clear evidence of substantial solution desupersaturation (see *Figure 2.1-4*).
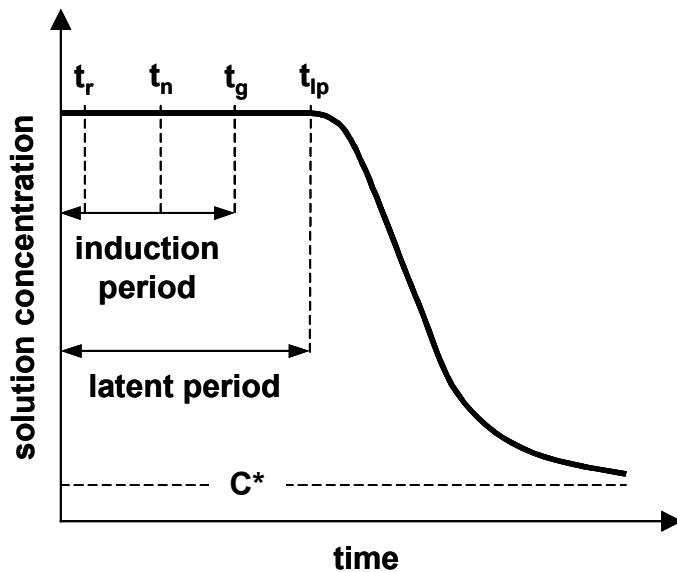
Fig. 2.1-4 Desupersaturation curve /MUL00/

This further distinction is helpful, because at the end of the induction period and often for a considerable time afterwards, no significant changes in the solution may be detected until, at the end of the latent period, rapid desupersaturation occurs. At very high supersaturations, the induction and latent periods can be extremely short and virtually indistinguishable. Factors that can influence the induction and latent periods are temperature, agitation, heat effects during crystallization, seed size, seed surface area, and the presence of impurities /MUL00/.

2.2 Crystal growth

Crystal growth depends to a great extent on the operating variables: *supersaturation*, *temperature* and *fluid dynamics*. The most critical factor in crystal growth processes is probably *supersaturation*, because the growth rate increases directly with the degree of supersaturation. Since the critical growth rate increases appreciably with *temperature*, good crystals can be grown more rapidly at higher temperatures - regardless of the solubility characteristics of the solution. In most crystal-growing systems, the growth rate depends on the *fluid dynamics* up to the point where the process is no longer diffusion-controlled.

Besides the operating variables, the character of the solution is dominating crystal growth. The choice of solvent, the purity, pH, and the presence of additives are often even more important than the apparatus design. Furthermore, the crystals' surface, history and size as well as the retention time of the crystals in suspension have to be considered /EGL63, KOH63, ULR93, VAU92/.

2.2.1 Fundamentals of crystal growth

Theories of crystal growth provide a theoretical basis for the correlation of experimental data and the determination of kinetic parameters from the data to be used in models of industrial crystallization processes. For the characterization of growth kinetics in solution crystallization the growth rate is determined as a function of supersaturation, because this way of describing growth kinetics allows the prediction of the dominating kinetic step. According to Kruse /KRU93/ volume diffusion, surface integration and heat transport exert an influence on the linear growth rate. His assumptions are comprised in a 3-step-model for combined mass and heat transfer /KRU93/.

The strongest reduction of supersaturation takes place during the rate determining step. For crystallization from pure melt, the heat transfer is rate determining, whereas the crystallization rate from solutions is normally controlled by the integration process, by diffusion, or by both. If the crystal growth rate is limited by the rate of diffusion through a laminar film, the growth is said to be diffusion-controlled. Especially in non-agitated systems, this is the controlling mechanism. However, in some cases, the growth rate reaches a maximum as agitation increases or as the relative velocity between crystal and mother liquor increases. This is consistent with the concept of diffusion-controlled growth for low relative solution velocities and with the concept of integration-controlled growth at high relative velocities /LAC99, RAN71/.

Volmer /VOL39/ suggested that crystal growth is a discontinuation process, taking place by adsorption, layer by layer, on the crystal surface. His suggestion led to the adsorption-layer theories, several modifications of which have been proposed in recent years (Volmer, Kossel, Frank, BCF-model). The diffusion theories presume that matter is deposited continuously on a crystal face at a rate proportional to the difference in concentration between the point of deposition and the bulk of the solution. Further models are the birth and spread model, which is assuming two-dimensional nuclei to spread across the crystal face, the mononuclear model, and the polynuclear model, just to name a few. Theories of crystal growth are described in detail by /BOI88, BUC58, MUL00, MYE02, VOL39/.

2.2.2 Crystal growth phenomena

Crystals kept in suspension will eventually change their size due to two phenomena, namely *growth rate dispersion* and *Ostwald ripening*.

Crystals of the same size growing in suspension exposed to identical conditions of supersaturation, temperature, and fluid dynamics, do not necessarily grow at the same rate. The effect that after some time a crystal size distribution emerges is called growth rate dispersion, meaning that the crystals have different growth rates. However, this is not the same as size-dependent growth in which crystals of different sizes display differences in their growth rate.

Two models are used to describe the effect of growth rate dispersion. In the constant crystal growth model it is assumed that all crystals or crystal faces grow with a constant crystal growth rate that is different from crystal to crystal and from face to face for faces of the same indication. In contrast to this, the random fluctuation model describes growth rate

dispersion by a change of growth rate during growth, assuming a uniform mean growth rate for all crystals and faces, respectively.

The effect of Ostwald ripening is to alter the CSD with time in a suspension of crystals that is in apparent equilibrium with its saturated solution. This is the result of the system trying to minimize its Gibbs free energy and thereby increasing the average crystal size.

Suspended particles with a size distribution have different solubilities based on their size (Gibbs-Thomson-relationship). A significant increase in solubility occurs when the crystal size is smaller than 1 µm and for larger particles at sharp edges and grain boundaries, i.e. at regions of very small radius. This difference in solubility results in the small particles dissolving and depositing on the larger particles, therewith decreasing the surface area and moving the system towards a minimum in Gibbs free energy. It is often taken advantage of Ostwald ripening in processes in which crystallization is rapid and crystal sizes are small. The smaller the particle size, or the higher the solubility for large particles, the faster the ripening process /LAC99, MYE02, MUL00/.

2.2.3   Methods to study crystal growth

Crystal growth data can be obtained by a number of experimental methods. Two main groups can be differentiated. The first group comprises methods that measure the growth of a single crystal to obtain the needed data (e.g. recirculation apparatus or flow apparatus /MYE02/, microscopic cell /NIE97/). Single crystal growth techniques, which can focus on growth rates of individual faces, are predominantly used for fundamental studies relating to growth mechanisms. The second group of methods involves the growth of a suspension of crystals (e.g. agitated vessel /MUL00/, fluidized bed /ULR93/). Measurements made on populations of crystals are useful for determining overall mass transfer rates and for observing size-dependent growth or growth rate dispersion. It often more useful for crystallizer design purposes to measure crystal growth rates in terms of mass change of the crystals rather than as individual face growth rates. The increase in mass of fractionated seed crystals under carefully controlled conditions with time can be directly related to the overall linear growth rate (see *section 3*) /MUL00, MYE02/.

2.2.4   Crystal habit

The crystal habit can have a major impact on a number of important properties relating to the slurry and the dry product, e.g. on the rheological properties of the suspension, the filtration or centrifugation efficiency, bulk density of the solid, flow properties of the solid, proneness to caking, handling or packaging of the material, and on storage characteristics. The control of crystal habit along with CSD is, therefore, an important task of industrial crystallization processes /KHAM76, MUL00, MYE02/.

The habit of a crystal depends on its different crystallographic faces and the relative growth rates of the individual faces. For instance, some crystals may grow more rapidly in one direction whereas others may be stunted. Thus, assuming a prismatic habit, an

elongated growth will give a needle-shaped crystal (acicular habit) whereas a stunted growth results in a plate-like crystal (tabular habit).

Some faces grow very fast and have little or no effect on the growth form. The ones that have the most influence are the slow-growing faces, because the slower a face grows the bigger its portion of the crystal surface. The opposite applies to dissolution. The faster a crystal surface is being carried off the bigger it will become /KLE85, KLU93, MUL00, VAU92/. The effect of "disappearing" fast growing faces is illustrated in *Figure 2.2-1*.
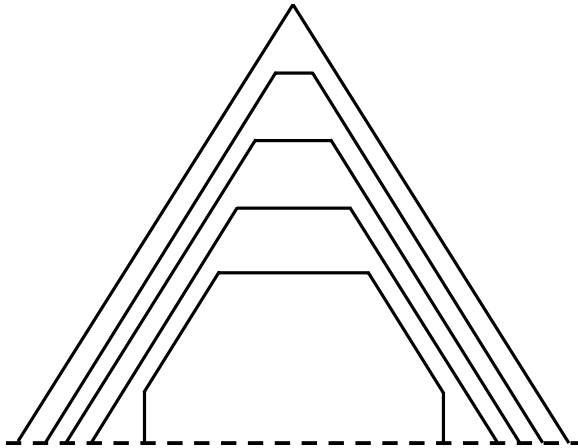
Fig. 2.2-1   Kinematics of crystal growth /KLE85/

Under conditions of very slow growth, the crystal habit is determined strictly by thermodynamics and the faces appearing on the crystal correspond to the smallest convex polyhedron having a minimum surface free energy. However, under most conditions the habit of a crystal is determined by kinetics rather than by thermodynamics.
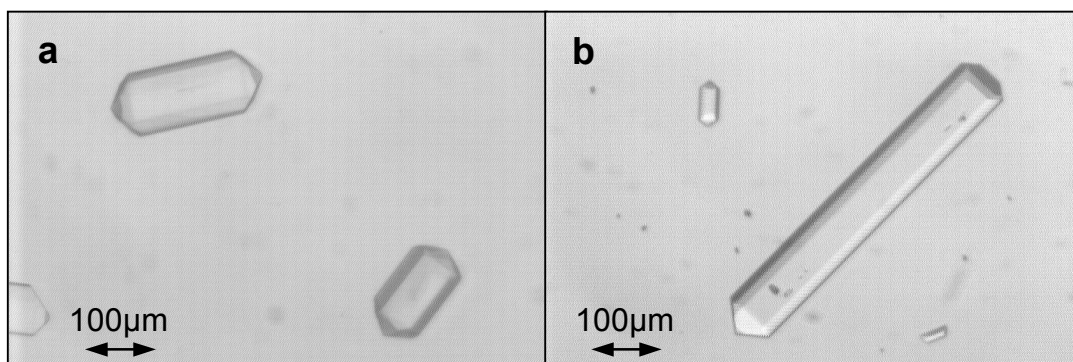
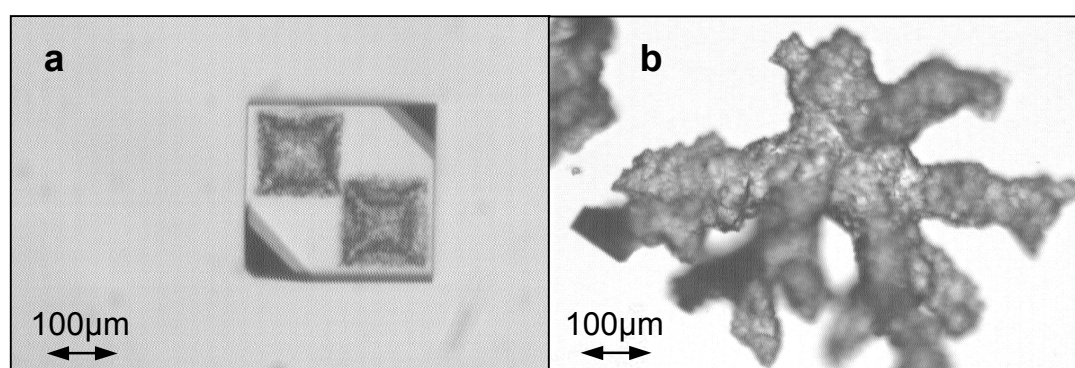**Fig. 2.2-2**   Influence of supersaturation on the habit of $MgSO_4 \cdot 7H_2O$ crystals
    a) Supercooling: 0.5 K, b) Supercooling: 3.0 K /ULR02/

The growth mechanisms and growth rates of a crystal depend on both, external and internal factors. Structure, bond and defects belong to the internal factors, whereas the external factors comprise environmental conditions. External factors include

supersaturation, temperature, agitation, solvent, pH, impurities, and the rate of crystallization, for instance the rate of cooling or evaporation. Furthermore, the purity of crystalline products strongly depends on the growth rate, since e.g. fast growth may lead to liquid inclusions /BOI88, KLU93, MUL00, VAU92/.

Exemplarily the effect of supersaturation on the crystal habit is shown in *Figure 2.2-2*. With increasing supersaturation the magnesium sulfate heptahydrate crystals become acicular, the (110) face being elongated. For magnesium sulfate heptahydrate, supercoolings larger 4 K cause veiled growth. For supercoolings larger 8 K no controlled growth is possible anymore, and e.g. dendritic growth occurs. The branches of the tree-like dendrites grow in directions in which the fastest crystallization is possible /CLO71, KLE85/.

Fig. 2.2-3   Influence of supersaturation on the habit of KCl crystals /ULR02/
Supercooling of the solution: 3.0 K
a) Warm surface of solution, b) Cold surface of solution

The considerable influence of supersaturation on the crystal habit is also illustrated for potassium chloride crystals (see *Figure 2.2-3*). Experiments have been carried out in a microscopic cell, described in *section 3*, with changing conditions of the solution surface, i.e. at the solution / air interface. With a warm solution surface, shown in *Figure 2.2-3 a*, distorted growth occurs in form of agglomerates (pyramids) on top of a seed crystal. In contrast to it, *Figure 2.2-3 b* shows the result for an experiment carried out with a distinctly colder solution surface. Under these conditions dendritic growth of the seed crystal occurs, leading to a distorted crystal without any sign of structure.

A comprehensive study of crystal growth has been published by Buckley /BUC58/, comprising subjects such as solution and solubility, supersaturation, preparation of crystals, theories of crystal growth, ideal and real crystals, dissolution phenomena, crystal habit modification by impurities, and peculiarities of crystal growth.
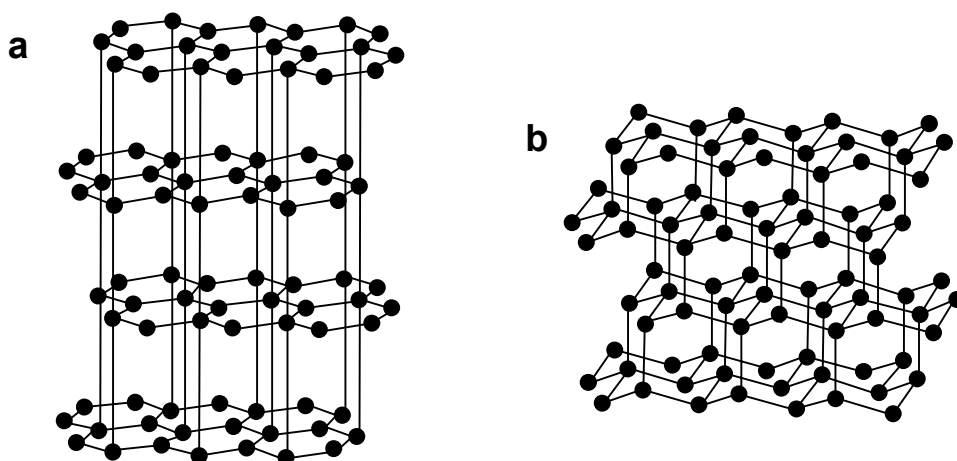
2.3 (Pseudo-) Polymorphism

In the context of crystallography, Mitscherlich was the first to use the term polymorphism in the year 1822. He had recognized different crystal structures of the same compound in a

number of arsenate and phosphate salts. In 1899, Ostwald wrote that almost every substance can exist in two or more solid phases and that, in general, the number of forms known for a given compound is proportionally to the time and money spent in research on that compound. Indeed, numerous organic materials, pharmaceutical and food substances, as well as inorganic substances are known to exhibit polymorphism. In addition, many of these materials can also crystallize as hydrates or solvates (pseudopolymorphs). Nowadays, more than 50 % of the pharmaceutical active agents are known to exist in several crystal forms as polymorphs or pseudopolymorphs or both /BER02, CAR85, HEN97, MCC65, MOHN01/.

2.3.1 Definitions

The term *polymorphism* applies to substances that can exist in at least two different crystal structures, having different arrangements and / or conformations of the molecules in the crystal lattice. Two polymorphs, although different in crystal structure, are identical in the liquid and vapor states, because melting or dissolution destroys any distinctions. Polymorphs often have different morphologies, solubilities, melting temperatures, densities, electrical or thermal conductivities and other physical properties. Furthermore, the crystalline form affects the filtering, drying, flow, tabletting, rate of dissolution, shelf life and bioavailability /BER02, BUE51, MCC65, MAT03, MOHN01, MYE02, THR95/.

Polymorphism of carbon with the two best known polymorphs diamond and graphite is probably the most popular example (see *Figure 2.3-1*) /BEC03/.

Fig. 2.3-1   Arrangement of C-atoms /CHR71/
a) Graphite-lattice , b) Diamond-lattice

The term pseudopolymorphism characterizes substances incorporating solvent in their crystal lattice. These substances are also called solvates or hydrates, if water molecules are part of the crystal structure. Like polymorphs, also different pseudopolymorphs of one substance can have distinctly different physical properties. However, due to the

incorporation of solvent, pseudopolymorphs are chemically not identical, and therefore not only the physical properties may be different, but also the chemical properties are different /BOI88, BYR82, KHA95, MOHN01, MYE02/.

2.3.2 Stability of (pseudo)-polymorphs

The *physical* nature of a system can be expressed in terms of phases. By altering one or more of the independent variables - temperature, concentration and pressure - the number of phases can be changed. The *chemical* nature of a system can be expressed in terms of components. For any given system, the number of components is fixed. The phase rule, which relates the number of components C, phases P, and degrees of freedom F of a given system, is expressed by the following equation:

$$P + F = C + 2 \qquad \textbf{(2.3-1)}$$

In this equation, P denotes the number of phases (solid, liquid, vapor), F is the number of degrees of freedom or independent variables, and C is the number of components. The number of independent variables that may be changed in magnitude without changing the number of phases present is called the number of degrees of freedom; and the number of components of a system is defined as the minimum number of chemical compounds required to express the composition of any phase /MUL00, USD98, VAU92/.

Since polymorphs are chemically identical, a system consisting e.g. of two solid phases can be considered a one-component system. The two variables that can affect the phase equilibria of a one-component system are temperature and pressure. In contrast to this, a system consisting of two pseudopolymorphs can be considered a two-component system due to the incorporation of solvent in the crystal lattice. The three variables that can affect the phase equilibria of a two-component system are temperature, pressure and concentration /MUL00/.

Materials crystallize into different crystal forms as a result of different molecular conformation or arrangement. This is a function of the conditions of growth like temperature, pressure, relative humidity, solvent, impurity content, growth rate, etc. along with intra- or intermolecular forces and the interaction of the solute with solvents and additives /BECH01, KLE85, MOHN01, MYE02/.

In many cases, a particular polymorph is metastable, meaning that this modification will eventually transform into a more stable state. These phase transformations can be relatively rapid in some systems while in others they can be infinitely slow. An example for the latter being diamond, which is a metastable form of carbon at room temperature. The transition from one polymorphic form to another usually occurs most rapidly when the crystals are suspended in solution, however, some materials will undergo transformation when in a dry solid state. Solution-mediated phase transformations proceed the more

rapidly the higher the solubility and the greater the solubility difference of the two forms /MCC65, MYE02/.

Phase transformations can be either reversible or irreversible. In *enantiotropic* systems each form has a temperature range over which it is stable with respect to the other form. At the so-called transition point the two forms are equistable and in principle interconvertible. Above the transition temperature, the thermodynamic tendency is to the formation exclusively of the form stable at higher temperatures. Below this temperature, the low-temperature form is the only stable one with respect to the other. Forms outside their range of stability are in general described as metastable.

In a *monotropic* system one form is metastable with respect to the other form at all temperatures. There is no observable transition point, although thermodynamics imply a theoretical transition point above the melting point. Therefore, two monotropically related modifications are not interconvertible. For instance, at room temperature graphite and diamond are monotropic forms of carbon /BER02, MUL00, MYE02, THR95/.
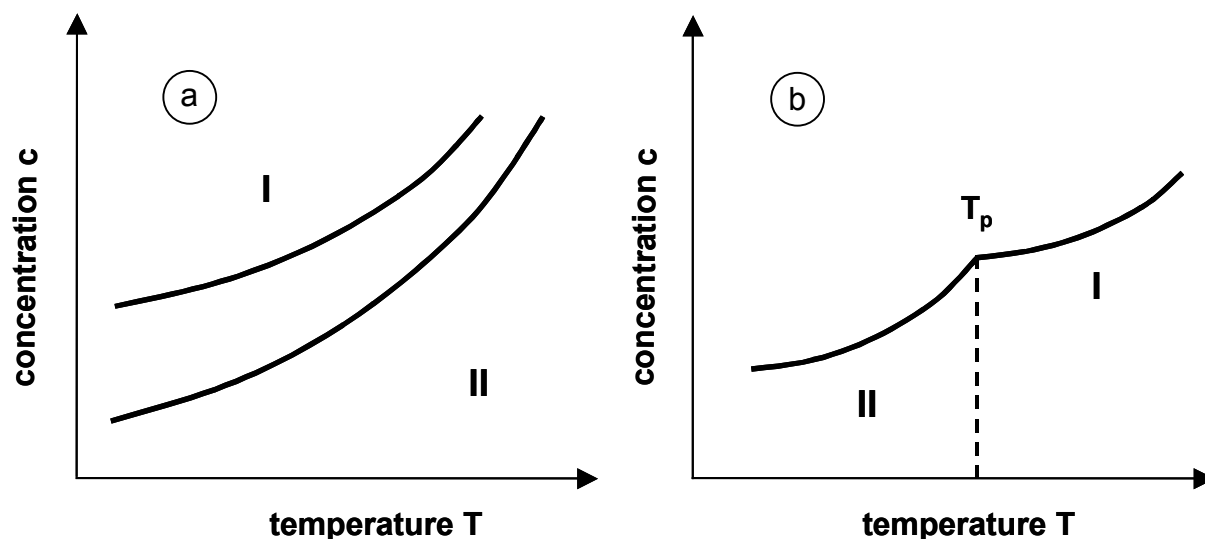
Fig. 2.3-2   Solubility curves exhibiting a) Monotropy, b) Enantiotropy /MUL00/

Typical solubility diagrams for substances that are monotropically or enantiotropically related are shown in *Figure 2.3-2*. In *Figure 2.3-2 a*, form II, having the lower solubility, is more stable than form I. These two non-interconvertible polymorphs are monotropic over the whole temperature range depicted. In *Figure 2.3-2 b*, form II is stable at temperatures below the transition point T_p and form I is stable at temperatures above T_p. The transition temperature is the temperature at which the solubilities of both forms are equal and at which the transformation rate in either direction is zero. However, a reversible transformation between these two enantiotropic forms I and II can be caused by a temperature change /MCC65, MUL00/.

15

At constant conditions of temperature and pressure, the relative stability of a series of polymorphs is determined by their free energies. At a particular temperature the most stable polymorph is always the one with the lowest free energy, the other forms tending to transform into it. This implies that the most stable phase will always be the least soluble, irrespective of the solvent used. At the transition temperature the two polymorphs have identical free energies, and hence, at that temperature, both forms have identical solubilities in any solvent as well as identical vapor pressures. However, it is often observed that the outcome of polymorphic forms can be varied by changing the crystallization solvent. Stearic acid, for instance, is obtained in the monoclinic B-form by slow crystallization from non-polar solvents, while rapid crystallization from polar solvents produces a second monoclinic C-form /DAV82/. Nonetheless, this is the result of kinetic phenomena and it does not imply that a change of solvent changes the order of stability of a polymorphic series. If crystallization of polymorphs is under kinetic control, solvent is important as it can accelerate the formation of one polymorph at the expense of the other. In crystallization processes being under thermodynamic control, the nature of the solvent will be immaterial in respect of the polymorphs produced /BUE51, CAR85, MCC65, THR00/.

Often competing thermodynamic and kinetic factors are governing the crystallization of polymorphs. According to thermodynamics, crystallization must result in an overall decrease in the free energy of the system, meaning in general that the crystal structures that appear will be those having the greater (negative) lattice (free) energies. However, in polymorphic systems there are a number of possible structures that have similar lattice energies. This drive towards free energy minimization will be balanced by the kinetic tendency of the system to crystallize as quickly as possible in order to relieve the imposed supersaturation. If some structures are able to form more quickly than others, then the system may for a certain period of time put up with less than the maximum energy decrease, providing such a situation can be achieved at speed. A further transformation into a lower energy state can take place later /BER02/.

Common representations of phase relationships of polymorphs are the energy versus temperature diagram and the vapor pressure versus temperature diagram, discussed in detail e.g. by /BER02, BUR79/. The combination of experience with polymorphic systems and the accumulation of sufficient thermodynamic and structural data have permitted the development of some useful rules concerning the relative stabilities of polymorphs. The most well-known rules are the heat-of-transition, entropy-of-fusion, enthalpy-of-sublimation, density, infrared, and the heat-capacity rule. More detailed accounts may be found elsewhere /BER99, BUR79/.

2.3.3 Ostwald rule of stages

The Ostwald rule of stages applies to substances that can exist in at least two different modifications. This rule states that an unstable modification does not necessarily transform directly into the most stable state, but into one which leads to the smallest loss in free energy. However, metastable modifications will subsequently transform stepwise to the

most stable crystal structure. The most probable explanation for this phenomenon lies in the kinetics of transformation, the decisive factor being the relative rates of crystal nucleation and growth of the relevant modifications. It is reported that seeding can be used to control the nucleation process and hence aid in the crystallization of a specific modification.

A kinetic versus thermodynamic control can be explained by nucleation theory (see *section 2.1.2*). For the formation of two polymorphs I and II, activation barriers must be overcome. The magnitudes of the activation barriers depend on the surface to volume ratio of the nucleus, because the existence of a phase boundary is associated with an increase in free energy of the system which must be offset by the overall loss of free energy. The nucleus must reach a critical size in order to be stabilized by further growth; the higher the supersaturation the smaller the critical size. If for a particular solution the critical size is lower for the metastable polymorph II, the activation free energy for nucleation is lower and kinetics will favor form II. Ultimately form II will have to transform into the stable form I /BEC03, BER02, BLA98, KLE85, MUL00, MYE02/.

2.3.4 Phase transformations

Due to the kinetics, a transformation of a metastable phase into a more stable phase is not certain even though a system enters a condition that will theoretically allow it. Transformation can only be ensured if a more stable solid phase is already present, is introduced by seeding, or nucleates /MUL00/.

Phase transformations may occur in a dry state, in which the metastable solid undergoes an internal rearrangement of molecules or atoms, as well as in suspension. When crystals are suspended in solution, transformations from one polymorph to another are termed solution-mediated transformations. The contact of the metastable phase with the solvent allows the crystals to dissolve, and the stable phase to nucleate and grow independently from solution /CAR85, MOHN01, MUL00/. Transitions in the solid state are discussed in detail by /BUE51, CAR85/, here only fundamentals of solution-mediated transformations will be presented.

The presence of solvent, even one in which the substance appears insoluble, will speed up the transition between different polymorphs. A large number of publications indicate that solution-mediated phase transformations are readily observed /BEC96, THR95/. Solution-mediated transformations have been reported for NaKGA monohydrate to the anhydrous form in methanol /BECH01/, abecarnil B- to the A-form /BEC96/, phase I and II of a dyestuff /DAV86/, L-glutamic acid α- to the β-form in aqueous solution /DAV97/, dihydroxybenzoic acid form I to form II /DAV02/, glycine β- to the α-form /FER03/, carbamazepine anhydrous form to dihydrate /MUR02/, vaterite to calcite /WEI03/, DL-methionine γ- to the α-form in aqueous solution /YAM02/ and chloropinnoite in boric acid solution /ZHI03/, just to name a few.

Transformations between solid phases in contact with a solvent are governed by the nucleation of the new phase, subsequent growth of the stable phase and dissolution of the metastable phase. However, the nucleation rate should be differentiated from the transformation rate. A transformation may be sluggish either with respect only to nucleation or to both, nucleation and growth. Many metastable systems, once the stable form has nucleated, will transform very rapidly, whereas others do not. Systems of polymorphs vary considerably in this respect, and the rates of nucleation and transformation usually depend as much on temperature, particle size, purity, and physical agitation as on the nature of the structural change involved /MCC65/.

The kinetics of a transformation are determined by the relative rates of dissolution and growth of the two phases and therewith depend on the solubility of each polymorph at that temperature, the rates of dissolution, and the diffusion rate of the molecules in solution. The transformation rate is higher the higher the solubility and the greater the difference in solubilities of the two phases. The overall rate is zero at the transition point, but increases both as the temperature rises and falls. However, as the temperature falls further, two factors cause the transformation rate to decrease again. On the one hand, the solubilities of both forms decrease, thus lowering the concentration in solution, and on the other hand, the viscosity of the solution increases. Both factors decrease the diffusion rate of the molecules in solution and lower the transformation rate. The transformation rate can be increased by agitation of the suspension, by using finely divided crystals, and by adding seed crystals of the stable form /BEC00, BEC03, BOI88, DAV82, DAV86, HAL75, MCC65/.

In some cases, however, transport phenomena play only a negligible role in phase transformations. For instance, the transformation kinetics of abecarnil in isopropyl acetate have been reported to be nearly independent of the slurry density and the agitation of the system. Photomicrographs of the crystals suggest that the transition follows a contact model type for transition, which describes the transformation to occur by nucleation of the new phase on the parent crystals and to proceed via the contact interface between both phases. Epitactic relationships between the new stable phase and the old metastable phase onto which it grows have also been reported by other authors /BEC96, BOI88/.

Nývlt /NYV97/ discussed the kinetics of solution-mediated phase transformations at three different conditions: If the starting point lies within the metastable zone of the stable phase, either above and below the transition point, the transformation starts only after a certain induction period. In the case when the starting point is situated outside the metastable zone of the stable phase, the transformation proceeds spontaneously /NYV97/.

Controlling factors in crystallization of polymorphs are supersaturation, temperature level, fluid dynamics, mixing rate of reactant solutions, and seed crystals (surface, size, history) as primary factors. Secondary factors are solvent, purity and additives, solid-liquid interface, pH and host-guest composition of a clathrate compound /BEC01, KIT02, KON02/.

Recently a method to grow crystals on a plurality of polymers has been presented for obtaining desired polymorphs and for generating previously unidentified polymorphs. By means of this method a novel polymorph of carbamazepine has been discovered /MAT03/.

Comprehensive information about (pseudo-) polymorphism including for instance methods to study polymorphism, phase transformations and applications of polymorphism in the pharmaceutical industry is given e.g. in /BRI99, HAL69, HAL75, KHA95, MCC65, THR95, VER66/.

2.4   Additives

The presence of impurities, synthesis by-products, and corrosion products can influence industrial crystallization processes, negating improvements that can be made using operating parameters such as temperature level, supersaturation, and residence time. At low impurity concentrations, an increase in supersaturation and metastable zone width compensates for a growth rate reduction and crystals even larger than in the pure system can be grown. However, at high impurity concentrations and increasing surface coverage of the crystals, supersaturation rises faster than the metastable zone width, causing increased nucleation rates and a higher fines content in the product. According to Rauls et al. /RAU00/, the optimum concentration of impurities depends strongly on the system, but may vary typically between 1-1000 µm.

Some impurities can exert an influence at concentrations less than 1 ppm, whereas others need to be present in fairly large amounts before having any effect. Even in so-called pure solutions the impurity levels are usually well within detectable limits and also instances are common, where properties are affected by impurities present in amounts below the usual analytical level /EGL63, KLU93, MUL00/.

2.4.1   Different kinds of additives

Additives may be soluble or insoluble, the effects of both kinds of additives being not completely predictable. Soluble impurities may for instance change the equilibrium solubility or the solution structure, the adsorption or chemisorption on nuclei or heteronuclei, and the chemical reaction or complex formation in the solution. For crystal growth from solution also the solvent can be considered an additive. Another frequently applied type of additive is a solution modifier that presumably changes the viscosity and surface tension of the system. A general distinction is made between metal ions, multifunctional and tailor-made additives /EGL63, MUL00, STE90/.

Metal ions are of considerable importance in crystallization, especially in aqueous systems. Commonly occurring ionic impurities, such as Cr^{3+}, Al^{3+}, Fe^{3+}, and Pb^{2+} are frequently observed to have a pronounced effect on the growth rate and crystal habit. In any case, the change in the ionic strength of the solution has an effect on the solubility of the crystallizing substance.

Multifunctional additives are capable of forming bonds with cationic species at the crystal-liquid interface. Examples of multifunctional additives are phosphonic acids, polycarboxylic acids, and polysulfonic acids, as well as high molecular weight copolymers with various acidic groups.

Tailor-made additives are designed to interact in very specific ways with selected faces of a particular crystalline phase. These additives contain e.g. chemical groups or moieties that mimic the solute molecule, and are thus readily adsorbed at growth sites on the crystal surface. Subsequent growth processes at the affected sites are disrupted causing a significant growth reduction and enlargement of the affected faces. With properly designed additives, the growth of nuclei of other crystalline phases will not be disturbed /EGL63, KHAM76, KLU93, WEIS03/.

2.4.2 Properties influenced by additives

Impurities, or additives if deliberately brought into the system, can exert an influence on many features of crystallization processes, e.g. on the solubility, nucleation, metastable zone, crystal growth and dissolution, crystal habit, crystal size and CSD, agglomeration, texture of the crystal, inclusions, purity, and polymorphic transformations. The choice of solvent influences solution properties like density, viscosity, and component diffusivities, the solute solubility, as well as the interfacial tension.

It is well known that already traces of additives have dramatic effects on *nucleation* and *crystal growth*. Generally, both is decreased, nucleation as well as the growth rate, but there are some examples known, where an increase is reported. A promotion of nucleation may be achieved by a heterogeneous process that takes places at an interface, thus lowering the activation barrier for nucleation. For example, in the case of microcomponents which can form stable complexes or binary salts with the macrocomponent, very low concentrations of the impurity can accelerate nucleation. On the other hand, small amounts of colloidal substances such as gelatin and of certain surface-active agents are known to suppress nucleation in aqueous solution /HER01, KAR93, KLU93, MUL00, WEIS03/.

Impurities can either suppress or enhance crystal growth entirely, or exert a highly selective effect, acting only on certain crystallographic faces and thus modifying the crystal habit. The growth rate can also change its nature. It has been shown that the growth rate of potassium chloride crystals exhibits a minimum value at the pH-range between 7 and 10, whereas the dissolution rate of potassium chloride in acidic solutions is higher than in alkaline solutions /MOH96a, MUL00/.

The *width of the metastable zone* of potassium sulfate has been measured in the presence of various concentrations of Cr^{3+}-, Cu^{2+}- and Al^{3+}-ions, and it is demonstrated that also the dependence of the metastable zone width on the impurity concentration in some cases changes its nature. Low concentrations of some impurities make the metastable zone narrower, whereas the metastable zone is broadened if these impurities are present in higher concentrations /KAR93/.

Often additives have *multiple effects*. The study of the influence of Al^{3+}, Cu^{2+}, Fe^{2+}, Mg^{2+}, Mn^{2+}, Na^+ and urea on the crystallization of ammonium sulfate showed that these additives broaden the metastable zone, and change the nucleation rate. Furthermore, the overall growth rate is affected as well as the growth rate of individual faces and in this way the habit of the ammonium sulfate crystals is changed /NYV99, RAU00/.

A change of the solvent used or the presence of an impurity may alter the *habit* of the crystal. Impurities or solvents that adsorb or interact with certain crystallographic faces slow down the growth rate of theses faces and can therewith increase their relative area. The effect of impurities is frequently employed in practice for altering the crystal habit. For instance, the habit can be changed from needle-like to a more compact form in order to have a more efficient filterability /EGL63, KLU93, KOH63, MYE02/.

In *Figure 2.4-1* the pronounced effect of Pb^{2+}-ions on the habit of potassium chloride crystals is shown. Single steps of the transformation of the crystal habit from cubic to octahedron are shown in *Figure 2.4-1 a*, whereas in *Figure 2.4-1 b* truncated octahedrons at different stages can be seen /ULR02/.
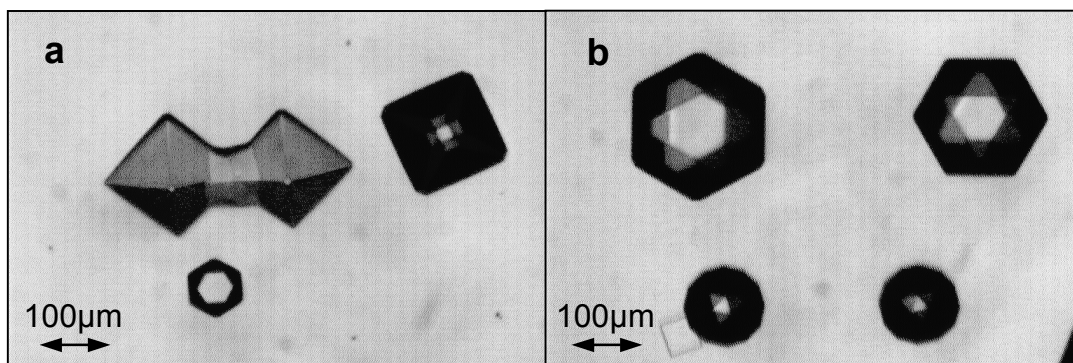
Fig. 2.4-1   Influence of Pb^{2+}-ions on the habit of KCl crystals /ULR02/

A comprehensive study of the influence of additives on the crystal habit is given by Buckley /BUC58/. Examples especially dealing with the effect of solvent on crystal growth and habit can be found elsewhere /DAV82, LAH01/. For a large number of admixtures, Nývlt and Ulrich /NYV95/ published a qualitative description of their effect on nucleation, crystal growth, crystal habit, crystal size and crystal size distribution.

2.4.3   Influence on (pseudo-)polymorphism

Transformation kinetics can significantly change when impurities are present in the system. The rate of transformation can be affected by introducing specific additives that act as inhibitors, retarding the nucleation of the new phase, the rate of dissolution of the less stable phase, and the growth of crystals of the stable phase. Already amounts on the ppm-level can have a pronounced influence on the kinetics of solution-mediated phase transformations. However, compared to other applications, the use of additives to control

the crystallization of polymorphs is a recent development /BEC00, BEC03, HAL75, HE01, MOHN01, MUL00/.

There are many examples for transformation-retardation agents, only a few of which are described here. For instance, the B-to-A transition of abecarnil can considerably be hindered by the presence of trace amounts of triethylamin hydrochloride and hydrochloric acid /BEC96/. The hydration of calcium sulfate hemihydrate to gypsum can be avoided by the addition of sodium polyacrylate, because the additive can block the heterogeneous and homogeneous gypsum nucleation /BOIV00/. Trimesic and transglutaconic acids are able to kinetically stabilize the metastable α-form of L-glutamic acid in aqueous solution /DAV97/. By isomorphic additives a stabilization of a metastable polymorph of 4-Methyl-2-nitroacetanilide can be achieved, and both, the solution and the solid-state transformation rate are reported to decrease /HE01/. On the other hand, additives may also increase the transition rate. The transformation from the thermodynamically unstable vaterite to the stable calcite was accelerated in the presence of polyvinylpyrrolidone. The additive promoted the formation of calcite as well as the rate of the solution-mediated transformation from vaterite to calcite /WEI03/.

Impurities may also influence the outcome of polymorphic forms. From pure aqueous solutions the most stable phase of sulphatiazole, form IV, was isolated. Different concentrations of a reaction by-product, ethamidosulphathiazole, stabilized the metastable modifications form I, II and III, respectively /BLA98/. Further experiments with sulphathiazole revealed that not all of the known polymorphic forms can be crystallized from any given solvent by a variation of the supersaturation. Some solvents selectively favor the crystallization of a particular form or forms. To explain this behavior, a kinetic mechanism is proposed, which assumes that the solvent acts by selective adsorption to certain faces of some of the polymorphs, and thereby either inhibits their nucleation or retards their growth to the advantage of others /KHO93/. Tailor-made inhibitors used for the control of crystal polymorphism must be designed to stereoselectively inhibit the precipitation of an undesired polymorph leaving the required form unaffected. The use of tailor-made additives for the control of crystal polymorphism is described in detail by Weissbuch et al. /WEIS03/. In the case when seeding is applied to obtain a specific polymorph, the purity of the starting material has a pronounced influence on the window of seeding /BEC01/.

2.5 Process control

In order to obtain products by crystallization with predefined properties, it is essential to directly monitor and control the supersaturation and metastability of the system. Without the online control of crystallization processes no desired and reproducible product quality including crystal size, CSD, habit, purity and yield can be ensured. Optimum conditions for crystallization processes can only be accomplished if the metastable zone width and the actual operation point of the crystallizer within this zone is known and controlled during the entire process. This necessitates sensors and control strategies capable of serving this

purpose. The same applies to the crystallization of polymorphs. If a specific polymorphic form is desired, the crystallization process has to be controlled in order to prevent crystallization of an undesired form or a phase transformation /GRO03, ULR02/.

2.5.1   Control of crystallization processes

Almost all conventional methods have disadvantages that become noticeable especially in process control. Specific measuring methods like gas-chromatography, IR- and UV-spectroscopy, play a minor role due to lack of robustness and economic aspects. Gravimetric determinations can easily be realized, however, they are not suitable for online process control because of the large amount of time required. Measuring heat emission can barely be kept under control, because of too many factors exerting influence. One of the most current methods is the measurement of density, but even negligible amounts of gas can alter the result of the measurement. Optical methods, like the measurement of turbidity, depend on the transparency of the medium. Furthermore, the measurement of the refractive index can only be carried out in homogeneous fluids /DIN97/.

In laboratories ATR-FTIR is often applied for the optimization of crystallization processes. With ATR-FTIR the solubility and the metastable zone width can be determined, and it is possible to measure online the supersaturation during batch crystallization processes /DUN97, FEV02, LEW01/. An approach for the determination of the optimum cooling profile without any prior knowledge of kinetic data or subsequent modeling has been proposed. In this study, an ATR-FTIR spectrometer was used to monitor the supersaturation level during batch cooling crystallization of succinic acid and therewith the maximum in the mean crystal size could be obtained /FEN02/. Inline measurements of the concentration with ATR-FTIR spectroscopy helped control the supersaturation during monosodium glutamate batch crystallization. The crystal size and its distribution as well as the habit of the monosodium glutamate crystals were controlled by applying different control strategies such as rapid desupersaturation, constant supersaturation and step-changing supersaturation profiles /BOR02, GRO03/. ATR-FTIR spectroscopy is also used for real-time evaluation of the concentration of impurities during organic batch cooling crystallization. In addition to the determination of the concentration of the main dissolved product, the online measurement of the concentration of one main process impurity is shown to be feasible before the onset of primary nucleation /DER03/. Also Raman spectroscopy is a common method used for the control of crystallization processes. For instance, fiber optic Raman spectroscopy was used for the in situ monitoring of aprotinin supersaturation in hanging-drop crystallization. The crystallizing agent, $(NH_4)_2SO_4$, is Raman active, which allows monitoring the salt concentration in the drop in addition to monitoring the aprotinin concentration /TAM02/.

Often, however, to assure optimum process conditions, two or more measuring methods are combined. For the quantitative analysis of various citrus oils ATR-FTIR and NIR-FT Raman spectroscopy have been applied /SCH02/. Crystallization of paracetamol in aqueous solution has been controlled in situ with ATR-FTIR and laser backscattering. In

this case, the metastable zone width is determined using laser backscattering as well as ATR-FTIR spectroscopy. The solubility curve and in situ solution concentration measurements are determined using ATR-FTIR /FUJ02/. Simultaneous ATR-FTIR and optical turbidometric measurements are used to monitor online the supersaturation and turbidity /GRO01/. Different inline analytical techniques are used simultaneously to facilitate online measurement and control of batch crystallization processes of monosodium glutamate. The measuring techniques include ATR-FTIR spectroscopy for supersaturation, ultrasonic spectroscopy for crystal size, x-ray diffraction for polymorphic form and particle perfection, and optical turbidometric measurements for metastable zone width /LAI02/.

2.5.2 Monitoring of polymorphs

For the control of the outcome of specific polymorphic forms, different measuring techniques can be applied. For instance, a Raman technique has been developed being capable of determining the relative concentrations of the polymorphic forms A, B and C of a pharmaceutical compound in real-time. This enables the acquirement of a robust process for the production of the desired metastable form B /HIL03/. The monitoring of crystallization experiments of highly concentrated aqueous citric acid solutions with a combination of online XRD and ATR-FTIR, revealed that under the applied conditions the anhydrate was formed /GRO01/. The crystallization of a pharmaceutical active ingredient, which exhibits three polymorphic phases, has been monitored using in situ ATR-FTIR spectroscopy coupled with in situ image acquisition. The ATR-FTIR spectroscopy is used to follow the solute concentration, whereas different polymorphic modifications can be clearly identified by use of in situ image acquisition and analysis /BOU02/. The same kind of control can be obtained by use of laser backscattering combined with a video-probe /NIEN02/. Ultrasonic attenuation spectroscopy was successfully applied for in-situ determination of particle size during the crystallization of ʟ-glutamic acid, which exhibits two polymorphic forms, α- and β-ʟ-glutamic acid. Since each polymorph yields a characteristic acoustic attenuation due to the different habits of the two polymorphs, data on particle size can be obtained. However, it was found that ultrasonic attenuation measurements were less sensitive than turbidometric measurements for the determination of the onset of crystallization /MOU02/. Second harmonic generation can be used in situ to monitor polymorph formation and transformation because each polymorph has a different second harmonic efficiency. In situ polymorph detection, especially during nucleation stages, is demonstrated for various crystal systems /LEC99/.

Also solution-mediated phase transformations can be monitored with a number of measuring techniques. Via ATR-IR spectroscopy the solubility of enantiomerically pure and racemic mandelic acid is measured, and nucleation and transformation of the racemate are studied /PRO02/. The concentration profile during a solution-mediated transformation of a photographic coupler was determined using an UV-Vis spectrometer /LIN01/. The ATR-FTIR technique is very promising for the monitoring of phase transitions during the crystallization of complex organic molecules, although, for complex polymorphic

systems, the calibration for the concentration measurement was found to be rather tricky /FEV02/. The progress of the transformation of anhydrous calcium sulfate into calcium sulfate dihydrate in aqueous solution was followed either by monitoring the conductivity, or measuring the solution calcium concentration with a calcium ion selective electrode coupled with a calomel reference electrode connected to a pH-meter /KON02/. In situ Raman spectroscopy was used to determine the rate of polymorphic transformation in a pharmaceutical system. It was found that Raman spectroscopy is a useful tool for in situ characterization of complex polymorphic slurry systems, particularly for the determination of transformation rates and elucidation of transformation pathways /STA02/. In situ Raman spectroscopy has been used to demonstrate the solution-mediated polymorphic transformation of progesterone. It has been shown that the appearance of form I progesterone is always proceeded by the formation of form II progesterone. The in situ monitoring capabilities of Raman spectroscopy allowed the definition of the processing parameters required to control the morphology of crystalline progesterone /WAN00/.

2.6 Aim of the present work

Nowadays, a multitude of organic as well as inorganic substances is known to exhibit polymorphism and / or pseudopolymorphism. Substances exhibiting (pseudo)-polymorphism are of particular interest e.g. for the pharmaceutical or the food industry, where it is often advantageous to use a metastable phase due to more advantageous properties. However, since metastable phases tend to successively transform into thermodynamically more stable forms, the possible risk of phase transformations during production, after-treatment and storage has to be considered. Often, kinetics play a more important role than thermodynamics and even if a transformation is thermodynamically probable, it might be kinetically hindered; thus the kinetics eventually determining the onset and the rate of transformation.

In general, solution-mediated phase transformations are more readily observed than transformations in a dry solid state. Many attempts have been undertaken over the years to predict and control solution-mediated phase transformations, all of these approaches being limited to specific substances, either organic or inorganic. With respect to the use of additives, it has been attempted to control the onset and the rate of transformation of (pseudo-) polymorphs, many examples for transformation-retardation agents and only few examples for transformation-acceleration agents being published. Since none of these approaches has a general applicability, the aim of the present work is to further carry out basic research in the field of phase transformations, leading to the following questions:

Is it possible to adequately predict the induction time for phase transformations in a given system?

Is it possible to exert well-aimed influence on the duration of phase transformations with additives?

Is there a general difference between phase transformations of inorganic and organic substances?

3. Experimental

For the studies different experimental set-ups and measuring techniques have been used. In general, samples have been analyzed by optical microscopy. For unequivocal characterization, some samples have also been analyzed by other techniques, such as x-ray diffraction, thermogravimetry or differential scanning calorimetry.

3.1 Ultrasonic measuring technique

The measurement of the ultrasonic velocity belongs to the group of integral measuring methods like density, refractive index, conductivity, viscosity and turbidity. Another group are the direct, specific methods, as e.g. gas and liquid chromatography, IR- / NIR-spectroscopy, UV-spectroscopy or Raman-spectroscopy. Both groups have in common that the target quantity is not identical with the physical measuring quantity, which has to be interrelated to the target quantity. Furthermore, the physical measuring quantities depend on a number of physico-chemical factors:

- chemical constitution of the components in pure substances and mixtures,
- physical state (temperature, pressure),
- composition of more-component systems,
- interaction of the components in more-component systems.

The main difference between the measuring methods is the kind of information that is gathered. With integral methods the result is one single measured value, whereas with the specific methods divers information is obtained. Therefore, with the specific methods several target quantities, e.g. concentrations, can be measured simultaneously. However, these methods cannot be employed without a minimum of mathematical processing. The reverse applies to the integral methods: Only one target quantity can be obtained, but measuring values are directly available, in real time and with a high density of the measured values /DIN03, ZIP00/.

Ultrasound is used in a wide range of commercial applications in the fields of chemistry, physics, biology, medicine and waste treatment. Chemical applications are e.g. degradation of aromatic pollutants, chemical synthesis, sonoelectrochemistry, cleaning, various leather processes etc. /ASH99/. Furthermore, since a long time the measurement of the ultrasonic velocity is used for monitoring the concentration of liquids in many processes in the chemical industry, in the production of food and beverages as well as in the pharmaceutical industry /BAU98, ZIP00/.

In the field of crystallization, high power ultrasound is applied to influence certain features of crystallization processes such as induction time or metastable zone width, nucleation rate, growth rate, crystal size and crystal size distribution /ARA87, LI03, MAS00, MIK02/. On the other hand, ultrasonic probes with low intensity and low energy input can be used

to measure the width of the metastable zone and to determine crystallization kinetics, e.g. desupersaturation curves /KIR98, OMA99, OMA99a, OMA99b, STR99, ULR00, ULR02/.

3.1.1   Ultrasonic probe

The spread velocity of sound waves through fluid media is a physical property like the viscosity of a medium or its refractive index. Since the ultrasonic velocity v in liquids depends on the density ρ and the adiabatic compressibility of the medium β_{ad}, it varies with temperature, concentration and pressure. However, the compressibility of a medium is the determining factor /DIN97/. The dependence between the ultrasonic velocity, density and adiabatic compressibility can be represented by the following equation:

$$v = \sqrt{\frac{1}{\rho\,\beta_{ad}}}$$

(3.1-1)

In *Figure 3.1-1*, the change of density and compressibility with temperature and concentration is shown exemplarily for aqueous magnesium sulfate solutions. Data of the density of the solution is taken from literature /GME53/ and the data of the compressibility is calculated from measurements of the ultrasonic velocity.

In the depicted temperature region, the density decreases with increasing temperature, whereas the compressibility exhibits a turning-point and is first decreasing and then again increasing with increasing temperature (however, due to the large graduation of the compressibility in *Figure 3.1-1* this can hardly be seen). At a constant temperature, the density is in inverse ratio to the compressibility; the density increasing and the compressibility decreasing with increasing concentration.
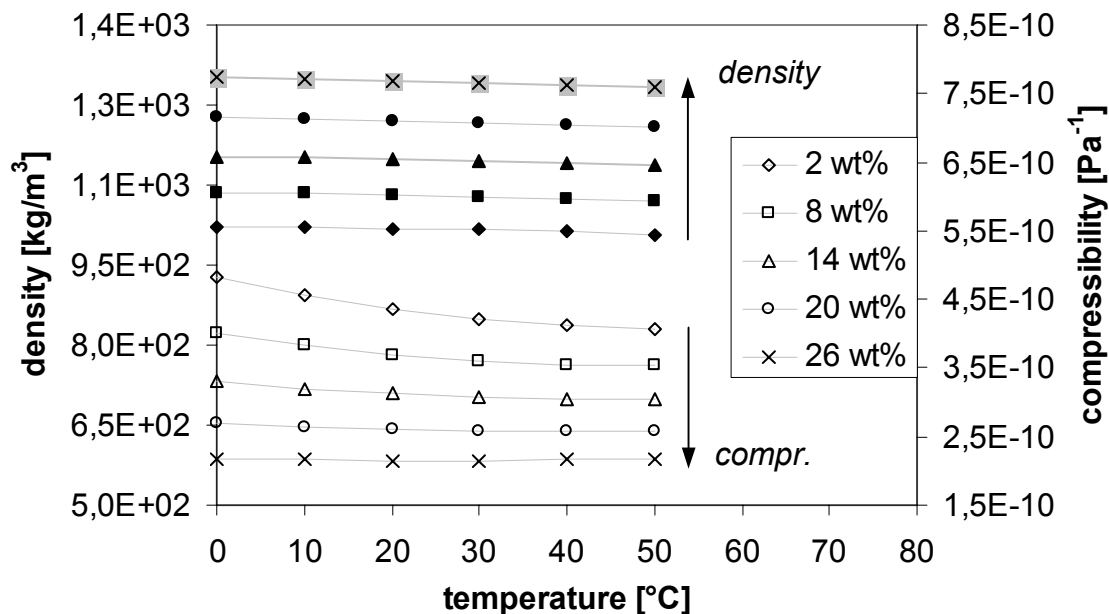
Fig. 3.1-1.   Changes in density and compressibility for magnesium sulfate solutions

In more-component systems, the resulting ultrasonic velocity depends on the ultrasonic velocity of each single component and on the temperature, concentration, pressure and the interaction between the components present in the system /BAU98, DIN97/.

For the experiments an ultrasonic sensor (LiquiSonic lab sensor developed by SensoTech GmbH, Magdeburg, Germany) has been used, which measures simultaneously the ultrasonic velocity and temperature. A more detailed description of the lab sensor is given by /OMA99a, SEN99/. In *Figure 3.1-2* a sketch of the measuring probe is shown.
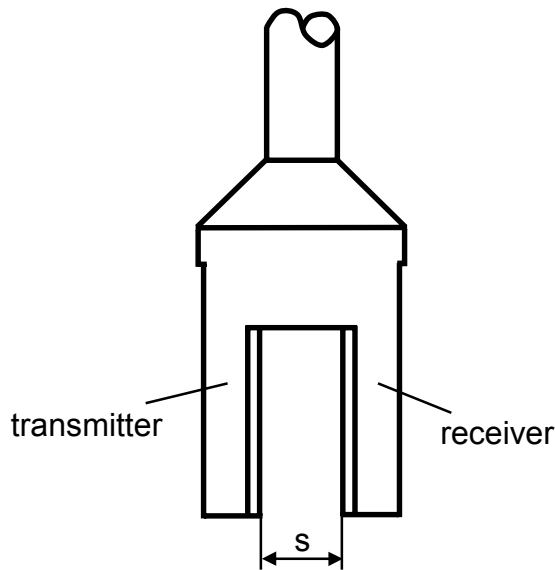
Fig. 3.1-2. Ultrasonic probe

A piezo-transmitter emits an ultrasonic signal at regular intervals. After covering the constant distance *s* between transmitter and receiver, the signal is detected and amplified (see *equation 3.1-2*). The time that the sound signal takes for covering this distance is constantly measured along with the temperature of the sample.

$$v = \frac{s}{t} \tag{3.1-2}$$

A comprehensive description of the use of ultrasound in crystallization is given e.g. by Povey /POV97/.

3.1.2   Suitability for measuring changes in concentration

Prior to the experiments, the suitability of the ultrasonic measuring technique for measuring changes in concentration has been tested. Exemplarily the dependence of the ultrasonic velocity on changes in concentration has been recorded for aqueous magnesium sulfate solutions. Measurements of the ultrasonic velocity in solutions with varying concentrations of magnesium sulfate have been carried out, and each resulting

curve has been correlated. In *Figure 3.1-3* the results of the correlation are shown, having a maximum deviation of ± 0.28 m/s between 0 and 75°C.
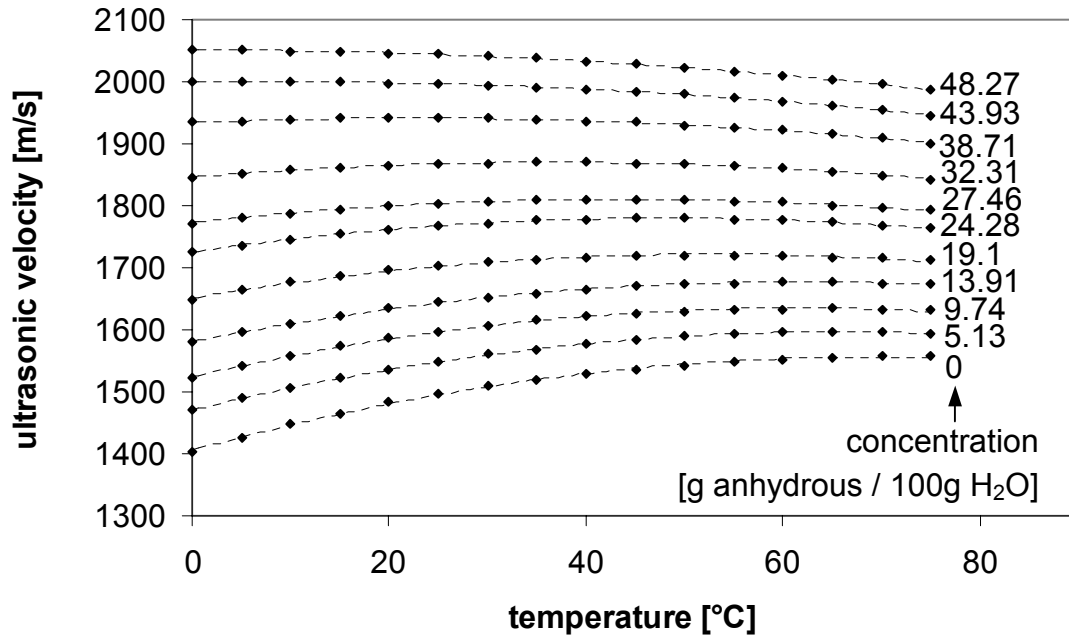
Fig. 3.1-3. Dependence of the ultrasonic velocity on the magnesium sulfate concentration
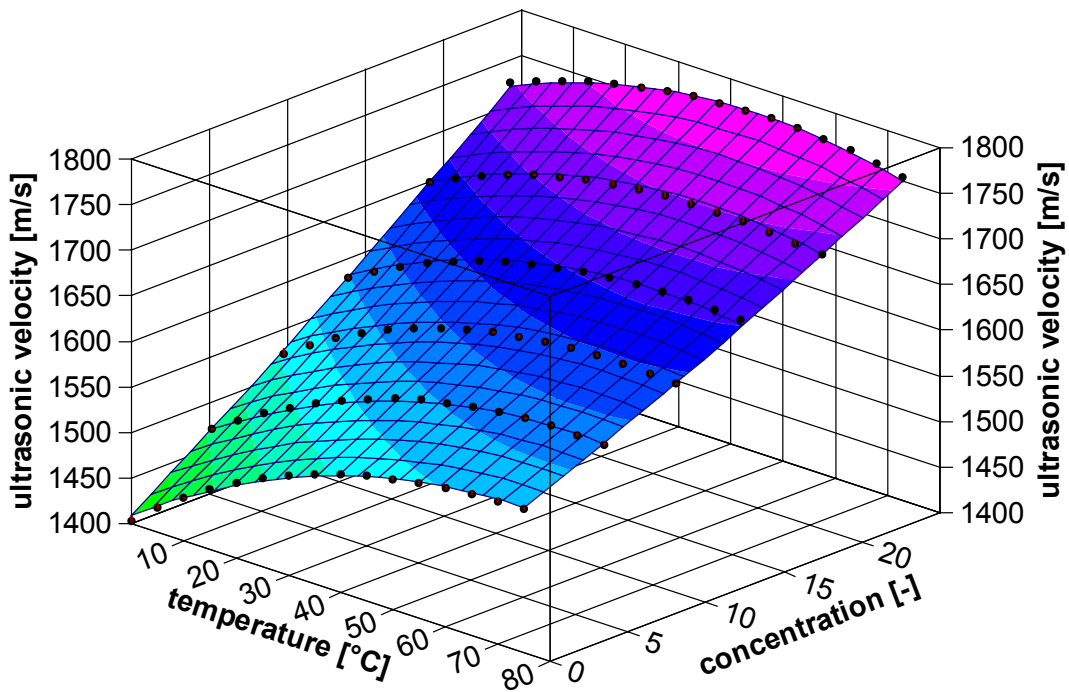
Fig. 3.1-4. Ultrasonic velocity for magnesium sulfate solutions with a concentration up to 25 wt%

From *Figure 3.1-3* it can be seen that the ultrasonic measuring technique responds even to small changes in concentration. Correlating all single measurements results in the graph shown in *Figure 3.1-4*. In this graph, the ultrasonic velocity is depicted as a function of concentration and temperature for concentrations between 0 and 25 wt% magnesium sulfate in a temperature range between 0 and 75°C. The coefficient of multiple determination R^2 is 0.9994, i.e. that 99.94% of the variation in the variables is explained by the model. Exact data about the regression and the model for concentrations from 0 to 25 wt% and from 25 to 48 wt% can be found in the *appendix, section 14.3*.

3.1.3   Monitoring of the experiments
3.1.3.1   Metastable zone

The determination of the metastable zone width was carried out by cooling an unsaturated solution at a constant rate – 10 K / h if not otherwise noted – and thereby moving its state into the metastable region until nucleation occurred. Subsequently, the suspension was heated at the same constant rate until all crystals were dissolved again. By evaluating the response of the ultrasonic velocity during this cycle, the nucleation as well as the saturation temperature can be determined.

In *Figure 3.1-5*, the change in ultrasonic velocity of an aqueous KCl-solution during such a heating / cooling cycle is shown. In the case of KCl, the ultrasonic velocity decreases linearly with decreasing temperature. When nucleation starts, a distinct decrease of the ultrasonic velocity is recorded. By heating the suspension after nucleation, the solid particles dissolve and the ultrasonic velocity increases linearly with temperature. The intersection of the cooling and the heating curve represents the saturation temperature. A detailed description of the use of ultrasound for the determination of the solubility and metastable zone width can be found elsewhere /OMA99, STR99/.
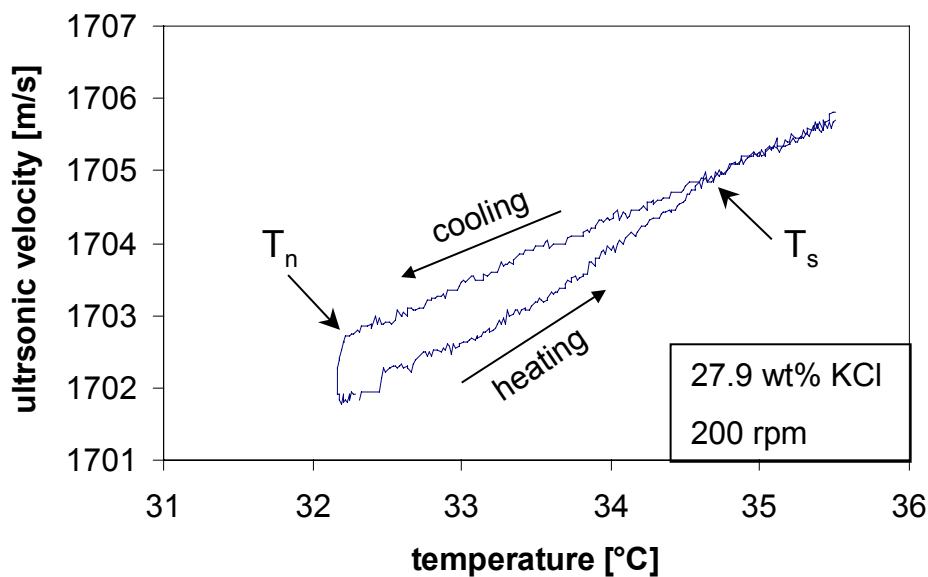

Fig. 3.1-5.   Determination of the metastable zone width by means of the ultrasonic sensor /ULR00/

Each solution was prepared with deionized water. The crystallizer consisted of a 600 ml jacketed glass vessel, which was brought to the desired temperature using a water-operated thermostat. The ultrasonic velocity and temperature were measured online and inline using the submerged LiquiSonic lab sensor. All experiments concerning the metastable zone width have been carried out as illustrated in *Figure 3.1-5*. Additionally, the saturation temperature has been verified optically by the Nývlt polythermal method /NYV85/.

3.1.3.2 Phase transformation

Since the ultrasonic velocity is a temperature and concentration dependent physical property, also phase transformations in solutions can be monitored. The change of the ultrasonic velocity during a phase transformation experiment can be seen in *Figure 3.1-6*. In this case, an experimental result for the transition of $Na_2B_4O_7 \cdot 5H_2O$ to $Na_2B_4O_7 \cdot 10H_2O$ is shown, which will be explained more detailed in *section 8.1 / phase transformations of other substances – borates*.
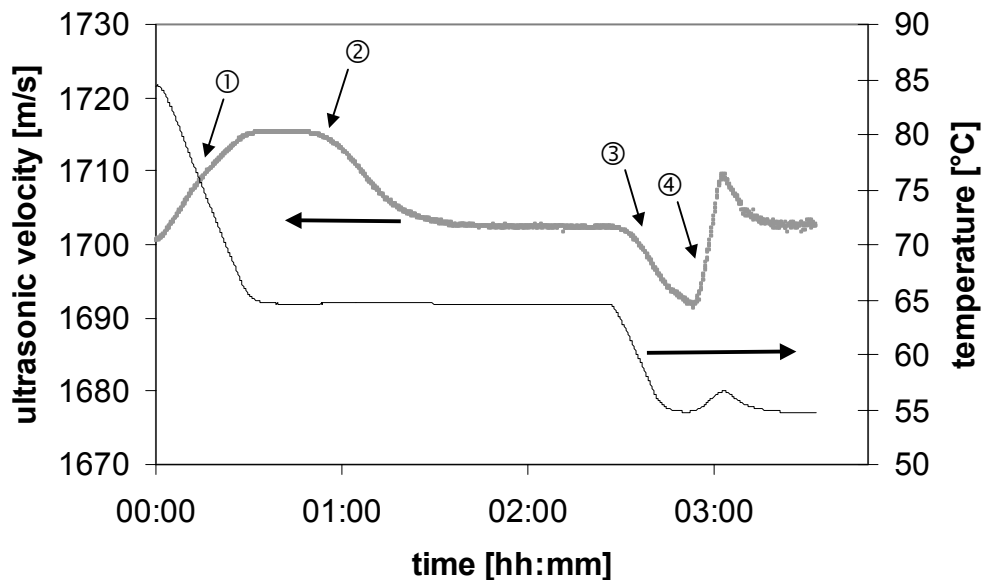
Fig. 3.1-6. Solution-mediated transformation of borate hydrates

The transition point of the penta- and the decahydrate is approximately 60.8°C /SMI02/. For the experiment, a solution - saturated at 75°C - is cooled to 65°C, thus into the metastable zone of the pentahydrate. In *Figure 3.1-6* it can be seen that while the temperature decreases, the ultrasonic velocity increases (1). During nucleation and subsequent growth of the pentahydrate, a distinct decrease of the ultrasonic velocity can be observed (2). When the solution is cooled to 55°C, i.e. below the transition point, the ultrasonic velocity decreases further (3). A temperature peak as well as a sudden increase of the ultrasonic velocity indicate nucleation of the decahydrate (4). Thereupon, growth of the decahydrate and dissolution of the pentahydrate take place simultaneously.

All experiments concerning solution-mediated phase transformations have been carried out in analogous manner: A solution, saturated with respect to the modification stable above the transition point, is prepared. The solution is slightly overheated and then cooled from an unsaturated state into the metastable region of that particular phase. After the supersaturation has been depleted completely by nucleation and subsequent crystal growth, the suspension has been cooled with ca. 20 K/h below the transition temperature. At a specific temperature, the suspension with crystals of the metastable phase is stirred until nucleation of the stable phase starts. The experiment is finished after complete dissolution of the metastable phase.

In all experiments, solutions have been prepared with deionized water and a 600 ml jacketed glass vessel served as crystallizer. Both, ultrasonic velocity and temperature, have been measured online and inline with the ultrasonic sensor during the experiment. The relevant modifications of most of the substances used, can be easily distinguished by optical microscopy due to their different crystal habits. If a visual determination is not unambiguously possible, the crystals have also been analyzed by x-ray diffraction, thermogravimetric analysis and/or differential scanning calorimetry.

3.2 Fluidized bed

According to Mullin /MUL00/ the fluidized bed principle, in which a mass of crystals is suspended in an upward flowing stream of liquor, is a common technique in industrial crystallization.
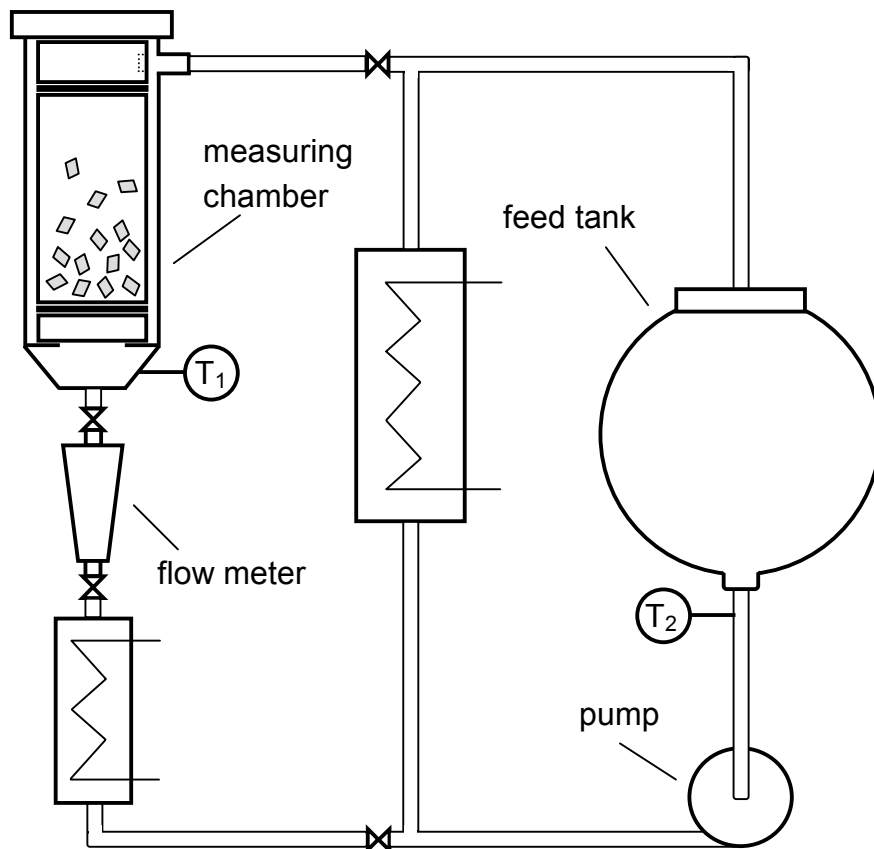
Fig. 3.2-1. Lab-scale fluidized bed

In *Figure 3.2-1*, the set-up of the lab-scale fluidized bed employed for the experiments is schematically shown, having proven to be very suitable and having been developed further over the years e.g. by /ALJ03, KRU93, MOH96, OMA99a, STE90, ULR89/. In this equipment, the solution is pumped from the feed tank into the measuring chamber with a constant flow velocity. Two heat exchangers are necessary to operate the system, one to keep the solution unsaturated and the other one to adjust the temperature of the solution to the desired supersaturation or undersaturation level, respectively. The lab-scale equipment is discussed in detail e.g. by /ALJ03, KRU93, MOH96, OMA99a, STE90, ULR89/.

Saturated solutions – 7 to 10 liters – have been prepared according to the solubility data of Mullin /MUL00/. For each run, 3 g seed crystals with a mean crystal size of 1 mm are filled into the measuring chamber. After 15 minutes the crystals are washed with ethanol, dried at ambient conditions and weight. The difference in weight before and after each run is used to calculate the growth rate.

The mass *m* of a crystal collective is defined as

$$m = k_v \, \rho \, N \, L^3 \tag{3.2-1}$$

with volume shape factor k_v, number of crystals N, density ρ and characteristic length L.

Assuming that during the experiment the volume shape factor, density and number of crystals in the measuring chamber are constant, the following equation can be used to calculate the linear growth rate:

$$G = \frac{L_1}{t} \left[\left(\frac{M_2}{M_1} \right)^{1/3} - 1 \right] \tag{3.2-2}$$

Conditions in the measuring chamber like flow velocity and temperature have to be constant. However, the growth of the seed crystals leads to a change in the relative velocity, i.e. the difference between the flow and the settling velocity. By re-adjusting the flow velocity, the relative velocity and therewith the porosity in the measuring chamber is kept constant during the experiment. Since the amount of crystals is small, it is assumed that the concentration of the solution does not change during growth of the crystals /STE90/.

3.3 Measuring cell

The measuring cell consists of two parts, one holding the solution and the other one serving as a cover. Since both parts are having windows made of glass, the cell can be used under a microscope. During the experiments, a fluid is circulated through both parts,

thereby enabling the adjustment of the temperature inside the cell. A detailed description of the measuring cell can be found e.g. in /MATT99, NIE97, WANN01/.

With the measuring cell the influence of additives on the crystal habit and on the growth rate of crystals has been determined. For each experiment, the temperature at which neither growth nor dissolution of the crystals occurred for at least 30 minutes, has been taken as the saturation temperature.

For the determination of the crystal habit, seed crystals were added to supersaturated solutions and nucleation was induced directly in the cell. After the crystals had grown, pictures were taken with a CCD-camera. The influence of additives on the growth and dissolution rate of crystals was observed by adding seed crystals (125 – 250 μm) to supersaturated or unsaturated solutions, respectively. Pictures were taken with a CCD-camera after periodical time intervals and the length and width of the crystals were measured. The change of the length and width with time was used to calculate the growth rate of the crystals.

3.4   Other measuring and analyzing techniques

In some experiments, the particle size distribution during the course of a phase transformation experiment has been measured. A **p**article **sy**stem **a**nalyzer developed by Meßtechnik Schwartz GmbH (MTS 523 PsyA CSD) equipped with a 3D ORM sensor has been used. This technique enables the determination of particle size distributions in concentration slurries up to 40 vol%. Particle sizes can be measured in the range from 10 to 1000 μm.

This measuring technique employs a highly focused laser beam to measure the particle size distribution in suspension. The laser beam illuminates individual particles in its path and the back-scattered light pulses are detected. By measuring the time that each particle remains in the scanning focal point, the size of the particle can be determined as a random chord length. Further information about this measuring technique is given by /ALL97, LYK01/.

In the following, the applied analyzing techniques are described very briefly. For more detailed information about these techniques, the quoted references should be drawn upon.

✖   TG and DSC

A *Netzsch STA 409* has been used, which combines different analyzing techniques (TG, DSC, Pulse-TA and MS).

Single TG or DSC measurements rarely give sufficient information to permit unequivocal interpretation of the reaction in a particular system. Therefore, alternative thermal methods are best applied simultaneously, providing information of the same sample under identical experimental conditions.

TG is used to measure the amount and rate of weight change in a material, either as a function of increasing temperature, or isothermally as a function of time. It can be used to characterize any material that exhibits a weight change and to detect phase changes due to decomposition, oxidation, or hydration.

DSC is concerned with the measurement of energy changes. The sample and an inert reference material are subjected to a temperature program while the temperature difference between both is monitored. Any temperature difference between the sample and the reference is directly proportional to the corresponding differential heat flow rate. DSC can be used for the study of endothermic or exothermic reactions, such as melting, glass transitions, solid-state transitions, or crystallization /UTS96, WAR01/.

✖   PXRD

Diffractograms have been taken with a *Bruker AXS D 4 Endeavor x-ray diffractometer* (ambient temperature (25°C), step: 0.020, step time: 2s).

X-Ray diffractometry is used for the identification and quantitative determination of crystalline phases within solid and powdered samples. A distinction can be made between two main XRD techniques: In single-crystal diffractometry the x-ray beam is focused onto a single crystal, whereas in powder diffractometry the beam is focused on powder being spread on a sample holder. The diffractogram, which can be considered as the *fingerprint* of a substance, can provide information about the phases present (peak positions), phase concentrations (peak heights), and the amorphous content (background bump) /FRA01, PAU01, WIL88/.

✖   ESEM and EDX[1]

A *Philips ESEM XL 30 FEG* combined with an *energy-dispersive x-ray diffractometer (EDX / EDAX)* has been applied.

EDX is used for the analysis of solids - restricted to areas close to the surface - or for the characterization of thin films. The energy distribution in the radiation emitted by the sample is analyzed by a solid state detector. EDX-spectra are plotted as intensity versus energy, the energies of characteristic K shell transitions of the elements can be found in literature. EDX is often combined with SEM or ESEM. Compared with a conventional SEM, the ESEM offers additional contrast mechanisms, based upon the interaction between gas molecules and electrons /HOP95, KRA01/.

---

[1] An dieser Stelle einen herzlichen Dank an den FB Physik der MLU für die Durchführung der Analysen.

4. Magnesium sulfate

Magnesium sulfate forms various hydrates in aqueous solution. Experiments have been conducted with two phases, the heptahydrate, $MgSO_4 \cdot 7H_2O$, also referred to as epsomite, and the hexahydrate, $MgSO_4 \cdot 6H_2O$, known as hexahydrite. A comprehensive study of the influence of additives on thermodynamics and kinetics of crystallization of magnesium sulfate hydrates is presented. Furthermore, phase transformations in pure and impure solutions have been studied, particularly with regard to induction times in dependence on the purity of the system or temperature, respectively.

4.1 Influence of additives on thermodynamics and kinetics of crystallization

The effect of several additives on the solubility, metastable zone width, growth rate and on the crystal habit has been determined experimentally. For a better basis for discussion, certain additives have been chosen of which the influence on some features of the crystallization process had already been published (see e.g. /KARP84, NYV95/). Furthermore, all additives chosen may occur as solution by-products in actual industrial crystallization processes.

4.1.1 Solubility

Due to the addition of an impurity, the solubility of a given substance my increase, decrease or not change at all within detectable limits. With magnesium sulfate, all three effects mentioned can be observed. The influence of twelve different additives on the solubility is qualitatively illustrated in *Figure 4.1-1*.
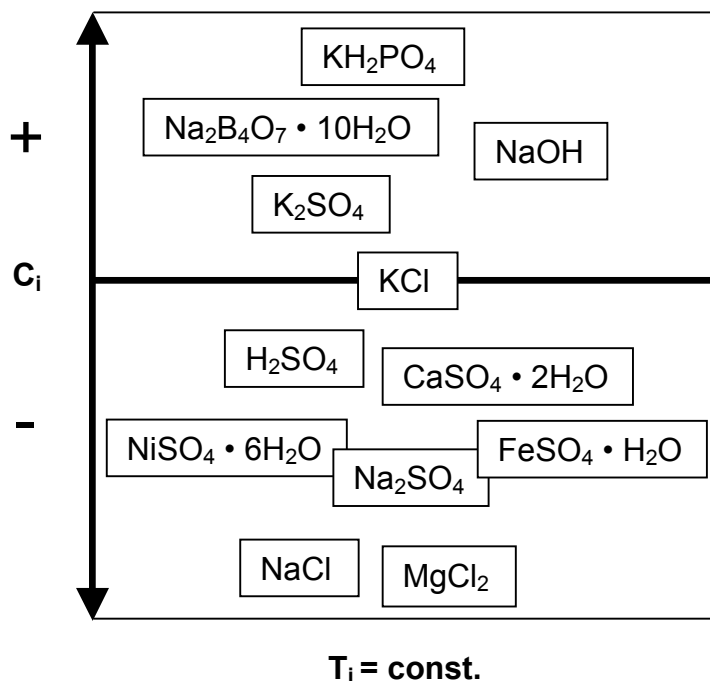
Fig. 4.1-1. Influence of additives on the solubility of epsomite

As can be taken from *Figure 4.1-1*, KCl is the only impurity that does not noticeably influence the solubility of epsomite. Some additives increase the solubility:

KH_2PO_4, K_2SO_4, $Na_2B_4O_7 \cdot 10H_2O$, NaOH

However, most additives lead to a decrease in solubility:

$CaSO_4 \cdot 2H_2O$, $FeSO_4 \cdot H_2O$, H_2SO_4, $MgCl_2$, NaCl, Na_2SO_4, $NiSO_4 \cdot 6H_2O$

Quantitative solubility data can be found in the *appendix / section 14.4* and *14.5*.

4.1.2   Metastable zone width

Additives might also exert an influence on the width of the metastable zone. Many cases of additives widening the metastable zone can be found in literature and only few examples are known in which an impurity decreases the metastable zone width. In *Figure 4.1-2*, the influence of twelve additives on the metastable zone width of magnesium sulfate solutions is illustrated. Since different amounts of additives are used, the respective amount is indicated in each column. The additives are listed in alphabetical order.
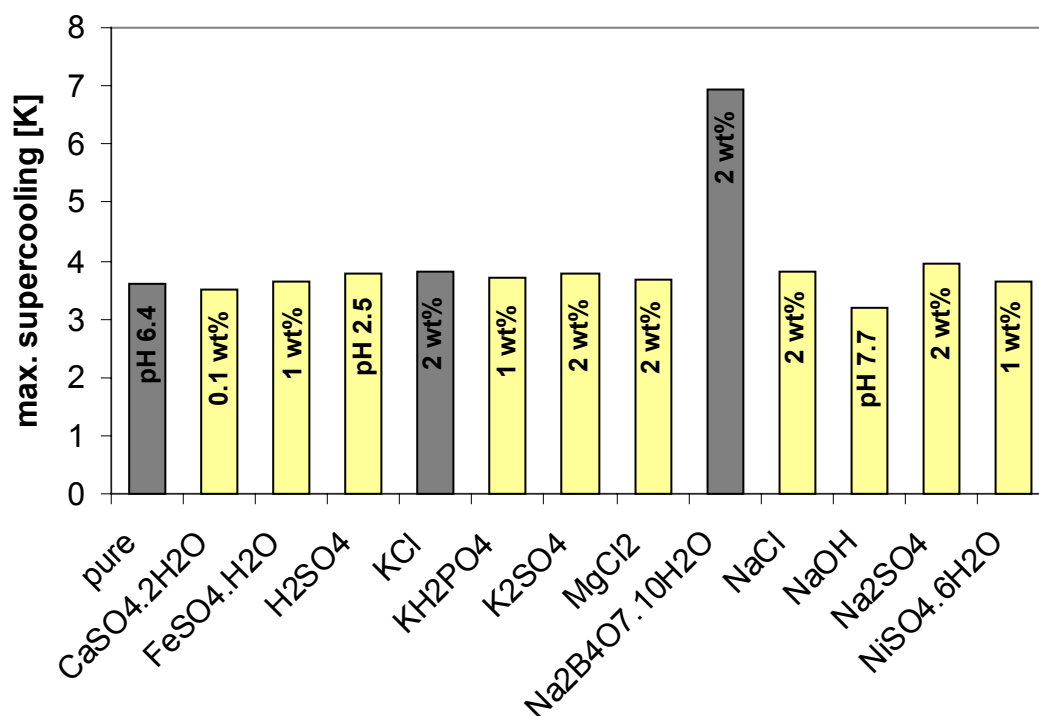
Fig. 4.1-2.   Influence of additives on the metastable zone width

The metastable zone width, or in other words the maximum possible supercooling, can be distinctly influenced by additives (see *Figure 4.1-2*). In *Figure 4.1-2* mean values of five measurements are shown, all of which have been carried out with the ultrasonic measuring technique. Most additives exert only little influence on the metastable zone

width. However, two additives have a pronounced effect: borax ($Na_2B_4O_7 \cdot 10H_2O$) and sodium hydroxide. The addition of borax causes a significant widening of the metastable region, whereas the addition of sodium hydroxide, i.e. the shift of pH into the alkaline region, reduces the maximum possible supercooling.

Comprehensive data on the influence of these additives on the metastable zone width of magnesium sulfate solutions is shown in the *appendix, section 14.6.* In this section, solely further information about the effect of potassium chloride (KCl) and di-sodium tetraborate decahydrate (borax) will be given.
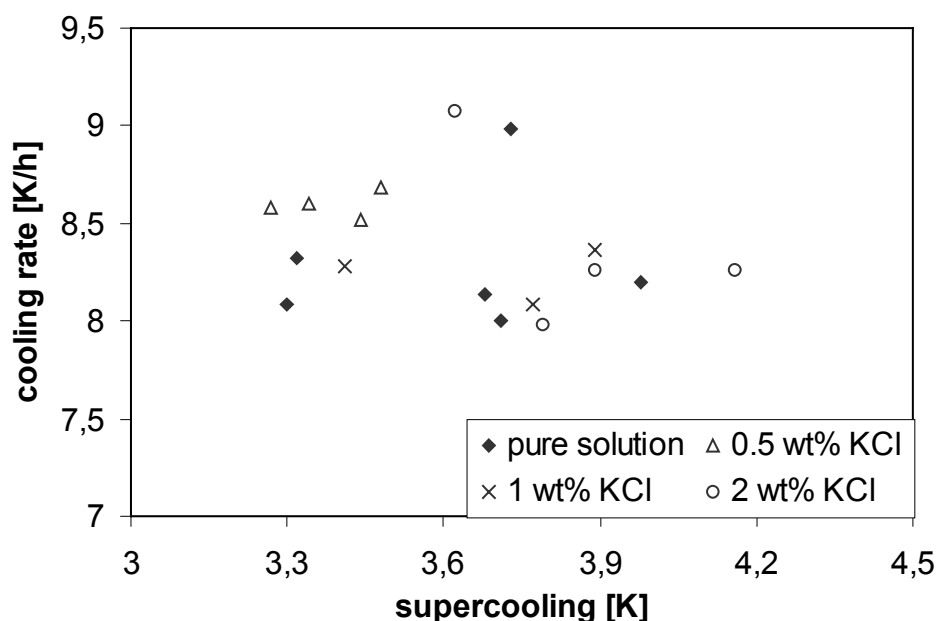
Fig. 4.1-3.   Influence of KCl on the maximum supercooling

The influence of different amounts of KCl on the maximum supercooling is shown in *Figure 4.1-3*. In this diagram the cooling rate – which has been kept constant in all experiments – is depicted above the maximum possible supercooling. Although for all experiments thermostatic baths have been programmed with a cooling rate of 10 K / h, the actual cooling rate ranged from approximately 8 to 9 K / h. Nevertheless, the influence of variations in the cooling rate have been neglected.

For pure magnesium sulfate solutions the maximum possible supercooling varies between 3.3 and 4.0 K. By the addition of KCl no distinct changes in the supercooling-behavior can be observed. Even amounts as high as 2 wt% KCl only have a negligible effect on the temperature at which nucleation takes place. Since the addition of KCl does not change the solubility of epsomite in aqueous solution within detectable limits, no significant effect of this additive on the metastable zone width is detected (see *Figure 4.1-3*).

As already shown in *Figure 4.1-2*, borax distinctly influences the metastable zone width. In the following diagram, *Figure 4.1-4*, the maximum supercooling of aqueous magnesium

sulfate solutions in dependence of the impurity concentration is illustrated. Experiments have been carried out in the same manner as described for KCl and, again, an almost constant cooling rate is employed. The maximum supercooling increases significantly even with additive amounts as low as 0.1 wt%. Experiments have been conducted with additive-concentrations ranging from 0.1 to 5 wt% borax. Up to 5 wt% borax a continuous increase in the width of the metastable zone with increasing additive concentration can be observed.
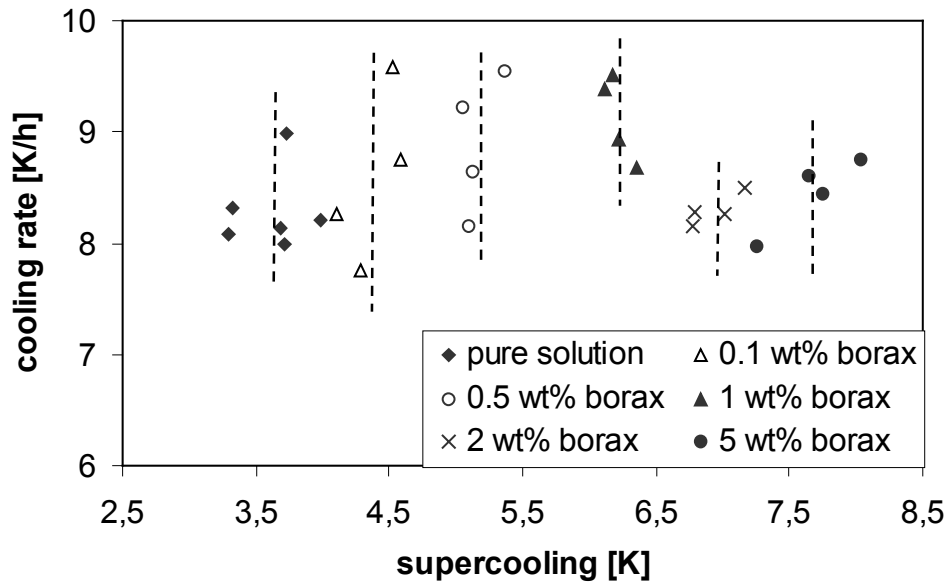
Fig. 4.1-4.   Influence of borax on the maximum supercooling

The influence of borax on the metastable zone width is also illustrated in *Figure 4.1-5*.
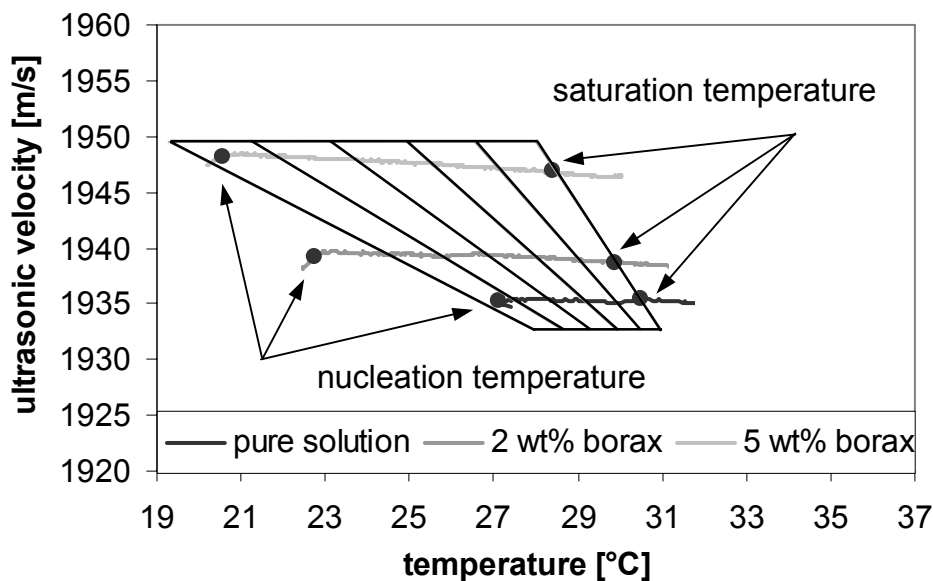
Fig. 4.1-5.   Influence of borax on the metastable zone width

The black line is the result obtained with the ultrasonic measuring technique for a pure magnesium sulfate solution. The medium gray and light gray lines represent results for solutions with 2 and 5 wt% borax, respectively. In each case, the ultrasonic velocity increases almost linearly with temperature. Only when nucleation starts, a sudden decrease of the ultrasonic velocity can be observed. Saturation and nucleation temperatures for each condition are marked with a black dot.

The saturation temperature for pure solutions is 30.5°C. With increasing amount of borax, saturation as well nucleation temperatures are shifted towards lower temperatures. However, the influence of borax on the nucleation temperature is stronger than on the saturation temperature and therefore the metastable zone width broadens. The metastable zone width in dependence on the amount of borax is also emphasized by the striped field (see *Figure 4.1-5*).

In addition, also experiments with varying cooling rates have been carried out with the same additives, KCl and borax. All solutions are saturated at approximately 30.5°C. A comparison between the maximum supercooling in pure and impure solutions in dependence on the cooling rate is presented in *Figure 4.1-6*.
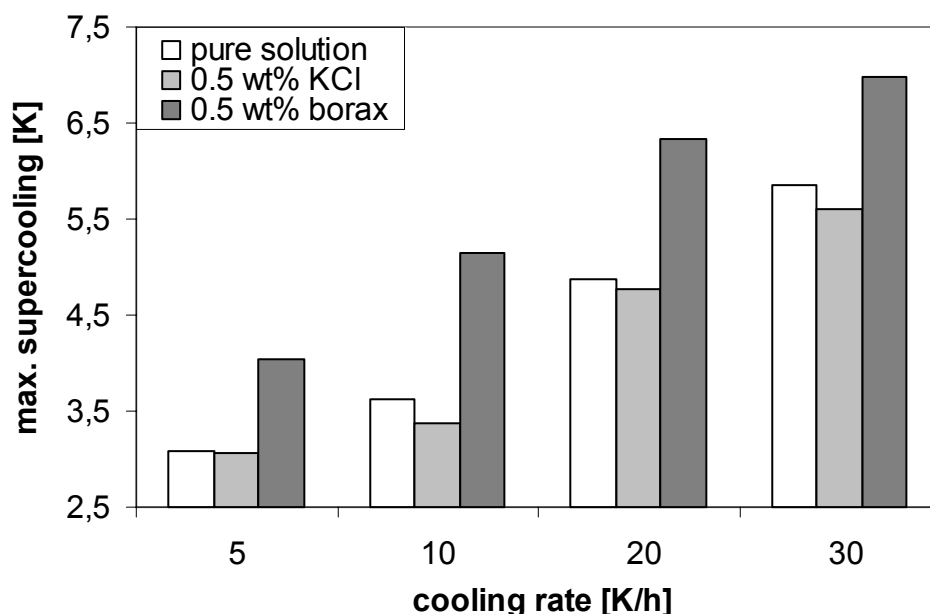
Fig. 4.1-6. Metastable zone width of pure and impure solutions for different cooling rates

Both additives have been used in quantities of 0.5 wt% and mean values of five measurements are taken as basis for the diagram / *Figure 4.1-6*. On an average, solutions with KCl exhibit a slightly smaller metastable zone than pure solutions. In contrast to it, solutions with borax can be supercooled to a larger extent than pure solutions, independent of the cooling rate employed. It is also apparent from *Figure 4.1-6*, that the metastable zone is a function of the cooling rate. The metastable zone broadens with increasing cooling rate, for pure solutions as well as for solutions containing additives.

The metastable zone width for the heptahydrate and the hexahydrate is depicted in *Figure 4.1-7*. It can be seen in *Figure 4.1-7* that the width of the metastable zone is not independent of temperature. The higher the temperature, the smaller the metastable zone width of both hydrates. According to literature /OTT02/, the transition temperature is approximately 48.1°C, indicated by the dotted line in *Figure 4.1-7*. Although the solubility curves are in good agreement with data published in literature /SEI65/ (see *appendix*, *section 14.4*), the experimentally obtained transition temperature is slightly higher, at ca. 50°C.
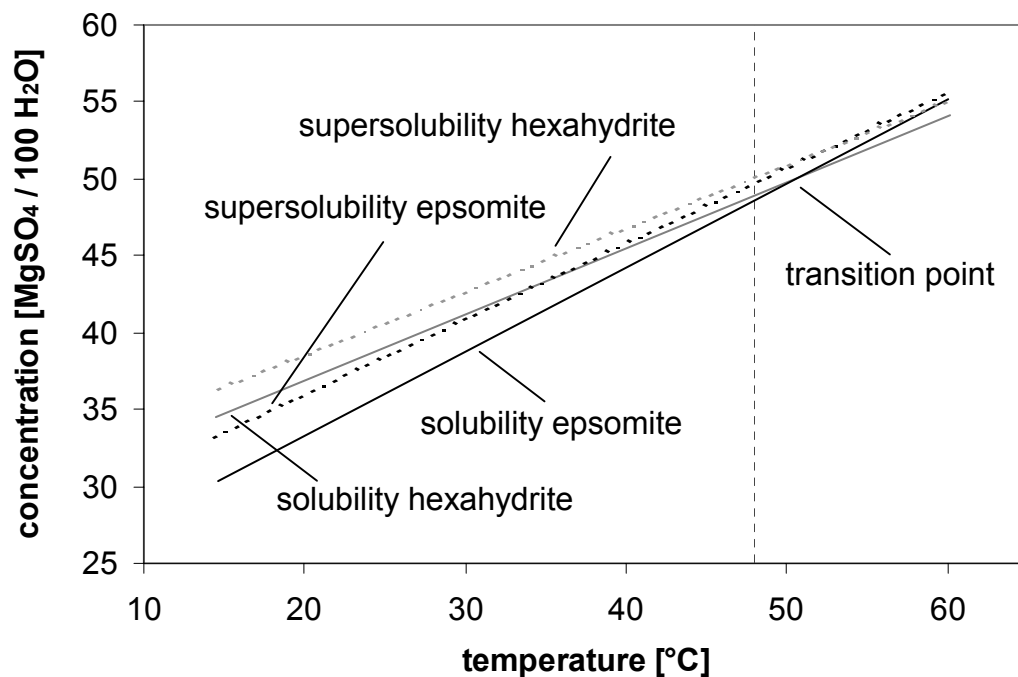
Fig. 4.1-7.   Metastable zone width: epsomite and hexahydrite

The solubility as well as the supersolubility curves for each hydrate can be approximated by linear trendlines, listed in *Table 4.1-1*.

Table 4.1-1.   Solubility and supersolubility of epsomite and hexahydrite

Epsomite	solubility	$c = 0.5471 \cdot T + 22.375$
	supersolubility	$c = 0.4906 \cdot T + 26.179$
Hexahydrite	solubility	$c = 0.4274 \cdot T + 28.358$
	supersolubility	$c = 0.4114 \cdot T + 30.356$

Quantitative data of the solubility and supersolubility of magnesium sulfate hexahydrate and heptahydrate is listed in the *appendix*, *section 14.4*.

4.1.3 Growth rate

Experiments concerning the influence of additives on the growth rate have been carried out in two ways: measurements of single crystals in a microscopic cell, and measurements with populations of crystals in a fluidized bed. Two additives, KCl and borax, have been used. The results from measurements in a fluidized bed are illustrated as the overall growth rate versus the supersaturation ratio. The supersaturation ratio, a common expression of supersaturation /MUL00/, is defined by

$$S = \frac{c}{c*}$$
(4.1-1)

In *Figure 4.1-8*, the growth and dissolution rate of magnesium sulfate heptahydrate crystals are shown. Experiments have been carried out in a fluidized bed, the solution having a saturation temperature of approximately 34°C.
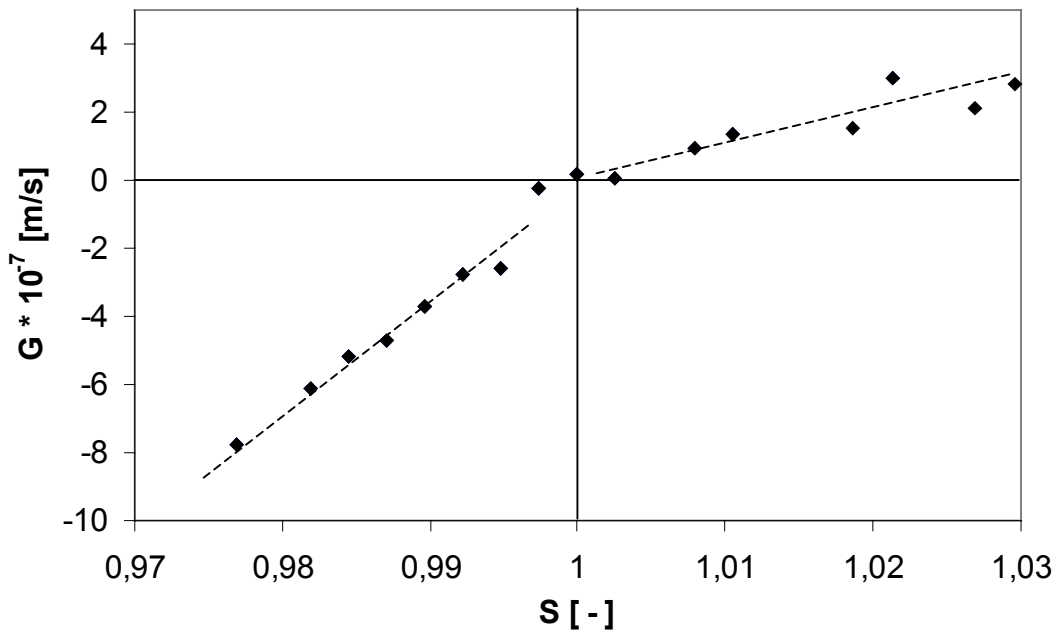
Fig. 4.1-8. Growth rate of magnesium sulfate heptahydrate

It can clearly be seen from *Figure 4.1-8*, that the growth rate is lower than the dissolution rate of the epsomite crystals. At a supersaturation ratio of 1.02 the growth rate is ca. $2 \cdot 10^{-7}$ ms^{-1}, whereas the dissolution rate at a supersaturation ratio of 0.98 is approximately $7 \cdot 10^{-7}$ ms^{-1}.

The influence of KCl on the growth and dissolution rate of epsomite crystals is illustrated in *Figure 4.1-9*. Measurements have been carried out with 1 and 5 wt% KCl, however, the results for the two different additive concentrations show no significant difference. It is obvious from *Figure 4.1-9*, that the dissolution rate of the epsomite crystals is reduced due to the addition of KCl. At a supersaturation ratio of 0.98, an overall dissolution rate of

$5 \cdot 10^{-7}$ ms^{-1} has been measured, in contrast to $7 \cdot 10^{-7}$ ms^{-1} for solutions containing no additive. Regarding the influence of KCl on the growth rate, no clear result is obtained. With both additive concentrations, the growth rate is not distinctly influenced, although the results give the impression that the growth rate slightly increases due to the addition of KCl. When 5 wt% KCl are added to the solution, the saturation temperature is slightly increased (about 0.2 K), i.e. the solubility is decreased. This effect has already been considered in *Figure 4.1-9*, the curve has been shifted to the zero point to show only the kinetic effect.
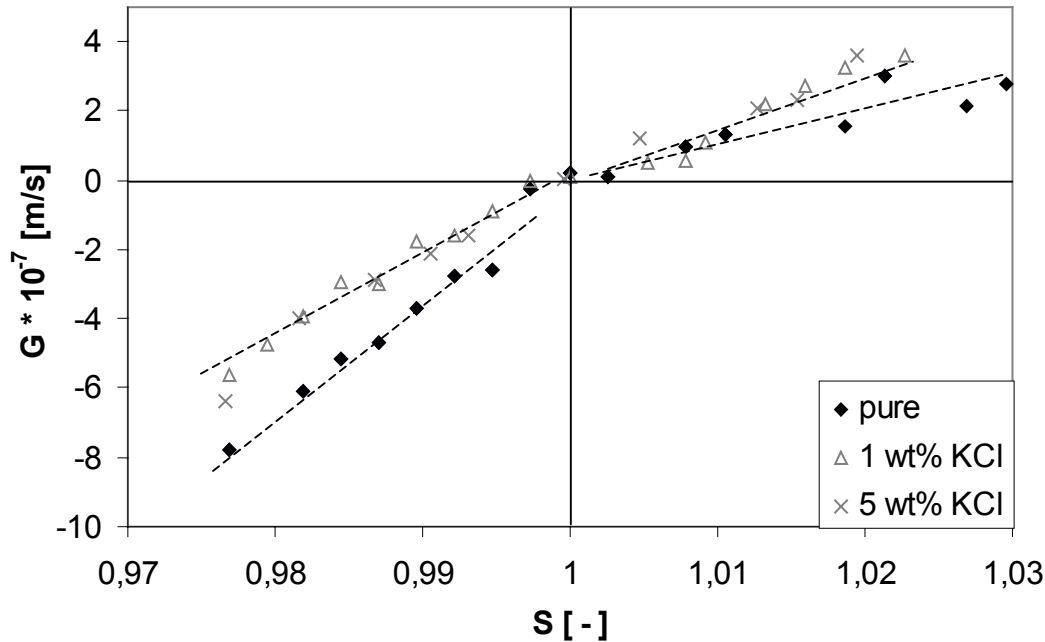
Fig. 4.1-9. Influence of KCl on the growth rate of magnesium sulfate heptahydrate

The influence of borax on the growth rate of epsomite crystals is already known /NYV95/. Therefore, no experiments with borax in the fluidized bed have been conducted. However, in order to find out about the influence of borax on single faces of a crystal, growth rate measurements have been carried out in a microscopic cell. For the same reason, also additional experiments with the additive KCl have been conducted in the microscopic cell.

In all experiments carried out in the microscopic cell, crystals have been measured according to the scheme shown in *Figure 4.1-10*.
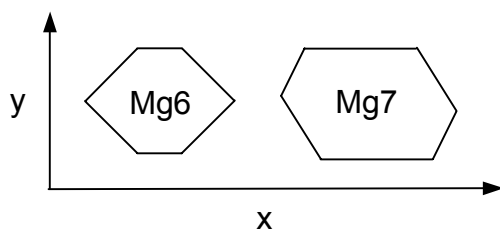
Fig. 4.1-10. Magnesium sulfate hexahydrate (Mg6) and heptahydrate (Mg7) crystals as measured in the microscopic cell

Results of experiments having been conducted in the microscopic cell with both additives, KCl and borax, are shown in *Figure 4.1-11*. The additive concentration amounts to 5 wt% in all experiments, and mean values of crystal growth rates from seven measurements are taken.
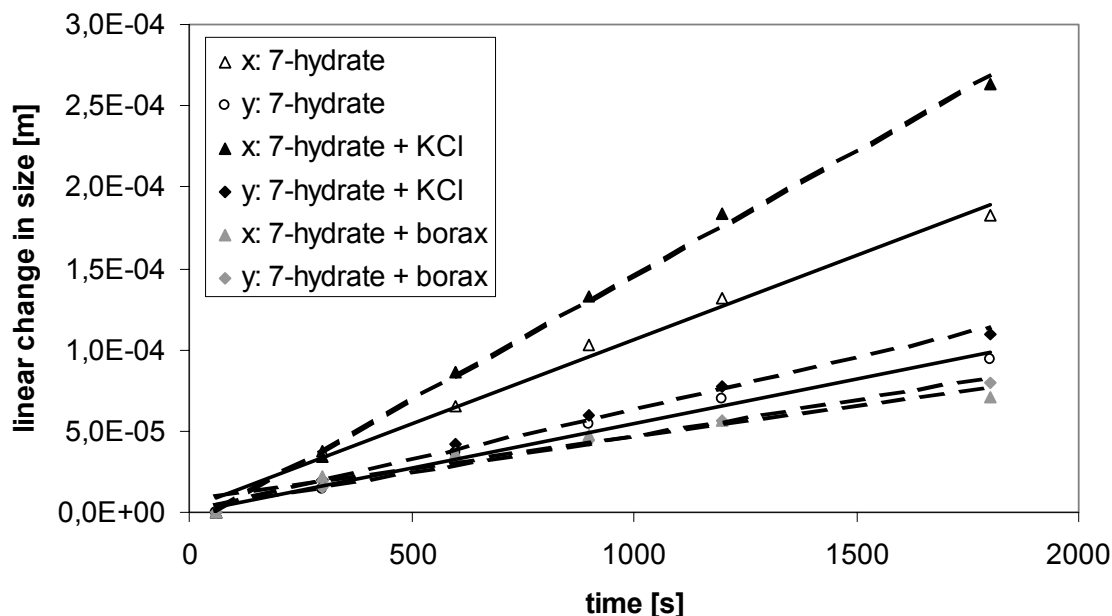
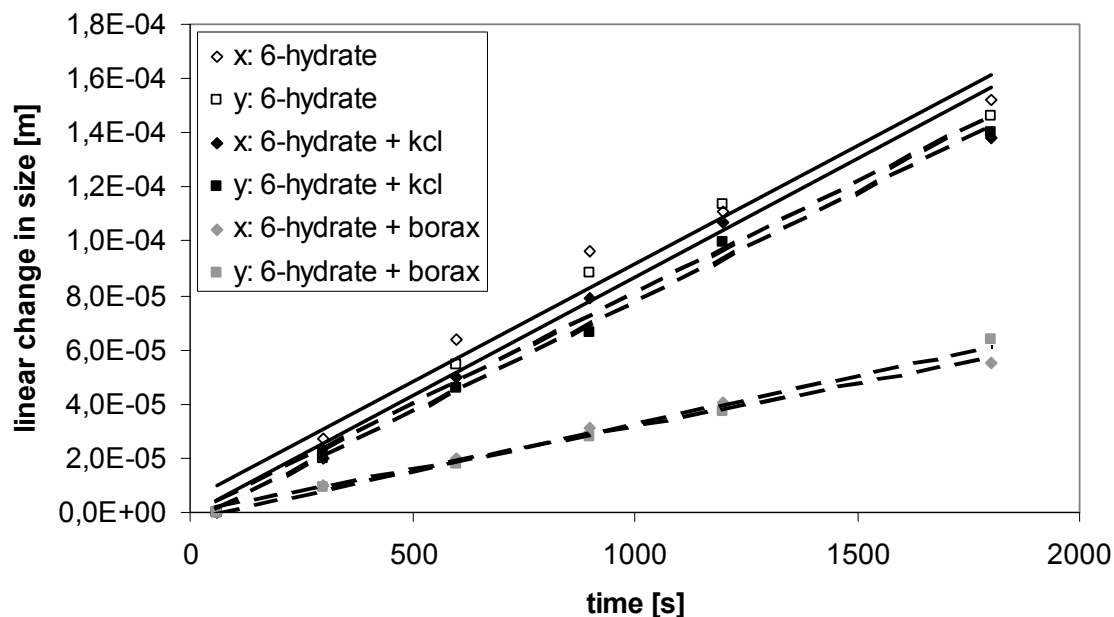**Fig. 4.1-11.** Influence of additives on the growth rate of magnesium sulfate heptahydrate

Experiments from growth rate measurements of single crystals in a microscopic cell show that the linear change in size in both directions increases with KCl, whereas it decreases due to the addition of borax. When borax is added, the growth rate of the epsomite crystals is almost the same in x- and y-direction.

Growth rates for crystals grown in pure solutions and in solutions with the respective additive are depicted in *Table 4.1-2*.

Table 4.1-2.   Growth rates of epsomite crystals in single crystal measurements

Epsomite	x-direction	$1 \cdot 10^{-7}$ ms^{-1}
	y-direction	$5 \cdot 10^{-8}$ ms^{-1}
Epsomite + 5 wt% KCl	x-direction	$2 \cdot 10^{-7}$ ms^{-1}
	y-direction	$6 \cdot 10^{-8}$ ms^{-1}
Epsomite + 5 wt% borax	x-direction	$4 \cdot 10^{-8}$ ms^{-1}
	y-direction	$5 \cdot 10^{-8}$ ms^{-1}

In the microscopic cell also the influence of KCl and borax and the growth rate of the hexahydrite has been measured. Results of these measurements are shown in *Figure 4.1-12*.

Fig. 4.1-12. Influence of additives on the growth rate of magnesium sulfate hexahydrate

In pure solutions, crystals of the hexahydrate grow in the same magnitude in both directions. When KCl is added to the solution, the crystals grow more slowly than in pure solutions. The linear change in size in the presence of KCl is influenced to the same extent in both, the x- and y-direction. Due to the addition of borax, the growth rate is decreased more distinctly. However with borax, the growth rate in the x-direction is reduced stronger than in the y-direction.

Growth rates of the hexahydrite with and without additives are comprised in *Table 4.1-3*.

Table 4.1-3. Growth rates of hexahydrite crystals in single crystal measurements

Hexahydrite	x-direction	$9 \cdot 10^{-8}$ ms^{-1}
	y-direction	$9 \cdot 10^{-8}$ ms^{-1}
Hexahydrite + 5 wt% KCl	x-direction	$8 \cdot 10^{-8}$ ms^{-1}
	y-direction	$8 \cdot 10^{-8}$ ms^{-1}
Hexahydrite + 5 wt% borax	x-direction	$3 \cdot 10^{-8}$ ms^{-1}
	y-direction	$4 \cdot 10^{-8}$ ms^{-}

4.1.4 Crystal habit

The habit of magnesium sulfate heptahydrate, which belongs to the rhombic-disphenoidic class /GME53/, is illustrated in *Figure 4.1-13*. The crystal shown in *Figure 4.1-13 b*, has been grown in a microscopic cell at low supersaturation, and thus, with a relatively slow growth rate. It can be seen from *Figure 4.1-13 b* that the faces of the epsomite crystal are well-developed.
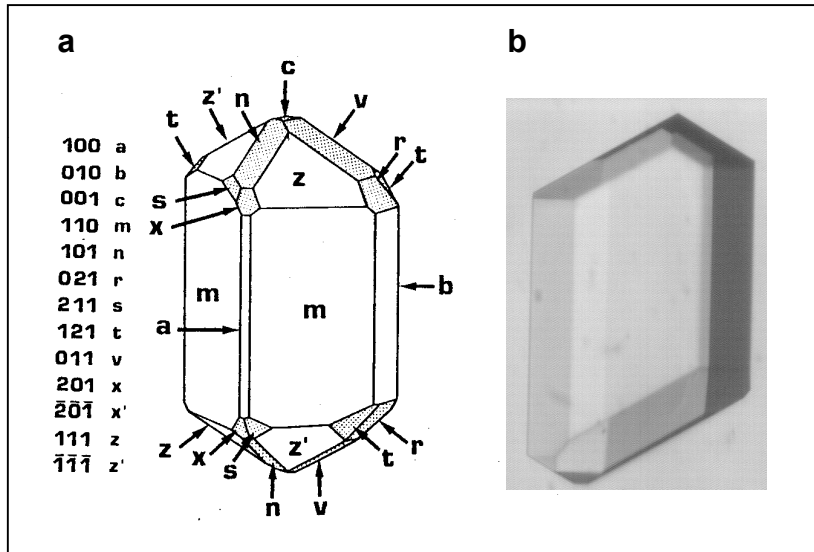
Fig. 4.1-13. Habit of epsomite crystals
a) theory /SGU87/, b) experiment
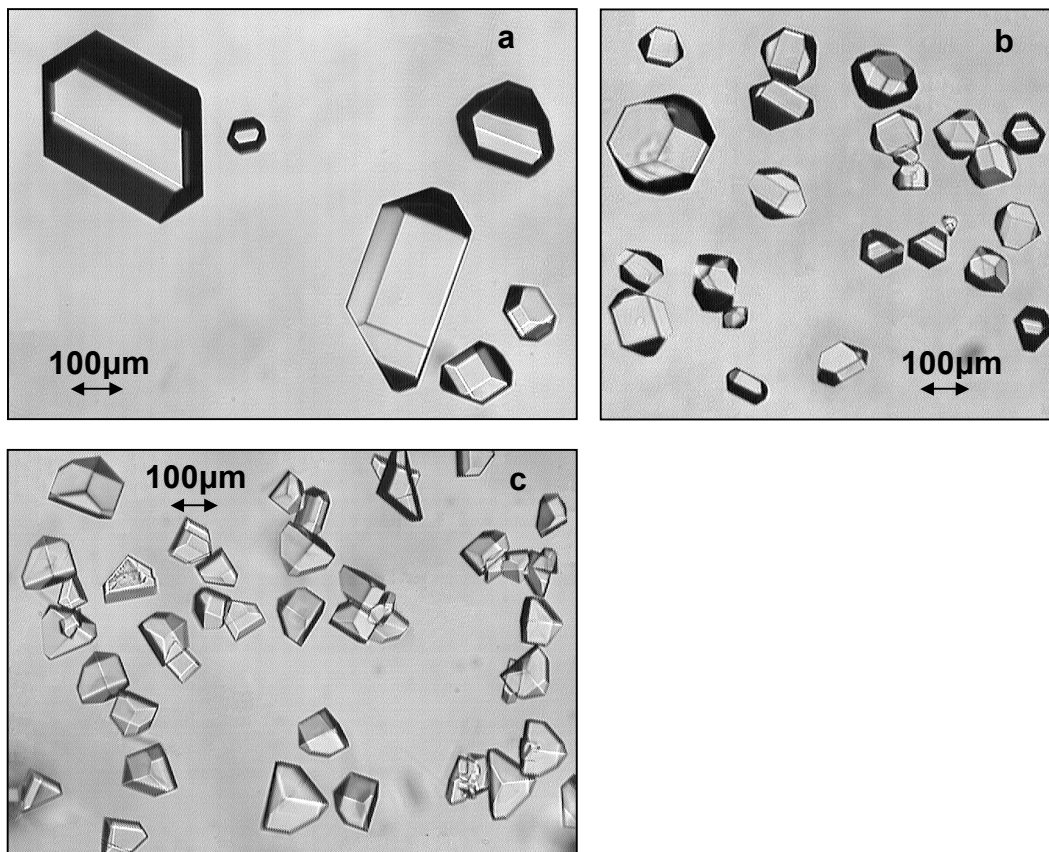
Fig. 4.1-14. Habit of magnesium sulfate heptahydrate crystals
a) without additive, b) with 5 wt% KCl, c) with 5 wt% borax

Comparing both crystals, the resemblance between the epsomite crystal obtained experimentally and the habit known from literature is emphasized (see *Figure 4.1-13)*.

46

Epsomite crystals which are grown in a pure magnesium sulfate solution are shown in *Figure 4.1-14 a*. It is obvious that even crystals grown in pure solutions show differences in their habit. Among crystals having the typical orthorhombic form, also shortened crystals with a higher length to width ratio are grown. In *Figure 4.1-14 b*, the influence of KCl on the habit of epsomite crystals is shown. Due to the addition of KCl, all crystals exhibit a shortened habit compared to the crystals grown in a pure solution. By the addition of borax, this effect is even more pronounced (see *Figure 4.1-14 c*). The epsomite crystals grown in the presence of borax do not have the typical orthorhombic form anymore, but look rather wedge-shaped.
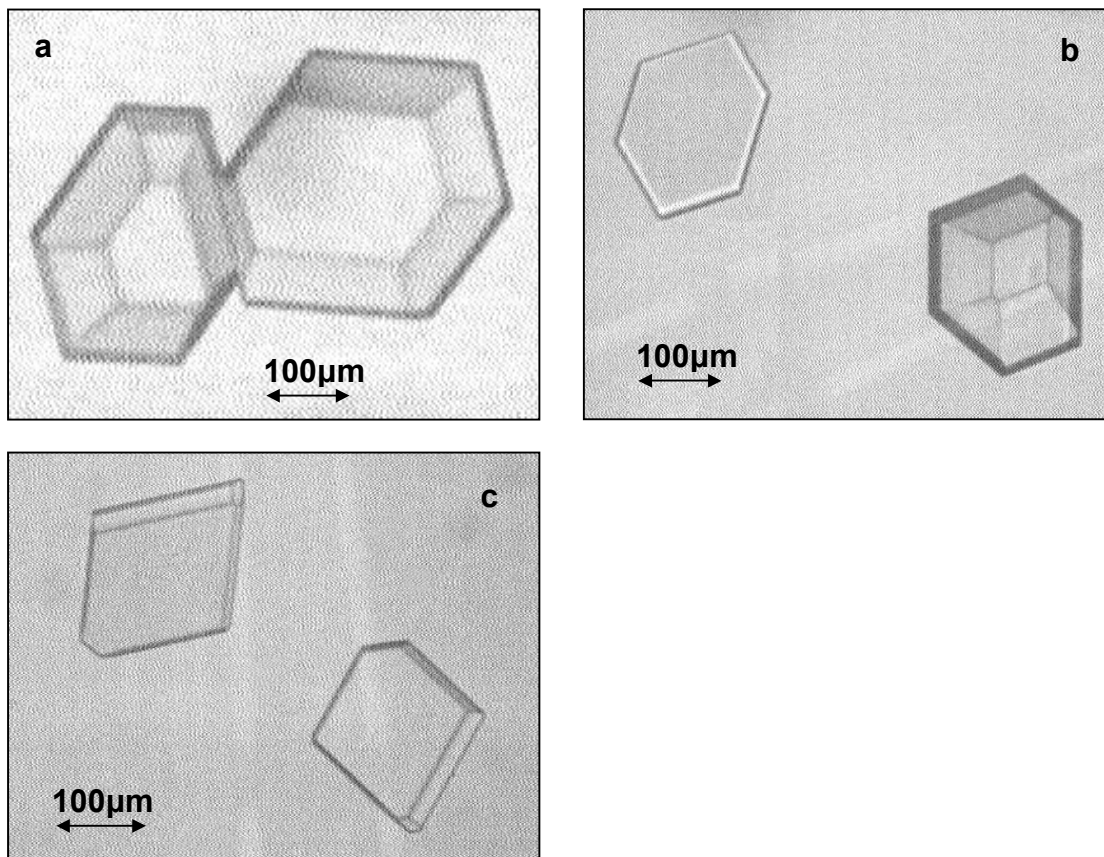
Fig. 4.1-15. Habit of magnesium sulfate hexahydrate crystals
a) without additive, b) with 5 wt% KCl, c) with 5 wt% borax

Both additives influence the habit of the hexahydrite crystals to a similar degree as they influence the habit of the epsomite crystals. In *Figure 4.1-15 a*, crystals of the hexahydrite grown in a pure solution are shown. Compared to the crystals grown without additive, KCl exerts only little influence on the habit whereas borax changes the external form of the hexahydrite more distinctly (see *Figures 4.1-15 b* and *4.1-15 c*). The generally hexagonal habit of the hexahydrite crystals is changed to an almost rhombic habit due to the addition of borax.
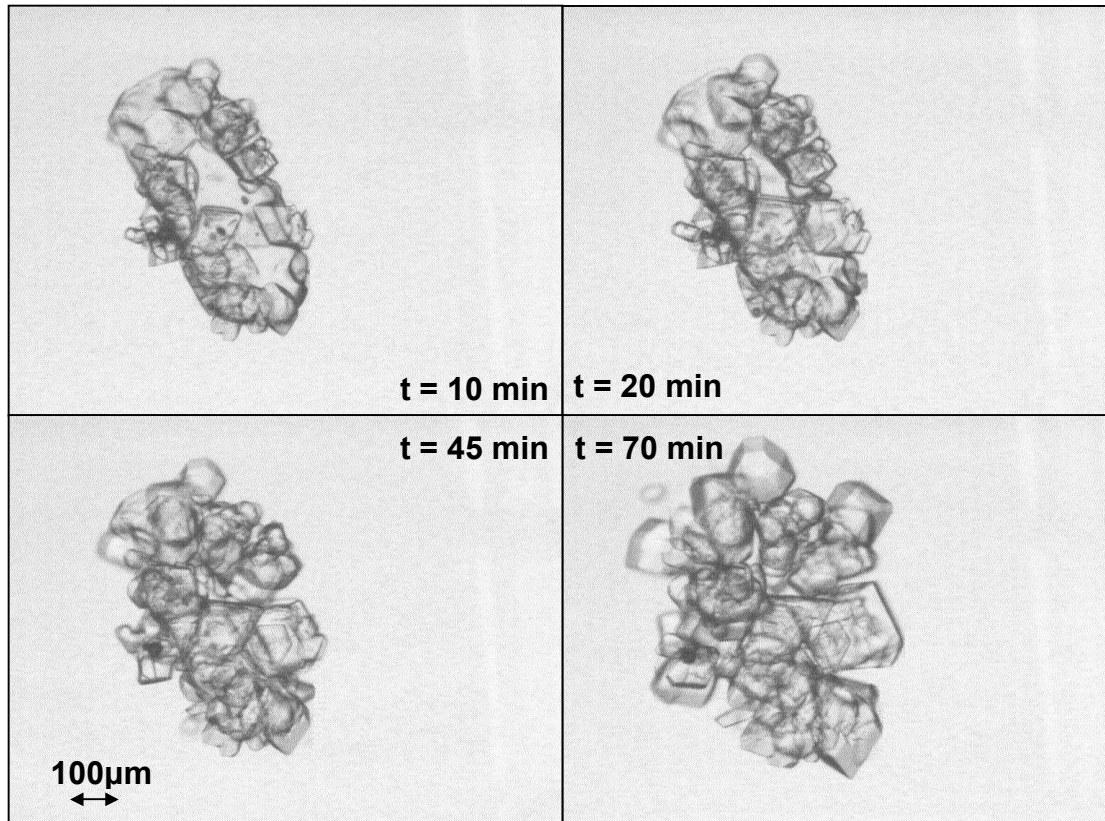
4.2 Phase transformation

The transition temperature between magnesium sulfate heptahydrate and hexahydrate is approximately 48.1°C /OTT02/. Above the transition point, the hexahydrate is the stable phase and the heptahydrate is metastable, below this point the opposite applies.

Phase transformations of magnesium sulfate heptahydrate to the hexahydrate and in reverse order have been observed in a microscopic cell. For the transformation of the hexahydrate to the heptahydrate, solutions have been prepared being saturated at ca. 30.5°C. During the experiment, the solution is slightly supersaturated with regard to the heptahydrate. A seed crystal of the hexahydrate, without special prior treatment, is added to the solution. The course of the transformation is illustrated in *Figure 4.2-1*. It can be seen that the crystal of the metastable hexahydrate gradually dissolves while the stable heptahydrate nucleates and grows onto the dissolving crystal of the hexahydrate.

t = 10 min t = 45 min
t = 65 min t = 110 min
100µm
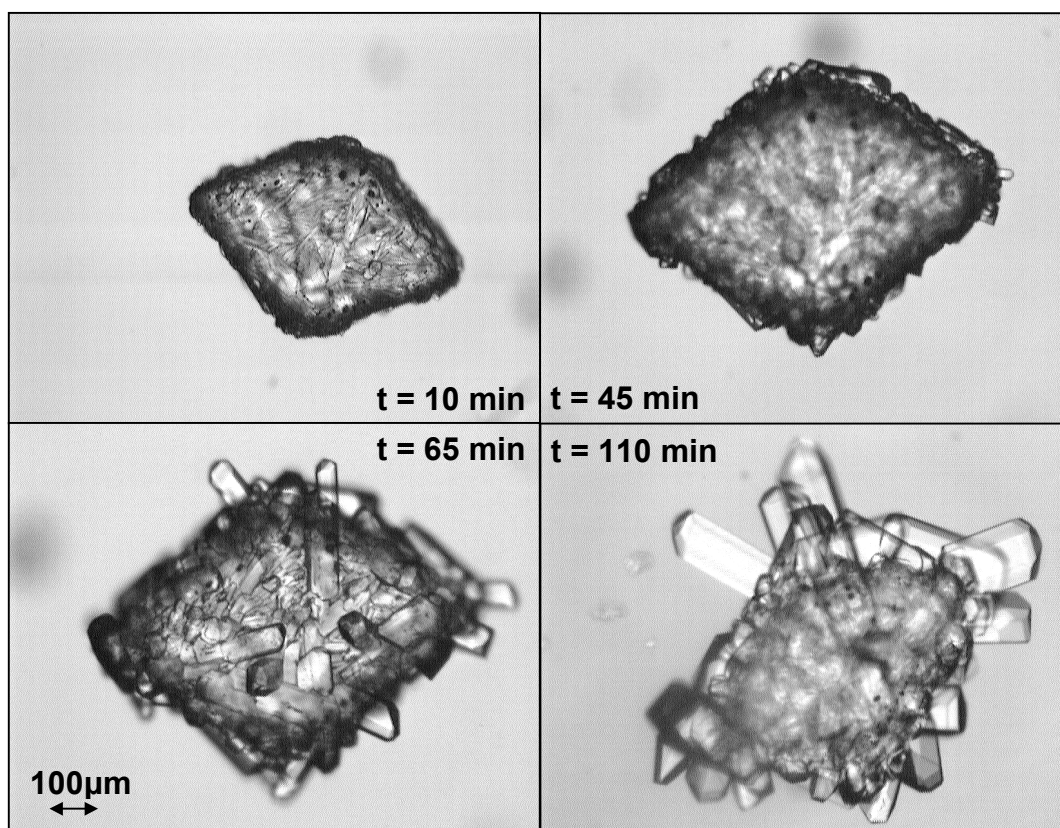
Fig. 4.2-1.   Phase transformation of magnesium sulfate hexahydrate to the heptahydrate

A transformation in reverse order has been carried out in a solution saturated at 55°C. During the experiment, the solution is slightly supersaturated with respect to the hexahydrate. A seed crystal of the heptahydrate, without special prior treatment, is added to the solution. In *Figure 4.2-2*, the course of the phase transformation is shown. The crystal of the metastable heptahydrate gradually dissolves and simultaneously the hexahydrate nucleates and grows onto the dissolving crystal of the heptahydrate.

Fig. 4.2-2.   Phase transformation of magnesium sulfate heptahydrate to the hexahydrate

Besides the phase transformation experiments in the microscopic cell, studies have also been carried out in a crystallizer. The transformation of the hexahydrate to the heptahydrate in these experiments has been monitored with the ultrasonic measuring technique. A schematic of how the phase transformation experiments are conducted is given in *Figure 4.2-3*.
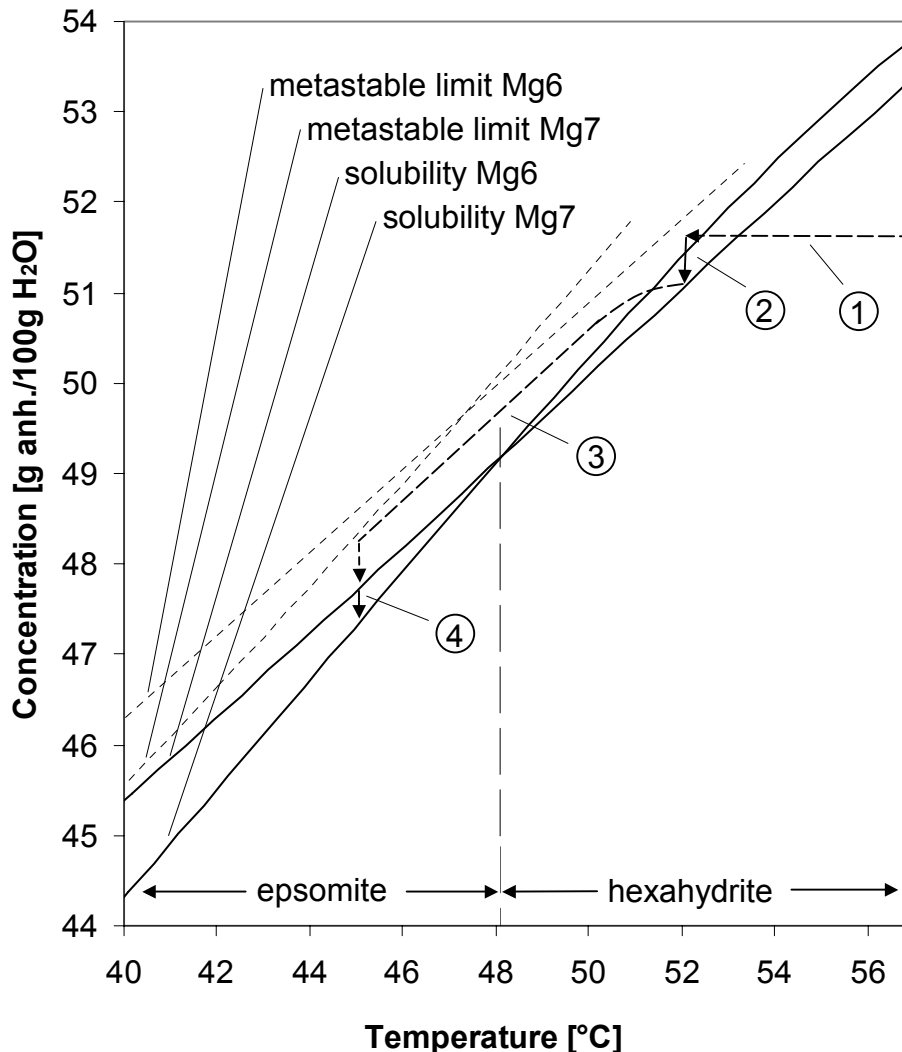
Single steps of the phase transformation experiments carried out in the crystallizer are as follows:
(1) cooling, addition of seed crystal, nucleation hexahydrite
(2) constant temperature, depletion of supersaturation by crystal growth
(3) cooling, growth hexahydrite
(4) nucleation epsomite, dissolution hexahydrite and growth epsomite

In this context, the induction time for nucleation of the stable phase is defined as the period of time starting when the final transformation temperature is reached until nucleation of the stable phase starts.

The course of a phase transformation monitored by the ultrasonic measuring technique is depicted in *Figure 4.2-4*. Both, ultrasonic velocity and temperature, have been measured in-line with the ultrasonic sensor. All solution-mediated transformations of the metastable

hexahydrate to the stable heptahydrate have been carried out as schematically shown in *Figure 4.2-3*.

Fig. 4.2-3.   Solution-mediated phase transformation: hexahydrate to heptahydrate

In the phase transformation experiments, solutions with a saturation temperature of 56°C are cooled to 53°C. If nucleation of the hexahydrate does not start within 15 minutes, a seed crystal is added to induce nucleation. After depletion of supersaturation by nucleation and crystal growth, the suspension is cooled to the final transformation temperature below the transition point. In this series of experiments, the solution-mediated phase transformation has been carried out at a constant temperature of 45°C. After reaching the final temperature of 45°C, the ultrasonic velocity increases linearly with time until nucleation of the stable phase starts. The starting point of nucleation of the heptahydrate is indicated by a distinct increase in ultrasonic velocity and by a temperature peak. In the pure solution, nucleation of the stable phase starts after an induction period of approximately 19 hours, as can be read from *Figure 4.2-4*.

The two additives, KCl and borax, significantly influence the induction time for nucleation of the heptahydrate. The effect of KCl on the phase transformation can be seen in

Figure 4.2-5. Experiments have been carried out in the same manner as for pure solutions. Adding KCl obviously accelerates the transformation. In solutions with 0.5 wt% KCl, nucleation of the heptahydrate already starts after an induction time of 45 minutes. In contrast to it, transformation in the presence of 0.5 wt% borax is distinctly prolonged (see *Fig. 4.2-6*). Nucleation of the stable phase can only be observed after an induction time of approximately 70 hours. In both cases, nucleation of the heptahydrate is accompanied by a distinct increase of the ultrasonic velocity and an increase in temperature.
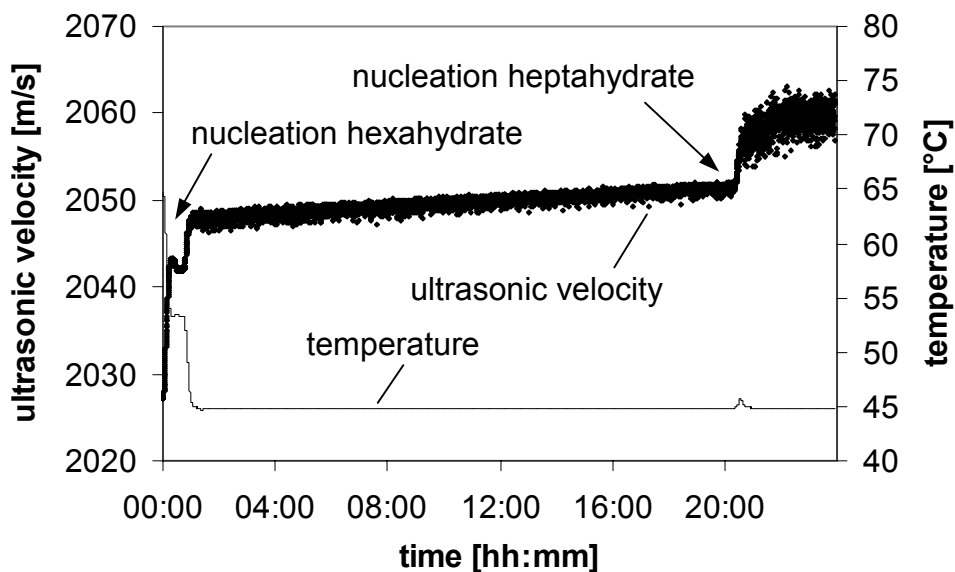
Fig. 4.2-4.   Phase transformation of magnesium sulfate heptahydrate to hexahydrate
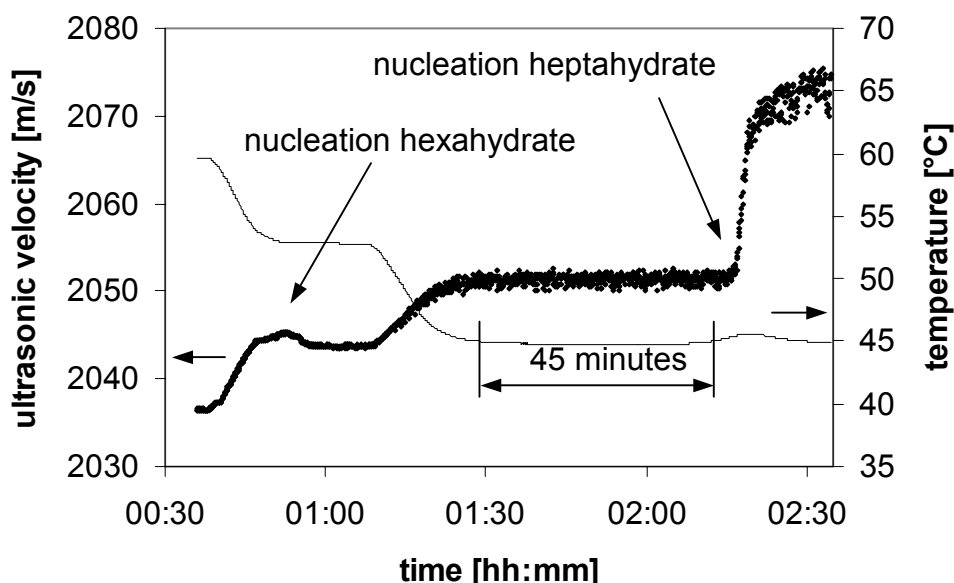
Fig. 4.2-5.   Phase transformation of magnesium sulfate with 0.5 wt% KCl

However, the induction times reported for the above mentioned phase transformations cannot be taken as given. Even if repetitive experiments are carried out in analogous

51

manner, the induction times until nucleation of the heptahydrate starts may vary experiment-to-experiment. In the case of pure solutions, nucleation of the heptahydrate starts after 10 to 19 hours. With 0.5 wt% KCl the induction times vary between 30 and 45 minutes, whereas with 0.5 wt% borax induction times from 27 to 70 hours have been monitored with the ultrasonic measuring technique.
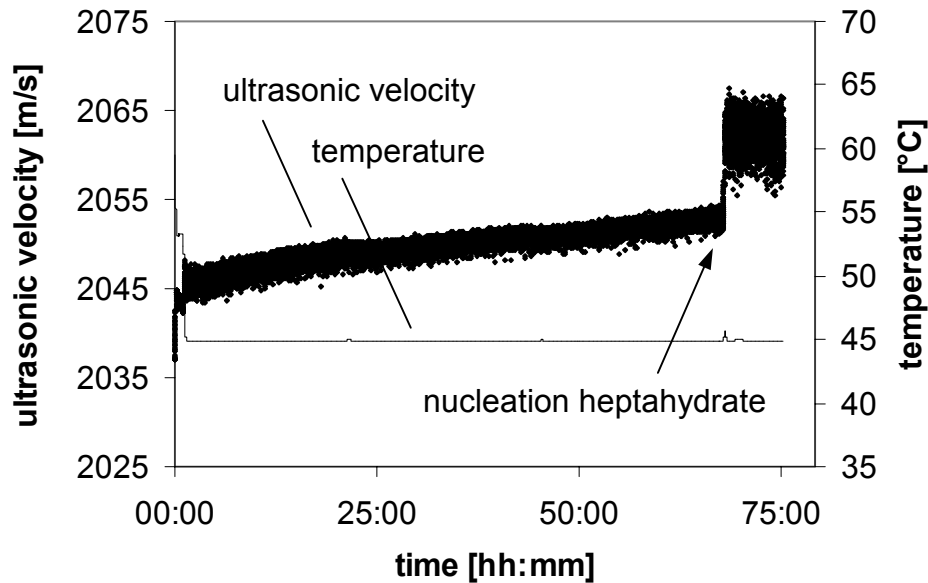

Fig. 4.2-6. Phase transformation of magnesium sulfate with 0.5 wt% borax

The phase transformation experiments have been monitored by means of the ultrasonic measuring technique. Furthermore, for optical evaluation of the progress of transformation, samples have been taken during a phase transformation experiment in pure solution. The crystals have been withdrawn from solution, filtered and dried at ambient conditions. After
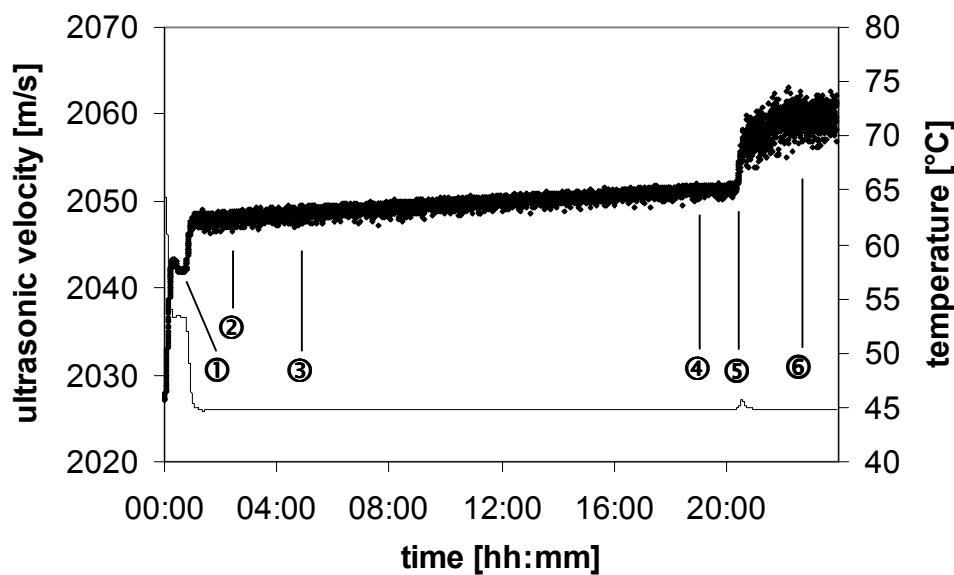
Fig. 4.2-7. Times of sampling in a phase transformation experiment

drying, all samples have been evaluated by optical microscopy. Times of sampling are indicated in *Figure 4.2-7*. The first sample (1) is taken at the beginning of cooling still above the transition temperature and the last sample (6) at the end of the transformation, when only crystals of magnesium sulfate heptahydrate are present in the slurry. Photographs of these samples are shown in *Figure 4.2-8*. Since different modifications are used, a scalar is plotted in each photograph.
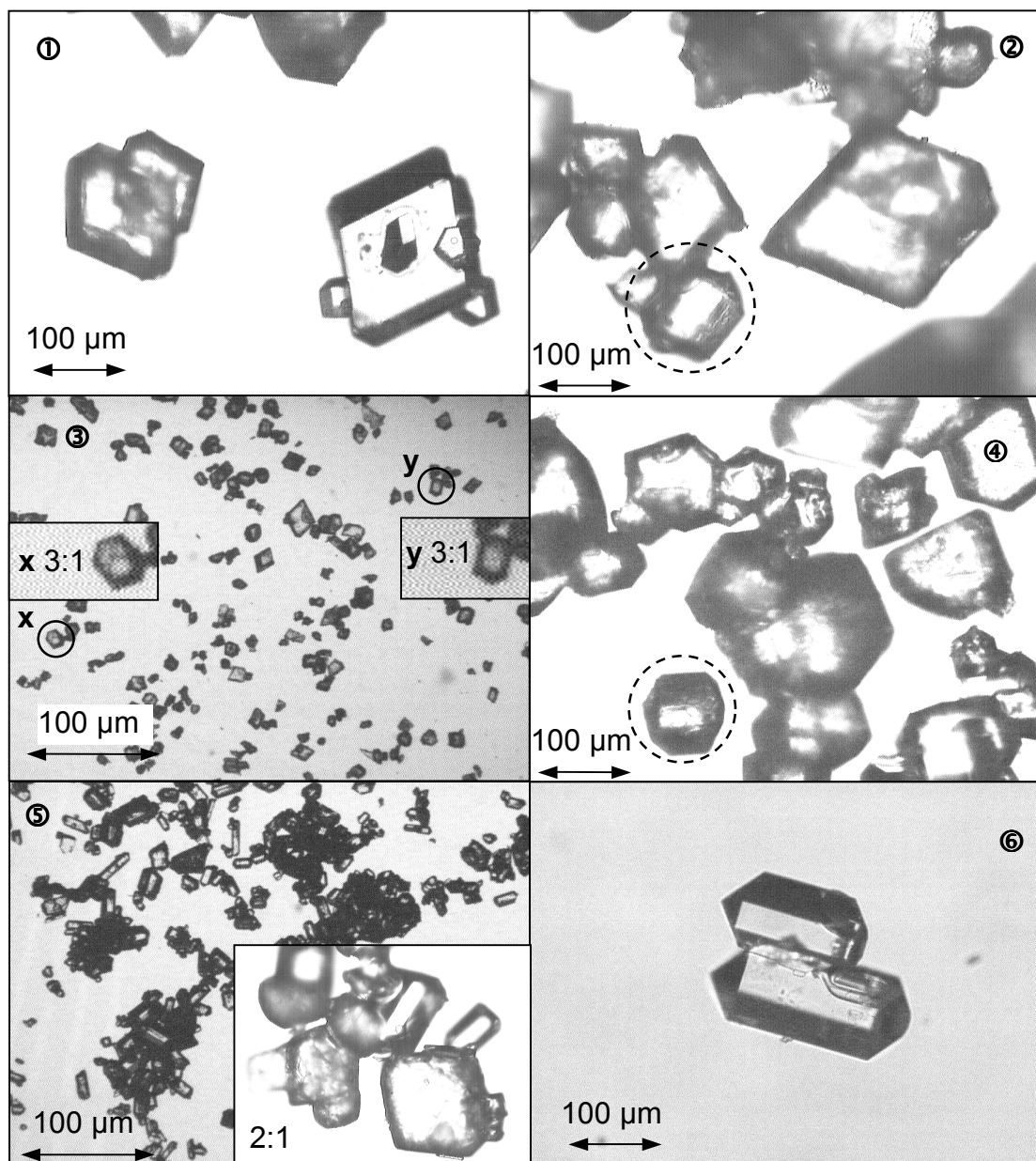
Fig. 4.2-8. Course of the phase transformation of magnesium sulfate hexahydrate to the heptahydrate

① 53°C, 45min   ④ 45°C, 19h 05min
② 45°C, 2h 40min   ⑤ 45°C, 20h 25min
③ 45°C, 4h 45min   ⑥ 45°C, 22h 55min

In the first photograph, taken at the beginning of cooling, only crystals of the hexahydrate can be seen. The fifth photograph, which is taken when nucleation of the heptahydrate is detected by the ultrasonic measuring technique, shows crystals of both phases, the hexahydrate as well as the heptahydrate. However, already before noticeable nucleation of the heptahydrate starts, single crystals of the heptahydrate can be found in the suspension, shown in the photographs (2), (3) and (4). About two and half hours after noticeable nucleation of the heptahydrate has started, no crystals of the hexahydrate can be observed anymore (see sixth photograph).

4.2.1 Induction times

Magnesium sulfate solutions with a saturation temperature of 56°C have been prepared. In the course of the experiments, solutions are cooled to 53°C into the metastable zone of the hexahydrate. If nucleation of the hexahydrate does not start within 15 minutes, a seed crystal is added to induce nucleation. After nucleation of the hexahydrate, the suspensions have been kept at a constant temperature of 53°C for at least 30 minutes to assure depletion of supersaturation by nucleation and growth of the crystals. Subsequently, the suspensions have been cooled to varying temperatures below the transition temperature, which is reported to be 48.1°C /OTT02/.

All experiments have been monitored by means of the ultrasonic measuring technique. The induction time is defined as the period of time between reaching the final transformation temperature and the start of nucleation of the stable heptahydrate. Thus, an induction time of zero means that nucleation of the heptahydrate starts instantaneously when the transformation temperature is reached. An example for instantaneous nucleation in a phase transformation experiment is shown in *Figure 4.2-9*.
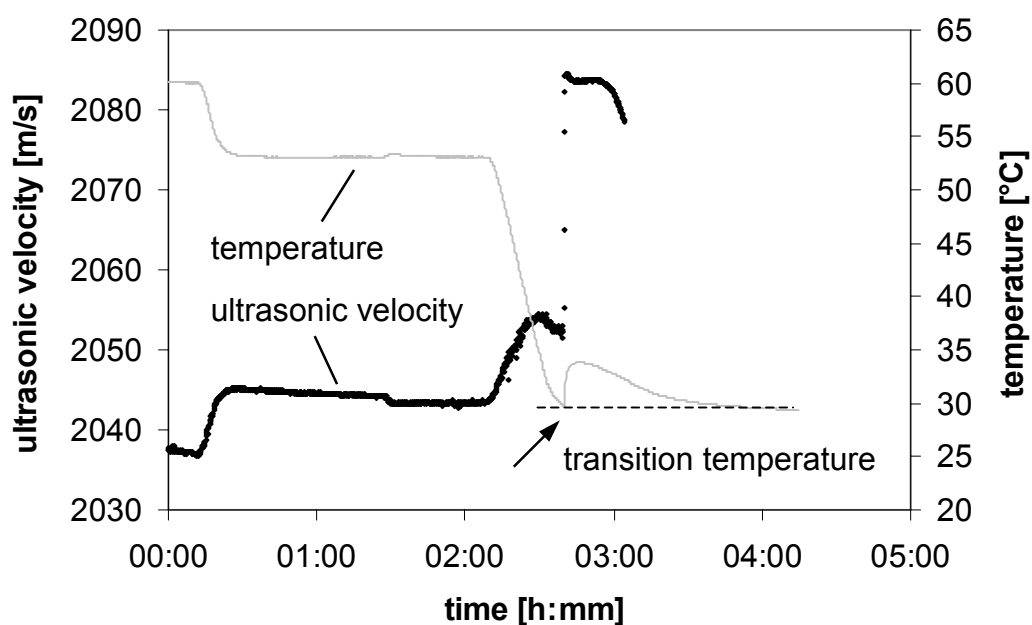

Fig. 4.2-9. Instantaneous nucleation at 30°C

Nucleation of the heptahydrate starts directly when the final transition temperature of 30°C is reached (see *Figure 4.2-9*). An arrow marks the onset of nucleation, which is accompanied by an increase in ultrasonic velocity and a temperature peak.

An example for varying induction times at one constant temperature can be seen in *Figure 4.2-10*. Both transformation experiments have been carried out at 45.5°C. At this temperature, the induction times do not differ distinctly. In one experiment, nucleation of the heptahydrate starts after almost 4 hours, in the other experiment an induction time of 5 hours has been monitored.
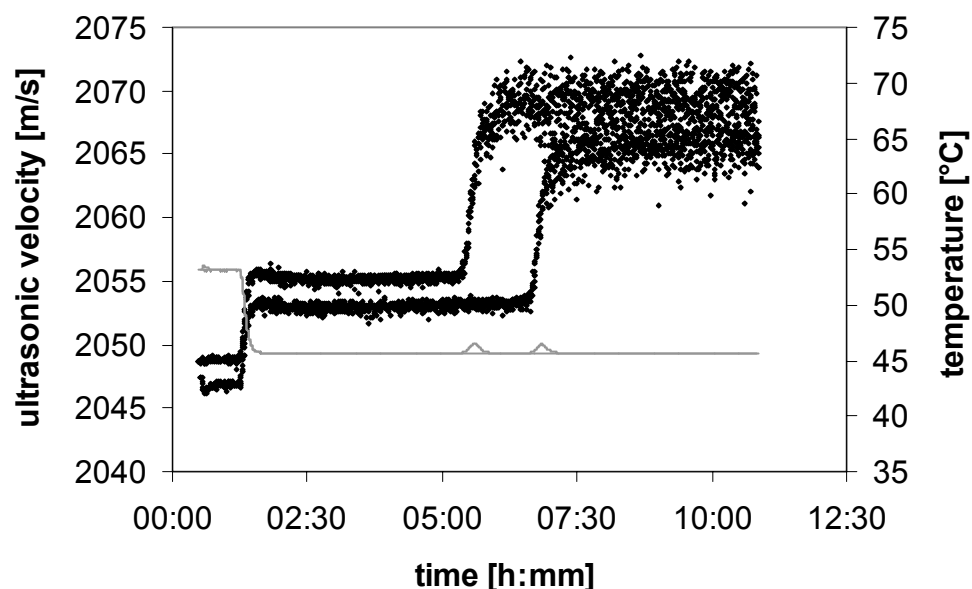
Fig. 4.2-10. Different induction times at 45.5°C in phase transformation experiments
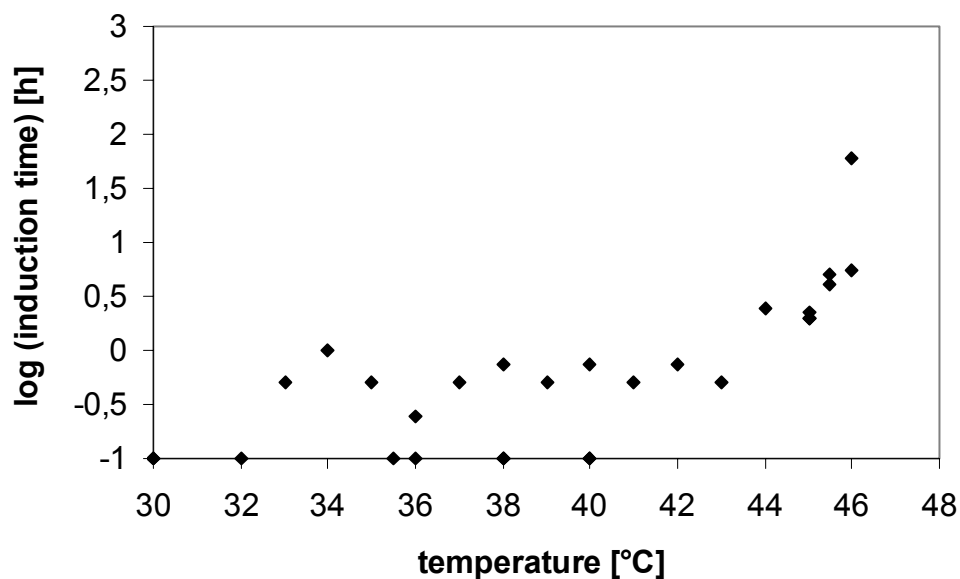
Fig. 4.2-11. Induction times for magnesium sulfate solutions as a function of temperature

Induction times as a function of temperature are depicted in *Figure 4.2-11*. Experiments have been carried out in the temperature range between 30 and 46°C. Temperatures below 30°C could not be reached, because in the respective experiments nucleation already started during cooling, i.e. before the final transition temperature has been reached. All experiments between 30 and 43°C have been repeated three times with very reproducible results. In this temperature range, nucleation always starts within one hour. Experiments at temperatures higher 46°C have been interrupted, because the induction times exceed 200 hours.

5. Discussion of the results for magnesium sulfate

The study of the influence of KCl and Borax has shown that the influence of KCl is often neglectable whereas borax has a strong inhibiting effect in every respect. Concerning the influence of additives on phase transformations it could be demonstrated that both is possible, a reduction as well as a prolongation of induction times attained with KCl and borax, respectively. However, it is also shown that a reliable prediction of induction times is not possible, neither in pure systems nor in systems with additives.

5.1 Influence of additives on thermodynamics and kinetics of crystallization
### 5.1.1 Solubility and metastable zone width
Even small traces of additives can influence the solubility and metastable zone width (see *Figures 4.1-1* and *4.1-2*). It is known that a pH more alkaline or acidic can influence the solubility as well as the amount of supersaturation tolerated by a system /EGL63/. Since all of the additives used in the experiments have changed the pH of the solution to some extent, this can be taken as a possible explanation for the influence of these additives on the solubility. The pH of a pure magnesium sulfate solution is approximately 6.4, a pH distinctly more acidic being obtained by adding e.g. 1 wt% $FeSO_4 \cdot H_2O$ (pH: 4.6) or 1 wt% KH_2PO_4 (pH: 3.2). It is possible that the additive either only increases the ionic strength I of the solution without forming complexes with the solute or the additive increases the ionic strength and simultaneously forms soluble complexes with the solutes /EGL63/. However, a possible formation of complexes has not been further prosecuted.

Concerning the influence of additives on the metastable zone width, two contrary effects have been observed: On the one hand, a slight decrease of the width of the metastable zone with 0.5 wt% KCl (see *Figures 4.1-3* and *4.1-6*), and on the other hand, an increase of the metastable zone width with 0.5 wt% borax (see *Figures 4.1-4* to *4.1-6*). From the state of the art it is known that the solution-composition influences the interfacial free energy γ between the solvent and the solute. Since any adsorption onto the surface of a nucleus decreases the interfacial free energy, an increase of the nucleation rate should be observed when impurities are present in the solution. However, this would be the sole result of the thermodynamic effect and does not take into account the kinetic effect. Since the growth of a nucleus proceeds only via a few growth sites, merely a few adsorbed impurity molecules are necessary for inhibiting the growth of a nucleus /EGL63/. In this

case, the impurity stabilizes the solution and, thus, the width of the metastable zone increases. Up to a certain point the efficiency of the additive increases with increasing concentration, as shown for borax in *Figure 4.1-4*.

The influence of varying amounts of borax on the metastable zone width is also shown in *Figure 5.1-1*. A logarithmic plot of the maximum supercooling versus the additive concentration yields a straight line for borax concentrations between 0.1 and 5 wt%.
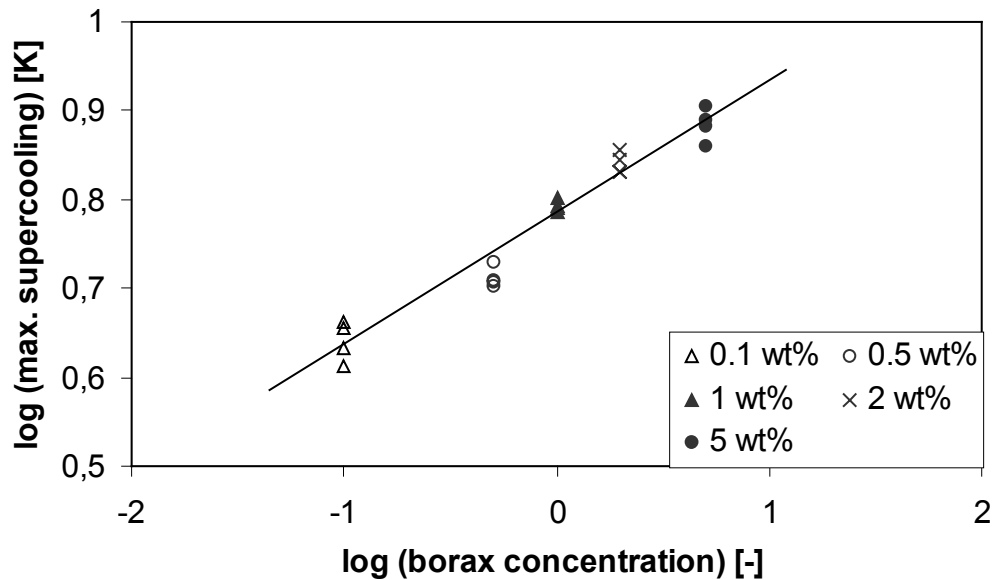
Fig. 5.1-1.   Influence of borax on the metastable zone width of magnesium sulfate
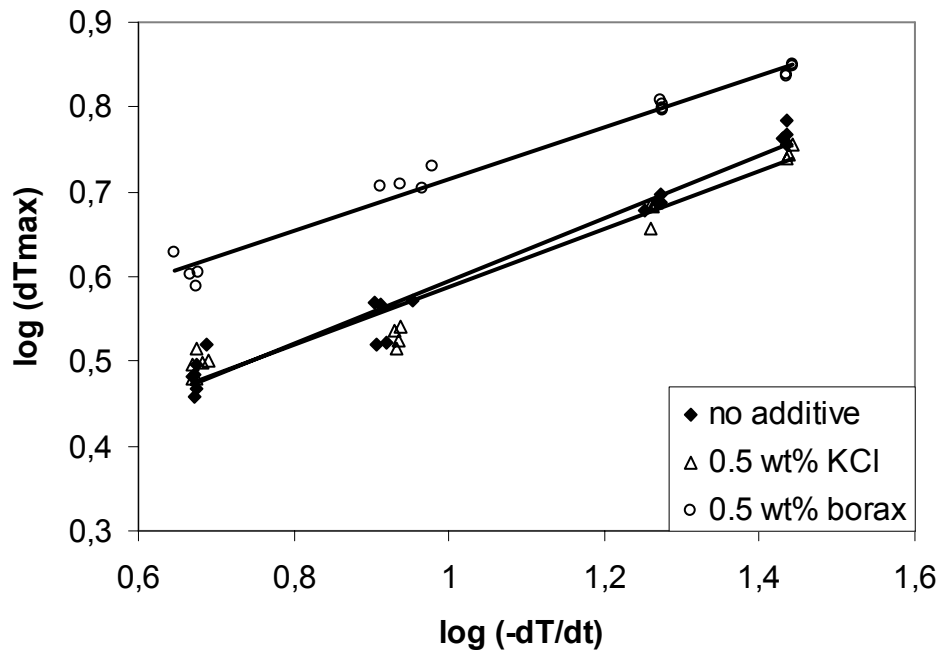
Fig. 5.1-2.   Metastable zone width in dependence on the cooling rate for magnesium sulfate solutions with and without additives

Furthermore, the width of the metastable zone has been determined for aqueous magnesium sulfate solutions without additives as well as for solutions with KCl and borax for four different cooling rates, 5, 10, 20, and 30 K/h (see *Figure 4.1-6*). As expected, the maximum supercooling which the solution tolerates increases with increasing cooling rate.

The measurements of the metastable zone width can give information on nucleation characteristics when both, the maximum supercooling and the cooling rate, are plotted in a logarithmic scale, as depicted in *Figure 5.1-2*. It can be seen that the gradient of the trendlines for solutions with additives is lower than for the magnesium sulfate solutions without additive, indicating that the influence of the cooling rate is less dominant in solutions with additives.

The metastable zone width in dependence on the cooling rate can be represented in an idealized manner by an equation of the type:

$$Y = A + B \cdot X \tag{5.1-1}$$

The constants A and B for magnesium sulfate solutions with and without additives derived from *Figure 5.1-2* are shown in *Table 5.1-1*.

Tab. 5.1-1.   Constants of *equation 5.1-1*

	A	B
no additive	0.2244	0.3707
0.5 wt% KCl	0.2475	0.3409
0.5 wt% borax	0.4123	0.3035

By using the constants depicted in *Table 5.1-1* nucleation parameters can be calculated with the following equation /NYV85/:

$$\log \Delta T_{max} = \frac{1-n}{n} \log \frac{dw_{eq}}{dT} - \frac{\log k_N}{n} + \frac{1}{n} \log \left(- dT / dt \right) \tag{5.1-2}$$

However, it should be noted that *equation 5.1-2* is simplified assuming that at the moment when nuclei are first detected the rate of supersaturation depletion is equal to the rate of nucleation. However, this assumption does not reflect the actual course, because the supersaturation is depleted in two ways, partly by growth on existing crystalline particles and partly by the formation of new nuclei. Furthermore, in the experimental determination of the metastable zone width nuclei are not detected directly at the moment of their creation but only when they have grown to a detectable size depending on the method employed for detection /MUL00/.

Nucleation parameters, in particular the nucleation rate constant and the nucleation order, obtained from measurements of the metastable zone width, are shown in *Table 5.1-2*.

Tab. 5.1-2.   Nucleation parameters

	n	$k_N \cdot 10^{-5}$
no additive	2.6976	3.192
0.5 wt% KCl	2.9334	3.831
0.5 wt% borax	3.2949	1.597

The nucleation order experimentally obtained is in good accordance with data found in literature. An exponent for nucleation of n = 2.6 for magnesium sulfate solutions at 25°C is given in /VAU92/, compared to ca. 2.7 given in *Table 5.1-2*. No appropriate value for the nucleation rate constant k_N has been found in literature, the constant being a function of many variables, in particular depending on temperature, fluid dynamics, and the presence of impurities /TAV87/. From *Table 5.1-2* it can be seen that borax significantly decreases the nucleation rate, whereas the nucleation rate is slightly increased by the addition of KCl, consequently resulting in a larger and a slightly smaller metastable zone width, respectively (see *Figure 4.1-6*).

Nucleation rates for different levels of supersaturation can be calculated with the following equation (homogeneous nucleation):

$$\dot{N}_N = k_N \Delta w^n \qquad \textbf{(5.1-3)}$$

Since in industrial crystallization usually a large number of solute molecules is involved, the steps of nucleation and crystal growth exhibit a probability behavior, justifying the use of a simple power law for the calculation of nucleation and growth rates /NYV92/.

5.1.2   Growth rate and crystal habit

Growth rate experiments have been conducted with single crystals in a microscopic cell as well as with crystal collectives in a fluidized bed. At first, the results of the "fluidized bed-experiments" will be discussed.

From *Figure 4.1-8* a linear growth rate G of $\approx 2 \cdot 10^{-7}$ ms^{-1} can be read whereas Mullin /MUL00/ states that for magnesium sulfate heptahydrate at 30°C and S = 1.02 a mean linear growth velocity of $\bar{v} = 1.5 \cdot 10^{-7}$ ms^{-1} is obtained. For comparison with the experimental data it should be noted that:

$$\bar{v} = \frac{1}{2} G \qquad \textbf{(5.1-4)}$$

Although in own experiments not the same result as stated by Mullin /MUL00/ has been obtained, the growth rate is well within the range expected in solution crystallization. Reasons for the deviation can be found e.g. in slightly different temperatures, the purity of the initial product crystals, the simplified calculation of the growth rate (see *equation 3.2-2*) and other sources of error, discussed in *section 5.3*.

The results plotted in *Figure 4.1.9* show that the dissolution rate of the epsomite crystals is reduced by the addition of KCl. In contrast to this, the growth rate tends to increase slightly when KCl is added. Even an increase of the amount of KCl from 1 to 5 wt% does not significantly influence the growth rate. However, this result is in accordance with the observation, that the metastable zone width is slightly smaller in the presence of KCl. The metastable zone width depends on the nucleation as well as on the growth rate, both being slightly increased in the presence of KCl, thus resulting in a smaller metastable zone width.

Furthermore, the influence of KCl and borax on the growth rate of both, magnesium sulfate heptahydrate and hexahydrate, have been explored in a microscopic cell to possibly aid in explaining the change of habit caused by these two additives.
With KCl, results similar to those of the "fluidized bed-experiments" are obtained. Again, the epsomite crystals are found to grow faster when KCl is added to the solution (see *Figure 4.1-11*). In contrast to it, borax significantly decreases the growth rate of the epsomite crystals. With both additives, the growth rate in the x- and y-direction has been affected.
The effect of KCl on the growth rate of the hexahydrate is different from that on the hexahydrate, because in this case the growth rate is reduced in both, the x- and the y-direction (see *Figure 4.1-12*). The growth rate of the hexahydrate crystals is even more reduced when borax is part of the solution composition.

The crystal habit depends on the one hand on internal factors like structure and bonds, and on the other hand on external factors such as supersaturation and solution composition. As already described in *section 2.2.4*, the smaller the growth rate the more extensive the development of a specific face. The only possibility to extend a face is to selectively decrease its velocity. One way to modify the relative growth rates of different faces is a change in supersaturation, because the different crystal faces do not have the same behavior at different levels of supersaturation. Also the solvent itself and impurities may play an important role. Since the solvent is always present it should be considered as the primary impurity for the crystal. When the solvent itself is not pure, it is likely that the growth rates of the faces of a crystal will be affected by the solution composition /EGL63, KHAM76/.

This might be taken as a possible explanation that even in so-called "pure solutions" different crystal habits are observed; among other influences such as the purity of the chemical substance and minor deviations in temperature and supersaturation.

Magnesium sulfate heptahydrate crystals grown in aqueous solution without any deliberately added impurity, illustrated in *Figure 4.1-14 a*, exhibit different habits.

The heptahydrate is a non-centrosymmetric crystal belonging to the orthorhombic-disphenoidal class. The $(\bar{1}\,\bar{1}\,\bar{1})$ faces exhibit SO_4^{2-}-groups pointing outside the crystal, these groups having a higher electronic polarizability than that of the complex $Mg(H_2O)_6^{2+}$ which outcrops on the (111) faces. The difference in the electronic polarizability should account for the two complementary forms having an unequal development. In particular, the $(\bar{1}\,\bar{1}\,\bar{1})$ faces should grow at a lower rate than the (111) faces /RUB85, SGU87/.
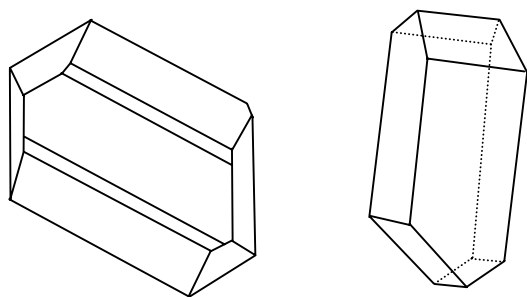
Fig. 5.1-3.   Different habits observed for the heptahydrate

Epsomite crystals are known to grow mainly in the direction of the c-axis with the prism (110) being the best-developed face /GME53/. This has proven to be true as can be seen in *Figure 5.1-3*, showing the outline of epsomite crystals grown in the microscopic cell. Although the faces are developed to a different extent and some faces are not at all developed (in comparison with *Figure 4.1-13 a*), both crystals outlined in *Figure 5.1-3* have a well-developed (110) face as well as the complementary {111} and $\{\bar{1}\,\bar{1}\,\bar{1}\}$ forms and, thus, can be easily identified.
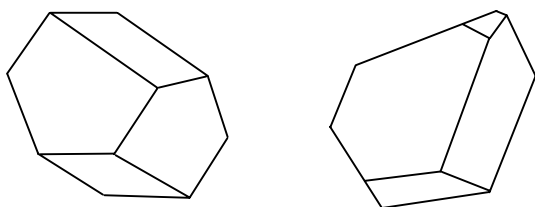
Fig. 5.1-4.   Different habits observed for the heptahydrate + KCl

Epsomite crystals grown in the presence of KCl exhibit a shortened habit compared to those grown in pure solutions (see *Figure 5.1-4*). The {111} and $\{\bar{1}\,\bar{1}\,\bar{1}\}$ forms are more pronounced and the (110) faces lose significance. From growth rate experiments in the microscopic cell it is known that the growth rate is increased in both directions, in the x- and in the y-direction (see *Figure 4.1-11*). However, the increase of the growth rate is more pronounced in the x-direction than it is in the y-direction. This indicates that the crystals should become more elongated when grown in the presence of KCl, which contradicts the outcome of the experiments concerning the crystal habit in the microscopic cell. Therefore, a selective adsorption of KCl on certain faces of the crystal is assumed to explain the change of habit, shown in *Figure 5.1-5*.

- inhibited growth
= unaffected growth
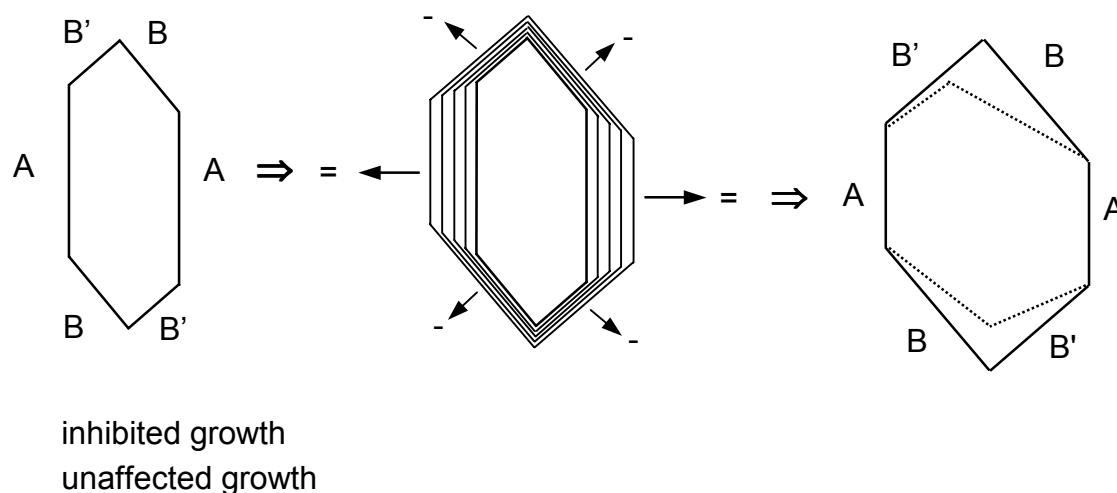
Fig. 5.1-5. Impact of KCl on crystal habit of magnesium sulfate heptahydrate

This face-specific adsorption might decrease the growth rate of the B/B'-faces and thus the A-faces will grow faster relatively to the B/B'-faces. Different angles of the disphenoids might result from different affinities of the impurity for the (111) and $(\bar{1}\,\bar{1}\,\bar{1})$ faces, indicated by the dotted lines in *Figure 5.1-5*.

Epsomite crystals grown in aqueous solution having borax added are known to exhibit hemiedry. Even small amounts of borax reduce the growth rate in the c-direction, which is ascribed to a selective adsorption of $B_4O_5(OH)_4^{2-}$-ions on the (111) and / or $(\bar{1}\,\bar{1}\,\bar{1})$ faces. However, borax is not build into the crystal lattices, at the most traces of this impurity are mechanically incorporated /GME53, RUB85/.

Own measurements in the microscopic cell confirm the distinct reduction of the growth rate in the c-direction or x-direction, respectively. With 5 wt% borax the growth rates in the x- and y-direction are almost the same, resulting in crystals having a compact from like those shown in *Figure 5.1-6*. Since the growth rate of the {111} and $\{\bar{1}\,\bar{1}\,\bar{1}\}$ forms is reduced, these forms develop more extensively whereas the {110} forms lose significance.
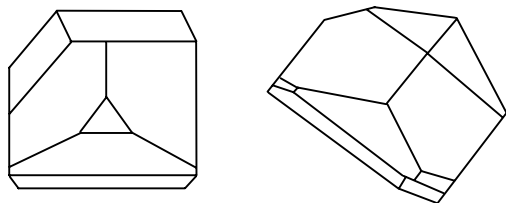
Fig. 5.1-6. Different habits observed for the heptahydrate + borax

A stepwise change of habit by successively increasing the borax-concentration is illustrated in *Figure 5.1-7*.

| 0 wt% | 0.1 wt% | 0.3 wt% |

| 1 wt% | 2 wt% | 5 wt% |
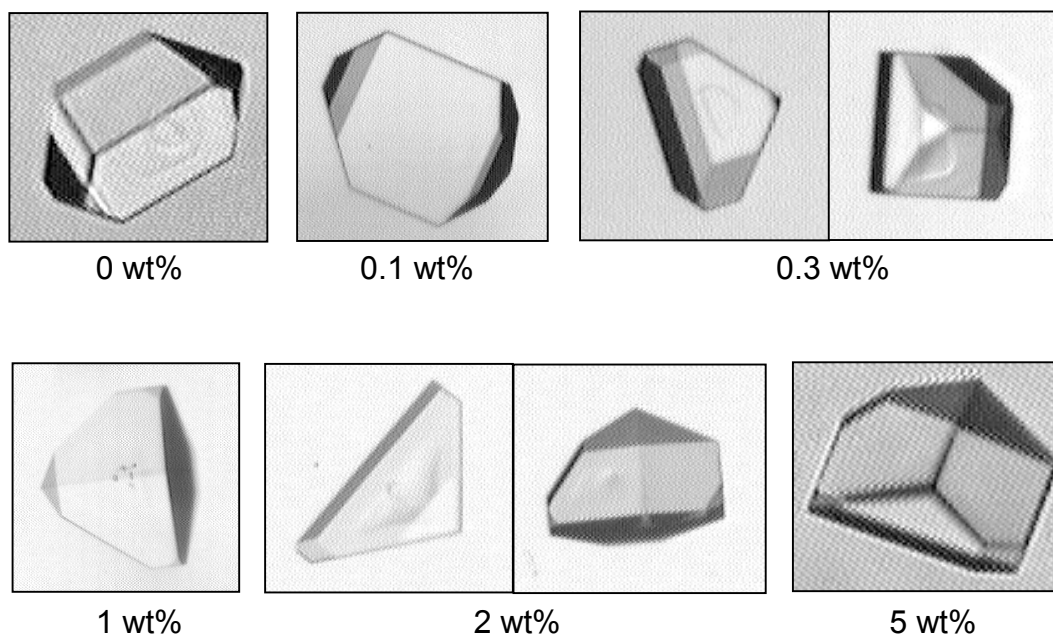
Fig. 5.1-7. The habit of epsomite in dependence on the borax-concentration

Adding 0.1 wt% borax to the solution results in crystals having a more compact form comparable to those crystals grown in solutions with 5 wt% KCl (see *Figure 5.1-4*). When the borax-concentration is increased to 0.3 wt% the (110) faces, being the best-developed faces of epsomite crystals grown in pure solutions, lose significance and the (111) and $(\bar{1}\,\bar{1}\,\bar{1})$ faces make up a major part of the crystal surface. Since this distinct change of habit is observed with 0.3 wt% borax, this concentration is regarded as the effective concentration for changing the habit of epsomite crystals from needle-like to cubic. At higher borax-concentrations, the disphenoids are well-developed at one end of the crystal, whereas they almost disappear at the other end, resulting in wedge-shaped crystals. An increase of the additive concentration from 2 to 5 wt% does not have a pronounced effect (see *Figure 5.1-7*).

Epsomite crystals grown in solutions with 0.3 wt% borax, the "effective concentration", have been analyzed with EDX (see *Figure 5.1-8*).
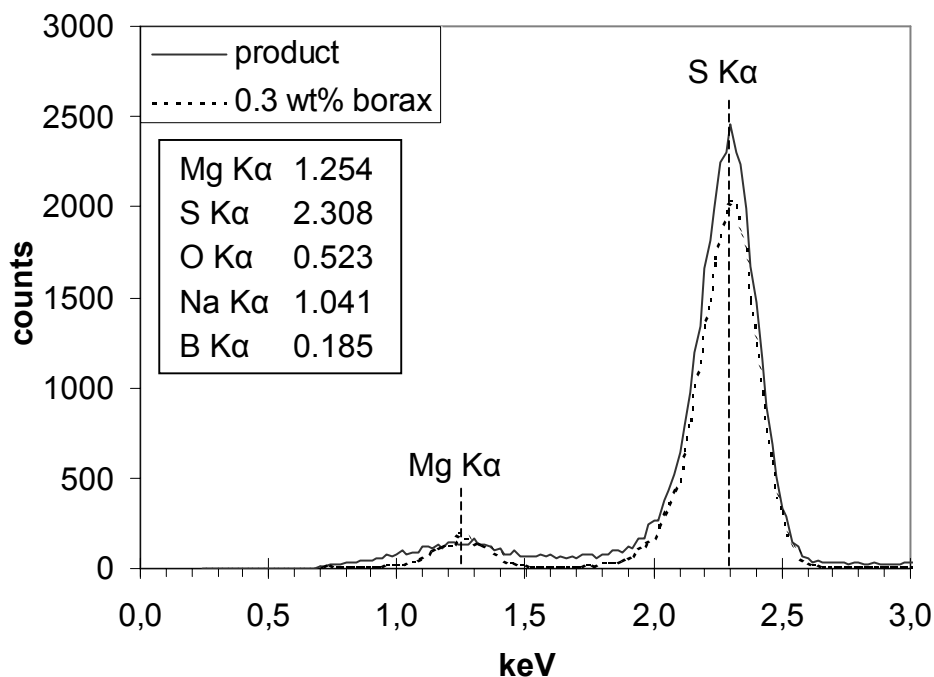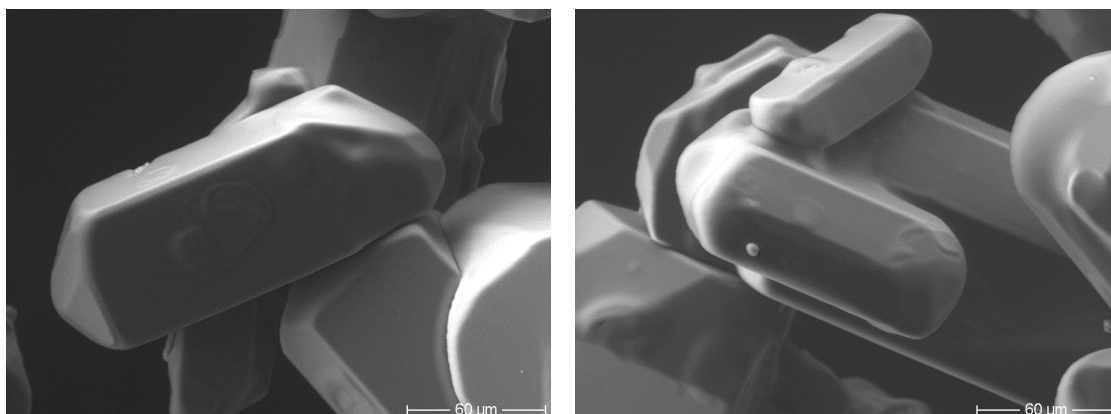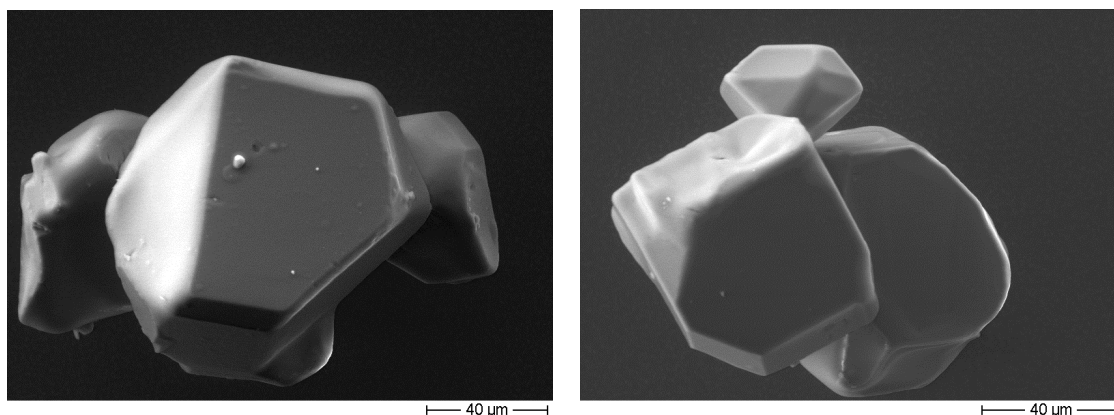
Fig. 5.1-8. EDX-Analysis of epsomite crystals grown in solutions with 0.3 wt% borax

Gmelin /GME53/ reported that at the most traces of borax are mechanically incorporated and also the EDX-analysis does not give any indication of borax being incorporated into the crystal lattice, at least not in areas close to the surface. From *Figure 5.1-8* it can be seen that the peaks of the product crystals are broader and not as distinct as those of the crystals grown in solutions with borax. However, in both cases only Kα-lines of magnesium and sulfur have been detected.

In combination with the EDX-analysis SEMs of the crystals have been taken, depicted in *Figures 5.1-9* and *5.1-10*.

Fig. 5.1-9. SEMs of epsomite crystals grown in pure solution

Fig. 5.1-10. SEMs of epsomite crystals grown in solutions with 0.3 wt% borax

In *Figure 5.1-9*, SEMs of crystals grown in pure solutions are shown, the epsomite crystals exhibiting the typical needle-like habit. SEMs of crystals grown in solutions with 0.3 wt% borax, the crystals being almost cubic, are shown in *Figure 5.1-10*. It can be seen from *Figure 5.1-10* that the (110) faces are less-developed whereas the (111) and $(\bar{1}\,\bar{1}\,\bar{1})$ faces are better-developed compared to the respective faces of the crystals shown in *Figure 5.1-9*.

Just like the heptahydrate, also magnesium sulfate hexahydrate crystals grown in aqueous solutions without any deliberately added impurity, illustrated in *Figure 5.1-11*, exhibit different habits.
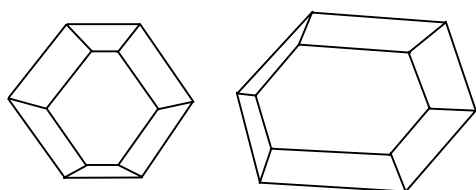
Fig. 5.1-11. Different habits observed for the hexahydrate

The habit of the hexahydrate, which is monoclinic-prismatic, strongly depends on temperature. At a crystallization temperature of 70°C long oblique crystals are obtained, whereas crystals sampled at 30°C are shorter and have more faces /GME53/. In experiments carried out at approximately 50°C crystals shown in *Figure 5.1-11* are obtained, having more well-developed faces than the product crystals (see *appendix*, *section 14.1*). By the addition of KCl, the habit of the hexahydrate is not distinctly changed, the crystals have the same faces as the crystals grown in pure solutions (see *Figure 5.1-12*). However, just like with the heptahydrate, the majority of the hexahydrate crystals grown in the presence of KCl exhibit a shortened habit.
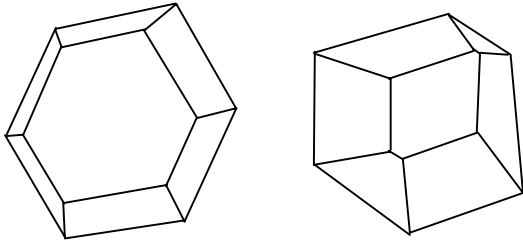
Fig. 5.1-12. Different habits observed for the hexahydrate + KCl

When borax is being added to the solution, the number of faces is reduced and the habit resembles a long oblique prism (see *Figure 5.1-13*).
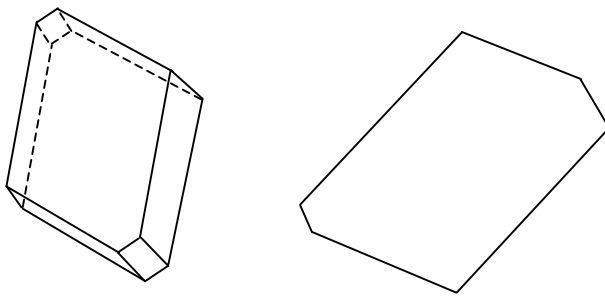
Fig. 5.1-13. Different habits observed for the hexahydrate + borax

It is assumed that both additives, KCl and borax, act only on certain crystallographic faces, shown schematically in *Figure 5.1-14*.


-     inhibited growth
=   unaffected growth
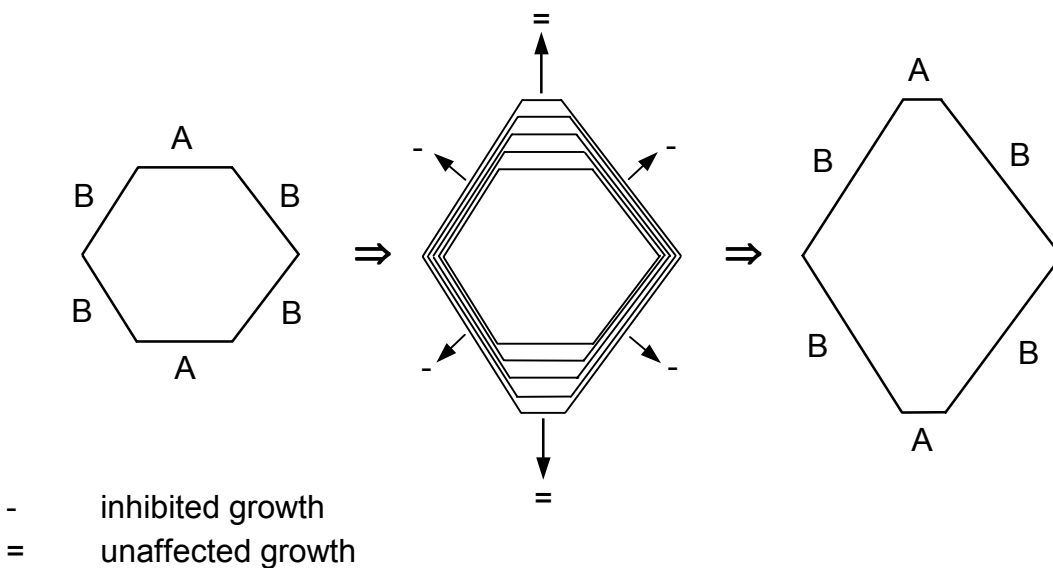
Fig. 5.1-14. Impact of additives on the crystal habit of magnesium sulfate hexahydrate

Under the assumption that the growth rate of the B-faces is affected by KCl, these faces will grow more slowly due to additive adsorption. If the growth rate of the A-faces is not affected by KCl, these faces will grow faster relative to the B-faces. Since faster growing faces disappear, the A-faces gradually disappear and the habit of the hexahydrate is changed to long oblique prisms.

Borax also seems to act only on certain crystallographic faces, similar to the interaction of KCl as described above. Furthermore, with borax certain side-faces present in pure solutions and in solutions with KCl - see *Figures 5.1-11* and *5.1-12* - disappear. This additive seems to have a more pronounced effect than KCl, since it does not only act on the A- and B-faces, but also on the side-faces which seem to grow relatively faster than the remaining faces and, therefore, disappear. Thus, with borax only crystals with a smaller number of faces than the crystals grown in pure solutions or in solutions with KCl are obtained.

5.2   Phase transformation

In phase transformation experiments with a duration of several hours, a linear increase of the ultrasonic velocity has been observed, for instance shown again in *Figure 5.2-1* for a phase transformation experiment with borax. The increase might be ascribed to the phenomena of Ostwald ripening, since the ultrasonic velocity increases without changing the temperature and concentration of the solution. This assumption is supported by experimental results from Sayan /SAY02/, showing that the ultrasonic velocity in aqueous magnesium sulfate solutions increases with increasing crystal size and suspension density, respectively.
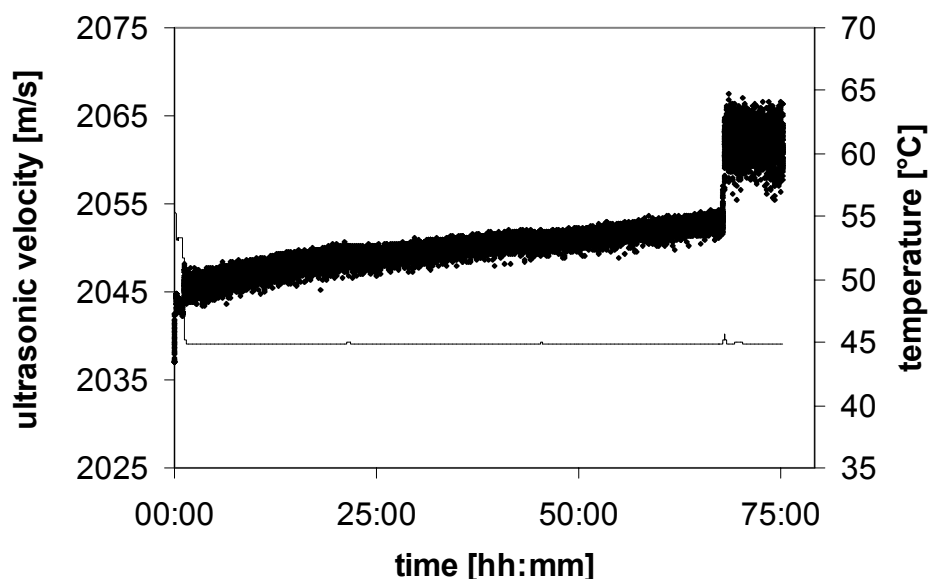
Fig. 5.2-1.   Phase transformation of magnesium sulfate with borax

The influence of KCl and borax on the duration of the phase transformation experiments has been shown in *section 4.2*. By adding 0.5 wt% KCl, which distinctly accelerated the transformation, the saturation temperature is not changed within detectable limits and the

metastable zone width is only slightly decreased, thus the solutions tolerating a slightly lower maximum supersaturation. The growth rate of the hexahydrate – the solution is also supersaturated with respect to the metastable phase – is slightly reduced compared to pure solutions. Therefore, it could be assumed that the supersaturation with respect to the stable phase is relatively higher compared to pure solutions, and since solutions in the presence of KCl only tolerate a lower supersaturation, nucleation of the stable phase starts earlier. However, this assumption presumably does not describe the real cause responsible for the reduction of the induction time, merely a promoting effect can be ascribed to it. Another possible explanation will be discussed subsequently in this section.

In contrast to the effect of KCl, the addition of borax significantly prolonged the induction times. An amount of 0.5 wt% borax in magnesium sulfate solutions influences the solubility as well as the metastable zone width (see *section 4.1*). Furthermore, the growth rate of the heptahydrate is distinctly decreased in the presence of small amounts of borax. The growth rate of the hexahydrate is also decelerated, but to a smaller extent. Since the growth of nuclei of the stable phase is drastically hindered, also the transformation will be retarded.

The experimental results clarify that although thermodynamically a transformation of a metastable phase into a more stable phase is possible, eventually the kinetics determine if and how fast a transformation takes place. Although the experiments have been carried out in analogous manner, the induction times differ considerably in some cases (see *Table 5.2-1*). Since the induction time for nucleation depends on many parameters (e.g. solution history, impurities present – including dust and dirt), it is not possible to obtain reproducible results in a series of experiments. However, nucleation always occurred within a certain time period, this time period most probably depending the purity of the product crystals.

Experiments with different batches of product crystals have shown that the induction times, although experiments carried out with one specific batch are reproducible within said time period, vary considerably from batch to batch (see *Table 5.2-1*).

**Table 5.2-1.** Induction times at 45°C

	pure	0.5 wt% KCl	0.5 wt% borax
Batch 1	10 - 19 h	0.5 – 0.75 h	27 – 70 h
Batch 2	> 100 h	>150 h	>300 h
Batch 3	1.5 – 2.5 h	-	-

Batch 1: 4 repetitions (pure, borax), more repetitions with KCl
Batch 2: in each case 2 repetitions
Batch 3: 4 repetitions

Experiments with different batches, which have been repeated several times, show significant differences between the induction times of the phase transformation experiments. In *Figure 5.2-2* a comparison between induction times of *batch 1* and *batch 3* is shown, the induction times being approximately two hours for *batch 3* and nineteen hours for *batch 1*.
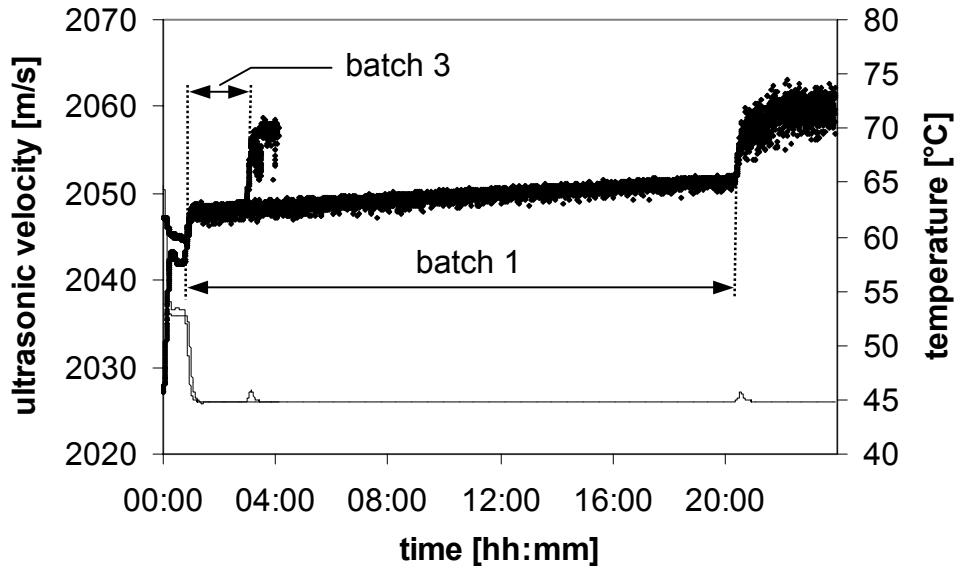

**Fig. 5.2-2.** Comparison between batch 1 and batch 3
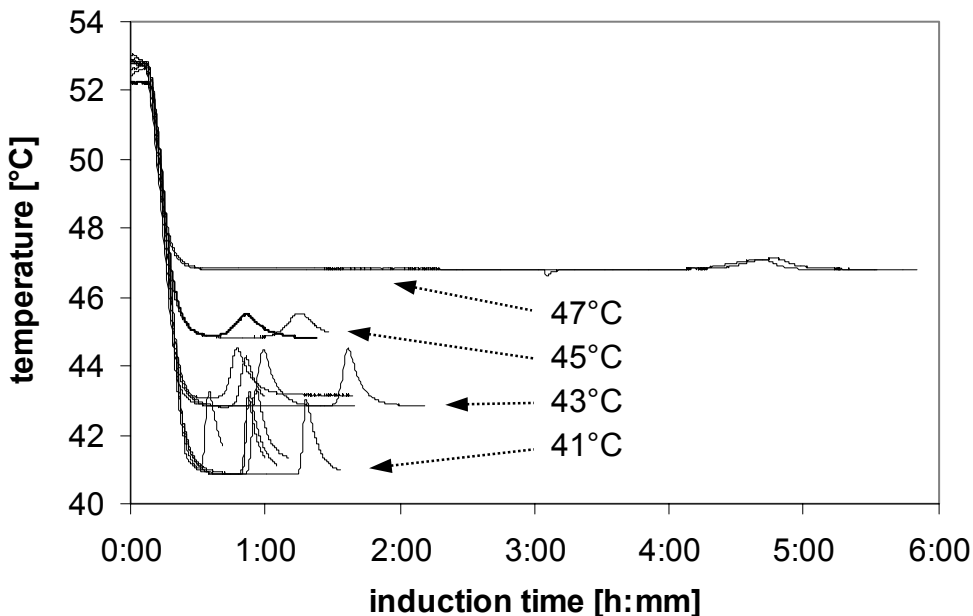
Fig. 5.2-3. Batch 1: Induction times with KCl at different temperatures

With *batch 1* and having KCl added to the solution, the induction times have been very reproducible, see *Figure 5.2-3*. For a better lucidity not the course of the ultrasonic velocity but that of the temperature course is depicted. Each temperature peak indicates nucleation

of the stable phase, the induction times at different temperatures being reproducible within a certain time period. Since the duration of the transformation experiments exceeded 150 hours with *batch 2*, further experiments have been carried out to find possible reasons.
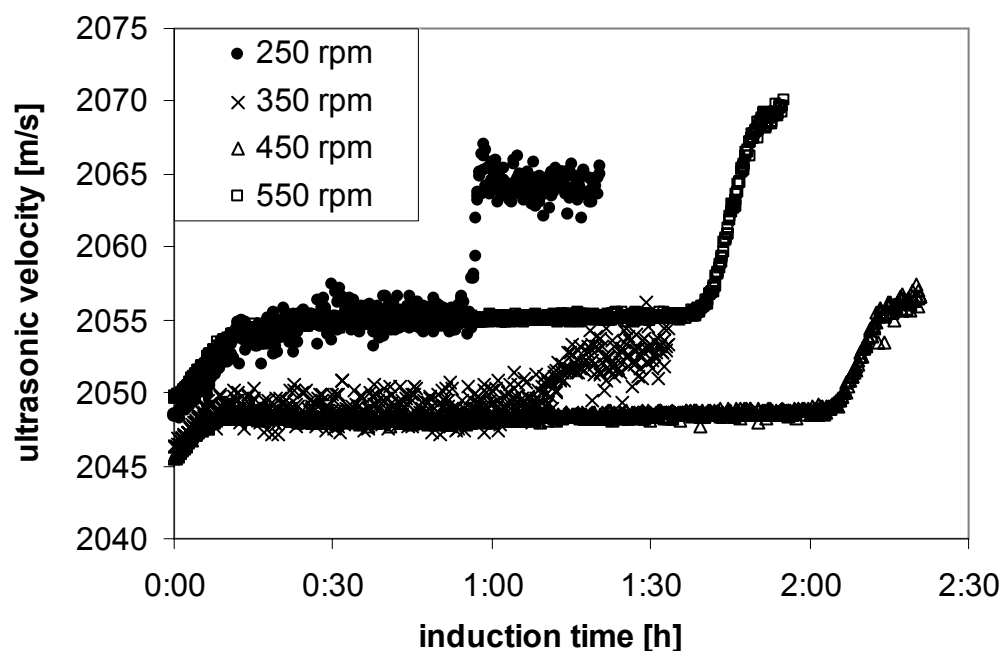
Fig. 5.2-4. Batch 3: Influence of the stirring rate on induction times
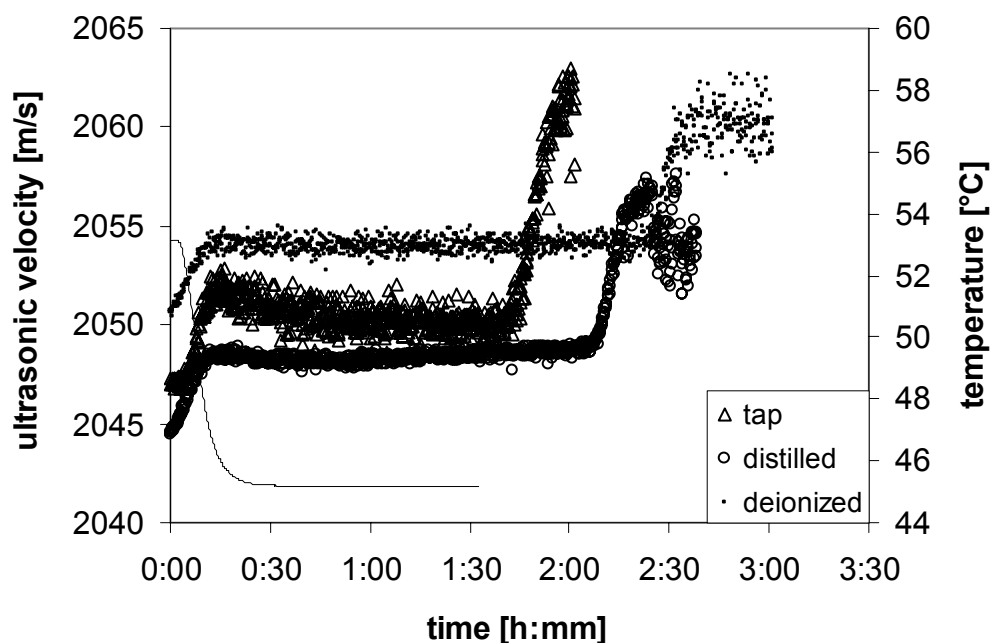
**Fig. 5.2-5.** Batch 3: Influence of the quality of the water on induction times

With *batch 3* the influence of fluid dynamics and the quality of the solvent on the induction time has been explored, the results being shown in *Figures 5.2-4* and *5.2-5*, respectively. These results indicate that differences in both, fluid dynamics and the quality of the

solvent, cannot be held responsible for the distinct difference in the induction times of two different batches.

Therefore, the assumption is near at hand that said differences between the induction times of different batches are caused by traces of impurities in the respective batches. It is known that the kinetics of solution-mediated phase transformations can depend on the purity of the system and even amounts on the ppm-level can have a pronounced effect on the induction time /BEC96/. Therefore, the strong influence of KCl on the phase transformation experiments conducted with *batch 1* is possibly due to the interaction of KCl with another impurity, not being present at this level in the other batches.

Phase transformations with magnesium sulfate indicate the presence of a latent period, which is supported by photographs taken in the course of a phase transformation experiment, showing single crystals of the stable phase prior to noticeable nucleation. Noticeable nucleation of the stable phase, magnesium sulfate heptahydrate, starts after ca. 19 hours, whereas single crystals of the stable phase have already been observed after less than 3 hours (see *Figures 4.2-7* and *4.2-8*).

Experiments in the microscopic cell have shown that in the course of a phase transformation crystals of the stable phase grow onto the dissolving metastable phase (see *Figure 4.2-1*). The same applies to solution-mediated phase transformations in agitated solutions in a crystallizer , supported by the photographs shown in *Figure 5.2-5*.
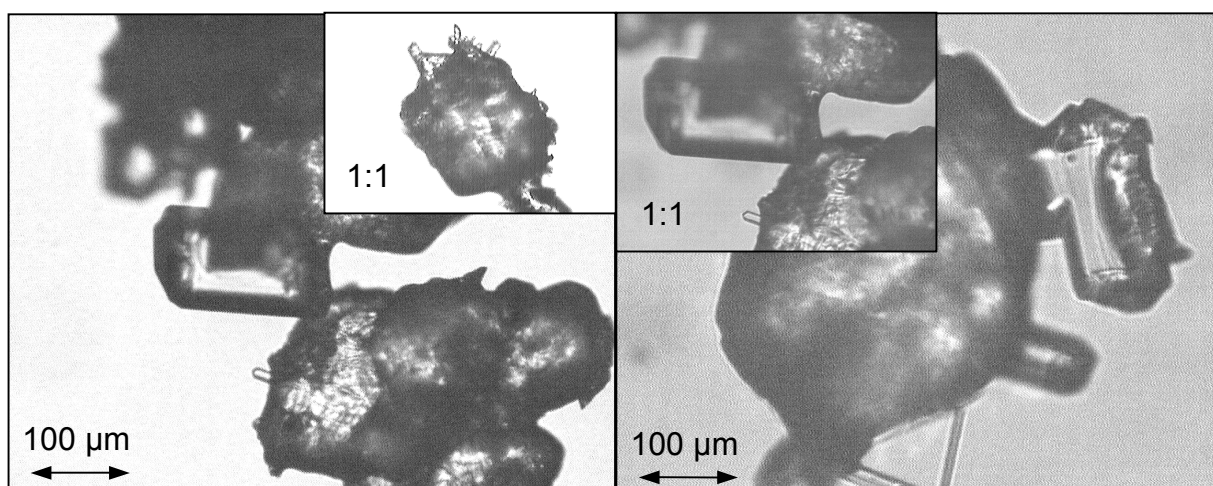
Fig. 5.2-5. Course of the phase transformation of magnesium sulfate hexahydrate to the heptahydrate

The pictures depicted in *Figure 5.2-5* have been taken directly after noticeable nucleation of the stable phase and it can be seen that crystals of the stable phase grow onto the crystals of the metastable phase. However, this behavior has not been observed during

the latent period; before noticeable nucleation only single independently growing crystals of the stable phase can be seen (see *Figure 4.2-8*).

5.2.1 Induction times

Induction times for phase transformations in aqueous magnesium sulfate solutions are depicted in *Figure 5.2-6*. The term "induction time" indicates the time until noticeable nucleation of the stable phase starts and it will not be differentiated between the induction period and the latent period as described in *section 2.1*. Accordingly, the term induction time does not mean the duration of the complete transformation, i.e. when all crystals of the metastable phase are dissolved.
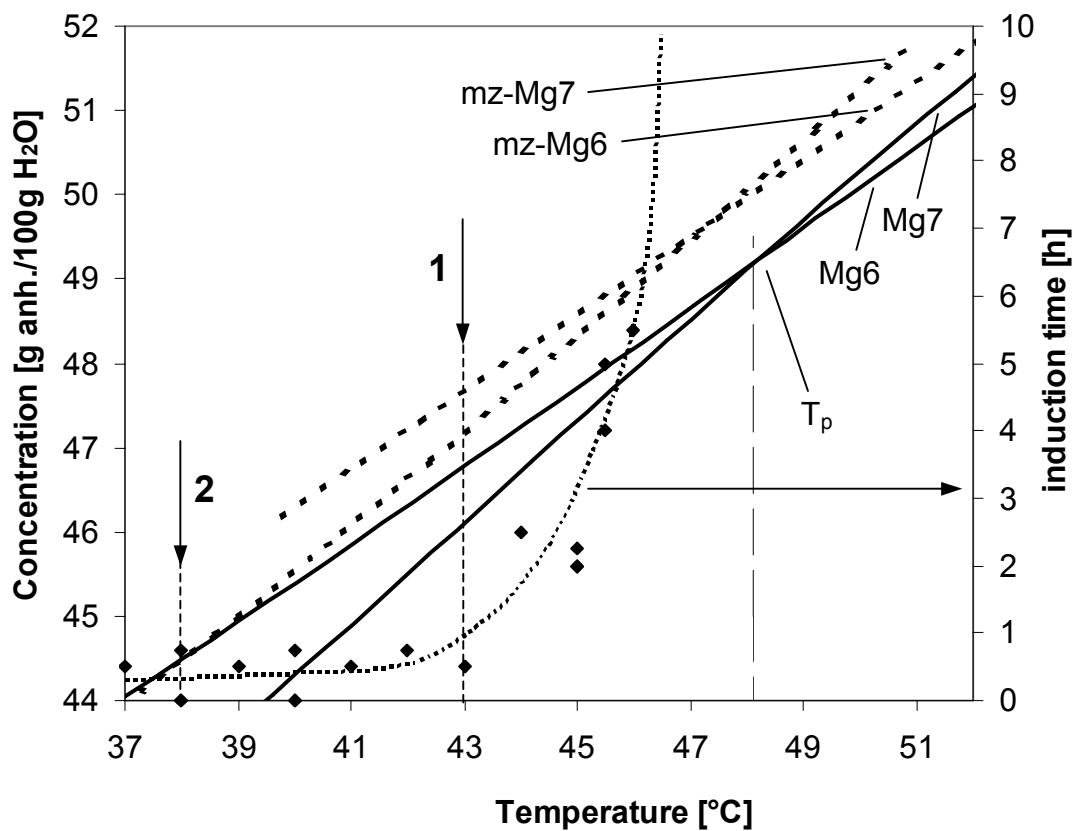
Fig. 5.2-6.   Induction times for magnesium sulfate solutions

Mg6   solubility of magnesium sulfate hexahydrate
mz-Mg6   metastable zone width of magnesium sulfate hexahydrate
Mg7   solubility of magnesium sulfate heptahydrate
mz-Mg7   metastable zone width of magnesium sulfate heptahydrate

The solubility curves and the metastable zones, for a cooling rate of ca. 10 K/h, have been idealized as linear lines. Data for the solubility and the metastable zone width of both hydrates can be found in the *appendix*, *section 14.4*.

As can be taken from *Figure 5.2-6*, the induction times tend to increase considerably at temperatures higher 43°C. Between 30°C and 43°C, nucleation of the stable phase started the latest after one hour and also at *point 2* of *Figure 5.2-6*, induction times of one hour have been monitored. This result is inconsistent with observations published by Nývlt /NYV97/, reporting that in phase transformation experiments nucleation of the stable phase starts spontaneously, if the solubility curve of the metastable phase is situated outside the metastable zone of the stable phase.

As can be seen in *Figure 5.2-6*, indeed all induction times at temperatures below *point 2* are less than one hour, however, this is also already given at temperatures below *point 1* where the solubility curve of the metastable phase is still well within the metastable zone of the stable phase. Since for the determination of the induction times a slightly higher cooling rate than for the determination of the metastable zone width has been employed, this result also cannot be weakened by possible variations of the cooling rate. The metastable zone during the transformation rate experiments should be broader not narrower – also in consideration of the error in measurement of the ultrasonic device - thus the intersection of the limit of the metastable zone with the solubility curve should even be at lower temperatures than indicated in *Figure 5.2-6*.

Therefore, phase transformations already started spontaneously under conditions in which they should only start after a certain induction time according to Nývlt's /NYV97/ assumption. In this case Nývlt's /NYV97/ rule of thumb does not seem to lead to satisfactory results. Shorter induction times for phase transformations rather seem to be determined by the higher difference between the solubilities of both phases at *point 1*, resulting in a high supersaturation with regard to the stable phase.

5.3   Discussion of errors

Since the sources of errors are identical for all experiments and do not depend on the substance, possible errors will only be discussed in this section, although also applying to the following sections.

The **solubility** has been determined optically with a thermometer having a temperature-scale with a subdivision of 0.1°C. To minimize the error, experiments have been repeated at least twice with a very slow heating rate of about 1 K/h. Although the results are subjective and depend on the person carrying out the experiments, a deviation of approximately ± 0.1°C seems to be appropriate.

The **metastable zone width** has been determined with the ultrasonic probe, measuring temperature and concentration with a precision of < ± 0.1°C and ± 0.1 m/s, respectively. However, not the onset of nucleation has been monitored, but the turbidity point and, therefore, the actual width of the metastable zone is smaller than indicated. In *Figure 5.3-1* a comparison between the maximum possible supercooling of magnesium sulfate solutions determined optically and by means of the ultrasonic probe, respectively, is shown (mean values of 3 measurements). The actual width of the metastable zone is still smaller than the value optically determined, since nuclei may only be optically observed when reaching approximately 10µm /MUL00/. Furthermore, it can be seen that the deviation

between optically determined values and the maximum possible supercooling determined with the ultrasonic probe increases with increasing cooling rate. In experiments with a cooling rate of 10 K/h the ultrasonic probe measures a metastable zone width being on an average ca. 0.5°C broader than the optically determined value.
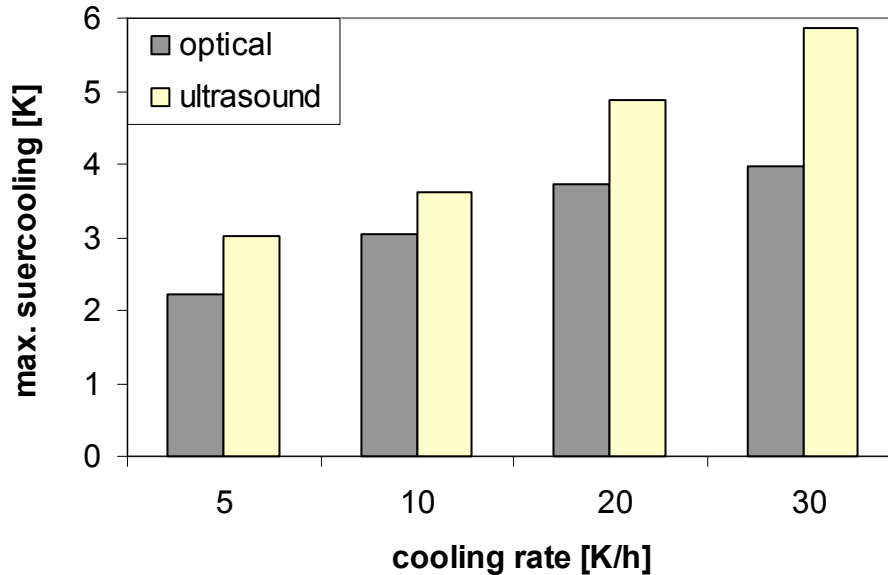
Fig. 5.3-1.   Metastable zone width: Determined optically and with the ultrasonic probe

In *transformation experiments*, the crystals in the suspension influence the result of the measurement with the ultrasonic probe and lead to higher values of the ultrasonic velocity, discussed in detail by /SAY02/. Extensive discussions of possible errors occurring during measurements in a *fluidized bed* and in a *microscopic cell* can be found in /KRU93/ and /MOH96/, respectively.

6   Zinc sulfate

The phase transformation of zinc sulfate hexahydrate to the heptahydrate has been monitored with the ultrasonic measuring technique. To follow the course of transformation, samples of crystals have been taken and evaluated by means of optical microscopy. Furthermore, induction times for nucleation of the heptahydrate have been determined at different temperatures.

6.1   Phase transformation

The transition temperature between zinc sulfate hexahydrate and the heptahydrate is 39°C /ROH02/.The hexahydrate is the stable form above the transition point, whereas the heptahydrate is stable below it. For the transformation experiments solutions with a saturation temperature of 44°C have been used. The solutions are cooled from an unsaturated state to 41°C, thus into the metastable zone of the hexahydrate. Nucleation of the hexahydrate starts after a certain induction time, as can be seen in *Figure 6.1-1*. When noticeable nucleation starts, a decrease of the ultrasonic velocity and a temperature peak can be observed. After nucleation the suspension is kept at 41°C for a while to assure that supersaturation is completely depleted by nucleation and subsequent growth of the crystals. Finally, the suspension is cooled with a linear cooling rate to 33.5°C. At ca. 34°C nucleation of the heptahydrate starts. Nucleation can be noticed by both, an increase in temperature and a drastic increase of the ultrasonic velocity. Until the end of the transformation, the suspension is kept at constant 33.5°C.
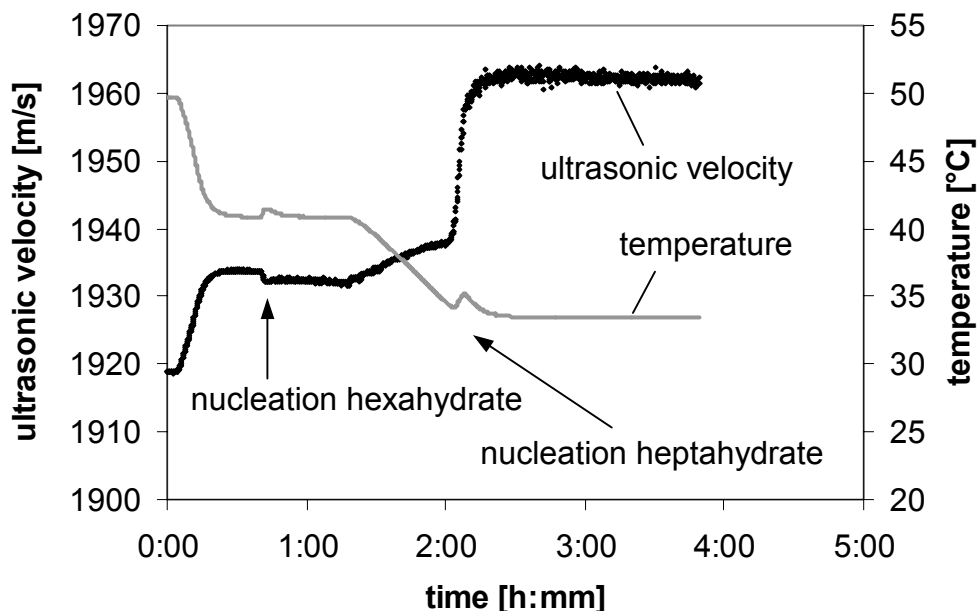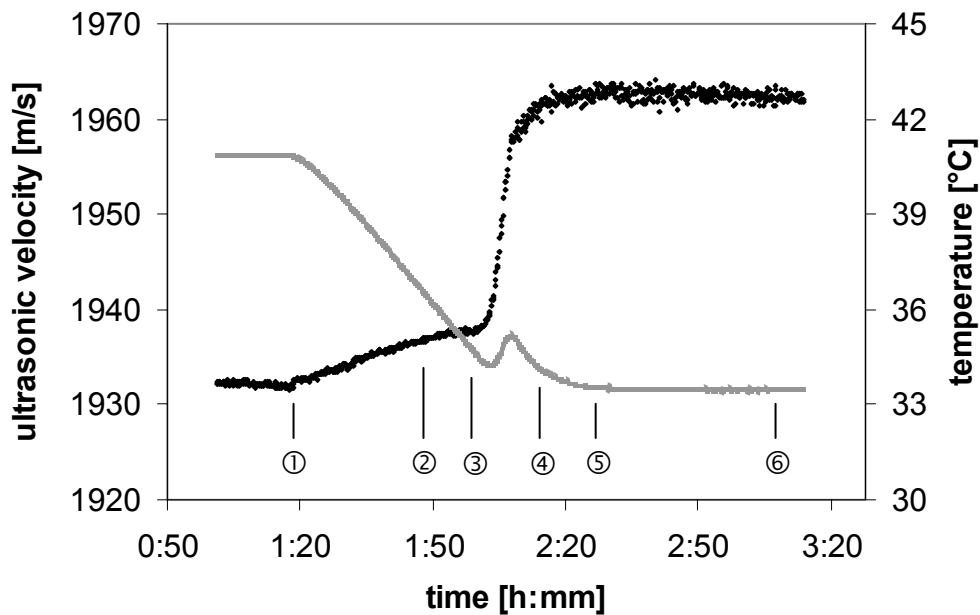

Fig. 6.1-1.   Solution-mediated transformation of zinc sulfate hydrates

Fig. 6.1-2.   Times of sampling in a phase transformation experiment

For optical evaluation of the experiment, samples have been taken at certain intervals. In *Figure 6.1-2*, the times are indicated at which samples of crystals have been withdrawn from the solution. *Figure 6.1-2* shows a detail of *Figure 6.1-1*.

The first sample (1) is taken at the beginning of cooling still above the transition temperature and the last sample (6) is taken at the end of the transformation, when only heptahydrate crystals are present in the solution. Photographs of these samples can be seen in *Figure 6.1-3*. Since different magnifications are used, the respective scale is plotted in each photograph.

In the first photograph, from the beginning of cooling, crystals of the hexahydrate can be seen. The fourth photograph is taken directly after nucleation has been detected by the ultrasonic measuring technique and the hexahydrate as well as the heptahydrate can be found. However, already before noticeable nucleation of the heptahydrate, single crystals of the heptahydrate can be detected, shown in photographs (2) and (3). About one hour after noticeable nucleation of the heptahydrate, no hexahydrate crystals can be found anymore in the sample (see sixth photograph).
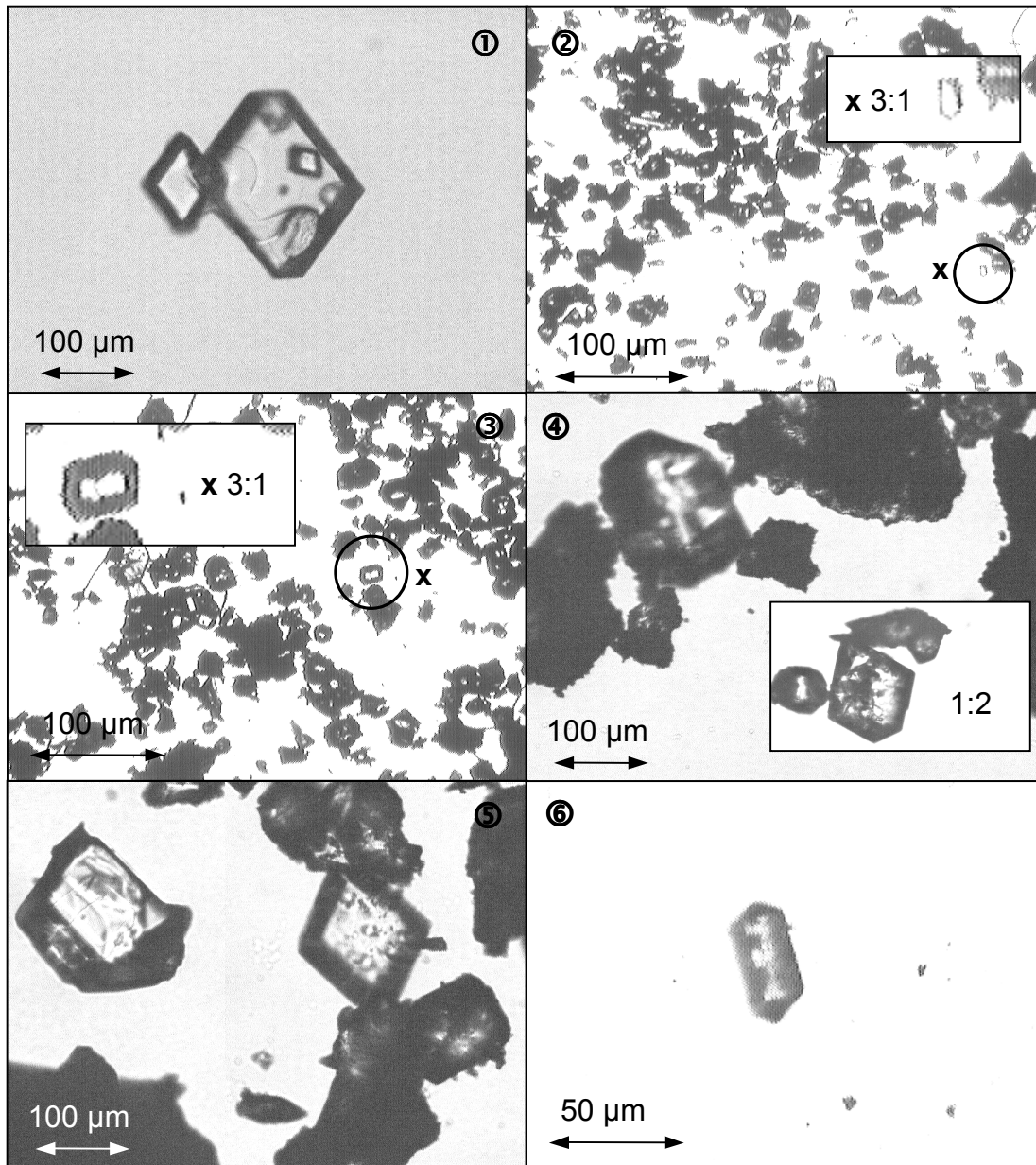
Fig. 6.1-3. Course of the phase transformation of zinc sulfate hexahydrate to the heptahydrate

①	41°C, 1h 20min	②	36.5°C, 1h 50min
③	34.5°C, 2h	④	34°C, 2h 15min
⑤	33.5°C, 2h 30min	⑥	33.5°C, 3h 10min

6.2 Induction times

Zinc sulfate solutions with a saturation temperature of 44°C have been prepared. In the course of the experiments, solutions are cooled to 41°C, into the metastable zone of the hexahydrate. After nucleation of the hexahydrate, the suspensions are kept at that temperature for at least 30 minutes to assure depletion of supersaturation by crystal growth. Subsequently, the suspensions are cooled to different temperatures below the

transition temperature, which is 39°C according to /ROH02/. The induction times for nucleation of the stable phase have been measured by means of the ultrasonic technique. For this set of experiments, the induction time is defined as the time between reaching the final transition temperature and the start of nucleation of the heptahydrate.

An induction time of zero, i.e. nucleation starts instantaneously when the transformation temperature is reached, is shown in *Figure 6.2-1*.
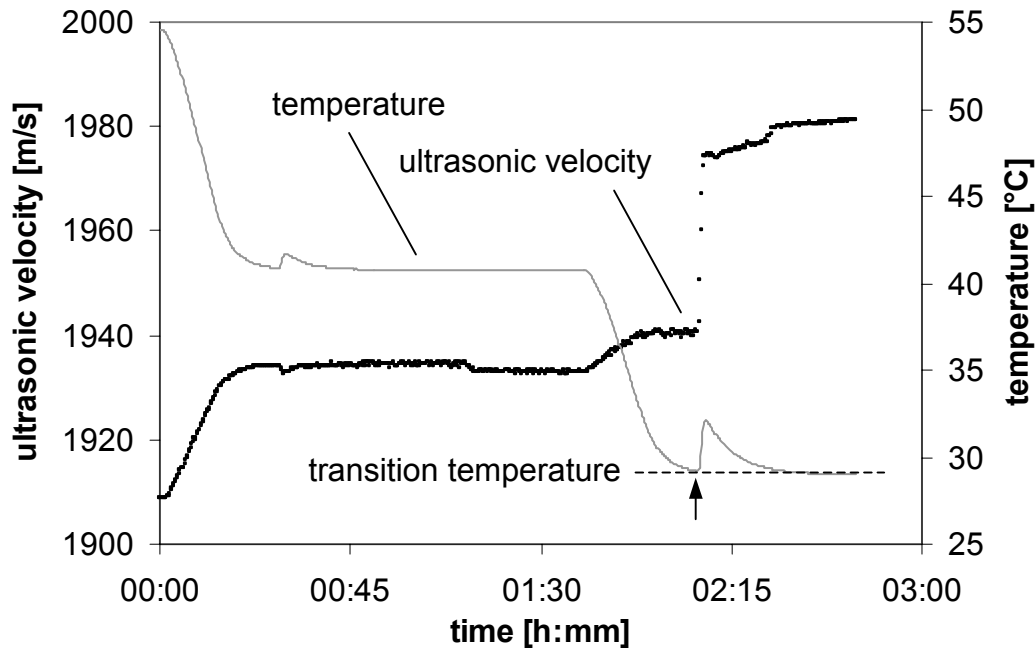
Fig. 6.2-1. Instantaneous nucleation in a phase transformation experiment

As can be seen from *Figure 6.2-1*, nucleation of the heptahydrate – marked by the arrow - starts directly after the final transition temperature of 29°C has been reached.
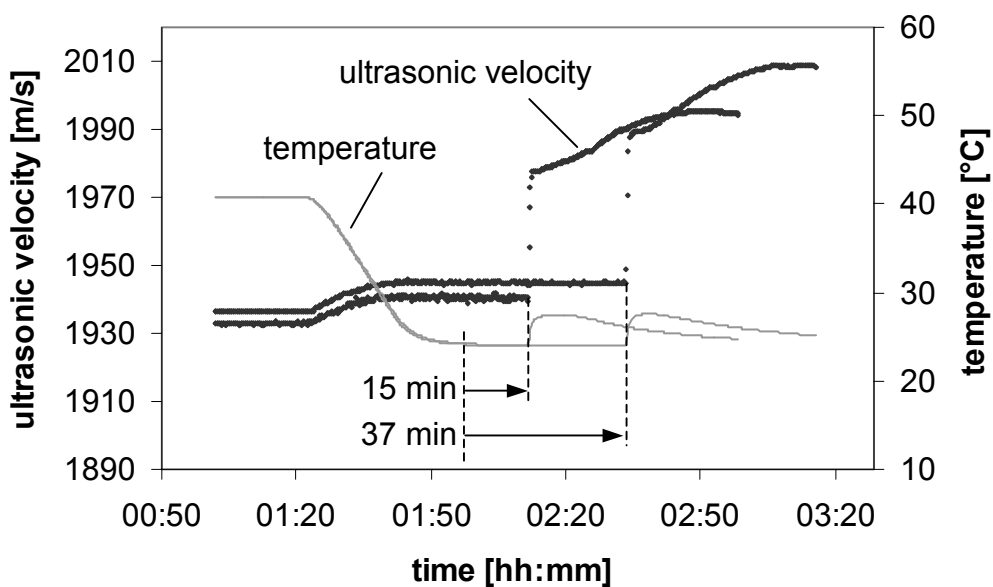

Fig. 6.2-2. Different induction times at 24°C in phase transformation experiments

Examples for longer induction times can be seen in *Figure 6.2-2*. The induction times have been determined with the ultrasonic measuring technique at a constant temperature of 24°C. At this temperature, the induction times differ only slightly. In one experiment noticeable nucleation starts after 15 minutes and in the other experiment after 37 minutes. Nucleation can be seen by both, increase in temperature and in ultrasonic velocity.

However, also larger differences between induction times at one temperature occur, as shown in *Figure 6.2-3*. Both experiments have been carried out at 32°C. In *Figure 6.2-3*, like in the previous diagrams, the ultrasonic velocity is represented by black rhombs and the course of temperature by a thin gray line. The starting point of nucleation of the heptahydrate can again be seen by a distinct increase in ultrasonic velocity and a temperature peak.

In this case, the induction times vary between approximately 30 minutes (see detail in *Figure 6.2-3*) and nearly 49 hours. Induction times for zinc sulfate solutions in a temperature range between 20 and 35°C are summarized in *Figure 6.2-4*.

In *Figure 6.2-4*, induction times for nucleation as a function of temperature are shown. Results of experiments in the temperature range from 20 to 34°C are depicted in the diagram. Temperatures below 20°C could not be reached, because in the respective experiments nucleation already started during cooling, i.e. before the final transition temperature had been reached. At temperatures higher 34°C the induction times exceed 200 hours and experiments had finally been interrupted. It can be seen from *Figure 6.2-4*, that the induction times start to increase considerably at temperatures around 30°C. Below 30°C, induction times between zero and eight hours can be observed. All experiments in the temperature range between 20 and 29°C have been repeated at least three times with very reproducible results. However, looking at *Figure 6.2-4*, it appears that in two experiments the induction times are significantly longer.
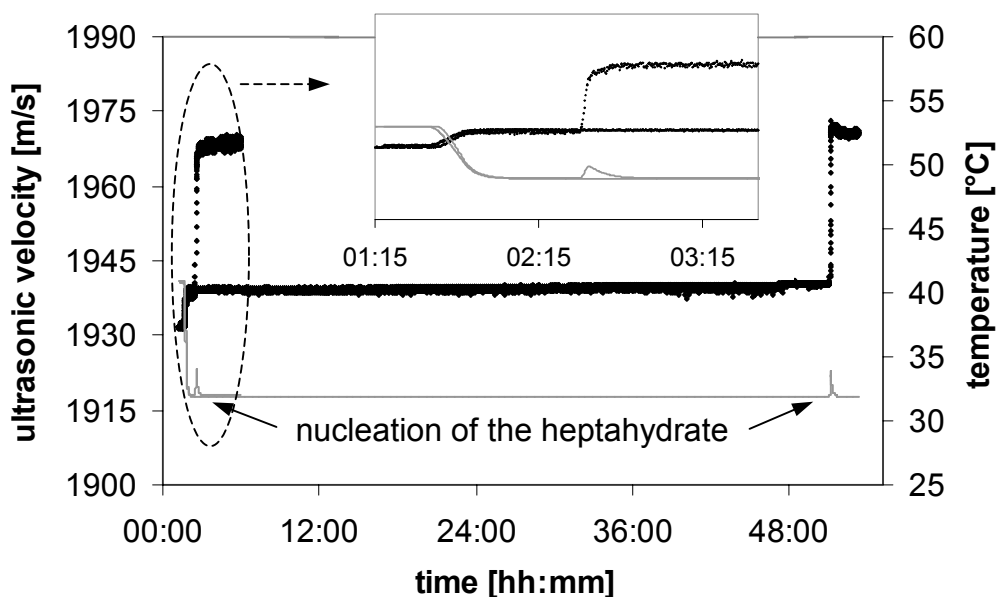
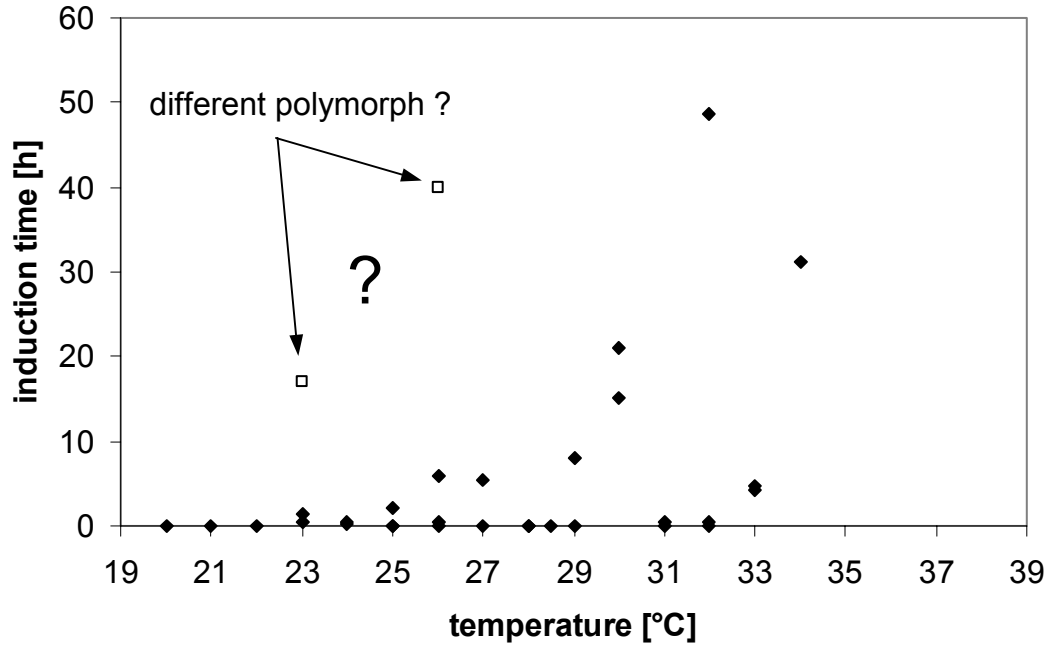**Fig. 6.2-3.** Induction times at 32°C in phase transformation experiments

Fig. 6.2-4. Induction times for zinc sulfate solutions

Exemplarily results for measurements carried out at 23°C are shown in *Figure 6.2-5*. In one experiment nucleation starts after 17 hours, whereas an induction time between 30 minutes and one and half hours in two other experiments had been measured (for a better lucidity only two experiments are depicted in *Figure 6.2-5*).
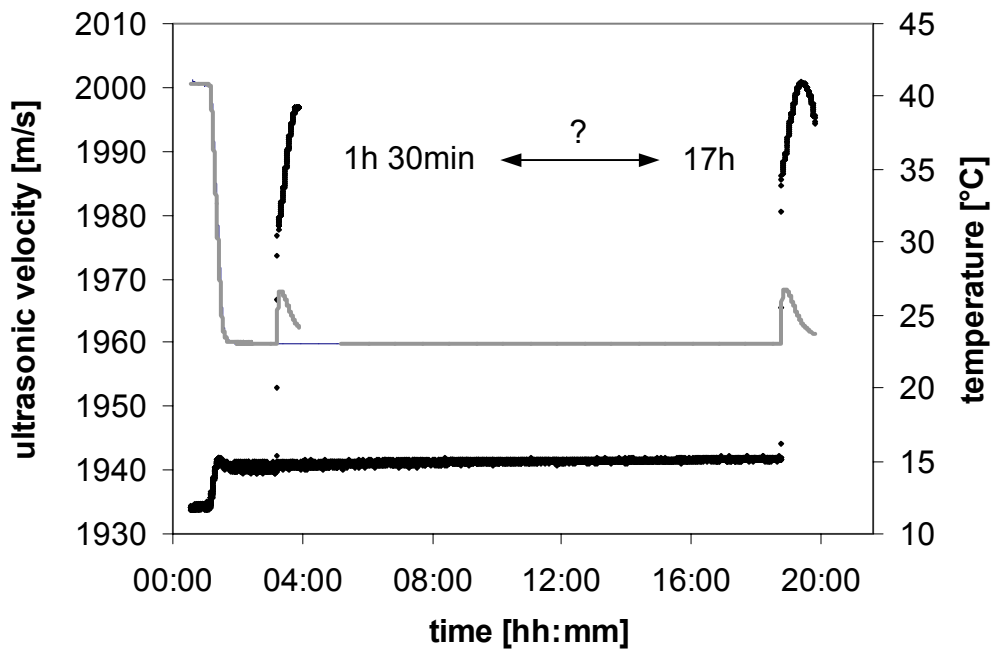

Fig. 6.2-5. Induction times at 23°C

7. Discussion of the results for zinc sulfate

The existence of a latent period for phase transformations in aqueous zinc sulfate solutions has been established by means of optical microscopy as well as by the measurement of crystal size distributions during phase transformation experiments. Furthermore, it is shown that the upper and the lower limit of inductions times for phase transformations can be described by an Arrhenius-function and different stages of stability for phase transformations are indicated.

7.1 Phase transformation

In addition to the measurement of the ultrasonic velocity, also the particle size distribution during a phase transformation experiment has been monitored. The result of this experiment, which has been carried out as described in *section 6.1*, is shown in *Figure 7.1-1*.

The measuring system needs a certain number of "counts" to work reliable, which is given when nucleation of the hexahydrate starts, indicated by (1). After the start of nucleation, the mean crystal size decreases due to further nucleation. After approximately 1 hour and 50 minutes, thus 30 minutes after nucleation started, the supersaturation is depleted by nucleation and crystal growth and the mean crystal size reaches a constant value. During cooling to the final transition temperature of 30°C, a slight increase in the mean crystal size can be observed, indicating that the metastable crystals in suspension grow. The mean crystal size stays almost constant after reaching the transition temperature.
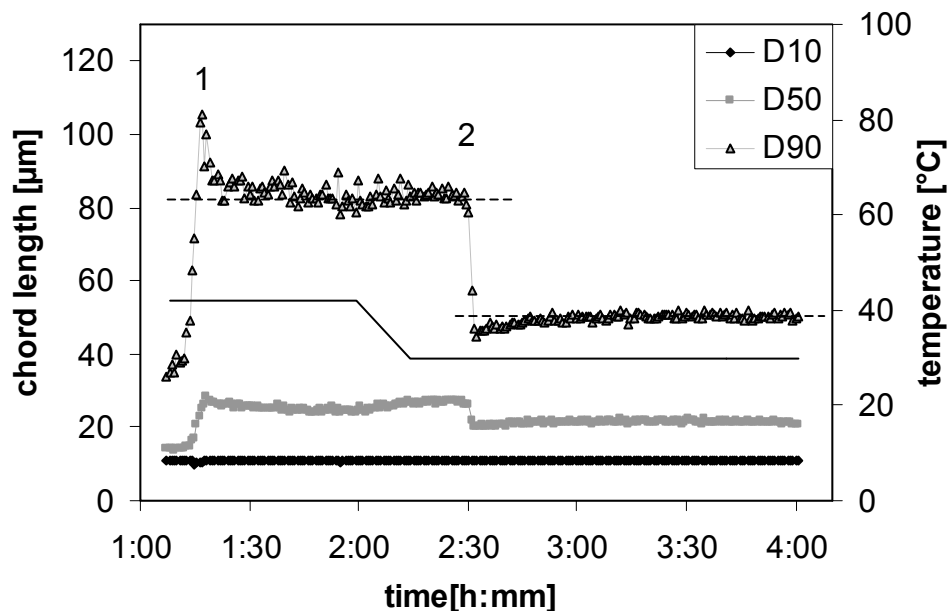
Fig. 7.1-1.   Particle size distribution during a phase transformation experiment

However, approximately 5 to 10 minutes before noticeable nucleation starts, the mean crystal size decreases slightly, indicating the start of nucleation. This can be taken as a proof for the so-called "latent period", meaning that after the end of the induction time and the start of nucleation, a certain time period elapses until rapid desupersaturation occurs. The presence of a latent period is also supported by photographs taken in the course of a phase transformation experiment, showing single crystals of the stable phase prior to noticeable nucleation (see *Figure 6.1-3*). Noticeable nucleation (2) of the stable phase, zinc sulfate heptahydrate, starts after ca. 2 hours and 30 minutes and is accompanied by a drastic decrease in the mean crystal size. Again, after about 30 minutes the supersaturation is depleted and a dynamic equilibrium is reached. The mean crystal size stays constant during the next 30 minutes.

7.2 Induction times

Induction times for phase transformations in aqueous zinc sulfate solutions are depicted in *Figure 7.2-1*. It should be noted, though, that the term "induction time" as it is used here, indicates the time until noticeable nucleation of the stable phase starts. In this case, it will not be differentiated between the induction period and the latent period. Furthermore, the induction time does not indicate the duration of the complete transformation, i.e. when all crystals of the metastable phase are dissolved.
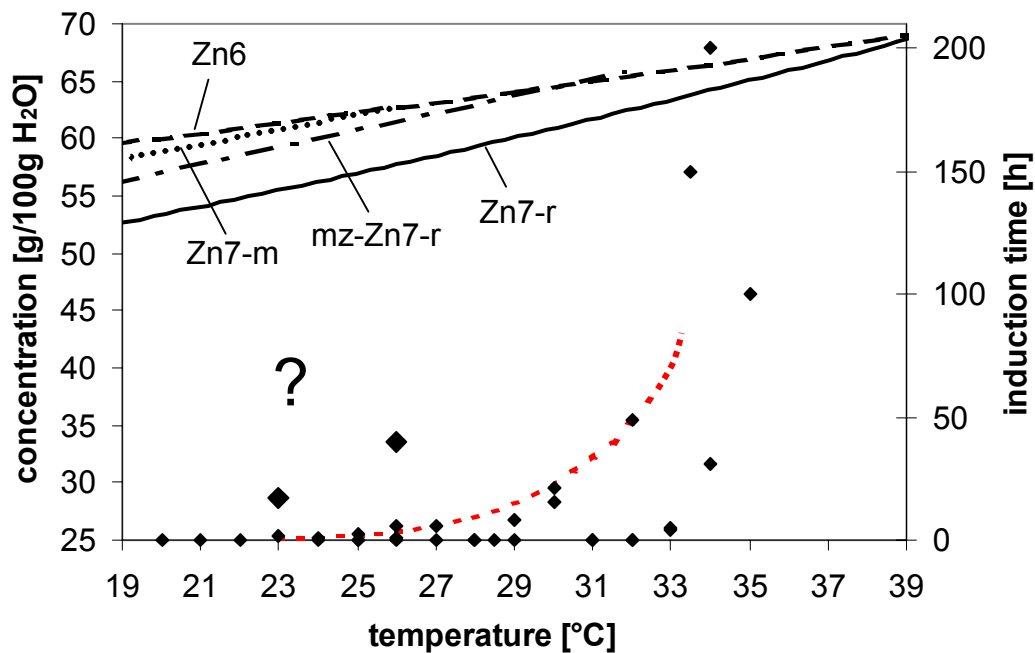

Fig. 7.2-1.   Induction times for zinc sulfate solutions

Zn6   solubility of zinc sulfate hexahydrate
Zn7-m   solubility of zinc sulfate heptahydrate monoclinic (metastable)
Zn7-r   solubility of zinc sulfate heptahydrate rhombic (stable)
mz-Zn7-r   metastable zone width of the rhombic zinc sulfate heptahydrate

The solubility curves and the metastable zone width, for a cooling rate of ca. 20 K/h, have been idealized as linear curves. Data for the solubility of the rhombic zinc sulfate heptahydrate is listed in the *appendix, section 14.7*, whereas the solubility data for the metastable monoclinic heptahydrate and the hexahydrate is taken from /GME56/.

In the temperature region experimentally covered, the maximum induction time for phase transformations of the metastable $ZnSO_4 \bullet 6H_2O$ into the stable $ZnSO_4 \bullet 7H_2O$ can be estimated by an Arrhenius-function:

$$t_{ind} = 4.935736875 \bullet 10^6 \bullet exp\ (-369.135 \bullet T^{-1}) \hspace{3cm} \textbf{(7.2-1)}$$

As can be seen from *Figure 7.2-1*, at temperatures higher 30°C the induction times considerably tend to increase. This result is consistent with observations published by Nývlt /NYV97/. Nývlt reported that nucleation of the stable phase in phase transformations starts spontaneously, if the solubility curve of the metastable phase is situated outside the metastable zone of the stable phase, whereas nucleation starts only after a certain induction time, if the solubility curve of the metastable phase lies within the metastable zone of the stable phase.

However, no such sharp division of the sections can be seen in *Figure 7.2-1*. The metastable zone of the heptahydrate intersects the solubility curve of the hexahydrate at approximately 30°C. Although below 30°C smaller induction times have been monitored with the ultrasonic measuring technique, spontaneous nucleation of the stable phase did
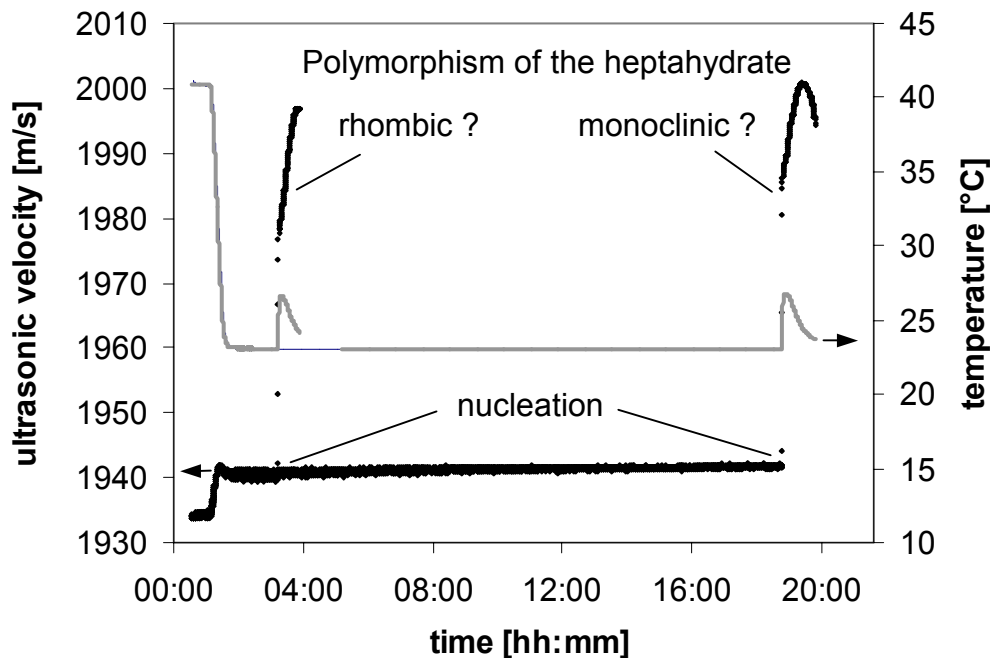

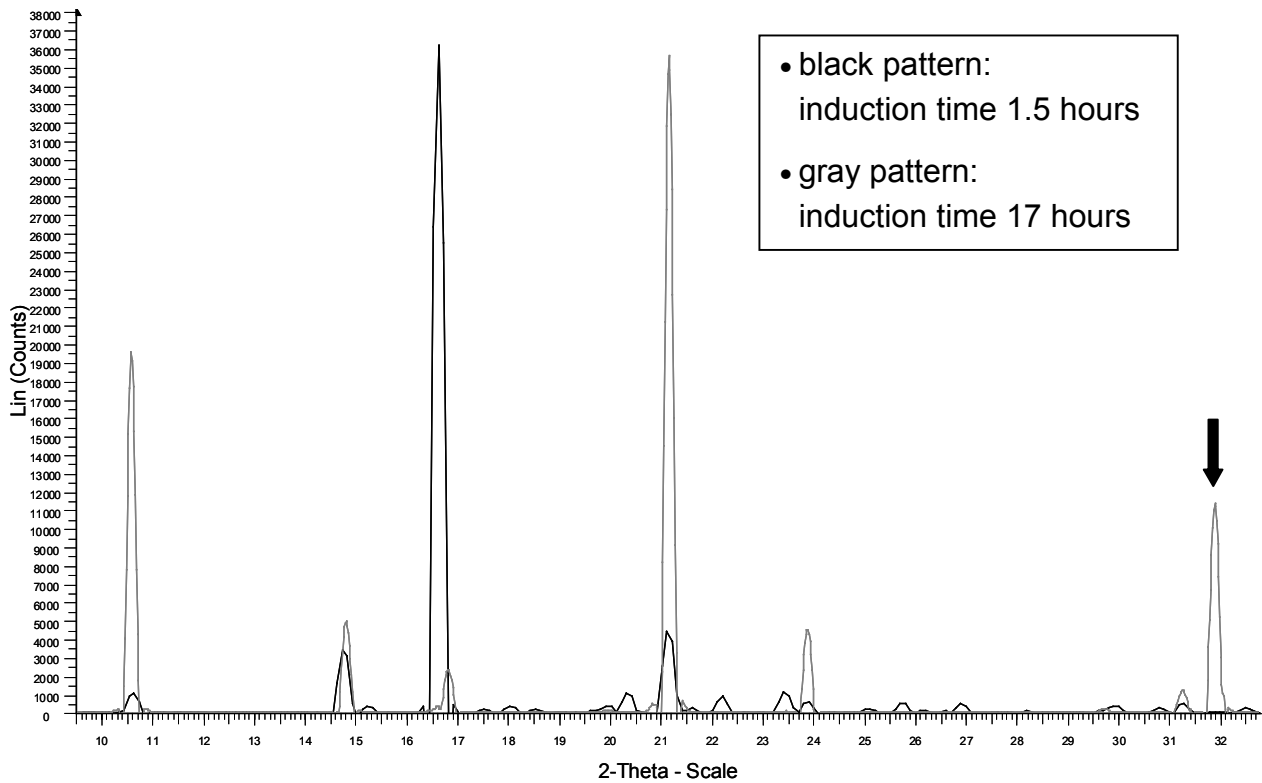**Fig. 7.2-2.**   Induction times for nucleation of the heptahydrate at 23°C

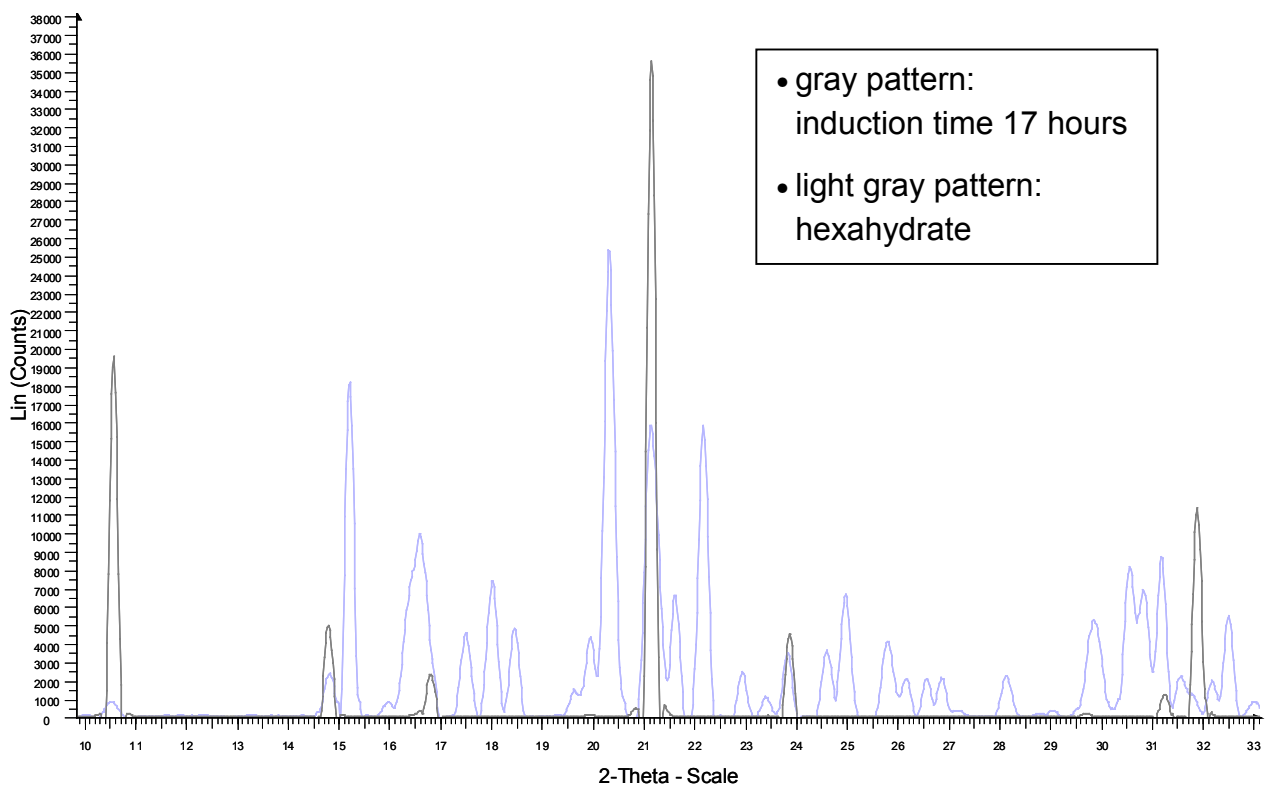**Fig. 7.2-3.**   PXRD-patterns of the crystals sampled at 23°C

Fig. 7.2-4.   PXRD-patterns of the hexahydrate and the crystals sampled at 23°C

not take place in all cases. This might be explained by the limit of the metastable zone of the heptahydrate, which depends on a variety of process parameters and cannot be taken as a "fixed line". For this reason, there is a strong presumption that in some experiments the solubility curve of the hexahydrate and the limit of the metastable zone of the heptahydrate intersect at lower temperatures, depending e.g. on the actual cooling rate employed. Still, in two experiments at 23 and 26°C significantly longer induction times have been monitored that cannot be explained by the aforementioned presumption. In *Figure 7.2-2*, the induction times for two experiments carried out at 23°C are shown. In both experiments, crystals have been sampled after nucleation and have been analyzed with PXRD (see *Figures 7.2-3* and *7.2-4*).

A comparison of the PXRD-patterns of the crystals sampled in different experiments at 23°C is depicted in *Figure 7.2-3*. The pattern of the crystals sampled after 1.5 hours is in good agreement with a pattern of the product crystals of zinc sulfate heptahydrate (not shown here). Therefore, this pattern shows most probably the phase stable at that temperature, the rhombic zinc sulfate heptahydrate. The most obvious difference between the two patterns of the crystals sampled at 23°C is the peak at $2\theta \approx 32$, indicated by the arrow. Moreover, the pattern of the crystals sampled after 17 hours has also been compared to a pattern of the hexahydrate (see *Figure 7.2-4*). Since this peculiar peak can neither be found in the pattern of the hexahydrate nor in the pattern of the stable heptahydrate, it is assumed that a phase different from the hexahydrate and the stable heptahydrate crystallized after 17 hours.

In literature /GME56/ is reported that two polymorphs of the heptahydrate exist, a metastable monoclinic form and the stable rhombic heptahydrate. Therefore, it is relatively save to assume that the significant deviations in the induction times at 23 and 26°C can be explained by the polymorphism of the heptahydrate, and that after 17 hours the metastable monoclinic heptahydrate had crystallized. However, this cannot be said with absolute certainty, because no PXRD-pattern for the monoclinic heptahydrate has been found in literature for comparison.

The deviations below 26°C may be explained by the polymorphism of the heptahydrate under the assumption that the actual metastable zone width is broader than illustrated in *Figure 7.2-1*. This hypothesis is supported by the fact that also in other phase transformation experiments at 23 and 26°C, nucleation of the stable phase did not always start spontaneously. When the actual metastable zone width is broader, the solubility curve of the monoclinic heptahydrate is crossed before the metastable zone of the rhombic heptahydrate is left. In this case, the outcome depends on the relative nucleation rates of the two polymorphs, and if the rhombic heptahydrate fails to nucleate spontaneously, it is likely that after a certain induction time the metastable monoclinic heptahydrate nucleates.
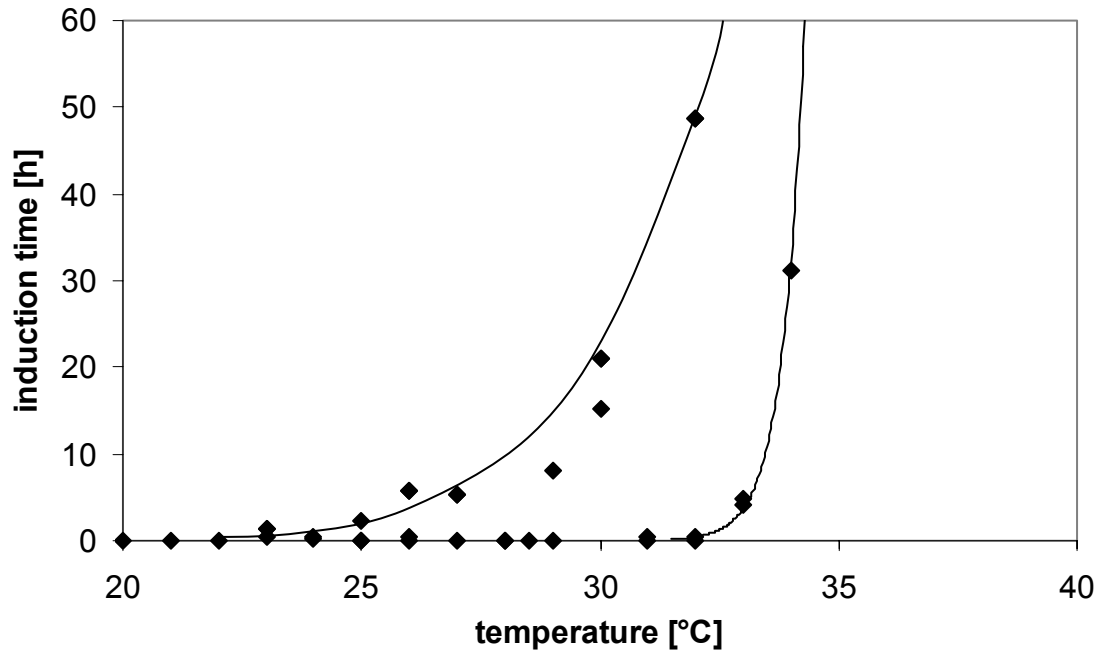
Fig. 7.2-5. Upper and lower limits for induction times in zinc sulfate solutions

The upper limit for phase transformations, i.e. the maximum induction time, can be described with an Arrhenius-function, as illustrated in *Figure 7.2-1*. In *Figure 7.2-5* is shown that also the lower limit, i.e. the minimum induction time until phase transformations occur, can as well be described with an Arrhenius-function. This dependence is even more evident when the data is depicted on a simple-logarithmic scale, shown in *Figure 7.2-6*.
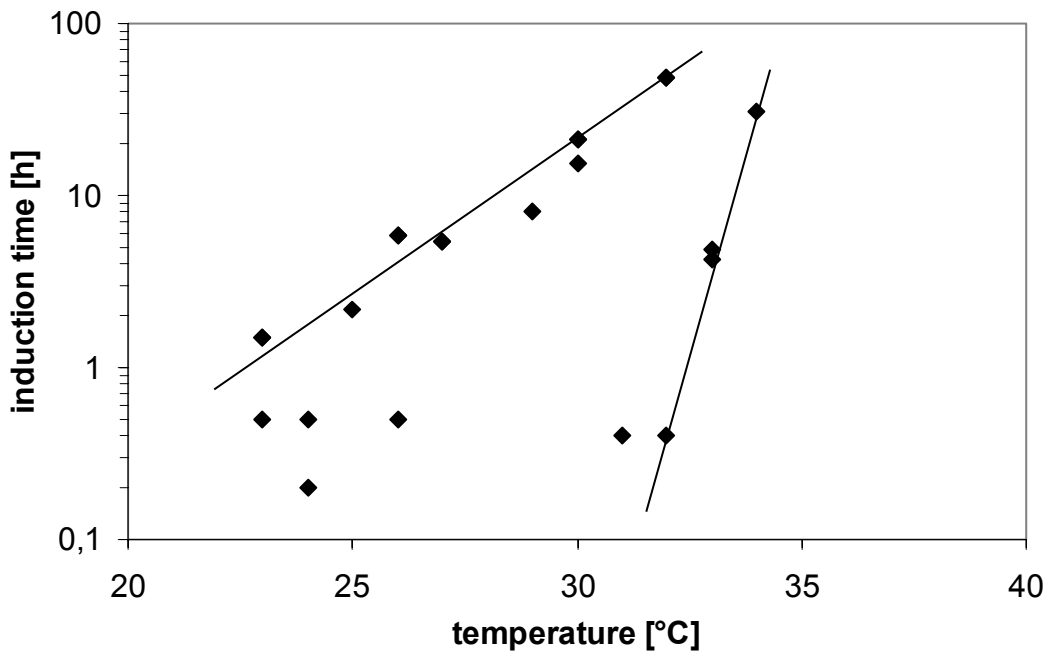
Fig. 7.2-6. Limits for induction times in zinc sulfate solutions

As can be seen in *Figure 7.2-6*, both, the upper and the lower limit for phase transformations, can be described by a straight line. This result is emphasized by a standardized representation of the stages of stability for phase transformations in *Figure 7.2-7*.
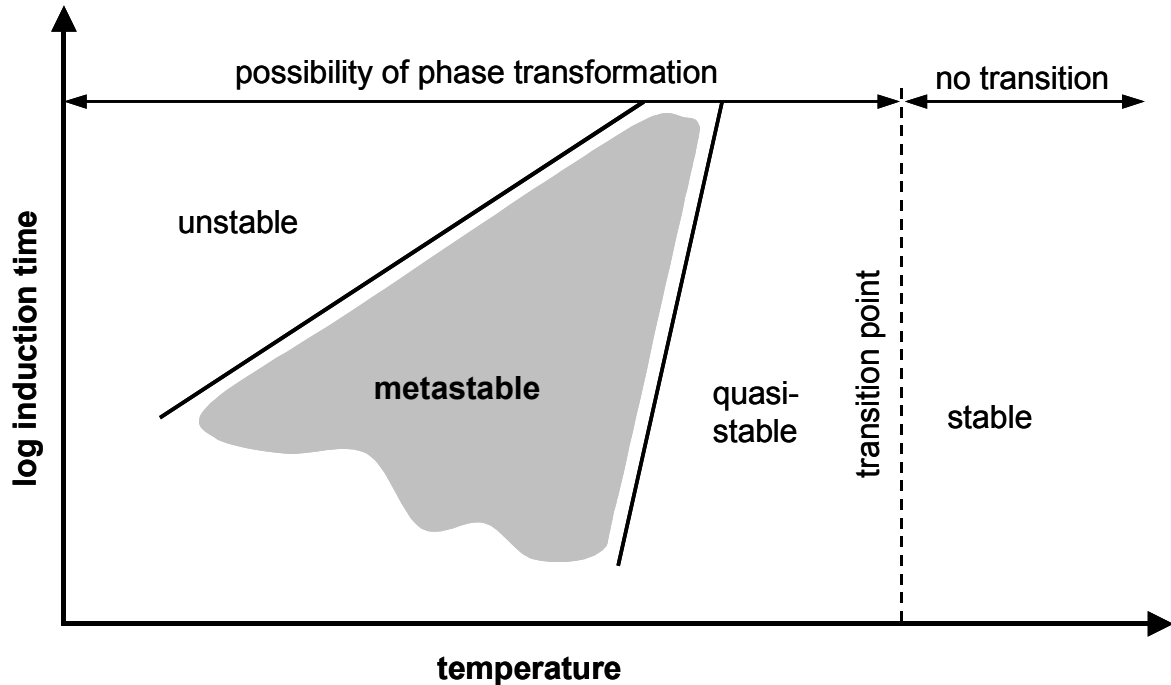
Fig. 7.2-7. Stages of stability for phase transformations

Different stages of stability are described in *Figure 7.2-7*. In principle, no phase transformations take place in the stable region above the transition point. However, below the transition point the possibility of phase transformations is generally given. The area below the transition point can be subdivided into three different "stages of stability" – quasi-stable, metastable and unstable. In the quasi-stable region no phase transformations have been observed up to a certain induction time. Therefore, the quasi-stable region determines the lower limit for phase transformations. The metastable area is characterized by phase transformations occurring at the same temperature after different induction times, depending on the process conditions and, thus, it represents the upper limit for phase transformations. The unstable region has not been reached in the experiments, because nucleation of the stable phase always started when crossing the line of the metastable region.

8. Phase transformations of other substances

The applicability of the ultrasonic measuring technique for determining phase transformations has been tested. In *section 4* and *6*, aqueous solutions of two different inorganic salts, namely magnesium sulfate and zinc sulfate, have been used. In this section, experimental results for two further inorganic salts in aqueous solution (sodium tetraborate and calcium chloride), one organic substance in aqueous solution (l-phenyl-alanine) and one organic substance in an organic solvent (stearic acid in methanol) are presented. All substances are pseudopolymorphs, or hydrates in this case, except for stearic acid which exhibits polymorphism.

8.1 Borates

The response of the ultrasonic velocity during the phase transformation of $Na_2B_4O_7 \bullet 5H_2O$ to $Na_2B_4O_7 \bullet 10H_2O$ is shown in *Figure 8.1-1*. The transition point of the penta- and the decahydrate is approximately 60.8°C /SMI02/. Above the transition temperature, the pentahydrate is the stable form, whereas the decahydrate is stable at temperatures below the transition point.

A solution, which is saturated at 75°C, has been cooled to 65°C. After an induction time of 15 minutes, nucleation of the pentahydrate starts, indicated by a distinct decrease of the ultrasonic velocity. The suspension is kept at 65°C for some time to assure depletion of supersaturation by nucleation and subsequent growth of the pentahydrate crystals. In the course of the experiment, the suspension is cooled to 55°C, i.e. below the transition temperature. After a short induction period, nucleation of the decahydrate sets in, causing a temperature peak as well as a sudden increase of the ultrasonic velocity.
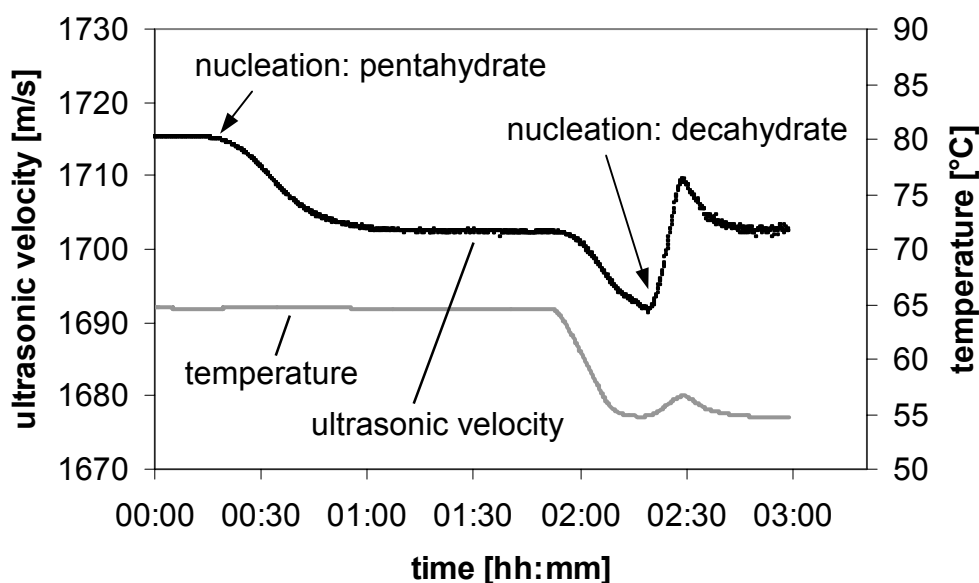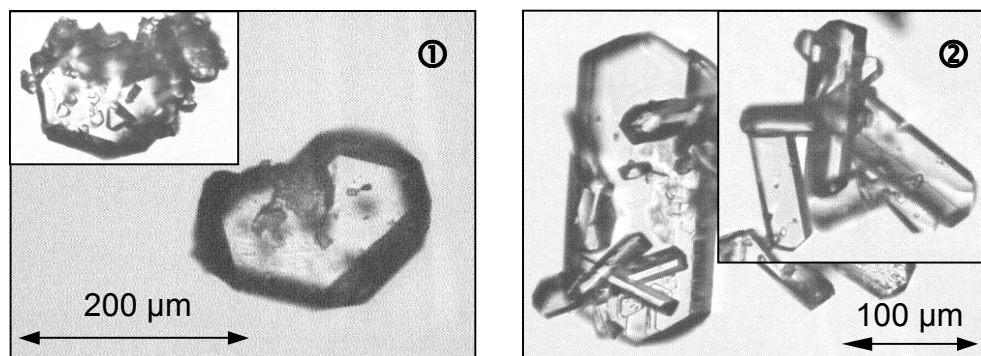

**Fig. 8.1-1.**   Solution-mediated transformation of borate hydrates

Fig. 8.1-2.   Borates (1) 65°C, (2) 55°C

Samples of sodium tetraborate hydrates taken during the experiment are shown in *Figure 8.1-2*. In *Figure 8.1-2 (1)* crystals taken out from suspension after nucleation at 65°C are shown. The crystals withdrawn from solution shortly after nucleation at 55°C, which are presented in the second photograph (2), have a different morphology than the crystals sampled at higher temperatures.

8.2   Calcium chloride

The solution-mediated phase transformation of $CaCl_2 \cdot 2H_2O$ to $CaCl_2 \cdot 4H_2O$ has also been monitored by the ultrasonic measuring technique (see *Figure 8.2-1*). The transition temperature of these two hydrates is approximately 45.3°C /KEM02/, the tetrahydrate being stable below this temperature, whereas the dihydrate is stable above this temperature.

In this experiment, a solution saturated at 65°C is cooled from an unsaturated state to 50°C at a constant rate. At about 51°C, nucleation of calcium chloride dihydrate starts, which can best be seen by the slight increase of the ultrasonic velocity, indicated by (1). The suspension is kept at that temperature for a certain period of time to assure the complete depletion of supersaturation by nucleation and subsequent crystal growth. In the course of the experiment, the suspension is then cooled to 35°C. It can be read from *Figure 8.2-1* that nucleation of the stable tetrahydrate starts after an induction period of approximately 45 minutes. The starting point of nucleation is indicated by a temperature peak as well as by a sudden increase of the ultrasonic velocity (2). During nucleation and subsequent growth of the tetrahydrate, the suspension density increases and so does the ultrasonic velocity. As the suspension density increases further, a point is reached where the ultrasonic velocity drastically decreases and finally the measuring technique is not able to detect the medium anymore (3).
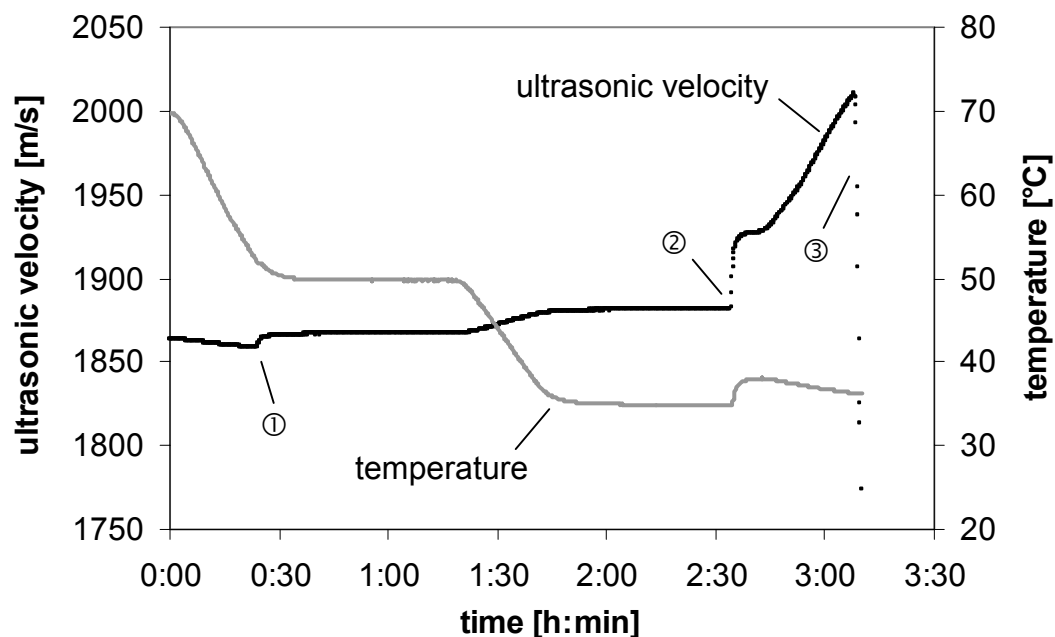
Fig. 8.2-1. Phase transformation of calcium chloride hydrates

① nucleation of the dihydrate
② nucleation of the tetrahydrate
③ measuring technique fails

Samples of calcium chloride crystals obtained during the experiment are shown in *Figure 8.2-2*. In *Figure 8.2-2 (1)*, a photograph of calcium chloride crystals withdrawn from suspension after nucleation at 51°C are presented. All crystals have an almost square shape. A photograph of crystals sampled after nucleation at 35°C is shown in *Figure 8.2-2 (2)*. In this photograph two different habits, designated "a" and "b", can be seen. Crystal habits "a" and "b" both differ distinctly from the habit of the crystals in *Figure 8.2-2 (1)*, indicating that two further crystalline forms have been obtained.
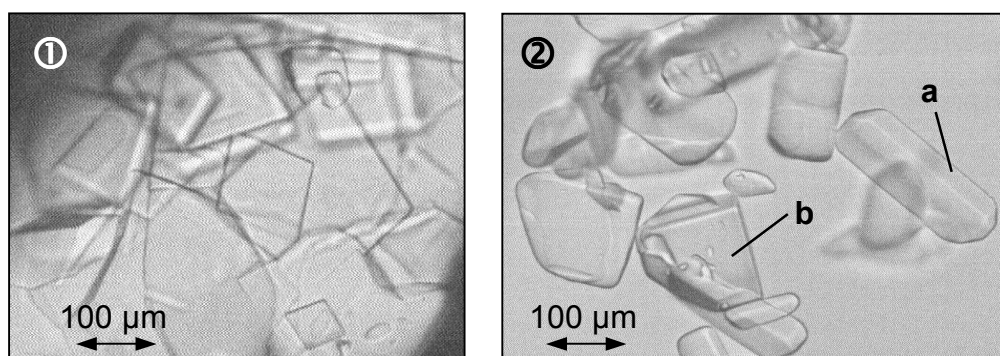

Fig. 8.2-2. Calcium chloride (1) 51°C, (2) 35°C

8.3 L-Phenylalanine

Two forms of l-phenylalanine are known, a hydrate and an anhydrous form. The transition temperature between the monohydrate and the anhydrous form is ca. 37°C /MOHN01/. Above the transition temperature, the anhydrate is the stable phase, the monohydrate being stable at lower temperatures.

The ultrasonic measuring technique has been applied to follow the phase transition of the anhydrous form to the monohydrate. In *Figure 8.3-1*, the result of a transformation experiment is shown.
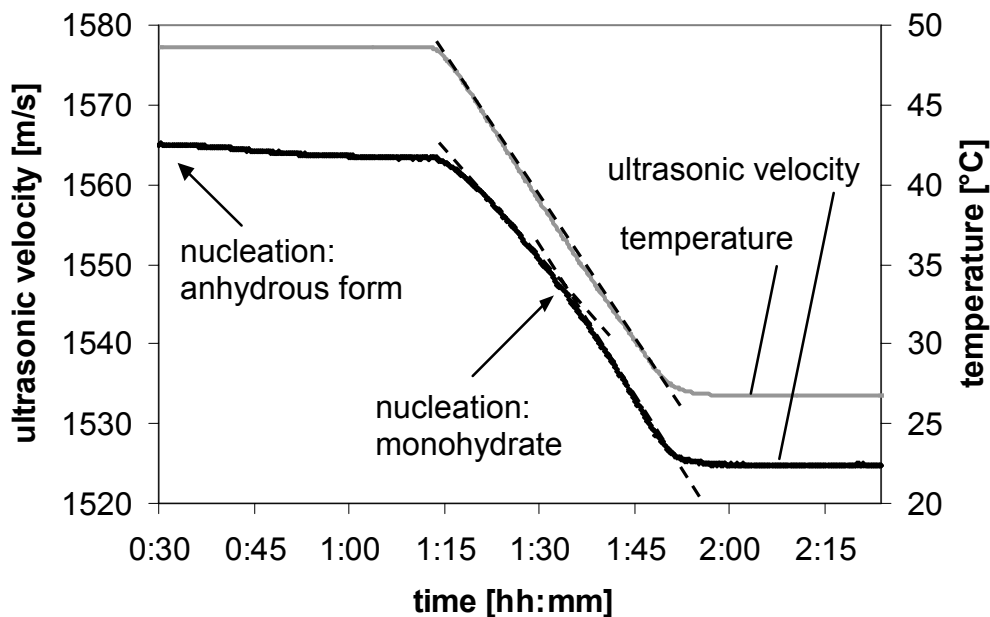
Fig. 8.3-1. Phase transformation of anhydrous l-phenylalanine to the monohydrate

A solution, saturated at 55°C, is cooled to 49°C. After an induction time of 30 minutes nucleation of the anhydrous form starts and the suspension is kept at that temperature further 45 minutes to deplete supersaturation by crystal growth. In the next step, the suspension is cooled to 27°C with a linear cooling rate. During cooling, at approximately 34.5°C, nucleation of the monohydrate is detected by means of the ultrasonic measuring device. However, no distinct change in ultrasonic velocity can be observed. By evaluating the response of the ultrasonic velocity during cooling and nucleation, a change in the gradient can be noted. Usually the ultrasonic velocity changes linearly when a linear cooling rate is employed, therefore this change in the gradient can be taken as an indication for nucleation of the new phase. Regarding the course of temperature during cooling and nucleation, no such change of the gradient or any temperature peak can be observed.
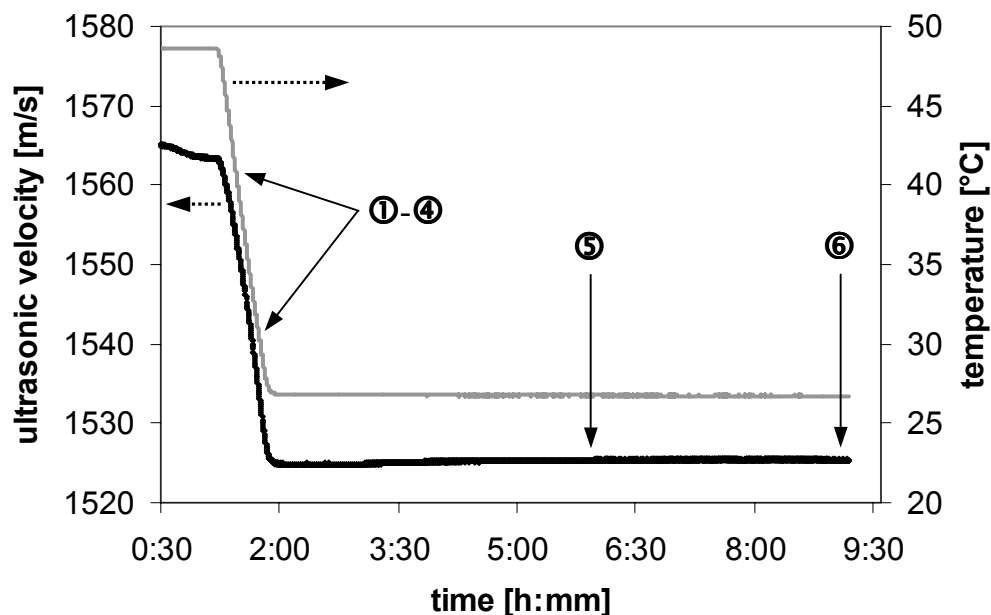
Fig. 8.3-2. Times of sampling

① 41.5°C, 1h 26min   ② 34.5°C, 1h 37min
③ 33.5°C, 1h 39min   ④ 31.5°C, 1h 43min
⑤ 27°C, 6h 05min   ⑥ 27°C, 9h 05min

At different stages of the transformation, samples have been taken from the suspension. Crystals have been sampled during cooling each 1 K, and at constant temperature every 20 minutes. In *Figure 8.3-2*, the times of sampling of the crystals, shown in the photographs documenting the transformation (see *Figure 8.3-3*) are marked. Starting at 41.5°C still above the transition temperature (1), until the end of transformation (6), i.e. when no anhydrous crystals can be detected anymore. Photograph 2 shows a sample taken at 34.5°C, thus directly after nucleation has been detected by means of the ultrasonic measuring technique. Samples 3 and 4 have also been taken during cooling, at 33.5°C and 31.5°C, respectively. After approximately 6 hours at constant 27°C still crystals of the anhydrous phase can be observed, as shown in photograph 5.

All photographs shown in *Figure 8.3-3* have been taken with the same magnification, therefore, the scale is plotted only exemplarily in one photograph.
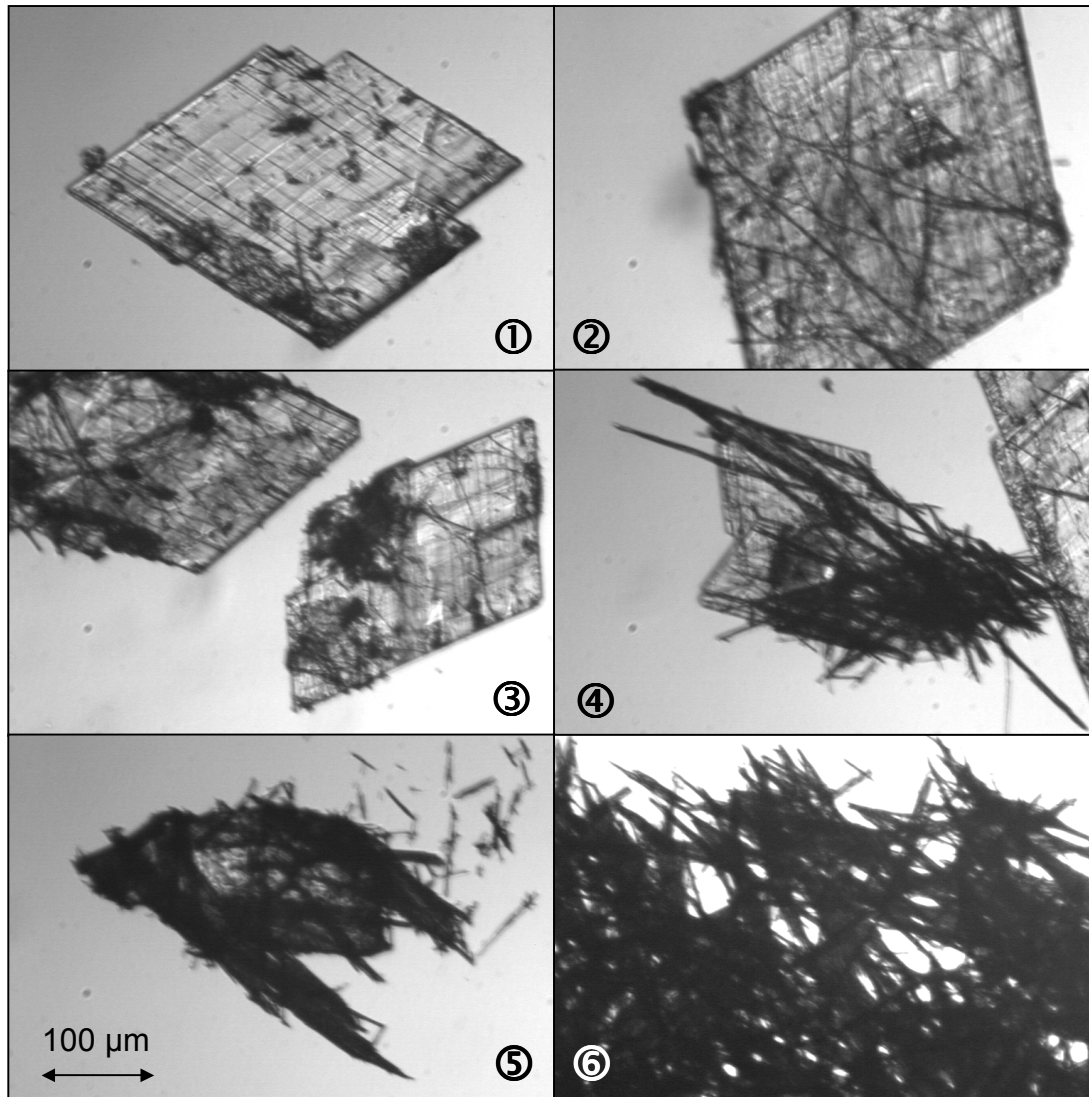
Fig. 8.3-3. Course of transformation

8.4 Stearic acid

The course of a phase transformation of stearic acid polymorphic modification C to modification B in methanol has been monitored with the ultrasonic measuring technique (see *Figure 8.4-1*). The transition temperature of these two polymorphs is reported to be between 29-32°C /BEC84, SAT84, SAT85/. Above the transition temperature modification C is stable and modification B is stable at lower temperatures. Modification A is metastable throughout the temperature range used for the experiments and has therefore not been considered any further.

For the experiment, a solution, which is saturated at 35°C, is cooled from an unsaturated state to 30°C. At ca. 30.5°C nucleation of modification C starts, which is indicated by a decrease of the ultrasonic velocity and a temperature peak. The suspension is kept at constant 30°C for a while to assure complete depletion of supersaturation by nucleation and subsequent crystal growth. At this temperature, only crystals of the C modification can

be observed. Thereafter, the suspension is cooled to 24°C to monitor phase transformation. At approximately 28°C, nucleation of the stable B modification is detected by the ultrasonic measuring technique. However, no distinct change of the ultrasonic velocity can be observed, just a small change in the gradient (see *Figure 8.4-1*).
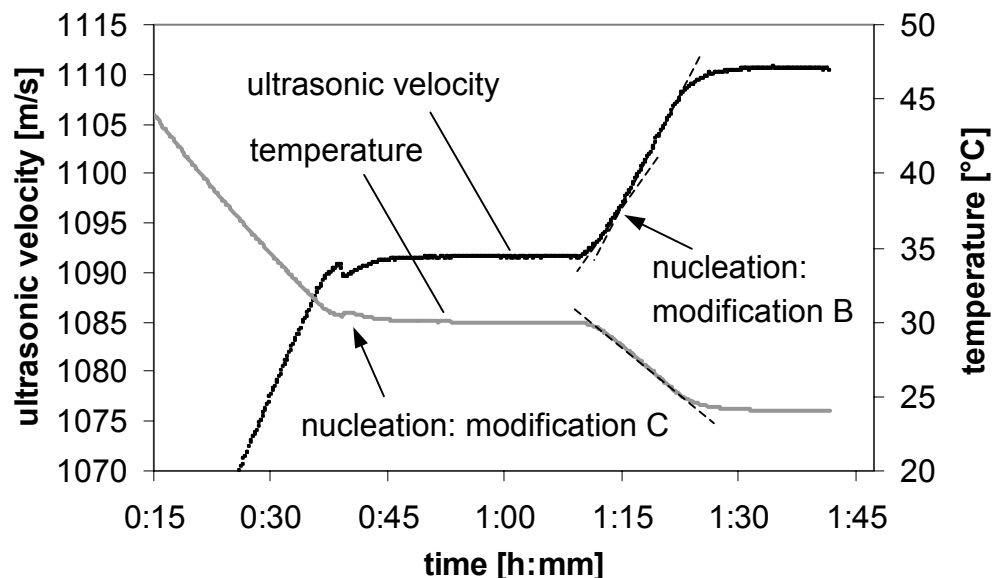
Fig. 8.4-1.   Solution-mediated transformation of stearic acid polymorphs

Samples taken at different stages during cooling confirm nucleation of the B modification. In *Figure 8.4-2*, crystals of the C and B modification can be seen, which have both been sampled in the course of the experiment.
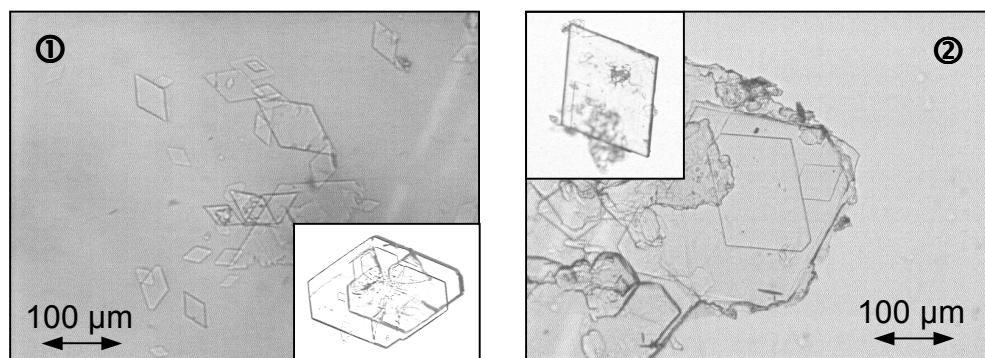
Fig. 8.4-2   Stearic acid polymorphs (1) C-modification (2) B-modification

Furthermore, it has been tested if the solution-mediated transformation of the C to the B modification at a constant temperature can be detected by the ultrasonic measuring technique. The result of such an experiment is shown in *Figure 8.4-3*.
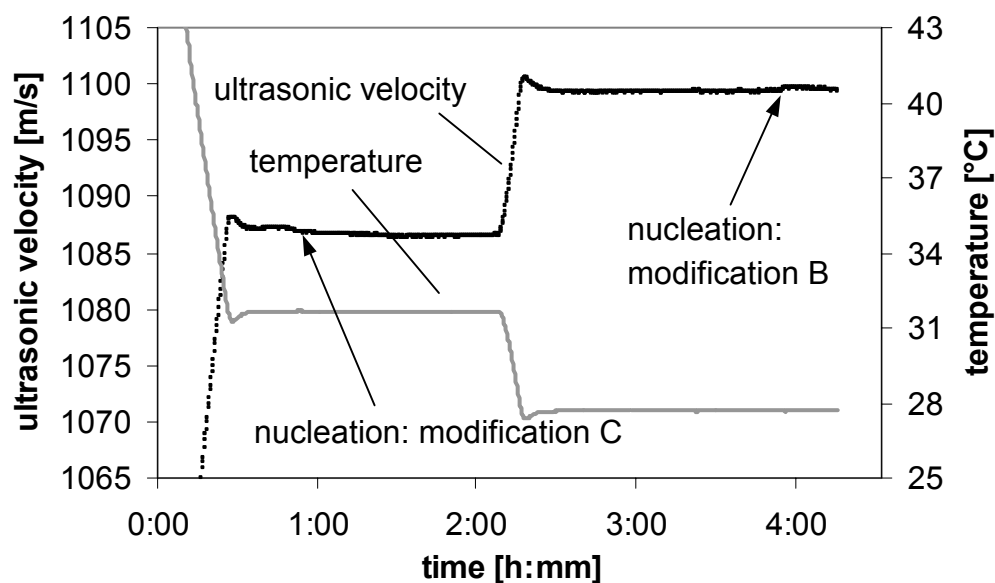
Fig. 8.4-3. Transformation of stearic acid polymorphs at constant temperature

For this experiment, a solution – saturated at 35°C – is cooled to 32°C. Nucleation of modification C starts after an induction period of about 20 minutes. Again, with nucleation of the C-modification a temperature peak and a decrease in the ultrasonic velocity can be observed. Like in the previous experiments, the suspension is kept at the chosen constant temperature after nucleation to assure depletion of supersaturation. After about one hour, the suspension is cooled to ca. 28°C. Nucleation of the stable B-modification starts after an induction time of approximately one hour. However, no unequivocal information can be gathered from *Figure 8.4-3*.
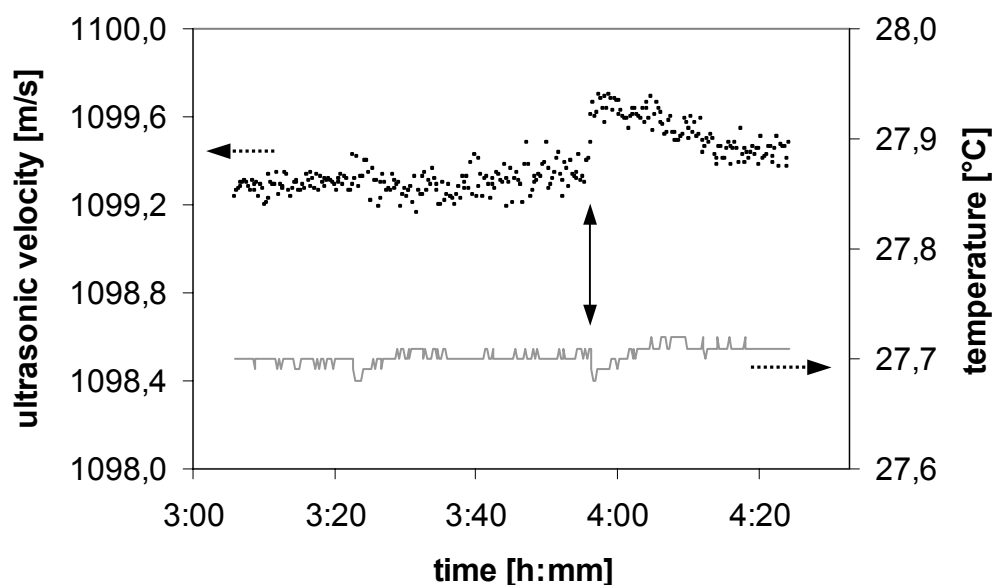

Fig. 8.4-4. Nucleation of modification B

Since no distinct changes occur, neither in the course of the ultrasonic velocity nor in temperature, a detail of *Figure 8.4-3* is shown in *Figure 8.4-4*.

In *Figure 8.4-4*, measured data of temperature and ultrasonic velocity during nucleation of the B-modification are shown. It can be seen that the ultrasonic velocity increases whereas the temperature does not change significantly during nucleation. Nucleation of the B-modification has also been confirmed by optical evaluation of samples taken at different times during the experiment.

9 Discussion of the results for other substances

In general, the applicability of the ultrasonic measuring technique is better given for inorganic substances than for organic substances. The reason for this can be found in the nature of the ultrasonic measuring technique.

As already mentioned in *section 3.1 / ultrasonic measuring technique*, the ultrasonic velocity in liquids depends on the density and the adiabatic compressibility of the medium. According to Dinger /DIN97/ the adiabatic compressibility of the medium is the determining factor. Since for the examined organic substances the compressibility changes less during nucleation than for the examined inorganic substances, with the organic substances also the resulting ultrasonic velocity does not change significantly during transformation.

9.1 Borates

For the experiments, a solution saturated at 75°C has been prepared. The solubility has been determined experimentally, whereas the transition point has been adopted from literature /SMI02/.
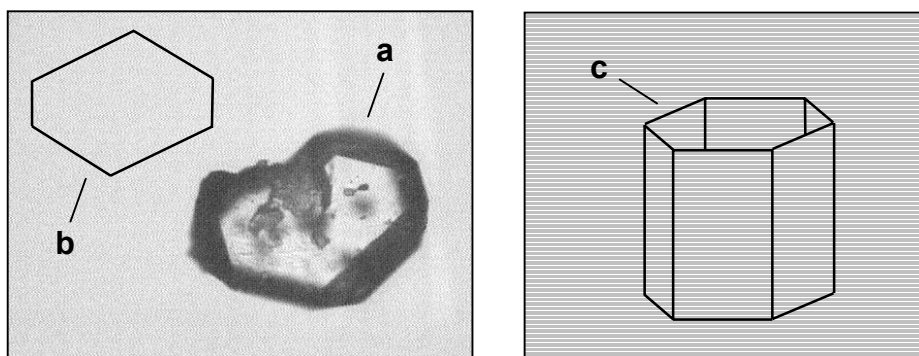
Fig. 9.1-1. Pentahydrate (a) sample, (b) habit as obtained experimentally, (c) habit according to theory /ROE79/

After nucleation at 65°C and at 55°C, samples have been taken and the crystals have been analyzed optically. At 65°C, in the stability region of the pentahydrate, crystals shown in *Figure 9.1-1* have been obtained. According to literature, the pentahydrate belongs to the trigonal-hexagonal class /ROEM95/ and crystallizes hexagonal-rhombohedral /GME73/.

Since in literature no illustration of the pentahydrate has been found, tabular compilations of mineralogy /ROE79/ are applied for analysis of the crystal habit. Assuming that the pentahydrate belongs to the trigonal crystal system and that the symmetry class is hexagonal-rhombohedral, the crystal habit shown in *Figure 9.1-1 c* is theoretically obtained. It can be seen from *Figure 9.1-1 a and b*, that the basic form of the crystals obtained experimentally is in good agreement with the habit that should theoretically appear (see *Figure 9.1-1 c*).

The pentahydrate is also called octahedral borax, because the habit of the crystals resembles octahedra /SMI02/. Due to the uneven faces of the crystals which have been sampled (see *Figure 9.1-1 a*), this can neither be confirmed nor denied.
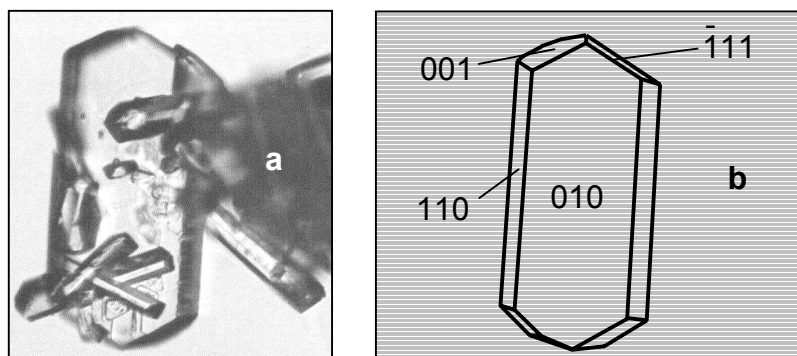
**Fig. 9.1-2.** Decahydrate (a) sample, (b) habit according to theory /ROE79/

The habit of di-sodium tetraborate decahydrate is well-described in literature. It is reported that the decahydrate crystallizes in monoclinic prisms /ROE79, ROEM95/ which resemble plates or columns. Crystals sampled after nucleation at 55°C, in the stability region of the decahydrate, are presented in *Figure 9.1-2*.

From *Figure 9.1-2* it can be seen that the crystals of the decahydrate which have been sampled during the experiment are in good accordance with the habit known from literature /ROE79/.

To find out for certain about the first form crystallized in the course of the experiment at 65°C, the sample has also been analyzed by TG/DSC. In the diagram (see *Figure 9.1-3*), data from the TG-measurement is represented by a solid line, whereas the dotted line represents data obtained from the DSC-measurement.

According to literature /SMI02/ the incorporated water is lost in two steps: 3 mol of water are lost on heating borax pentahydrate up to 160°C and the last 2 mol of water are slowly lost up to about 400°C. Furthermore, the pentahydrate is known to dehydrate reversibly to an amorphous dihydrate on heating at 140°C in air. Own measurements confirm the dehydration of the pentahydrate being a two-step process (see *Figure 9.1-3*). However, both steps take place at lower temperatures than mentioned in literature, the second step starting already at ca. 140°C. Also the total loss of mass is higher than the theoretic value of ca. 30.9 wt%, which is already lost at about 200°C. Regarding the extra loss of weight,

the conditions of drying have to be considered. The pentahydrate, being hygroscopic, is known to adsorb water from the air /GME73/. Since no defined conditions of drying could be obtained, the pentahydrate might have adsorbed water during drying which then leads to a higher loss of weight than theoretically calculated. However, it can be excluded that the sampled crystals are decahydrates. The decahydrate should theoretically lose 47.2 wt% during heating up to 400°C /SMI02/ and the TG/DSC-analysis of the crystals sampled at 55°C is in good agreement with this theoretical value.
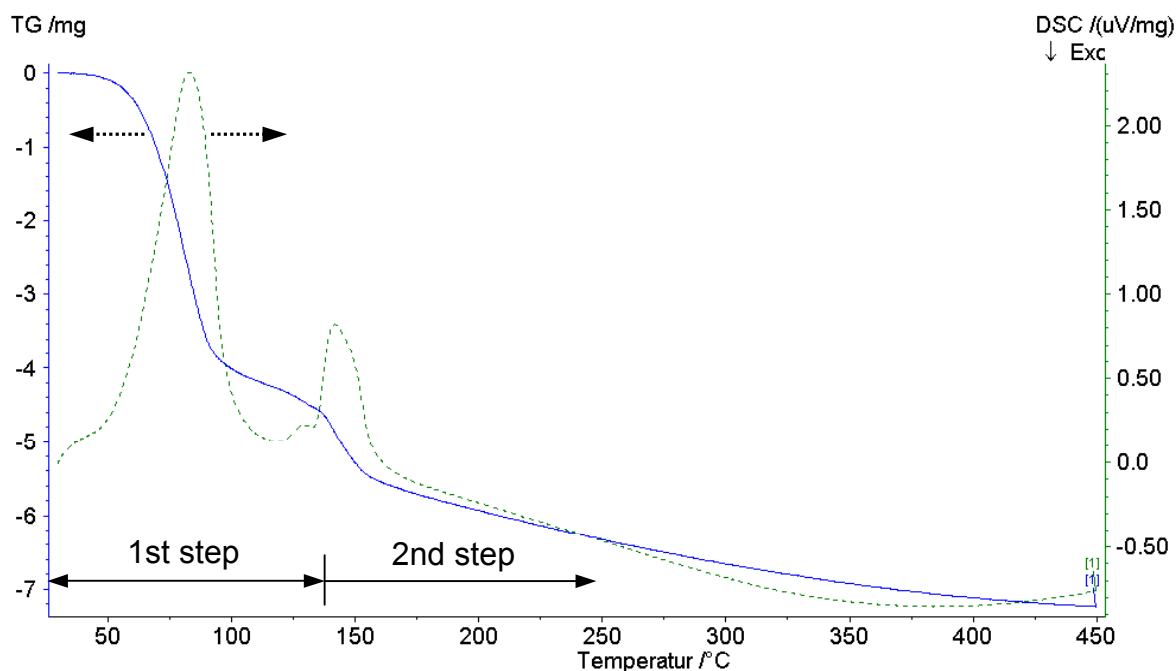

Fig. 9.1-3. TG/DSC analysis of the pentahydrate

Thus, in combination with the optical evaluation, it is save to assume that the pentahydrate has crystallized first, followed by nucleation of the decahydrate.

The phase transformation of the penta- to the decahydrate has been monitored with the ultrasonic measuring technique. In the experiments, simultaneously the ultrasonic velocity and temperature are measured, yet the temperature measurement turns out to be not always a reliable method for the determination of the onset of nucleation (see *Figure 8.1-1*). No distinct change in the course of temperature can be observed during nucleation of the pentahydrate. A detail of *Figure 8.1-1* is shown in *Figure 9.1-4*.

From *Figure 9.1-4* it is clear to see that the temperature increases only slightly about 0.1 K during nucleation of the pentahydrate. In contrast to it, the ultrasonic velocity decreases distinctly during nucleation, approximately 10 m/s, and can therefore be counted a reliable method to monitor the onset of nucleation for this substance. In cases where the heat of crystallization, ΔH_{cryst}, is very low, as for the pentahydrate, a simple temperature measurement cannot be applied as a measuring technique. In this case, other measuring

techniques, e.g. concentration-dependent measuring techniques like the tested ultrasonic measuring technique, have to be used.
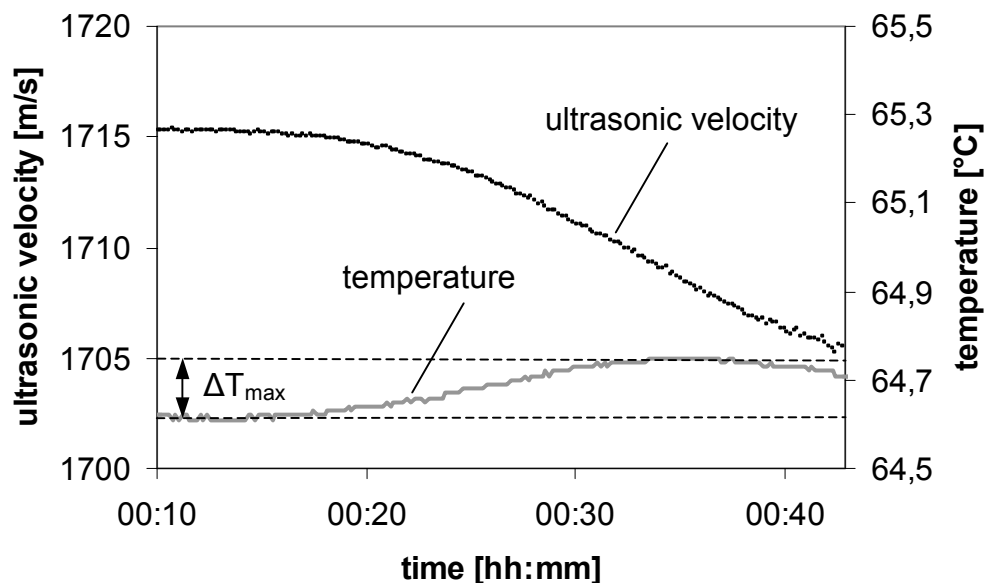
Fig. 9.1-4. Nucleation of the pentahydrate

In this experiment, the solution has been saturated at 75°C and nucleation of the pentahydrate started at 65°C. The difference in concentration between these two temperatures is ca. 6 g anhydrous substance / 100 g solvent. Since the ultrasonic measuring technique is very sensible even to small changes in concentration, see e.g. *section 3.1.2, suitability for measuring changes in concentration* or /OMA99a/, the change in ultrasonic velocity can indicate nucleation of the pentahydrate without any doubt.
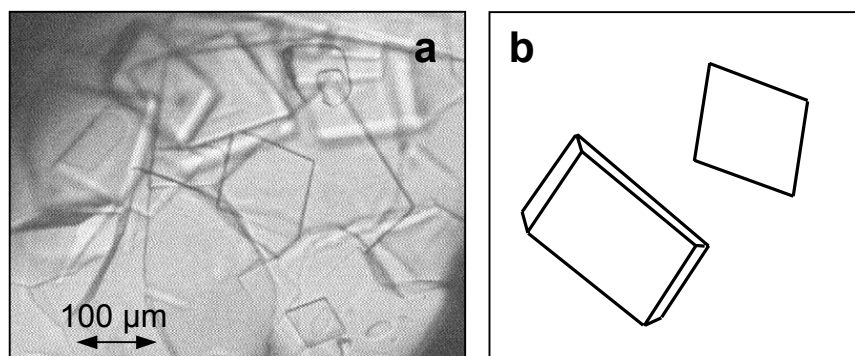
9.2 Calcium chloride

For the preparation of aqueous calcium chloride solutions, solubility data of Kaltofen /KAL94/ has been used. The solubility data taken from literature has only been checked in points, since both, the experimental values and the values taken from literature, were almost identical.

After nucleation had been detected by the ultrasonic measuring technique, samples have been taken and the crystals have been analyzed by optical microscopy. Since the transition temperature of the di- and the tetrahydrate is about 45.3°C /KEM02/, it should be save to assume that the crystals sampled at 51°C are the dihydrate. Calcium chloride dihydrate belongs to the tetragonal crystal system, and the crystals are shaped like slender prisms /SIN03/.

In *Figure 9.2-1*, the crystals which have been sampled at 51°C are shown. For a better lucidity, the habit of the dihydrate crystals is also illustrated schematically in *Figure 9.2-1 b*. The obtained crystals do look like slender prisms, as described in literature /SIN03/,

however, no further analysis of the crystals was possible for reasons described later in this section.

Fig. 9.2-1.   Calcium chloride dihydrate

Also at 35°C, in the stability region of the tetrahydrate, crystals have been sampled after nucleation had been detected by means of the ultrasonic measuring technique. These crystals (see *Figure 9.2-2*) differ distinctly from the crystals obtained after nucleation at 51°C, which have been discussed before. Therefore, the phase transformation which has been monitored successfully with the ultrasonic technique, can also be proven by means of optical analysis. However, looking at *Figure 9.2-2* gives the impression that two different phases are present, yet both deviating from the crystals sampled at 51°C (see *Figure 9.2-1*).

It is known from literature /GME71/ that the tetrahydrate exhibits polymorphism. Three different polymorphs of the tetrahydrate may occur: the α-, the β- and the γ-form. The α-tetrahydrate, which is the stable form, forms granular and well-defined, diamond-like crystals. Crystals of the β-form are square or rectangular prisms, often having beveled edges. The γ-tetrahydrate forms big hexagonal plates which easily disintegrate to long needles. According to the description of the habits of the three different polymorphs, probably the β-form (*Figure 9.2-2* (1)) and the γ-form (*Figure 9.2-2* (2)) have been obtained, both being metastable polymorphs. However, the crystals cannot be identified with certainty by means of optical methods. Also, further analysis for instance with DSC and x-ray diffraction has not been possible, because of the reasons pointed out below.
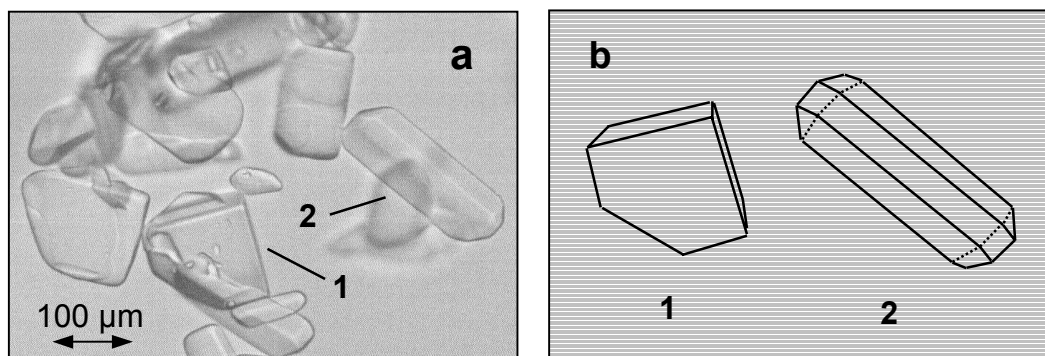
**Fig. 9.2-2.**   Calcium chloride tetrahydrate

Both hydrates of calcium chloride have been difficult to analyze due to the following reasons:

- The dihydrate is very deliquescent, and the crystals absorb water from the air and melt or otherwise deteriorate /SIN03/.
- The tetrahydrate is hygroscopic and melts at 35°C /MERC99/.

Thus, these crystals can only be adequately analyzed under defined conditions regarding temperature and humidity. However, under the prevailing conditions, the crystals were molten within less than one minute after sampling, which is also indicated by the rounded corners of the crystals in *Figures 9.2-1* and *9.2-2*.

The phase transformation of calcium chloride dihydrate to tetrahydrate has been monitored with the ultrasonic measuring technique. For the phase transformation experiment, an unsaturated solution is cooled into the metastable zone of the dihydrate. Nucleation of the dihydrate starts already during cooling, and the change in ultrasonic velocity is more significant than in temperature. The response of the ultrasonic velocity and temperature during nucleation of the dihydrate is shown in *Figure 9.2-3*, which is a detail of *Figure 8.2-1* displayed in the previous section.

As can be seen in *Figure 9.2-3*, the temperature hardly increases during nucleation, whereas a distinct increase in the ultrasonic velocity can be observed. Thus, the heat of crystallization, ΔH_{cryst}, of the dihydrate has to be very low, and a simple temperature measurement cannot be applied as a measuring technique. In contrast to it, nucleation of the tetrahydrate can be monitored with both, a simple temperature measurement and the measurement of the ultrasonic velocity (see *Figure 8.2-1*).
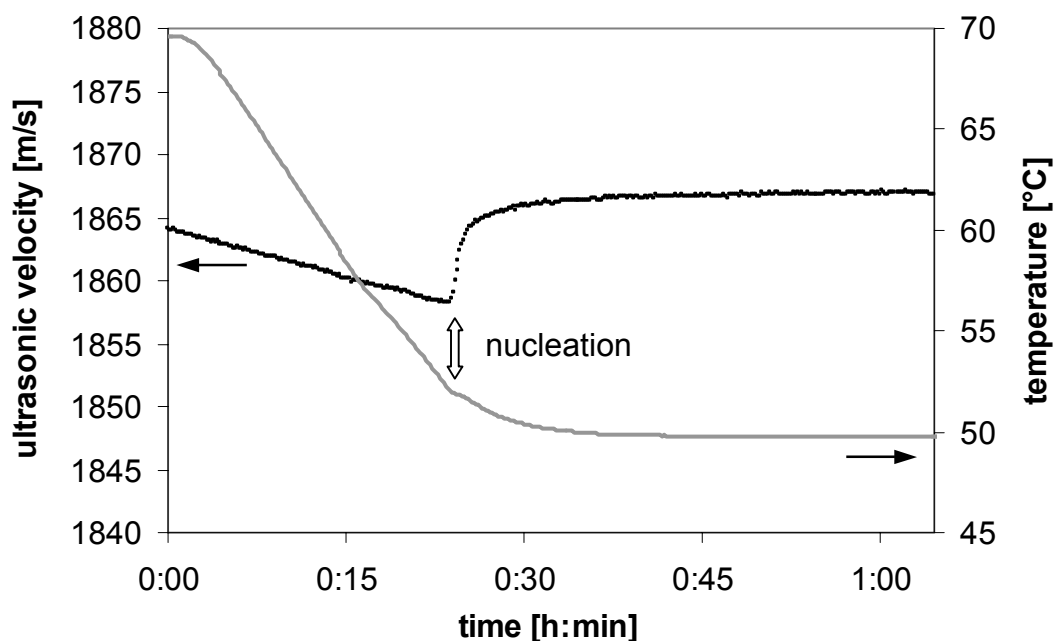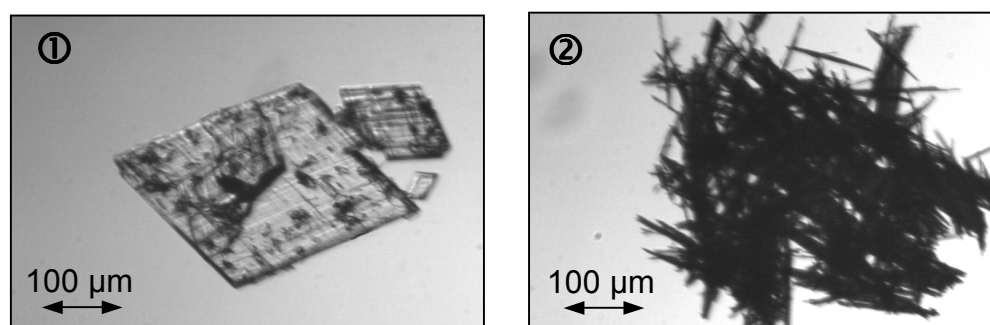

Fig. 9.2-3. Nucleation of the dihydrate

It can also be taken from *Figure 8.2-1* that the ultrasonic measuring technique can only be applied up to a certain suspension density. After nucleation of the tetrahydrate at 35°C, a theoretical solid-content of 46% is expected. However, the ultrasonic velocity can only be reliably measured up to approximately 40%, at higher solid-contents the measuring technique fails.
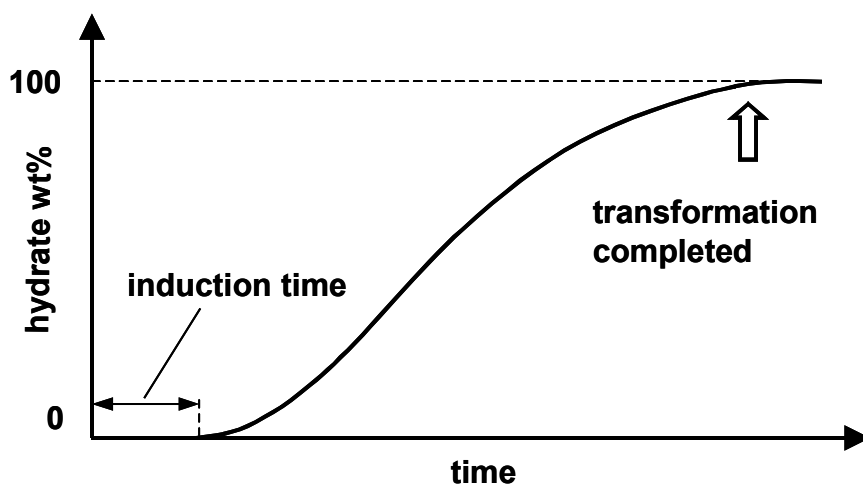
9.3   L-Phenylalanine

The solubility of l-phenylalanine in aqueous solution previously reported by Mohan et al. /MOHN01/ has been found to be in good agreement with the solubility data obtained in the course of these experiments. Therefore, the reported transition point of the monohydrate and the anhydrous form at 37°C /MOHN01/ has been adopted without further verification.

Fig. 9.3-1.   L-Phenylalanine (1) anhydrous form, (2) monohydrate

Both, nucleation of the anhydrous form and the subsequent transformation to the monohydrate, have been confirmed by optical microscopy (see *Figure 8.3-3*). The monohydrate and the anhydrous form can be easily distinguished by their habit, and therefore, optical microscopy represents a fast and reliable characterization method. Crystals of the anhydrous form exhibit a plate-like shape, whereas crystals of the monohydrate occur in the form of needles (see *Figure 9.3-1*).

The phase transformation of the anhydrous form to the monohydrate proceeds in such a way that the anhydrous form gradually dissolves, while crystals of the monohydrate nucleate and grow on the surface of the metastable phase (see *Figure 8.3-3*). However, no sudden noticeable nucleation is observed and the transformation proceeds rather sluggish. This result is in accordance to phase transformation experiments carried out by Mohan et al. /MOHN01/. They have observed phase transformations of the anhydrous form to the monohydrate in pure aqueous solutions and in solutions with different additives. In each case, the transformation proceeded rather sluggish, resulting in a sigmoidal-curve. This result is supported by own experiments /STR99a/, carried out previously. The course of a phase transformation for l-phenylalanine is schematically shown in *Figure 9.3-2*.

Fig. 9.3-2. Phase transformation of l-phenylalanine

In *Figure 9.3-2* is illustrated that the transformation of anhydrous l-phenylalanine to the monohydrate follows a sigmoid-curve. Often, phase transformations do not start spontaneously, but only after a certain induction time /MOHN01, NYV97/. The reason for this phenomena can be found in the metastable zone width of the system. When the metastable phase is within the metastable zone width of the stable phase, nucleation of the stable phase will only start after a certain induction period. On the other hand, if the metastable phase is outside the metastable zone of the stable phase, the stable form will nucleate spontaneously.

As shown in *Figure 8.3-1* in the previous section, nucleation of the anhydrous form is accompanied by a decrease of the ultrasonic velocity, however, no significant change in temperature can be observed. Although there is only a relatively small change in concentration before and after nucleation of ca. 0.4 g, nucleation can be detected by means of the ultrasonic measuring technique. The heat of crystallization, ΔH_{cryst}, which is usually liberated when a substance with a positive solubility crystallizes, is neglectable in this case. Thus, the onset of crystallization of the anhydrous form cannot reliably be indicated by a sole temperature measurement. The same applies to the crystallization of the monohydrate, which is taking place during cooling to the final transformation temperature. In the course of the ultrasonic velocity a change in the gradient during nucleation of the monohydrate is visible, whereas in the course of the temperature no such change can be observed (see *Figure 8.3-1*). During the experiment, samples have been taken at certain intervals, confirming that the start of nucleation of the monohydrate can be reliably indicated by the change of the gradient of the ultrasonic velocity.

9.4 Stearic acid

The solubility of the B- and C-modification of stearic acid in methanol over a temperature range from 6 to 39°C was published by Beckmann /BEC84/ and has been checked in points. Since the solubility experiments give only a slightly lower solubility than the

published data, the latter is taken as reference and solutions are prepared in accordance to it. The transition temperature of the B- and C-modification is reported to be between 29 and 32°C /SAT84/. Due to the fact that the solubilities of the two polymorphs are nearly equal in this range, an exact transition point is difficult to determine.

For the transformation experiments, a solution is cooled into the metastable zone until spontaneous nucleation of the C-modification starts. In the course of the experiment, the suspension is cooled further to induce the solution-mediated transformation of the C- to the B-modification. Both, nucleation of the C-modification at 30.5°C and the subsequent transformation to the B-modification at ca. 28°C have been confirmed by optical microscopy (see *Figures 8.4-2*).

The two polymorphs can be easily distinguished by their habit. Both modifications are lozenge-shaped, however, they can be identified by the angles of the lozenge /SAT84/:

B-modification: 75°
C-modification: 55°

Photographs of both modifications are shown in *Figure 9.4-1*.
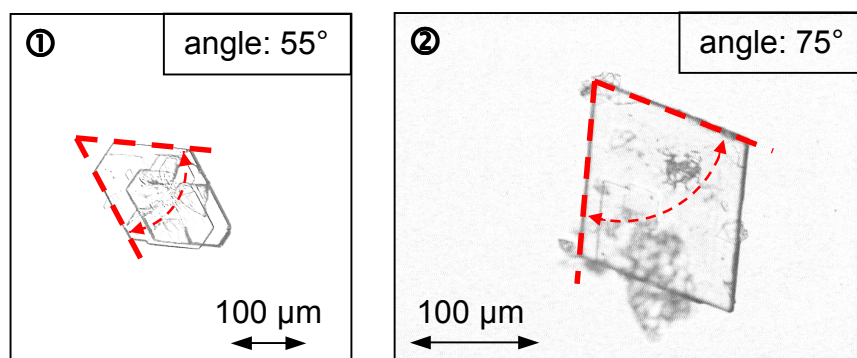
Fig. 9.4-1.   Stearic acid polymorphs (1) C-modification (2) B-modification

Since the two polymorphs can easily be distinguished by their habit, optical microscopy is a fast and reliable analyzing technique.

Nucleation of the C-modification leads to a visible change in temperature as well as in the ultrasonic velocity. However, the onset of the transformation can better be monitored by the ultrasonic measuring technique than by a temperature measurement. The start of transformation during cooling is not at all indicated by a change of temperature (see *Figure 8.4-1*). Although the ultrasonic velocity is not influenced significantly by nucleation of the B-modification, a change in the gradient can be observed. In the case of the transformation taking place at a constant temperature, as shown in *Figure 8.4-3*, again a small change in ultrasonic velocity, but not in temperature can be seen. The ultrasonic velocity increases noticeably about 0.5 ms^{-1} during nucleation of the B-modification (see *Figure 8.4-4*), whereas the temperature varies between 26.8 and 27.2°C with a mean

temperature of 27.0°C before nucleation and 27.1°C after nucleation. However, these deviations in temperature are too small to draw any conclusions.

Due to the low solubility of stearic acid in methanol, no distinct changes in concentration occur during transformation. Under given conditions, the difference in concentration is ca. 0.14g / 100g solvent. Therefore, the heat of crystallization ΔH_{cryst}, which is usually liberated on crystallization and which leads to an increase in solution temperature for substances with a positive solubility, seems to be negligible for the nucleation of modification B. Due to this reason, no satisfying results can be obtained by a sole temperature measurement. The measurement of the ultrasonic velocity, which is concentration-dependent, gives better results, but still the applicability for monitoring phase transformations might not be given in all cases.

10. Summary of the discussion

An extensive study of the influence of twelve different additives on the solubility and the metastable zone of magnesium sulfate solutions has shown that most of the additives increase the width of the metastable zone, whereas the influence of these additives on the solubility is more diverse.

- Effect on the solubility

   All three possible ways of influence: decrease, increase or no detectable change.

- Effect on the metastable zone width

   Slightly broader metastable zone width in most of the cases.

The influence of borax and KCl, having distinctly different effects on the solubility and metastable zone width, has been further examined.

- Borax

   Small amounts increase the solubility and considerably broaden the metastable zone.

- KCl

   Small amounts do not change the solubility within detectable limits and slightly reduce the metastable zone.

To round off preceding experiments, the effect of different amounts of KCl and borax on the solubility, metastable zone width, crystal habit and growth rate have been studied; confirming that borax has a strong inhibiting effect in every respect whereas the influence of KCl is more complex, promoting as well as inhibiting, but always less strong than the effect of borax.

Furthermore, the effect of both additives on solution-mediated phase transformations has been explored.

- Borax considerably slows down phase transformations.
- KCl considerably accelerates phase transformations.

It has been shown, however, that induction times for phase transformations cannot be reliably predicted even in "pure solutions" and therefore, possibly due to the interaction with inevitably present by-products, also the effect of additives often is too complex to be predicted. In this respect, also the aforementioned strong promoting effect of KCl cannot be generalized. Although experiments were very reproducible with one batch of product crystals, it could not be repeated with another batch, emphasizing the difficulty of reliably predicting phase transformations.

In Addition, experiments with zinc sulfate, which is structurally related to magnesium sulfate, have been carried out. Transformation experiments with zinc sulfate and their comparison with the respective experiments with magnesium sulfate led to the following results:

- Maximum induction times for phase transformations can be estimated by an Arrhenius-function.

106

- Predicting induction times in dependence on the metastable zone width does not always yield reliable results.
- Different stages of stability for phase transformations have been identified.

Although more pronounced for zinc sulfate, the maximum induction times for both substances, zinc sulfate and magnesium sulfate, can be reasonably described by an Arrhenius-function. The rule of thumb that nucleation of the stable phase starts spontaneously if the solubility curve of the metastable phase is situated outside the metastable zone of the stable phase, however, does not always lead to satisfactory results. For instance, phase transformations in magnesium sulfate solutions already started spontaneously under conditions in which they should only start after a certain induction time; the shortened induction times probably being determined by the higher difference of the solubilities of the two relevant phases. Furthermore, for practical purposes, the area below the transition point has been subdivided into three different stages of stability - quasi-stable, metastable and unstable - indicating the probability of phase transformations.

In order to test the general applicability of the ultrasonic measuring technique for monitoring phase transformations, transformation experiments have also been carried out with further substances, inorganic as well as organic substances.

- The ultrasonic measuring technique can be applied for monitoring phase transformations of organic as well as inorganic substances.
- The mechanism for phase transformations of organic and inorganic substances is identical.
- The course of phase transformations for organic and inorganic substances is different.

Although the ultrasonic velocity changed more distinctly during phase transformation experiments with inorganic substances, the ultrasonic measuring technique has also been successfully applied for monitoring the onset of phase transformations with organic substances. For both kinds of substances, inorganic as well as organic substances, it has been shown that during a solution-mediated phase transformation crystals of the stable phase start to grow onto the metastable phase. The subsequent course of the phase transformation, however, has been significantly different for the examined inorganic and organic substances. The course of phase transformations for organic and inorganic substances is schematically shown in *Figure 10.1*.

Regarding the difference between phase transformations of the examined organic and inorganic substances, the existence of a latent period and a sudden onset of nucleation of the stable phase has been observed with inorganic substances, whereas with organic substances a gradual, continuous transformation has been observed.
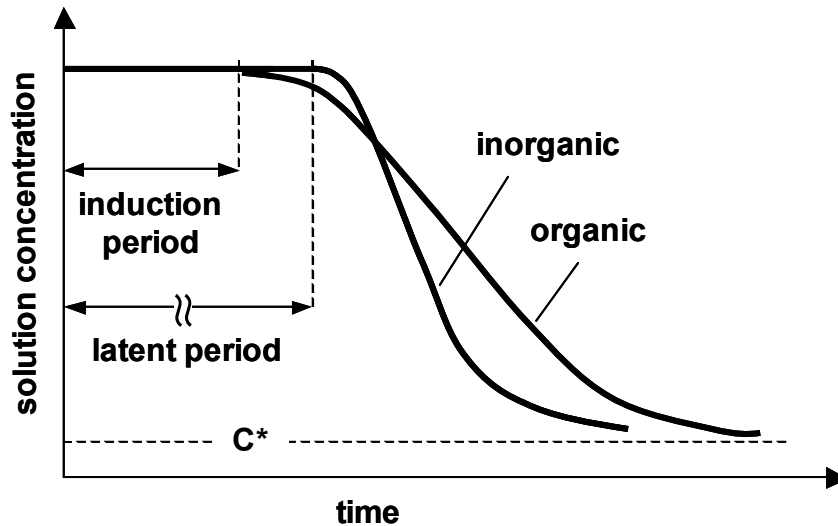
Fig. 10.1.   Course of phase transformations for inorganic and organic substances

Summing up, it may be said that future works should be focused more detailed on the factors determining the kinetics of phase transformations. Although a general prediction of the onset of phase transformations does not seem to be possible, a more reliable rule of thumb could be developed. The prediction of induction times could be based on improving Nývlts' /NYV97/ rule of thumb that nucleation of the stable phase only starts spontaneously if the solubility curve of the metastable phase is situated outside the metastable zone of the stable phase, which did not always lead to satisfactory results. Furthermore, it should be examined with a representative number of substances, if the discovered difference between the course of phase transformations of organic and inorganic substances is of general nature or if it might at least be assigned to specific substance groups or certain characteristics of the substances.

11. Summary

In many cases, crystallization leads to the formation of a metastable (pseudo-) polymorph, which will eventually transform into a more stable one. Influencing the stability of (pseudo-) polymorphs is a crucial aspect of product design since often, e.g. due to more advantageous processing and application properties, a metastable form is demanded. This applies particularly to pharmaceuticals and foods, because different modifications frequently exhibit different physical properties such as bioavailability, dissolution rate and shelf life. In addition, in many cases a change in crystal structure also leads to different crystal habits, which might play an important role in downstream processing. Knowledge and control of the crystallizing solid phase and its stability during formation, after-treatment or storage is therefore decisive for the quality of the final product.

Transformation rates of (pseudo-) polymorphs strongly depend on kinetics. Therefore, the transformation of a metastable phase into a more stable phase is not certain even though the system enters a condition in which, considering solely thermodynamics, a transformation would have to take place. Thus, it would be desirable to be able to predict and control the kinetics of phase transformations.

Within the scope of this work, solution-mediated phase transformations in systems with and without additives have been carried out, the ultrasonic measuring technique having proven to be suitable for monitoring phase transformations of organic as well as inorganic substances. However, it has been demonstrated that a reliable prediction of induction times for phase transformations might not be possible, even with so-called "pure solutions" and limited to one substance, due to inevitably present by-products. A prediction of induction times according to the rule of thumb that nucleation of the stable phase only starts spontaneously if the solubility curve of the metastable phase is situated outside the metastable zone of the stable phase did also not lead to satisfactory results for all substances. Furthermore, although the extension and therewith the control of induction times by the use of additives has been successively demonstrated, it has also been shown, possibly due to the interaction with inevitably present by-products, that the effect of additives often might be too complex to be predicted.

However, it has been shown that maximum induction times of phase transformations with zinc sulfate and magnesium sulfate can be sufficiently described by an Arrhenius-function. Furthermore, for practical purposes, the area below the transition point can be subdivided into three different stages of stability - quasi-stable, metastable and unstable – indicating the probability of phase transformations in a standardized manner.

Regarding differences of phase transformations with organic and inorganic substances, experiments indicate that the course of the phase transformation is different for inorganic and organic substances. With inorganic substances, a latent period and a sudden onset of nucleation of the stable phase has been observed, whereas with organic substances a gradual, continuous transformation has been observed.

12. Zusammenfassung

In Kristallisationsprozessen bildet sich oftmals zunächst eine metastabile Phase, die sich schließlich in eine stabilere Phase umwandelt. Die Beeinflussung der Stabilität von (Pseudo-) Polymorphen ist deshalb ein entscheidender Aspekt der Produktplanung, z.B. aufgrund vorteilhafterer Verarbeitungs- und Anwendungseigenschaften der metastablen Form. Neben anderen physikalischen Eigenschaften weisen verschiedene Modifikationen in vielen Fällen auch verschiedene Habitii auf, die wiederum eine wichtige Rolle in den nachfolgenden Verarbeitungsprozessen spielen können. Kenntnis und Kontrolle der kristallisierenden festen Phase und ihrer Stabilität während Entstehung, Nachbehandlung oder Lagerung ist deshalb entscheidend für die Qualität des Endproduktes.

Da Phasenumwandlungen sehr stark von der Kinetik beeinflußt sind, ist die Umwandlung einer metastabilen Phase in eine stabilere Phase selbst dann nicht sicher, wenn das System einen Zustand erreicht in dem, bei alleiniger Betrachtung der Thermodynamik, eine Umwandlung stattfinden müßte. Aus diesem Grund wäre es wünschenswert, die Kinetik von Phasenumwandlungen kontrollieren und voraussagen zu können.

Im Rahmen dieser Arbeit wurden Phasenumwandlungen in Lösungen sowohl mit Additiven als auch ohne Additive durchgeführt, wobei sich die Ultraschallmeßtechnik als geeignet zur Überwachung von Phasenumwandlungen organischer und anorganischer Substanzen erwiesen hat. Es wurde jedoch gezeigt, daß selbst für "reine Lösungen" eine zuverlässige Vorhersage der Induktionszeiten von Phasenumwandlungen nicht unbedingt möglich ist. Eine Vorhersage der Induktionszeiten gemäß der Faustregel, daß die Keimbildung der stabilen Phase nur dann spontan anfängt, wenn die Löslichkeitskurve der metastabilen Phase außerhalb des metastabilen Bereichs der stabilen Phase liegt, führte nicht für alle Substanzen zu einem befriedigenden Ergebnis. Obwohl eine Verlängerung und damit die Kontrolle der Induktionszeit durch Additive erfolgreich demonstriert wurde, ist auch deutlich geworden, daß der Effekt von Additiven häufig, möglicherweise infolge der Wechselwirkungen mit unvermeidlich präsenten Nebenprodukten, zu komplex zur Vorhersage ist.

Es wurde jedoch gezeigt, dass die maximalen Induktionszeiten von Phasenumwandlungen mit Zink- und Magnesiumsulfat hinreichend genau durch eine Arrhenius-Funktion beschrieben werden können. Des Weiteren wurde das Gebiet unter dem Umwandlungspunkt aus praktischen Gesichtspunkten in drei verschiedene Stabilitätsbereiche – quasi-stabil, metastabil und instabil - unterteilt, welche in einer standardisierten Art die Wahrscheinlichkeit von Phasenumwandlungen anzeigen.

Hinsichtlich der Unterschiede von Phasenumwandlungen bei organischen und anorganischen Substanzen, deutet sich ein generell unterschiedlicher Verlauf an. Bei anorganischen Substanzen wurde eine Latenzzeit und ein plötzlicher Beginn der Keimbildung der stabilen Phase beobachtet, während bei organischen Substanzen eine allmähliche, kontinuierliche Umwandlung beobachtet wurde.

13. Nomenclature

c	concentration	-
C	number of components	-
F	number of degrees of freedom	-
G	Gibbs free energy	kJ
G	linear growth rate	m s^{-1}
I	ionic strength	mol kg^{-1}
J	rate of nucleation	nuclei m^{-3} s^{-1}
k	(shape) factor	-
k_N	rate constant of nucleation	s^{-1}
L	crystal size	m
m, M	mass	kg
n	nucleation order	-
N	number of crystals	-
P	number of phases	-
r	radius	m
s	distance	m
S	supersaturation ratio	-
t	(residence) time	s
T	temperature	°C, K
v	ultrasonic velocity	m s^{-1}
$\bar{v}$	mean linear growth velocity	m s^{-1}
w_{eq}	solubility	-
ΔH_{cryst}	heat of crystallization	kJ mol^{-1}

Greek letters

β	compressibility	Pa^{-1}
γ	interfacial free energy	N m^{-1}
ρ	density	kg m^{-3}
σ	surface tension	N m^{-1}

Indices

*	equilibrium
1	initial
2	final
ad	adiabatic
crit	critical

cryst   crystallization

g   growth

ind   induction

lp   latent period

n   nucleation, nucleus

r   relaxation

s   saturation

s   surface

v   volume

Abbreviations

ATR-FTIR   attenuated total reflectance Fourier transform infrared

BCF-model   Burton-Cabrera-Frank-model

CCD   charge-coupled device

CSD   crystal size distribution

DSC   differential scanning calorimetry

EDX   energy-dispersive x-ray

ESEM   environmental scanning electron microscopy

MS   mass spectroscopy

NIR   near-infrared

ppm   part per million

PXRD   powder x-ray diffraction

rpm   revolution per minute

TGA   thermo-gravimetric analysis

T_p transition point

UV-Vis   ultraviolet-visible

vol   volume

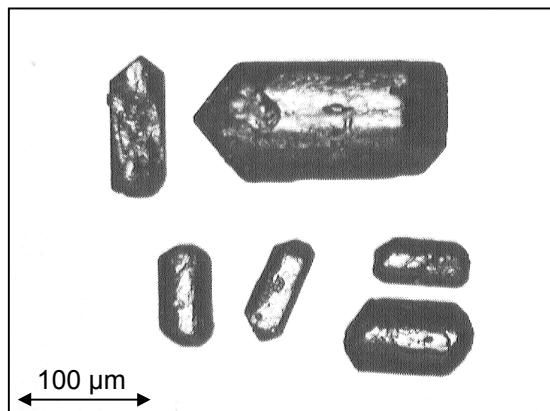wt   weight

14. Appendix

14.1 Substances and solvents

Magnesium sulfate hydrates

Transition point: $MgSO_4 \cdot 7H_2O \leftrightarrow MgSO_4 \cdot 6H_2O$ at 48.1°C /OTT02/

$MgSO_4 \cdot 7H_2O$
Magnesium sulfate heptahydrate

       Mineral name: epsomite
       Mol wt: 246.48
       Purchased from: Merck (pure)
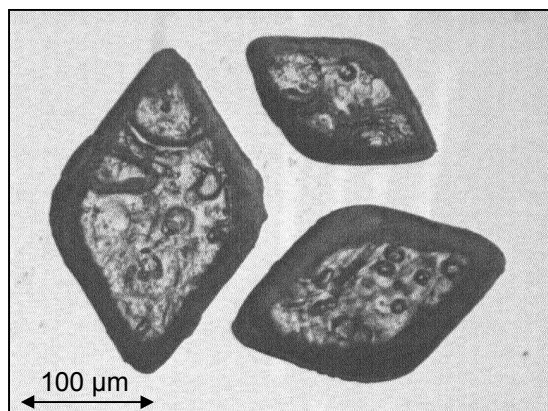

100 µm

    $MgSO_4 \cdot 7H_2O$ crystals

$MgSO_4 \cdot 6H_2O$
Magnesium sulfate hexahydrate

       Mineral name: hexahydrite
       Mol wt: 228.47
       Purchased from: Fluka (puriss. p.a.)
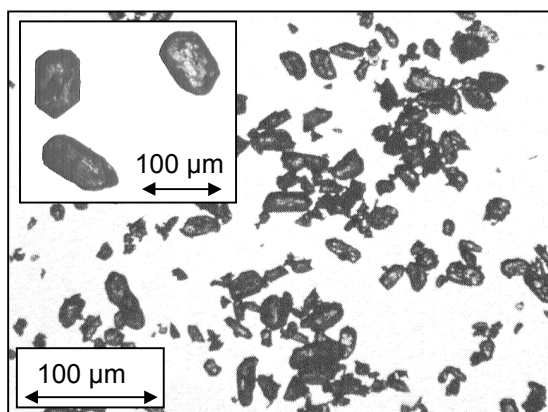

100 µm

    $MgSO_4 \cdot 6H_2O$ crystals

Zinc sulfate hydrates

Transition point: $ZnSO_4 \cdot 7H_2O \leftrightarrow ZnSO_4 \cdot 6H_2O$ at 39.0°C /ROH02/

$ZnSO_4 \cdot 7H_2O$
Zinc sulfate heptahydrate

Mineral name:	zinc vitriol
Mol wt:	287.55
Purchased from:	Merck (pure)

ZnSO$_4$ · 7H$_2$O crystals

L-Phenylalanine

Transition point $C_9H_{11}NO_2 \cdot H_2O \leftrightarrow C_9H_{11}NO_2$ at 37.0°C /MOHN01/

$C_9H_{11}NO_2$ or $C_6H_5CH_2CH(NH_2)CO_2H$
L-Phenylalanine anhydrate

Mol wt:	165.19
Purchased from:	Lancaster (assay, formula >99%)
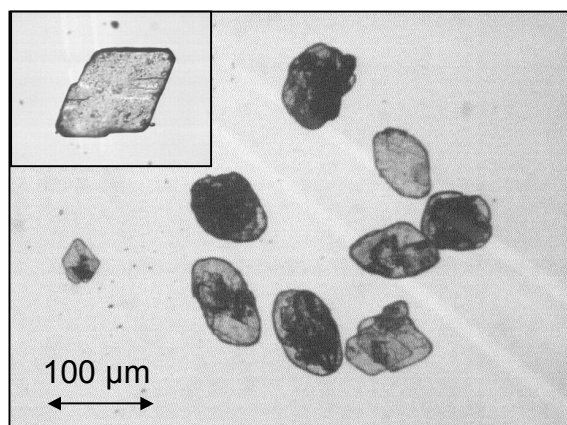
C$_9$H$_{11}$NO$_2$ crystals

Borax hydrates

Transition point: $Na_2B_4O_7 \cdot 10H_2O \leftrightarrow Na_2B_4O_7 \cdot 5H_2O$ at 60.8°C /SMI02/

$Na_2B_4O_7 \cdot 10H_2O$
di-Sodium tetraborate decahydrate

       Mineral name: tincal, borax
       Mol wt: 381.37
       Purchased from: Merck (extra pure)

100 µm
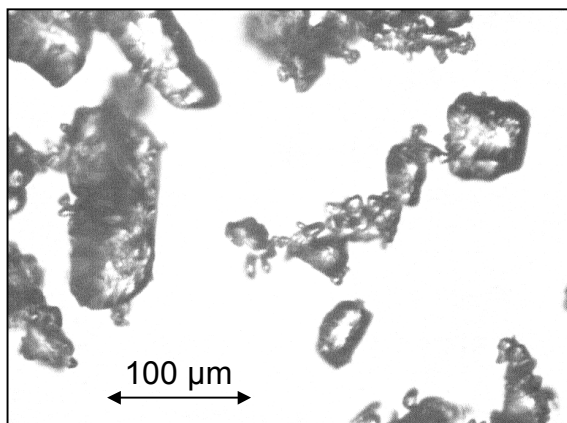
      $Na_2B_4O_7 \cdot 10H_2O$ crystals

Calciumchloride hydrates

Transition point $CaCl_2 \cdot 4H_2O \leftrightarrow CaCl_2 \cdot 2H_2O$ at 45.3°C /KEM02/

$CaCl_2 \cdot 2H_2O$
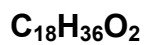Calciumchloride dihydrate

       Mineral name: sinjarite
       Mol wt: 147.02
       Purchased from: Merck (cryst. GR for analysis)

100 µm
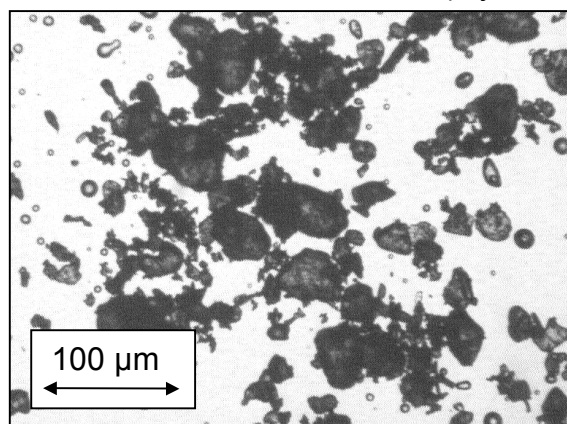
      $CaCl_2 \cdot 2H_2O$ crystals

Stearic acid

Transition point B ↔ C between 29-32°C /BEC84, SAT84, SAT85/

$C_{18}H_{36}O_2$
Stearic acid

       Mol wt: 284.47
       Purchased from: Merck

100 µm
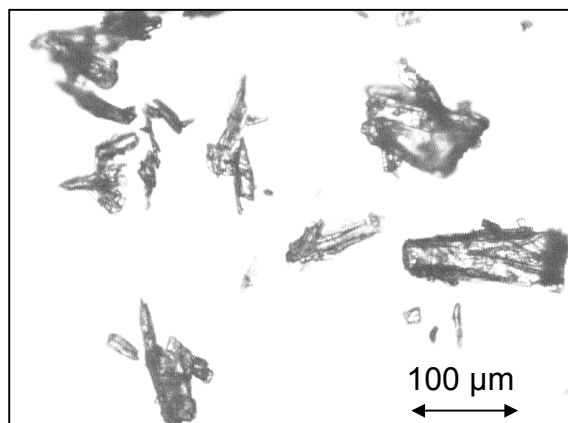
      stearic acid crystals

Methanol
Methanol, dried, max. 0.005% H_2O, Merck

14.2 Additives
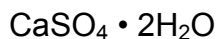
$CaSO_4 \cdot 2H_2O$
   Calcium sulfate dihydrate, Merck (precipitated, GR for analysis)
$FeSO_4 \cdot H_2O$
   Iron(II) sulfate hydrate, Merck (extra pure)
H_2SO_4
   Sulfuric acid, Merck (95-98%, extra pure)
KCl
   Potassium chloride, Merck (GR for analysis)
KH_2PO_4
   Potassium dihydrogen phosphate, Merck (GR for analysis)
K_2SO_4
   Potassium sulfate, Merck (cryst. GR for analysis)
$MgCl_2$
   Magnesium chloride, Merck (anhydrous, for synthesis)
$Na_2B_4O_7 \cdot 10H_2O$
   di-Sodium tetraborate decahydrate, Merck (GR for synthesis)
NaCl
   Sodium chloride, Merck (extra pure)
NaOH
   Sodium hydroxide, Riedel-de Haën (GR for analysis)
Na_2SO_4
   Sodium sulfate, Riedel-de Haën (anhydrous, GR for analysis)
$NiSO_4 \cdot 6H_2O$
   Nickel(II) sulfate hexahydrate, Merck (GR for analysis)
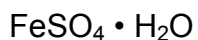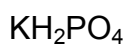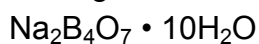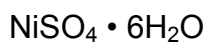
14.3 Ultrasonic velocity of magnesium sulfate solutions

Ultrasonic velocity of magnesium sulfate solutions for concentrations between 25 and 48 wt%.
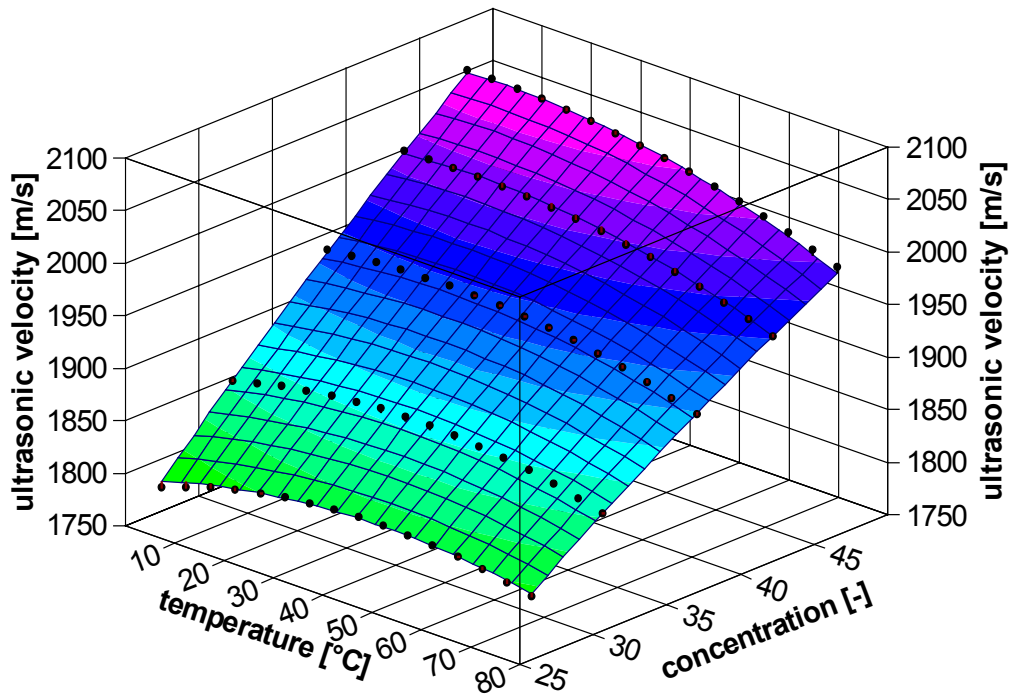
The ultrasonic velocity y in aqueous magnesium sulfate solutions in dependence on temperature x_1 and concentration x_2 can be correlated by the following equation:

$$y = a + b\,x_1 + c\,x_2 + d\,x_1^2 + e\,x_2^2 + f\,x_1\,x_2$$

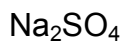Variables for concentrations between 0-25 and 25-48 wt% magnesium sulfate

variables	concentration 0-25 wt% ($R^2 = 0.9994$)	25-48 wt% ($R^2 = 0.9993$)
a	1409.648757	1335.664605
b	4.048246101	2.826807026
c	11.55346016	17.96038865
d	-0.02739812	-0.0151228834
e	0.05267242271	-0.06620185994
f	-0.06127042746	-0.05364606128

14.4 Solubility of magnesium sulfate in aqueous solution

Comparison between own experimental data (exp.) and data from literature (lit.) /SEI65/.
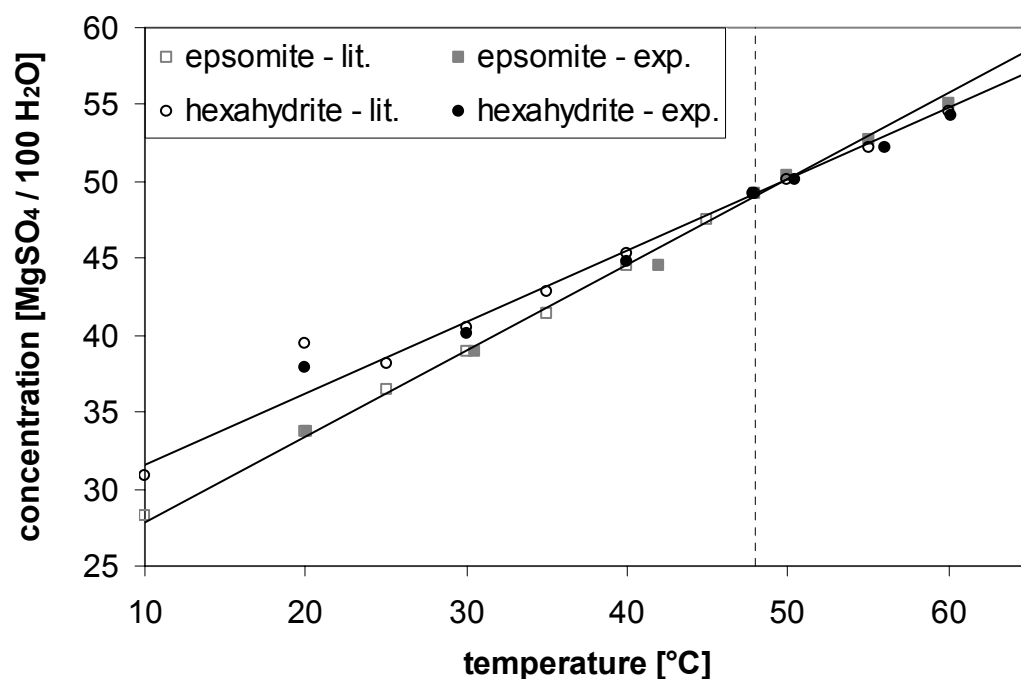
Solubility of epsomite

saturation temperature [°C]		concentration [g anh. / 100g H_2O]
(exp.)	(lit.)	
20.1	20.0	33.69
30.5	30.0	38.89
42.0	40.0	44.51
50.0**	--	50.38
55.0**	--	52.67
60.0**	--	55.04

Solubility of hexahydrite

saturation temperature [°C]		concentration [g anh. / 100g H_2O]
(exp.)	(lit.)	
20.0**	--	37.93
30.0**	--	40.06
40.0**	--	44.72
50.5	50.0	50.15
56.0	55.0	52.21
60.2	60.0	54.32

** solubility of the metastable phase

Supersolubility of epsomite

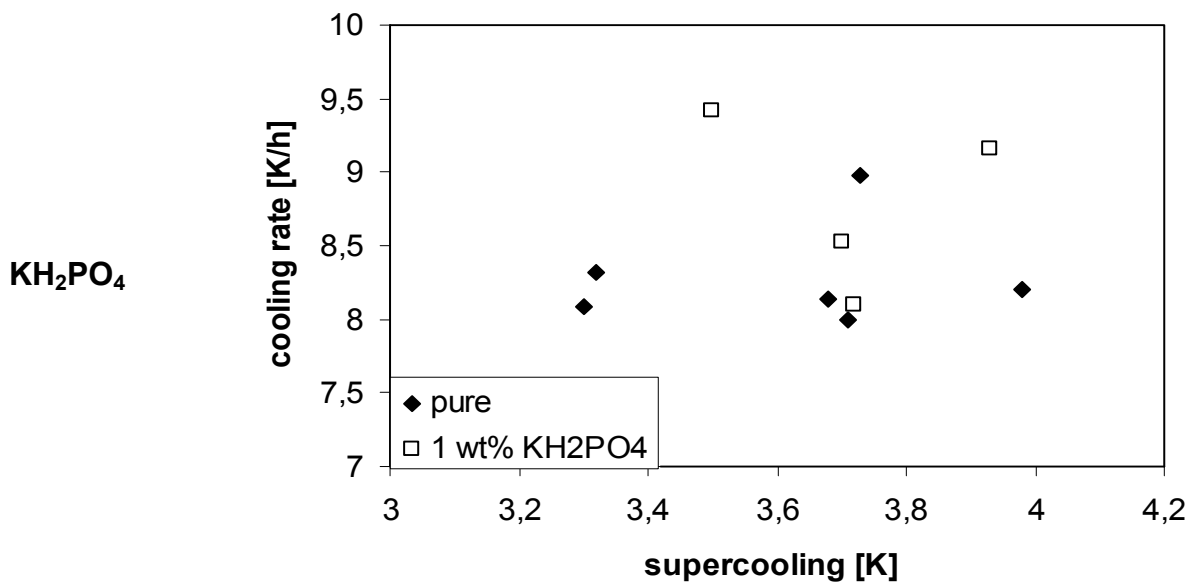| concentration [g anh. / 100g H_2O]	saturation temperature [°C]	nucleation temperature [°C]	ΔT_{max}* [K]
33.69	20.1	14.3	5.8
38.89	30.5	26.9	3.6
44.51	42.0	38.8	3.2
50.38	50.0	47.9	2.1

Supersolubility of hexahydrite

concentration [g anh. / 100g H_2O]	saturation temperature [°C]	nucleation temperature [°C]	ΔT_{max}* [K]
49.25	47.8	45.6	2.2
50.15	50.5	48.4	2.1
52.21	56.0	53.4	2.6
54.32	60.2	58.0	2.2

* average of 3-5 measurements with ultrasound, 10 K / h, seed crystal, moderate stirring

14.5 Influence of additives on the solubility of magnesium sulfate

Additive	Concentration [wt%]	Saturation temperature [°C]
--	pH: 6.4	30.5
$CaSO_4 \cdot 2H_2O$	0.1	30.6
$FeSO_4 \cdot H_2O$	1	30.8
H_2SO_4	pH: 2.5	30.8
KCl	0.5	30.5
KCl	1.5	30.5
KCl	2	30.5
KH_2PO_4	1	30.1
K_2SO_4	2	30.3
K_2SO_4	5	29.4
$MgCl_2$	0.1	30.8
$MgCl_2$	1	31.3
$MgCl_2$	2	32.8
$Na_2B_4O_7 \cdot 10H_2O$	0.1	30.5
$Na_2B_4O_7 \cdot 10H_2O$	0.5	30.4
$Na_2B_4O_7 \cdot 10H_2O$	1	30.2
$Na_2B_4O_7 \cdot 10H_2O$	2	30.1
$Na_2B_4O_7 \cdot 10H_2O$	3.5	29.1
$Na_2B_4O_7 \cdot 10H_2O$	5	28.6
NaCl	2	31.6
NaCl	5	32.5
NaOH	pH: 7.7	30.2
Na_2SO_4	2	30.9
Na_2SO_4	5	31.9
$NiSO_4 \cdot 6H_2O$	1	30.8

14.6 Metastable zone (maximum allowable supercooling) of magnesium sulfate in aqueous solution with additives

$CaSO_4 \cdot 2H_2O$

$FeSO_4 \cdot H_2O$

KH_2PO_4

Na$_2$SO$_4$

NiSO$_4$ • 6H$_2$O

pH
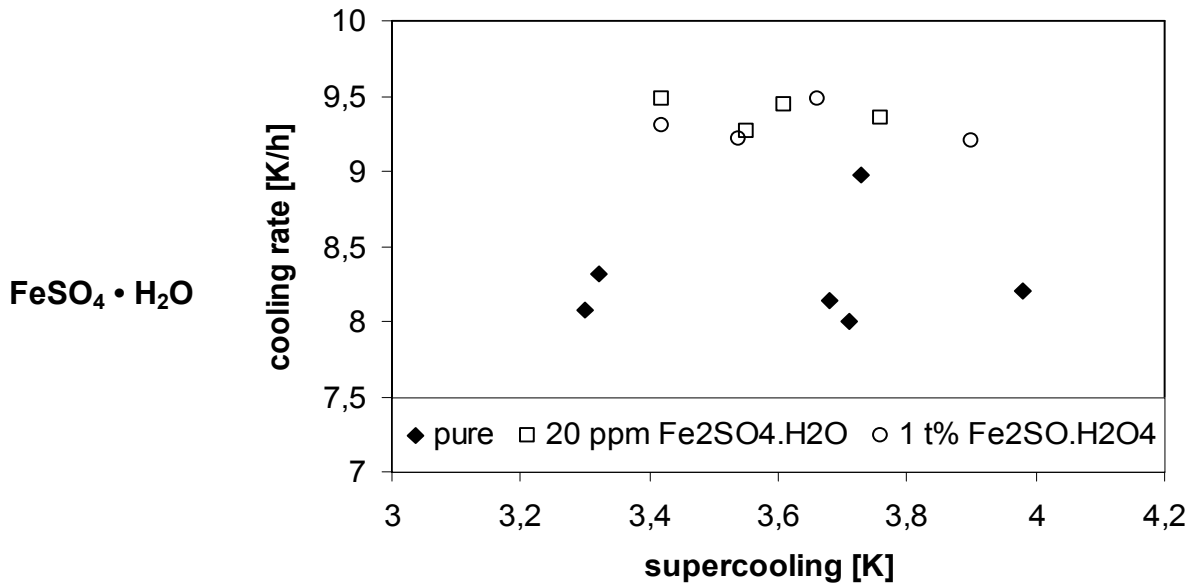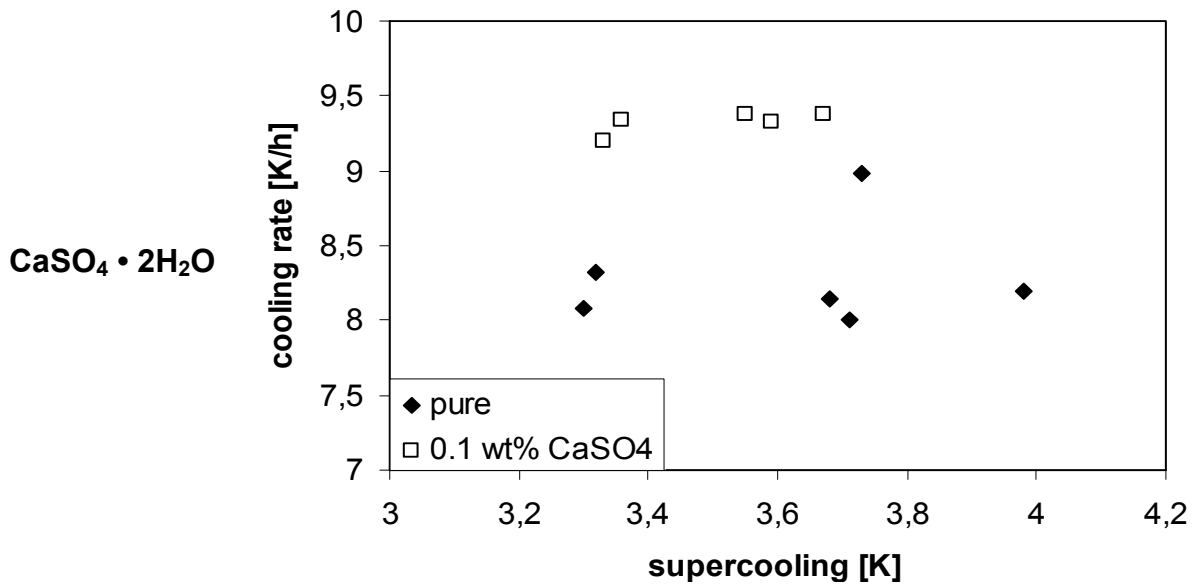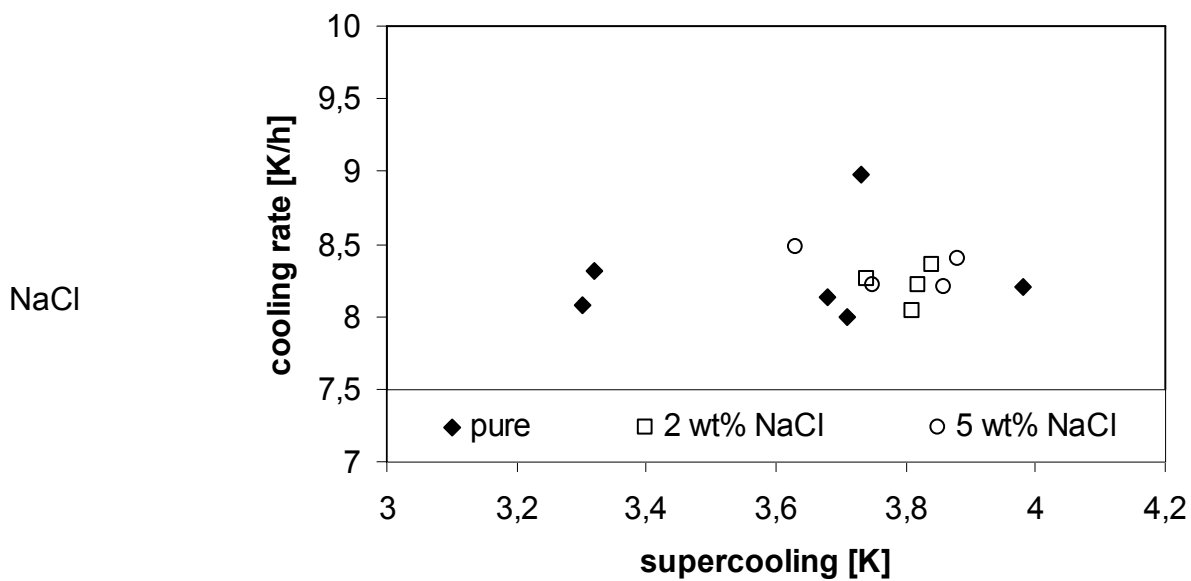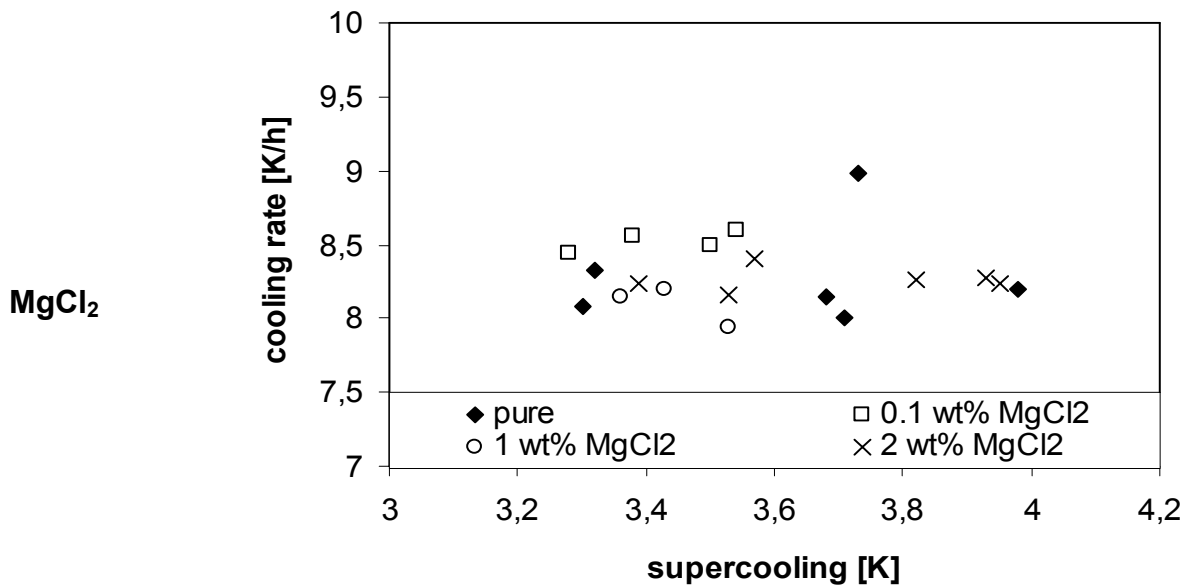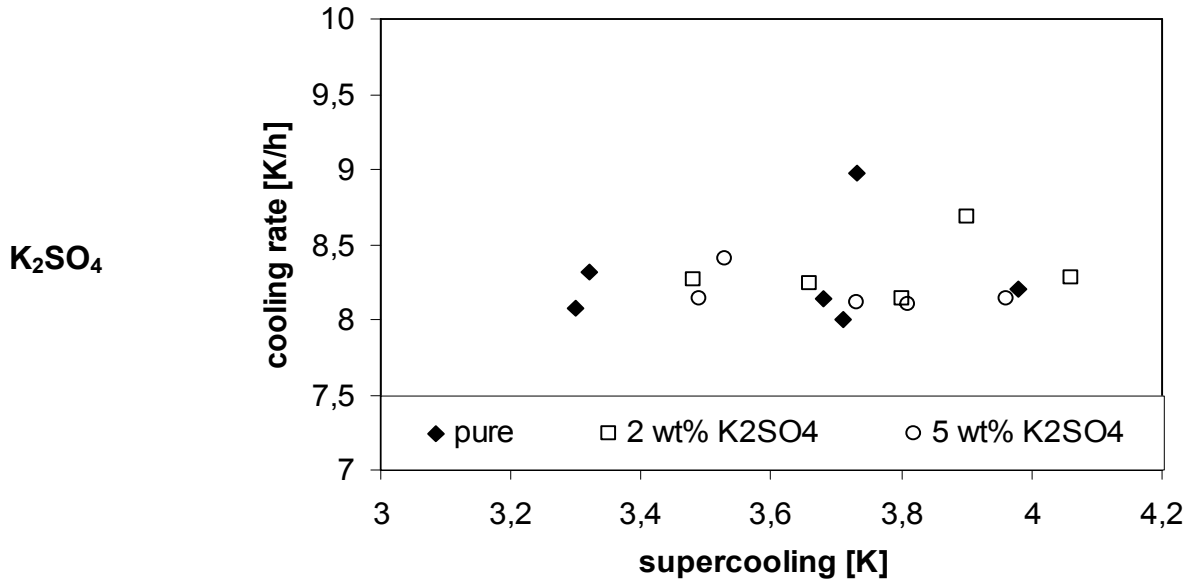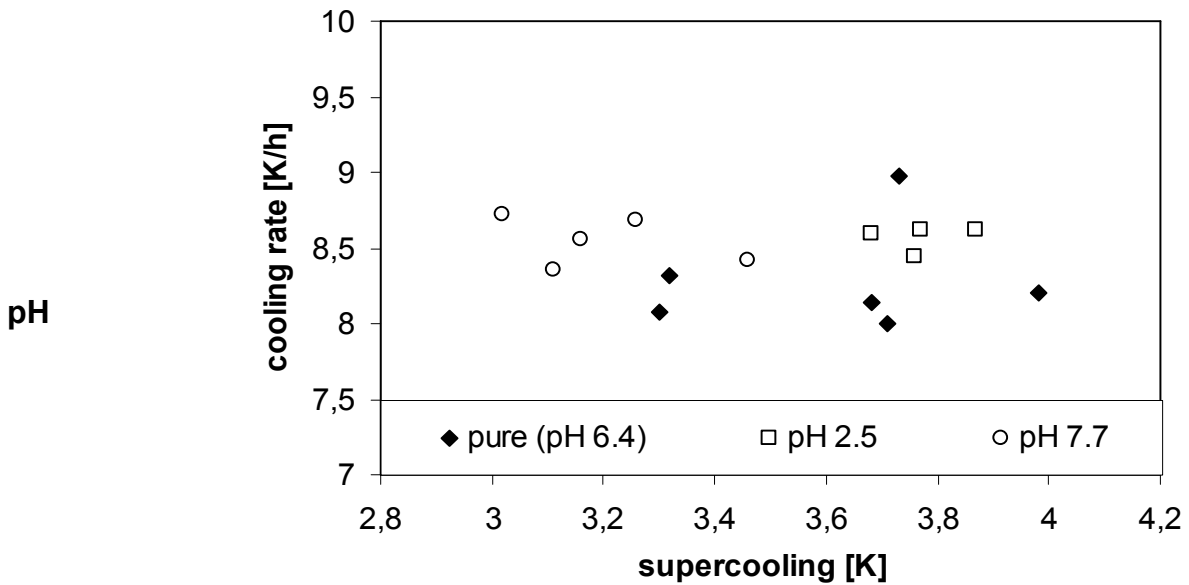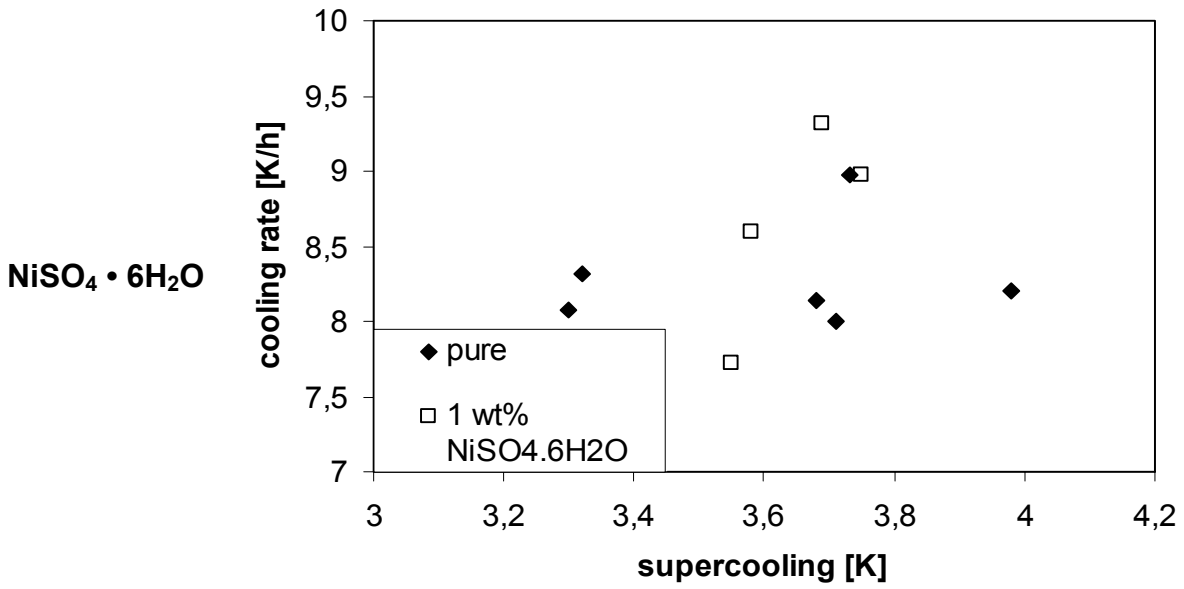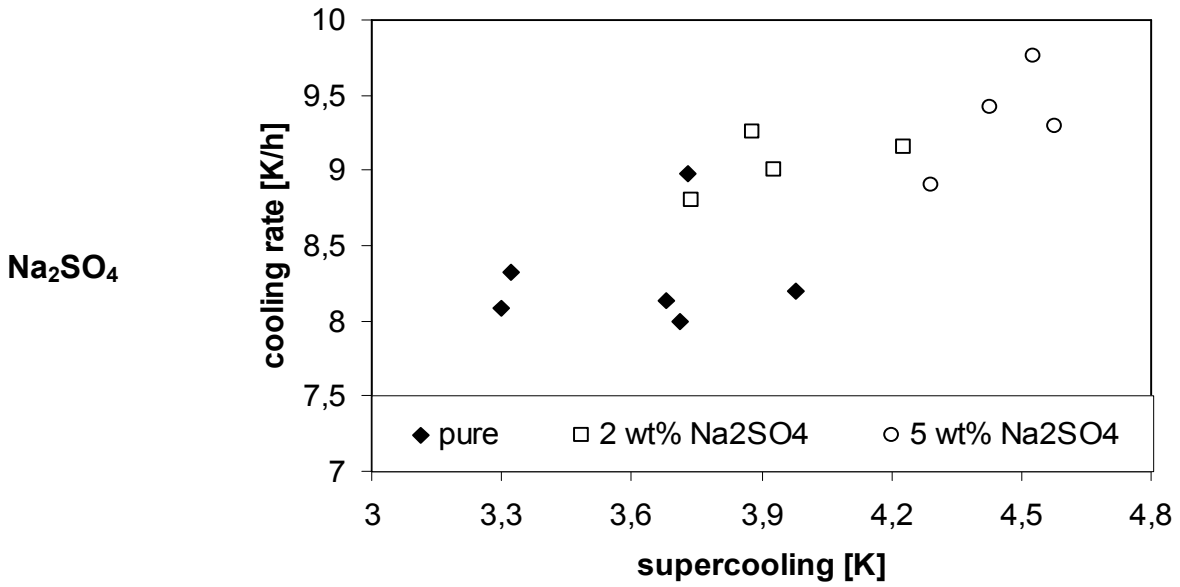
14.7 Solubility of zinc sulfate heptahydrate in aqueous solution

Solubility of zinc sulfate heptahydrate

saturation temperature [°C]	concentration [g anh. / 100g H_2O]
10.15	47.09
15.45	50.33
20.70	53.78
25.60	57.44
30.40	61.28
35.90	66.15
38.45	68.77
38.70	68.58
39.75**	69.46
44.00[+]	72.48

** solubility of the metastable phase
[+] solubility of zinc sulfate hexahydrate

Supersolubility of zinc sulfate heptahydrate

concentration [g anh. / 100g H_2O]	saturation temperature [°C]	nucleation temperature [°C]	ΔT_{max}* [K]
53.78	20.7	16.95	3.75
57.44	25.6	22.42	3.18
61.28	30.4	27.74	2.66
66.15	35.9	33.32	2.58

*average of 3-5 measurements with ultrasound, 10 K/h, seed crystal, moderate stirring

15. References

/ALJ03/ Al-Jibbouri, S. Effects of additives in solution crystallization. Online-Dissertation der Martin-Luther-Universität Halle-Wittenberg an der Universitäts- und Landesbibliothek Sachsen-Anhalt, 2003.

/ALL97/ Allen, T. Particle size measurement. Vol. 1: Powder sampling and particle size measurement. London: Chapman & Hall, 1997. 362-363.

/ARA87/ Arakelyan, V.S. Effect of ultrasound on crystal growth from melt and solution. Acta Phys. Hung. 61 (1987) 2, 185-187.

/ASH99/ Ashokkumar, M.; F. Grieser. Ultrasound assisted chemical processes. Rev. Chem. Eng. 15 (1999) 1, 41-83.

/BAU98/ Baumegger, A.; T. te Kloese. Einfache Messprinzipien für höchste Ansprüche. VT 32 (1998) 1, 76-78.

/BECH01/ Bechtloff, B.; S. Nordhoff; J. Ulrich. Pseudopolymorphs in industrial use. Cryst. Res. Technol. 36 (2001) 12, 1315-1328.

/BEC84/ Beckmann, W.; R. Boistelle; K. Sato. Solubility of the A, B, and C polymorphs of stearic acid in decane, methanol, and butanone. J. Chem. Eng. Data 29 (1984) 2, 211-214.

/BEC96/ Beckmann, W.; W.H. Otto. Occurrence, stability, kinetics of crystallization and polymorphic transition of the A, B and C modification of abecarnil – Influence of supersaturation, temperature, solvents and impurities. Trans IChemE 74 (1996) Part A, 750-757.

/BEC00/ Beckmann, W. Seeding the desired polymorph: Background, possibilities, limitations, and case studies. Org. Process Res. Dev. 4 (2000) 5, 372-383.

/BEC01/ Beckmann, W.; W. Otto; U. Budde. Crystallisation of the stable polymorph of hydroxytriendione: Seeding process and effects of purity. Org. Process Res. Dev. 5 (2001) 4, 387-392.

/BEC03/ Beckmann, W. Crystallisation of pharmaceutical compounds – Polymorphs, pseudo-polymorphs and particle formation. Eng. Life Sci. 3 (2003) 3, 113-120.

/BEC03a/ Beckmann, W. Personal communications, 2003.

/BER99/ Bernstein, J.; R.J. Davey; J.-O. Henck. Concomitant polymorphs. Angew. Chem. Int. Ed. 38 (1999) 3440-3461.

/BER02/ Bernstein, J. „Polymorphism". Strength from weakness: Structural consequences of weak interactions in molecular, supermolecules, and crystals. Eds. A. Domenicano and I. Hargittai. Dordrecht: Kluwer Adademic Publishers, 2002. 247-260.

/BLA98/ Blagden, N.; R.J. Davey; R. Rowe; R. Roberts. Disappearing polymorphs and the role of reaction by-products: the case of sulphathiazole. Int. J. Pharm. 172 (1998) 169-177.

/BOI88/ Boistelle, R.; J.P. Astier. Crystallization mechanisms in solution. J. Cryst. Growth 90 (1988) 14-30.

/BOIV00/	Boisvert, J.-P.; M. Domenech; A. Foissy; J. Persello; J.-C. Mutin. Hydration of calcium sulfate hemihydrate into gypsum. The influence of the sodium poly(acrylate)/surface interaction and molecular weight. J. Cryst. Growth 220 (2000) 579-591.
/BOR02/	Borissova, A.; K. Roberts; H. Groen. "Batch crystallization of monosodium glutamate with defined particle size via the use of in-process ATR-FTIR spectroscopy operated in closed-loop control". Chemical Engineering Transactions. Ed. A. Chianese. I (2002) 1467-1472.
/BOU02/	Boukerche, M.; D. Mangin; A. Rivoire; O. Monnier; C. Hoff; J.P. Klein. "Monitoring of polymorphs crystallization using in situ FTIR ATR spectroscopy coupled with in situ image acquisition". Chemical Engineering Transactions. Ed. A. Chianese. II (2002) 659-664.
/BRI99/	Brittain, H.G. Polymorphism in pharmaceutical solids. New York; Marcel Dekker, Inc., 1999.
/BUC58/	Buckley, H.E. Crystal Growth. New York: John Wiley & Sons, Inc., 1958.
/BUE51/	Buerger, M.J. "Crystallographic aspects of phase transformations". Phase Transformations in Solids. Eds. R. Smoluchowski, J.E. Mayer. New York: John Wiley & Sons, Inc., 1951. 183-211.
/BUR79/	Burger, A.; R. Ramberger. On the polymorphism of pharmaceuticals and other molecular crystals. I. Theory of thermodynamic rules. Mikrochim. Acta 11 (1979) 259-271.
/BYR82/	Byrn, S.R. Solid-State chemistry of drugs. New York: Academic Press, 1982.
/CAR85/	Cardew, P.T.; Davey, R.J. The kinetics of solvent-mediated phase transformations. Proc. R. Soc. Lond. A 398 (1985) 415-428.
/CHR71/	Christen, H.R. Einführung in die Chemie. Frankfurt a.M.: Diesterweg Salle, 1971.
/CLO71/	Clontz, N.A.; W.L. McCabe. Contact nucleation of Magnesium Sulfate Heptahydrate. Symp. Ser. AIChE 110 (1971) 67, 6-17
/DAV82/	Davey, R.J. "Solvent effects in crystallization processes". Current Topics in Materials Science. Ed. E. Kaldis. Vol. 8. Amsterdam: North-Holland Publishing Company, 1982. 429-479.
/DAV86/	Davey, R.J.; P.T. Cardew; D. McEwan; D.E. Sadler. Rate controlling process in solvent-mediated phase transformations. J. Cryst. Growth 79 (1986) 648-653.
/DAV97/	Davey, R.J.; N. Blagden; G.D. Potts; R. Docherty. Polymorphism in molecular crystals: Stabilization of a metastable form by conformational mimicry. J. Am. Chem. Soc. 119 (1997) 1767-1772.
/DAV02/	Davey, R.J.; N. Blagden; S. Righini; H. Alison; E.S. Ferrari. Nucleation control in solution mediated polymorphic phase transformations: The case of 2,6-Dihydroxybenzoic Acid. J. Phys. Chem. B 106 (2002) 1954-1959.

/DER03/	Derdour, L.; G. Févotte; F. Puel; P. Carvin. Real-time evaluation of the concentration of impurities during organic solution crystallization. Powder Technol. 129 (2003) 1-7.
/DIN97/	Dinger, F. Flink wie der Schall – Konzentrationsmessung mit Ultraschall. Process 5 (1997) 40-44.
/DIN03/	Dinger, F. Inline-Prozessanalytik und Reaktionsverfolgung mit Ultraschall. CHE Manager 5 (2003) 12, 9.
/DUN97/	Dunuwila, D.D.; K.A. Berglund. ATR FTIR spectroscopy for in situ measurement of supersaturation. J. Cryst. Growth 179 (1997) 185-193.
/EGL63/	Egli, P.H.; L.R. Johnson. "Ionic salts". The art and science of growing crystals. Ed. J.J. Gilman. New York: John Wiley & Sons, Inc., 1963. 194-213.
/FEN02/	Feng, L.; K.A. Berglund. ATR-FTIR for determining optimal cooling curves for batch crystallization of succinic acid. Cryst. Growth Des. 2 (2002) 5, 449-452.
/FER03/	Ferrari, E.S.; R.J. Davey; W.I. Cross; A.L. Gillon; C.S. Towler. Crystallization in polymorphic systems: The solution-mediated transformation of β to α glycine. Cryst. Growth Des. 3 (2003) 1, 53-60.
/FEV02/	Févotte, G. New perspectives for the on-line monitoring of pharmaceutical crystallization processes using in situ infrared spectroscopy. Int. J. Pharm. 241 (2002) 263-278.
/FRA01/	Fransen, M. Faster x-ray powder diffraction measurements. Int. Lab. 21 (2001) 16-22.
/FUJ02/	Fujiwara, M.; P.S. Chow; D.L. Ma; R.D. Braatz. Paracetamol crystallization using laser backscattering and ATR-FTIR spectroscopy: Metastability, agglomeration, and control. Cryst. Growth Des. 2 (2002) 5, 363-370.
/GME53/	Gmelin, L. "Magnesium". Gmelins Handbuch der anorganischen Chemie. 8th ed. Berlin: Verlag Chemie, 1953.
/GME56/	Gmelin, L. "Zink". Gmelins Handbuch der anorganischen Chemie. 8th ed. Berlin: Verlag Chemie, 1956.
/GME71/	Gmelin, L. "Calcium". Gmelins Handbuch der anorganischen Chemie. 8th ed. Berlin: Verlag Chemie, 1971.
/GME73/	Gmelin, L. "Natrium". Gmelins Handbuch der anorganischen Chemie. 8th ed. Berlin: Verlag Chemie, 1973.
/GRO01/	Groen, H.; K.J. Roberts. Nucleation, growth, and pseudo-polymorphic behavior of citric acid as monitored in situ by attenuated total reflection fourier transform infrared spectroscopy. J. Phys. Chem. B. 105 (2001) 43, 10723-10730
/GRO03/	Groen, H.; A. Borissova; K.J. Roberts. In-process ATR FTIR spectroscopy for closed-loop supersaturation control of batch crystallizer producing monosodium glutamate crystals of defined size. Ind. Eng. Chem. Res. 42 (2003) 1, 198-206.
/HAL69/	Haleblian, J.; W. McCrone. Pharmaceutical applications of polymorphism. J. Pharm. Sci. 58 (1969) 8, 911-929.

/HAL75/ Haleblian, J.K. Characterization of habits and crystalline modification of solids and their pharmaceutical applications. J. Pharm. Sci. 64 (1975) 8, 1269-1288.

/HE01/ He, X.; J.G. Stowell; K.R. Morris; R.R. Pfeiffer; H. Li; G.P. Stahly; S.R. Byrn. Stabilization of a metastable polymorph of 4-methyl-2-nitroacetanilide by isomorphic additives. Cryst. Growth Des. 1 (2001) 4, 305-312.

/HEN97/ Henck, J.-O.; U.J. Griesser, A. Burger. Polymorphie von Arzneistoffen – Eine wirtschaftliche Herausforderung. Pharm. Ind. 59 (1997) 2, 165-169.

/HER01/ Herden, A.; C. Mayer; S. Kuch; R. Lacmann. About the metastable zone width of primary and secondary nucleation. Chem. Eng. Technol. 24 (2001) 12, 1248-1254.

/HIL03/ Hilfiker, R. Bioverfügbarkeit optimieren. cav 4 (2003) 70-73.

/HOF91/ Hofmann, G. Verfahren zur Kristallisation: Die Praxis der Kristallisation. Haus der Technik, Essen, 24.-25. April 1991.

/HOP95/ Hopfe, J.; M. Füting. "Fundamentals of environmental scanning electron microscopy". In situ scanning electron microscopy in materials research. Eds. K. Wetzig and D. Schulze. Berlin: Akademie Verlag, 1995. 219-226.

/KAL94/ Kaltofen, R. Tabellenbuch Chemie. Ed. Thun. Braunschweig: Vieweg, 1994.

/KAR93/ Karel, M.; Nývlt, J. Effect of impurities on the width of the metastable region of potassium sulfate. Collect. Czech. Chem. Commun. 58 (1993) 1997-2001.

/KARP84/ Karpinski, P.H.; J. Butz; M. Larsen. "Influence of cationic admixtures on kinetics of crystal growth from aqueous solution". Industrial Crystallization 1984, ed. J. de Jong, Amsterdam: Elsevier, 1984, 85-89.

/KAS00/ Kashchiev, D. Nucleation: Basic theory with applications. Oxford: Butterworth-Heinemann, 2000.

/KEM02/ Kemp, R. "Calcium chloride". Ullmann's Encyclopedia of Industrial Chemistry. Ed. M. Bohnet. Electronic release. Weinheim: Wiley-VCH, 2002.

/KHA95/ Khankari, R.K.; D.J.W. Grant. Pharmaceutical hydrates. Thermochim. Acta 248 (1995) 61-79.

/KHAM76/ Khamskii, E.V. "Some problems of crystal habit modification". Industrial Crystallization. Ed. J.W. Mullin. New York: Plenum Press, 1976. 215-221.

/KHO93/ Khoshkhoo, S.; J. Anwar. Crystallization of polymorphs: The effect of solvent. J. Phys. D: Appl. Phys. 26 (1993) B 90-93.

/KIR98/ Kirchheim, J.; R. Bismark. Mehr Möglichkeiten – Messung von Kristallisations-parametern mit Ultraschall. Chem. Tech. 27 (1998) 4, 94-95.

/KIT02/ Kitamura, M. Controlling factor of polymorphism in crystallization process. J. Cryst. Growth 237-239 (2002) 2205-2214.

/KLE85/ Kleber, W. Einführung in die Kristallographie. Berlin: VEB Verlag Technik, 1985.

/KLU93/ Klug, D.L. "The influence of impurities and solvents on crystallization". Handbook of Industrial Crystallization. Ed. A.S. Myerson. Boston: Butterworth-Heinemann, 1993. 65-87.

/KOH63/   Kohman, G.T. "Precipitation of crystals from solution". The art and science of growing crystals. Ed. J.J. Gilman. New York: John Wiley & Sons, Inc., 1963. 152-162.

/KON02/   Kontrec, J.; D. Kralj; L. Brečević. Transformation of anhydrous calcium sulphate into calcium sulphate dihydrate in aqueous solutions. J. Cryst. Growth 240 (2002) 203-211.

/KRA01/   Krawitz, A.D. Introduction to diffraction in materials science and engineering. New York: John Wiley John & Sons, Inc., 2001.

/KRU93/   Kruse, M. Zur Modellierung der Wachstumskinetik in der Lösungskristallisation. Fortschr.-Ber. VDI Reihe 3, Nr. 309. Düsseldorf: VDI-Verlag, 1993.

/LAC99/   Lacmann, R.; A. Herden; C. Mayer. Kinetics of nucleation and crystal growth. Chem. Eng. Technol. 22 (1999) 4, 279-289.

/LAH01/   Lahav, M.; L. Leiserowitz. The effect of solvent on crystal growth and morphology. Chem. Eng. Sci. 56 (2001) 2245-2253.

/LAI02/   Lai, X.; K.J. Roberts; R.B. Hammond. "On-line analytical techniques for monitoring and controlling crystallization processes of organic speciality chemicals". Chemical Engineering Transactions. Ed. A. Chianese. I (2002) 1485-1490.

/LEC99/   LeCaptain, D.J.; K.A. Berglund. "In-Situ polymorph determination using second harmonic generation". Abstracts of Papers. Washington D.C.: ACS, 1999. 109-anyl.

/LEW01/   Lewiner, F.; G. Févotte; J.P. Klein; F. Puel. Improving batch cooling seeded crystallization of an organic weed-killer using on-line ATR FTIR measurement of supersaturation. J. Cryst. Growth 226 (2001) 348-362.

/LI03/   Li, H.; J. Wang; Y. Bao; Z. Guo; M. Zhang. Rapid sonocrystallization in the salting-out process. J. Cryst. Growth 247 (2003) 192-198.

/LIN01/   Li, N.; A. Shanks; D.M. Murphy. Solution-mediated transformation of photographic coupler. J. Cryst. Growth 224 (2001) 128-133.

/LYK01/   Lyko, H. Optische Verfahren zur Partikelanalyse. F & S 15 (2001) 5, 296-299.

/MAS00/   Mason, T.J. Large scale sonochemical processing: aspiration and actuality. Ultrason. Sonochem. 7 (2000) 4, 145-149.

/MAT03/   Matzger, A.; M. Lang; K. Kim. Systems and methods for the generation of crystalline polymorphs. Patent. WO 03/033462 A2, 24.04.2003. The regents of the University of Michigan.

/MATT99/   Mattos, M.V.C. Zur Übertragung der Einbau-Annäherung auf die Kristallhabitusänderung durch Adsorption. Dissertation. Universität Bremen. Aachen: Shaker Verlag, 1999.

/MCC65/   McCrone, W.C. "Polymorphism". Physics and chemistry of the organic state. New York: Interscience Publishers, 1965. 726-767.

/MER80/   Mersmann, A. Thermische Verfahrenstechnik. Berlin: Springer, 1980.

/MER95/   Mersmann, A. "Fundamentals of crystallization". Crystallization Technology Handbook. Ed. A. Mersmann. New York: Marcel Dekker, 1995. 1-74

/MER96/   Mersmann, A. Supersaturation and nucleation. TransIChemE A 74 (1996) 812-819.

/MERC99/   Merck Sicherheitsdatenblatt. CAS-Nr.: 25094-02-4. http://www.chemdat.de/, 1999.

/MIK02/   Mikonsaari, I.; U. Teipel; J. Ulrich. Kristallisation unter Anwendung von Ultraschall. Symposium Produktgestaltung in der Partikeltechnologie, Proceedings. Fraunhofer Institut für Chemische Technologie, 14.–15. November 2002, Pfinztal, Germany.

/MOH96/   Mohameed, H.A.; J. Ulrich. Wachstumskinetik in der Lösungskristallisation mit Fremdstoffen. Dissertation. Universität Bremen. Aachen: Shaker Verlag, 1996.

/MOH96a/   Mohameed, H.A.; J. Ulrich. Influence of the pH-value on the growth and dissolution rate of potassium chloride. Cryst. Res. Technol. 31 (1996) 1, 27-31.

/MOHN01/   Mohan, R.; K.-K. Koo, C. Strege; A.S. Myerson. Effect of additives on the transformation behavior of l-phenylalanine in aqueous solution. Ind. Eng. Chem. Res. 40 (2001) 26, 6111-6117.

/MOU02/   Mougin, P.; D. Wilkinson; K.J. Roberts. In situ measurement of particle size during the crystallization of L-glutamic acid under two polymorphic forms: Influence of crystal habit on ultrasonic attenuation measurements. Cryst. Growth Des. 2 (2002) 3, 227-234.

/MUL00/   Mullin, J.W. Crystallization. Oxford: Butterworth-Heinemann, 2000.

/MUR02/   Murphy, D.; F. Rodríguez-Cintrón; B. Langevin; R.C. Kelly; N. Rodríguez-Hornedo. Solution-mediated phase transformation of anhydrous to dihydrate carbamazepine and the effect of lattice disorder. Int. J. Pharm. 246 (2002) 121-134.

/MYE93/   Myerson, A.S. "Solutions and solution properties". Handbook of Industrial Crystallization. Ed. A.S. Myerson. Boston: Butterworth-Heinemann, 1993. 1-31.

/MYE02/   Myerson, A.S.; R. Ginde. "Crystals, crystal growth, and nucleation". Handbook of Industrial Crystallization. Ed. A.S. Myerson. Boston: Butterworth-Heinemann, 2002. 33-63.

/NIE97/   Niehörster, S. Der Kristallhabitus unter Additiveinfluß: Eine Modellierungs-methode. Dissertation. Universität Bremen, 1997.

/NIEN02/   Nienhaus, B.; E. Schweers. Keimbildung und Wachstum optimiert. cav 9 (2002) 84-86.

/NYV85/   Nývlt, J.; O. Söhnel; M. Matuchová; M. Broul. The kinetics of industrial crystallization. Prague: Academia Praha, 1985.

/NYV92/   Nývlt, J. Design of crystallizers. Boca Raton: CRC Press, 1992.

/NYV95/   Nývlt, J.; J. Ulrich. Admixtures in crystallization. Weinheim: VCH Verlagsgesellschaft, 1995.

/NYV97/   Nývlt, J. On the kinetics of solid-liquid-solid phase transformation. Cryst. Res. Technol. 32, 695-700.

/NYV99/   Nývlt, J. Effect of additives on crystallization of ammonium sulphate. Hung. J. Ind. Chem. 27 (1999) 2, 155-159.

/OMA99/   Omar, W.; C. Strege; J. Ulrich. Bestimmung der Breite des metastabilen Bereichs von realen Lösungen mit der Ultraschallmesstechnik zur on-line Prozessregelung bei Kristallisationsverfahren. Chem. Tech. 51 (1999) 5, 286-290.

/OMA99a/   Omar, W. Zur Bestimmung von Kristallisationskinetiken auch unter der Einwirkung von Additiven mittels Ultraschallmesstechnik. Dissertation. Universität Bremen, 1999.

/OMA99b/   Omar, W.; J. Ulrich. Application of ultrasonics in the on-line determination of supersaturation. Cryst. Res. Technol. 34 (1999) 3, 379-389.

/OTT02/   Otto, W. "Magnesium compounds". Ullmann's Encyclopedia of Industrial Chemistry. Ed. M. Bohnet. Electronic release. Weinheim: Wiley-VCH, 2002.

/PAU01/   Paulus, E.F.; A. Gieren. "Structure analysis by diffraction". Handbook of Analytical Techniques. Eds. H. Günzler and A. Williams. Vol. I. Weinheim: Wiley-VCH, 2001. 373-414.

/POV97/   Povey, M.J.W. Ultrasonic techniques for fluids characterization. London: Academic Press, 1997.

/PRO02/   Profir, V.M.; E. Furusjö; L.-G. Danielsson; Å.C. Rasmuson. Study of the crystallization of mandelic acid in water using in situ ATR-IR Spectroscopy. Cryst. Growth Des. 2 (2002) 4, 273-279.

/RAN71/   Randolph, A.D.; M.A. Larson. Theory of particulate processes. New York: Academic Press, 1971.

/RAU00/   Rauls, M.; K. Bartosch; M. Kind; S. Kuch; R. Lacmann; A. Mersmann. The influence of impurities on crystallization kinetics – a case study on ammonium sulfate. J. Cryst. Growth 213 (2000) 116-128.

/ROE79/   Rösler, J. Lehrbuch der Mineralogie. Leipzig: Deutscher Verlag für Grundstoff-industrie, 1979.

/ROEM95/   Römpp Chemielexikon a-z. 9th ed. Electronic release. Stuttgart: Georg Thieme Verlag, 1995.

/ROH02/   Rohe, D.M.M. "Zinc compounds". Ullmann's Encyclopedia of Industrial Chemistry. Ed. M. Bohnet. Electronic release. Weinheim: Wiley-VCH, 2002.

/RUB85/   Rubbo, M.; D. Aquilano; M. Franchini-Angela. Growth morphology of epsomite ($MgSO_4 \cdot 7H_2O$). J. Cryst. Growth 71 (1985) 470-482.

/SAT84/   Sato, K.; R. Boistelle. Stability and occurrence of polymorphic modifications of stearic acid in polar and nonpolar solutions. J. Cryst. Growth 66 (1984) 441-450.

/SAT85/	Sato, K.; K. Suzuki; M. Okada. Solvent effects on kinetics of solution-mediated transition of stearic acid polymorphs. J. Cryst. Growth 72 (1985) 699-704.
/SAY02/	Sayan, P.; Ulrich, J. The effect of particle size and suspension density on the measurement of ultrasonic velocity in aqueous solution. Chem. Eng. Proc. 41 (2002) 281-287.
/SCH02/	Schulz, H.; B. Schrader; R. Quilitzsch; B. Steuer. Quantitative analysis of various citrus oils by ATR/FT-IR and NIR-FT Raman spectroscopy. Appl. Spectrosc. 56 (2002) 1, 117-124.
/SEN99/	Sensotech GmbH. SensoTech GmbH – LiquiSonic Produktbeschreibung. http://www.sensotech.com/de/liquisonic, 1999.
/SGU87/	Sgualdino, G.; G. Vaccari; D. Aquilano; M. Rubbo. Growth kinetics of epsomite ($MgSO_4 \cdot 7H_2O$). J. Cryst. Growth 83 (1987) 523-527.
/SEI65/	Seidell, A.; W.F. Linke. Solubilities of inorganic and metalorganic compounds. Vol. 2: K-Z. Ed. W.F. Linke. 4th edition. Washington: ACS, 1965.
/SIN03/	Sinjarite mineral data. http://www.webmineral.com/data/sinjarite.shtml, 2003.
/SMI02/	Smith, R.A. "Boric oxide, boric acid, and borates". Ullmann's Encyclopedia of Industrial Chemistry. Ed. M. Bohnet. Electronic release. Weinheim: Wiley-VCH, 2002.
/STA02/	Starbuck, C.; A. Spartalis; L. Wai; J. Wang; P. Fernandez; C.M. Lindemann; G.X. Zhou; Z. Ge. Process optimization of a complex pharmaceutical polymorphic system via in situ Raman spectroscopy. Cryst. Growth Des. 2 (2002) 6, 515-522.
/STE90/	Stepanski, M. Zur Wachstumskinetik in der Lösungskristallisation. Dissertation. Universität Bremen, 1990.
/STR99/	Strege, C.; W. Omar; J. Ulrich. "Measurements of metastable zone width by means of ultrasonic devices". 7th International Workshop on Industrial crystallization BIWIC 1999. Ed. J. Ulrich. Halle (Saale): Verlag Martin-Luther-Universität Halle-Wittenberg, 1999. 219-230.
/STR99a/	Strege, C. Effect of additives on the solubility and the transformation behavior of l-phenylalanine. Studienarbeit. Universität Bremen / Polytechniy University of Brooklyn, 1999.
/TAM02/	Tamagawa, R.E.; E.A. Miranda, K.A. Berglund. Simultaneous monitoring of protein and $(NH_4)_2SO_4$ concentrations in aprotinin hanging-drop crystallization using Raman spectroscopy. Cryst. Growth Des. 2 (2002) 6, 511-514.
/TAV87/	Tavare, N.S. Batch crystallizers: A review. Chem. Eng. Comm. 61 (1987) 259-318.
/THR95/	Threlfall, T.L. Analysis of organic polymorphs. Analyst 120 (1995) 2435-2453.
/THR00/	Threlfall, T. Crystallisation of polymorphs: Thermodynamic insight into the role of solvent. Org. Process Res. Dev. (2000) 4, 384-390.

/ULR93/	Ulrich, J. Kristallwachstumsgeschwindigkeiten bei der Kornkristallisation – Einflussgrössen und Messtechniken. Habilitationsschrift. Universität Bremen. Aachen: Shaker Verlag, 1993.
/ULR00/	Ulrich, J.; C. Strege. "Metastable limits of salts: measurements and consequences". 8th World Salt Symposium. Ed. R.M. Geertman. Amsterdam: Elsevier Science B.V., 2000. 477-481.
/ULR02/	Ulrich, J.; C. Strege. Some aspects of the importance of metastable zone width and nucleation in industrial crystallizers. J. Cryst. Growth 237-239 (2002) 2130-2135.
/ULR02a/	Ulrich, J. "Crystallization". Kirk-Othmer Encyclopedia of Chemical Technology. Electronic Release. New York: John Wiley John & Sons, Inc., 2002.
/USD98/	Usdowski, E.; M. Dietzel. Atlas and data of solid-solution equilibria of marine evaporites. Berlin: Springer Verlag, 1998.
/UTS96/	Utschick, H. Anwendungen der thermischen Analyse: anorganische Chemie – organische Chemie – Polymerchemie – Anwendungstechniken. Landsberg: ecomed, 1996.
/VAU92/	Vauck, W.R.A.; H.A. Müller. Grundoperationen chemischer Verfahrenstechnik. Leipzig: VEB Deutscher Verlag für Grundstoffindustrie, 1992.
/VER66/	Verma, A.R.; P. Krishna. Polymorphism and polytypism in crystals. New York: John Wiley & Sons, Inc., 1966.
/VOL39/	Volmer, M. "Kinetik der Phasenbildung". Die chemische Reaktion. Ed. K.F. Bonhoeffer. Band IV. Dresden u. Leipzig: Verlag von Theodor Steinkopff, 1939.
/WAN00/	Wang, F.; J.A. Wachter; F.J. Antosz; K.A. Berglund. An investigation of solvent-mediated polymorphic transformation of progesterone using in situ Raman spectroscopy. Org. Process Res. Dev. 4 (2000) 5, 391-395.
/WANN01/	Wangnick, K.; J. Ulrich. Experimentelle Untersuchung zum Einfluss von Additiven auf den Habitus von Benzophenon. Chem. Tech. 52 (2001) 5/6, 210-216.
/WAR01/	Warrington, S.B.; G.W.H. Höhne. "Thermal analysis and calorimetry". Handbook of Analytical Techniques. Eds. H. Günzler and A. Williams. Vol. II. Weinheim: Wiley-VCH, 2001. 827-849.
/WEI03/	Wei, H.; Q. Shen; Y. Zhao; D.-J. Wang; D.-F. Xu. Influence of polyvinylpyrrolidone on the precipitation of calcium carbonate and on the transformation of vaterite to calcite. J. Cryst. Growth 250 (2003) 516-524.
/WEIS03/	Weissbuch, I.; M. Lahav; L. Leiserowitz. Toward stereochemical control, monitoring, and understanding of crystal nucleation. Cryst. Growth Des. 3 (2003) 2, 125-150.
/WIL88/	Willard, H.H.; L.L. Merritt; J.A. Dean; F.A. Settle. Instrumental methods of analysis. 7th edition. Belmont: Wadsworth Publishing Company, 1988.

/YAM02/   Yamanobe, M.; H. Takiyama; M. Matsuoka. Polymorphic transformation of DL-methionine crystals in aqueous solutions. J. Cryst. Growth 237-239 (2002) 2221-2226.

/ZET69/   Zettlemoyer, A.C. Nucleation. New York: Marcel Dekker, Inc., 1969.

/ZHI03/   Zhihong, L.; G. Shiyang; X. Shuping. FT-IR spectroscopic study of phase transformation of chloropinnoite in boric acid solution at 303 K. Spectrochim. Acta A 59 (2003) 265-270.

/ZIP00/   Zips, A. Prozesskontrolle mittels Ultraschall. tm 67 (2000) 5, 201-207.

LEBENSLAUF

Persönliche Daten

Christine Strege
geboren am 24. Juli 1973
in Nienburg (Weser)

Schulausbildung und Hochschulausbildung

1980-1993:	Grundschule, Orientierungsstufe, Gymnasium Abschluss: Abitur am SZ Holter Feld, Bremen
1993-1999:	Studium der Produktionstechnik an der Universität Bremen Abschluss: Dipl.-Ing. Produktionstechnik

Berufspraxis

1999-2003:	Wissenschaftliche Mitarbeiterin am Institut für Verfahrenstechnik / TVT an der Martin-Luther-Universität Halle-Wittenberg, Halle (Saale)
Seit Nov. 2003:	Patentanwaltskandidatin bei der Sozietät von Patent- und Rechtsanwälten Hoffmann·Eitle in München

München, November 2004